Complexation between flaxseed proteins, polyphenols and gums: Mechanism and application

A Thesis submitted in fulfilment of the requirements

for the degree of Doctor of Philosophy

Bao Loc Pham

B.Sc. (Food Technology), An Giang University, Vietnam

M. Sc. (Post-harvest technology), Can Tho University, Vietnam

School of Science

College of Science, Engineering and Health

RMIT University

June 2020

Declaration

I certify that except where due acknowledgement has been made, the work is that of the author alone; the work has not been submitted previously, in whole or in part, to qualify for any other academic award; the content of the Thesis is the result of work which has been carried out since the official commencement date of the approved research program; and any editorial work, paid or unpaid, carried out by a third party is acknowledged; and ethics procedures and guidelines have been followed.

Bao Loc Pham
30 June 2020

Copyright

Bao Loc Pham

2020

Acknowledgements

Apart from my own efforts, a number of people provided me with their valuable support during my PhD journey and I wish to express my gratitude to each and every of them.

First of all, I wish to express my deepest gratitude to my Senior Supervisor Professor Benu Adhikari for his intellectual guidance and continuous support during the course my PhD candidature. I wish to express my sincere gratitude to my Associate Supervisors Dr. Bo Wang, Dr. Bogdan Zisu and Dr. Tuyen Truong for their constructive and timely feedback and motivational support. Every piece of their advice was invaluable. The high-quality supervision from my supervisors enabled me to complete this study.

I gratefully acknowledge the Vietnam International Education Development and RMIT University for providing jointed scholarship for my PhD study.

I also acknowledge the technical staffs of School of Science, RMIT University for providing support on instrument training and safety induction. My gratitude goes to Mary Karagiozakis, Mina Dokouhaki, Hadi Ranjiburachaloo, Sanaz Salehi, Spiros Tsaroumis, Lillian Chuang, Yan Chen, Frank Antolasic, Nadia Zakhartchouk, Stephen Grist, Matthew Field and Billy Murdoch for providing me with essential technical support.

I wish to thank the colleagues of Food and Bioscience laboratories including Thi Lan Huong Nguyen, Minh Khanh Chau, Thi Nham Linh Tran, Thi Hong Anh Nguyen, Bo wang, Yakindra Timilsena, Tai NyokLing, A.K.M Masum, Arissara Phosanam, Billy Lo, Pranita Mhaske, Juhi Saxena, Mayumi Silva, Vilia Darma, Paramita Mhaske, Carine Semasaka, Jasmeet Kaur, Nelum Pematilleke, Shahla Teimouri, Geethu Kurup, Lloyd Condict, Mehran Ghasemlou, Manisha Singh, and Kingshuk Dhali, for their company during this journey.

Last but not least, I would like to thank my family for their enduring support and encouragement. Endless supports and encouragement from my parents, parents-in-law, my brothers and sisters enable me to overcome most of obstacles in order to achieve this goal. My understanding wife (Thi Diep Hoang Mai) and lovely children (Nghi, Thinh and Thai) are the reasons I chose undertake this PhD study in Australia.

Publications

The following are journal papers that form part of this Thesis.

A list of Journal articles:

1. **Pham, L. B.**, Wang, B., Zisu, B., & Adhikari, B. (2019). Covalent modification of flaxseed protein isolate by phenolic compounds and the structure and functional properties of the adducts. *Food chemistry*, *293*, 463-471.
   (This published research paper is presented as **Chapter 3** in this Thesis)
2. **Pham, L. B.,** Wang, B., Zisu, B., & Adhikari, B. (2019). Complexation between flaxseed protein isolate and phenolic compounds: Effects on interfacial, emulsifying and antioxidant properties of emulsions. *Food hydrocolloids*, *94*, 20-29.
   (This published research paper is presented as **Chapter 4** in this Thesis)
3. **Pham, L. B.**, Wang, B., Zisu, B., Truong, T., & Adhikari, B. (2020). Microencapsulation of flaxseed oil using polyphenol-adducted flaxseed protein isolate-flaxseed gum complex coacervates. *Food Hydrocolloids, 107*, 105944
   (This published research paper is presented as **Chapter 5** in this Thesis)

Manuscripts under preparation

4. **Pham, L. B.**, Wang, B., Zisu, B., Truong, T., & Adhikari, B. *In-vitro* digestion of flaxseed oil encapsulated in phenolic compound adducted flaxseed protein isolate-flaxseed gum complex coacervates.
   (This manuscript is accepted for publication in *Food Hydrocolloids* on 09 September 2020 and is presented as **Chapter 6** in this Thesis)

TABLE OF CONTENTS

Thesis title page		
Declaration		i
Copyright		ii
Acknowledgements		iii
Publications		iv
Table of contents		v
List of abbreviations		xi
List of units and symbols		xiii
Explanatory notes		xvi
Summary		xvii
Chapter 1	**Introduction**	1
1.1	**Introduction**	2
1.2	**Research hypotheses and research questions**	5
1.3	**Research objectives**	5
1.4	**Expected outcomes of Thesis**	6
1.5	**Outline of Thesis**	6
	References	9
Chapter 2	**Literature Review**	
	Complexation between protein and phenolic compounds and the application of the adducts and complex coacervates as emulsifiers and encapsulants	12
	Abstract	13
2.1	**Introduction**	14
2.2	**The mechanism of covalent conjugation between proteins and phenolic compounds**	16
2.3	**The effects of covalent conjugation of proteins with phenolic compounds on their physicochemical properties**	17
2.3.1	Effect of covalent conjugation of protein with phenolic compounds on the free amino and thiol groups and tryptophan content	19
2.3.2	Effect of covalent conjugation of protein with phenolic compounds on their molecular weight	20
2.3.3	Effect of covalent conjugation of phenolic compounds on structural conformation of proteins	21
2.3.4	Effect of covalent conjugation of phenolic compounds on the solubility and hydrophobicity of proteins	22

2.3.5	Effect of covalent conjugation with phenolic compounds on the thermal stability of proteins	22
2.3.6	Effect of covalent conjugation with phenolic compounds on the antioxidative property of proteins	23
2.3.7	Effect of covalent conjugation of proteins with phenolic compounds on their interfacial/emulsifying properties	23
2.3.7.1	*Effect of conjugation with phenolic compounds on the interfacial behaviour of proteins*	24
2.3.7.2	*Effect of conjugation of phenolic compounds with proteins on the emulsifying properties*	26
2.4	**Stabilisation of polyunsaturated fatty acids (PUFAs) rich oils using protein/gum complex coacervates as wall material**	26
2.5	**Microencapsulation of PUFAs rich oil using plant based-wall materials**	29
2.6	***In-vitro* digestion of oil microcapsules produced using complex coacervates as shell material**	30
2.7	**Composition and physicochemical properties of flaxseed protein, polyphenol, gum and oil**	33
2.7.1	Flaxseed protein	33
2.7.2	Flaxseed polyphenols	35
2.7.3	Flaxseed gum	37
2.7.4	Flaxseed oil	37
2.8	**Hydroxytyrosol**	38
2.9	**Concluding remarks**	38
	References	
Chapter 3	**Covalent modification of flaxseed protein isolate by phenolic compounds and the structure and functional properties of the adducts**	49
	Abstract	50
3.1	**Introduction**	50
3.2	**Materials and methods**	49
3.2.1	Materials	52
3.2.2	Methods	52
3.2.2.1	*Extraction of flaxseed protein isolate (FPI)*	52
3.2.2.2	*Extraction of flaxseed polyphenol (FPP)*	52
3.2.2.3	*Determination of chemical composition of FPI and FPP*	52
3.2.2.4	*Preparation of protein-phenolic adducts*	52
3.2.2.5	*Determination of free amino, thiol and tryptophan contents*	52
3.2.2.6	*Determination of molecular weight of FPI in protein-phenolic adducts*	53

3.2.2.7 Characteristic infrared absorption bands of functional groups using Fourier transform infrared spectroscopy (FTIR) 53
3.2.2.8 Determining the secondary structural features of FPI and its adducts 53
3.2.2.9 Determination of thermal behaviour of FPI and its FPI-phenolic adducts 53
3.2.2.10 Determination of surface hydrophobicity 53
3.2.2.11 Determination of antioxidative capacity of FPI and FPI-phenolic adducts 53
3.2.2.12 Statistical analysis 54
3.3 Results and discussion 54
3.3.1 Chemical composition of FPI and FPP 54
3.3.2 Free amino, thiol and tryptophan contents in FPI and FPI-phenolic adducts 54
3.3.3 Change in molecular weight of FPI due to reaction with phenolic compounds 54
3.3.4 Conformation of FPI and phenolic compound reaction through FTIR 55
3.3.5 Conformational structure of FPI and FPI-phenolic adducts 55
3.3.6 Thermal stability of FPI-phenolic adducts 55
3.3.7 Surface hydrophobicity of FPI and FPI-phenolic adducts 56
3.3.8 Antioxidative capacity of FPI-phenolic adducts 56
3.4 Conclusions 56
References 57

Chapter 4 Complexation between flaxseed protein isolate and phenolic compounds: Effects on interfacial, emulsifying and antioxidant properties of emulsions 59
Abstract 60
4.1 Introduction 60
4.2 Materials and methods 61
4.2.1 Materials 61
4.2.2 Sample preparation 61
4.2.2.1 Extraction of flaxseed protein isolate, flaxseed polyphenols and flaxseed oil 61
4.2.2.2 Preparation of protein-phenolic complexes 61
4.2.3 Methods 62
4.2.3.1 Determination of chemical composition of FPI and FPP 62
4.2.3.2 Determination of solubility of FPI and its complexes 62
4.2.3.3 Determination of zeta potential and particle size of FPI and its complexes 62
4.2.3.4 Measurement of dynamic interfacial tension and dilatational rheology 62

4.2.3.5 Measurement of adsorption of FPI and its phenolic complexes at oil/ water interface 62
4.2.3.6 Preparation of emulsions 63
4.2.3.7 Determination of particle size and zeta potential of emulsions 63
4.2.3.8 Determination of emulsifying activity and emulsion stability indices 63
4.2.3.9 Measurement of lipid oxidation 63
4.2.3.10 Measurement of colour parameters 63
4.2.3.11 Statistical analysis 63
4.3 Results and discussion 63
4.3.1 Chemical composition of FPI and FPP 63
4.3.2 The physical properties of FPI and FPI-phenolic complexes 64
4.3.3 Effect of FPI-phenolic compound complexation on dynamic interfacial tension and adsorption kinetics 64
4.3.4 Effect of FPI-phenolic complexation on dilatational rheology of FPI 65
4.3.5 Effect of FPI-phenolic complexation on emulsifying properties of FPI 66
4.3.6 Effect of FPI-phenolic reaction on the oxidation of oil-in-water emulsion 66
4.3.7 Effect of FPI-phenolic complexation on the colour of emulsions 66
4.4 Conclusion 68
References 68
Chapter 5 Microencapsulation of flaxseed oil using polyphenol-adducted flaxseed protein isolate-flaxseed gum complex coacervates 70
Abstract 71
5.1 Introduction 71
5.2 Materials and methods 72
5.2.1 Materials 72
5.2.2 Extraction of FPI, FPP, FG gum and flaxseed oil 72
5.2.3 Determination of the proximate composition of FPI and FG 72
5.2.4 Preparation of protein-phenolic adducts 72
5.2.5 Determination of optimum pH and protein/gum ratio for complex coacervation 73
5.2.6 Preparation of liquid microcapsules using FPI, FPI-phenolic adducts/FG complex coacervates 73
5.2.7 Spray drying 73
5.2.8 Determination of particle size of re-constituted microcapsules 73
5.2.9 Determination of viscosity of emulsion and liquid microcapsules 73
5.2.10 Determination of physicochemical properties of microcapsules 73
5.2.10.1 Moisture content and water activity 73
5.2.10.2 Surface oil and total oil contents of microcapsules 73
5.2.10.3 Encapsulation efficiency 74

5.2.10.4 Glass transition temperature 74
5.2.11 Determination of surface morphology of microcapsules 74
5.2.12 Determination of surface composition of solid microcapsules 74
5.2.13 Oxidative stability of solid microcapsules 74
5.2.13.1 Peroxide value 74
5.2.13.2 p-Anisidine value 74
5.2.14 Determination of secondary structure of protein in adducts and complex coacervates 74
5.2.15 Statistical analysis 74
5.3 Results and discussion 75
5.3.1 Chemical composition of FPI and FG 75
5.3.2 Optimum pH for complex coacervation between FPI and phenolic compound adducted FPI with FG 75
5.3.3 Optimal ratio for complex coacervation between FPI, (FPI-FPP), and (FPI-HT) and FG 77
5.3.4 Viscosity and particle size of emulsion and liquid microcapsules 78
5.3.5 Other physical properties of microcapsules 78
5.3.6 Surface elemental composition of microcapsules 78
5.3.7 Morphological characteristics of solid microcapsules 78
5.3.8 Oxidative stability of encapsulated flaxseed oil 79
5.3.9 Effect of complex coacervation on the secondary structure of FPI and FPI-phenolic adducts 81
5.4 Conclusion 81
References 81
Chapter 6 *In-vitro* digestion behaviour of flaxseed oil encapsulated using phenolic adducted flaxseed protein isolate-flaxseed gum complex coacervates 83
Abstract 84
6.1 Introduction 85
6.2 Materials and methods 86
6.2.1 Materials 86
6.2.2 Extraction of FPI, FO, FPP, FG and preparation of phenolic adducted FPI 86
6.2.3 Preparation of FO microcapsules using phenolic compound adducted FPI/FG complex coacervates 88
6.2.4 Preparation of simulated digestive fluids and in-vitro digestion of FO microcapsules 89
6.2.4.1 Simulated oral digestion 89
6.2.4.2 Simulated gastric digestion 89
6.2.4.3 Simulated intestinal digestion 89
6.2.4.4 Determination of particle size and zeta potential of digesta 90

6.2.5	Proteomic analysis	90
6.2.5.1	*Quantification of free amino groups in digesta*	90
6.2.5.2	*Determination of molecular weight of protein in the digesta*	91
6.2.6	*Determination of lipolysis of digesta*	91
6.2.6.1	*Quantification of released oil*	91
6.2.6.2	*Quantification of released free fatty acids*	92
6.2.7	*Observation of change of microstructure of microcapsules during digestion*	92
2.2.8	Statistical analysis	93
6.3	**Results and discussion**	93
6.3.1	Particle size, zeta potential and microstructure of digesta	93
6.3.1.1	*Particle size and size distribution*	93
6.3.1.2	*The surface charge of digested microcapsules*	98
6.3.1.3	*The microstructure of digested microcapsules*	99
6.3.2	Proteolysis during digestion	102
6.3.2.1	*Concentration of free amino groups in digested samples*	102
6.3.2.2	*Change of molecular weight of protein*	103
6.3.3	Release of oil and lipolysis during digestion	105
6.3.3.1	*Release of oil*	105
6.3.3.2	*Lipolysis of encapsulated oil*	106
6.4	**Conclusion**	108
	References	109
Chapter 7	**General Discussion, Overall Conclusion and Recommendation**	112
7.1	**Introduction**	113
7.2	**Key findings**	114
7.2.1	Effect of covalent conjugation of FPI with phenolic compounds (FPP, FA, HT) on its physicochemical and functional properties	114
7.2.2	Investigation of the interfacial and emulsifying properties of FPI-phenolic adducts	115
7.2.3	Microencapsulation of FO using phenolic adducted FPI-FG complex coacervates	116
7.2.4	*In-vitro* digestion behaviour of FO encapsulated in phenolic-adducted FPI/FG complex coacervates	117
7.3	**Contribution made by this Thesis to the body of knowledge**	117
7.4	**Recommendations for future research**	118
	References	119

List of abbreviations

AAA	Aromatic amino acids
ABTS	2,2′-Azino-bis(3-ethylbenzothiazoline-6-sulfonic acid
AI	Acidic isoelectric precipitation
ALA	Alpha-linolenic acid
ANOVA	Analysis of variance
AOAC	Association of Official Analytical Chemists
BCAA	Branched-chain amino acids
BSA	Bovine serum albumin
CA	Chlorogenic acid
CD	Circular dichroism
CC	Carboxymethyl chitosan
CLMS	Confocal scanning microscopy
DIT	Dynamic interfacial tension
DPPH	2,2-diphenyl-1-picrylhydrazyl
DSC	Differential scanning calorimeter
EAI	Emulsifying activity index
EGCG	Epigallocatechin gallate
ESI	Emulsion stability index
FA	Ferulic acid
FAE	Ferulic acid equivalence
FG	Flaxseed gum
FM	Flaxseed mucilage
FO	Flaxseed oil
FPI	Flaxseed protein isolate
FPP	Flaxseed polyphenols
FFA	Free fatty acids
FSD	Fourier self-deconvolution
FTIR	Fourier-transform infrared spectroscopy
GA	Gum Arabic
HMP	High methyl pectin
HT	Hydroxytyrosol
IDT	Initial decomposition temperature
MALDI-TOF-MS	Matrix-assisted laser desorption/ionization time of flight mass spectrometry
LCPUFAs	Long chain polyunsaturated fatty acids
MI	Micellization
MW	Molecular weight
RMIT	Royal Melbourne institute of technology

SDG	Secoisolariciresinol diglucoside
SDS-PAGE	Sodium dodecyl sulphate polyacrylamide gel electrophoresis
SECO	Secoisolariciresinol
SEM	Scanning electron microscope
SF	Simulated fluid
SSF	Simulated salivary fluid
SGF	Simulated gastric fluid
SIF	Simulated intestinal fluid
SPI	Soy protein isolate
TPC	Total phenolic content
WPI	Whey protein isolate
XG	Xanthan gum
XPS	X-ray Photoelectron Spectrometry
α-La	α-Lactalbumin
β-Lg	β-Lactoglobulin

List of units and symbols

A	Surface area
AU_{350}/g	Absorbance unit at 350 nm per gram
a*	Green-red
a_w	Water activity
B	Time at which the amount of free fatty acid released is equal to half of that at the "pseudo-equilibrium"
b*	Blue-yellow
C_0	Concentration of protein in the bulk phase
C	Carbon
D	Diffusion coefficient
$D_{1/2}$	Temperature for 50 wt% decomposition
Da	Dalton
$d_{4,3}$	Volume mean diameter
$d_{3,2}$	Surface mean diameter
E	Dilatational modulus
E′	Dilatational elasticity
E″	Dilatational viscosity
FFA_{max}	Amount of free fatty acids released at the "pseudo-equilibrium"
g	Gram
h	Hour
Hz	Hertz
K	Boltzmann constant
kcal	Kilo calorie
kDa	Kilo Dalton
kV	Kilovolt
KU mL^{-1}	Kilounit per millilitre
K_0^{FFA}	Initial free fatty acid release rate
K^{FFA}	Overall free fatty acid release rate
MRDT	Temperature for the maximum rate of decomposition
K_{diff}	Diffusion rate constant
K_p	Penetration rate constant
kg	Kilogram
L*	Lightness
M	Molar
mbar	Millibar
min	Minute
mg	Milligram
mol m^{-3}	Mole per cube meter

m^2 kg s^{-2} K^{-1}	Square meter per kilogram per square second per kelvin degree
mN m^{-1}	Millinewton per meter
$mNm^{-1}s^{-0.5}$	Millinewton per meter per square root of second
m^2/g	Square meter per gram
m^2 s^{-1}	Square meter per minute
m^{-1}	Per minute
mm^2	Square millimeter
mM	Millimolar
mg mL^{-1}	Milligram per litre
mL	Millilitre
ms	Millisecond
mV	Millivolt
MPa	Megapascal
N	Nitrogen
nm	Nanometer
O	Oxygen
pH	The power of Hydrogen
psi	Pounds per square inch
R^2	Coefficient of determination
rpm	Rotation per minute
S	Sulphur
S_0	Hydrophobicity index
s	Second
s^{-1}	Per second
t	Time
T	Absolute temperature
T_0	Turbidity of fresh emulsion
T_d	Denaturation temperature
T_g	Glass transition temperature
T_{onset}	Onset denaturation temperature
T_{endset}	Endset denaturation temperature
W	watt
w/w	Weight by weight
w/v	Weight by volume
µL	Microliter
µmol	Micromole
π_f	Interfacial pressure at final adsorption time
π_t	Interfacial pressure at a chosen time
π_0	Interfacial pressure at initial time

α	Alpha
β	Beta
σ_0	Interfacial tension of pure water
σ_t	Interfacial tension of protein solution at oil/water interface
γ	Interfacial tension
$\emptyset$	Phase shift between the sinusoidal perturbation of the interfacial tension and that of the interfacial area
%	Percentage
°C	Degree Celsius
ΔH	Denaturation enthalpy

Explanatory Notes

The following notes briefly delineate the points that were taken into consideration during the writing of this Thesis.

(i) Attempts have been made to use British spellings in the text except in the published journal articles where the journal guidelines have been followed.

(ii) Symbols or abbreviations, used in place of a lengthy name or expression, have been defined or explained in appropriate places as far as practicable.

(iii) Wherever possible, SI units have generally been used in expressing results throughout this Thesis.

(iv) APA referencing format has been followed in this Thesis except in the published articles where journal guidelines have been followed.

(v) Details of materials and reagents, method of calibration of equipment and experimental parameters used are depicted in each experimental chapter (Chapter 3-6) of this Thesis.

(vi) The term of complex/complexation in chapter 2 is equivalent to those of adduct/adduction in chapter 1 and the rest of this Thesis

SUMMARY

The interaction between proteins and polyphenols can produce complexes that can be used as emulsifiers and encapsulants for food application. Protein-polyphenol interaction can be of non-covalent and covalent nature; the latter produces protein-phenolic conjugates/adducts with improved thermal stability, antioxidant activity and emulsion stability compared to the native protein. However, most of the reported studies on protein-phenolic interactions are performed using animal proteins. The studies conducted on plant protein-phenolic interaction such as to explain the astringency of wine, cloudiness in beer and certain fruit juices, which have negative implication, and cannot necessarily explain the positive outcome of protein-phenolic interaction in developing useful food ingredients. Given that the use of plant-based ingredients is becoming increasingly popular, it is of practical important to understand the covalent interaction between plant proteins and polyphenols, as well as the physicochemical and functional characteristics of the resulting conjugates for their potential use as novel food ingredients. Therefore, the main objective of this Thesis was to understand the mechanism of formation of plant protein-phenolic adducts/conjugates, determine the optimum conditions under which these adducts produce complex coacervates with polysaccharide gum, and use the knowledge to produce emulsions and microcapsules of omega-3 rich oils. The resulting emulsions and microcapsules will have increased stability against oxidation, and improved controlled/targeted release of oil in simulated gastro-intestinal environment.

Protein, polysaccharide gum and polyphenol used in this study were extracted and purified from a single plant (flaxseed). Firstly, the covalent reaction between flaxseed protein isolate (FPI) with phenolic compounds (flaxseed polyphenol (FPP), small molecular weight phenolic compounds: ferulic acid (FA), and hydroxytyrosol (HT)] was investigated. The effect of conjugation of phenolic compounds with FPI on its physicochemical (molecular weight, conformational structure, and thermal stability) and functional (solubility, surface hydrophobicity, and antioxidant capacity) was studied. It was found that the degree and nature of conjugation depended on the structure of the phenolic compounds. HT was oxidised into hydroxytyrosol quinone and subsequently reacted with the nucleophiles in the side chain of FPI to form C-N and C-S linkages with its aromatic ring. The regenerated HT was re-oxidised and reacted with a second side chain of FPI to form a cross-link. The dimerization of two HT quinones, each carrying one side chain of FPI, also produced a cross-link. FA and FPP were oxidised to phenolate ions and subsequently formed semiquinone intermediate radicals which

reacted with the amino or sulfhydryl side chain of FPI to form uncross-linked FPI-FA and FPI-FPP adducts. Overall, all FPI-phenolic adducts showed improved thermal stability and antioxidant capacity. The FPI-HT adduct appeared to have higher solubility in water than FPI-FPP and FPI-FA. These findings suggest that the plant protein-phenolic adducts can be used as plant-based emulsifiers.

Secondly, the emulsifying and interfacial (diffusion, absorption and realignment) properties of cross-linked (FPI-HT) and uncross-linked (FPI-FPP) adducts were examined to explore their potential use as emulsifiers, compared with unmodified FPI. All the FPI-phenolic adducts exhibited similar surface activity to the unmodified FPI; however, the emulsion stability of emulsions stabilised by the adducts was weaker. Importantly, the emulsions stabilised by FPI-FPP and FPI-HT adducts had better stability against oxidation compared to that of the FPI-stabilised one. Given the substantially improved oxidative stability of FPI-FPP and FPP-HT adducts, they can be considered as emulsifiers of polyunsaturated fatty acid (PUFA)-rich oils.

Thirdly, flaxseed gum (FG) was used as the oppositely charged biopolymer to induce the complex coacervate with FPI-phenolic adducts. The optimum conditions for complex coacervation between these adduct, un-adducted FPI and FG were determined and found to be within a narrow pH range (4.6±0.1). The optimum protein-to-gum and adducts-to-gum ratio was also identical (6:1). Then the FPI/FG and (FPI-adducts)/FG complex coacervates were used as wall materials to encapsulate flaxseed oil (FO) at a wall:core ratio of 2:1 and the resulting microcapsules were spray dried into powder. Microcapsules produced using FPI/FG and (FPI-adducts)/FG had similar irregular shape and wrinkled surface morphology. The (FPI-HT)/FG was found to be the most protective wall matrix to stabilise FO with the lowest surface oil (1%) and the highest microencapsulation efficiency (95.4%). The microcapsule produced using (FPI-FPP)/FG had the highest oxidative stability.

Finally, the powder FO microcapsules were subjected to *in-vitro* digestion, and breakdown of the microcapsule and release of the FO in oral, gastric and intestinal stages was determined. These microcapsules exhibited significant resistance against digestion at the oral and gastric environments with a low degree of proteolysis and oil release; there was also insignificant change in particle size and microstructure. The microcapsules were substantially digested (break down of shell structure, release of FO and formation of free fatty acids (FFA) formed) intestinal stage. The (FPI-HT)/FG/FO microcapsule had the highest degree of oil release (80

%) and free fatty acid formation (FFA; 38.5%) the intestinal stage. The (FPI-FPP)/FG/FO capsule had the lowest extent of oil (66.3%) and FFA (28.9%) release. These findings suggest that the (FPI-FPP)/FG coacervate can be a promising delivery vehicle for PUFA-rich oils and other hydrophobic compounds to gastrointestinal system.

This thesis makes the following important contribution the body of knowledge: (1) Some phenolic compounds (e.g. HT) can crosslink plant protein molecules (e.g. FPI) while others (e.g. FPP) can form covalent conjugate at their side chain but cannot produce crosslinks; (2) The interfacial and emulsifying properties of plant protein-phenolic adducts depends on the nature of the adducted phenolic compounds; (3) The stability against oxidation of emulsions stabilised by plant protein-phenolic adducts can be substantially higher yet the such emulsions can be less stable compared to those produced using native (unconjugated) proteins; (4) The plant protein-phenolic adduct can be effectively used as wall materials for complex coacervate-based microencapsulation of unstable hydrophobic ingredients (e.g. omega-3 rich oils) as they impart promising controlled/targeted release properties.

CHAPTER 1

Introduction

1.1 Introduction

The interaction between proteins and polyphenols involves non-covalent and covalent bonding. The former occurs via hydrogen, ionic and/or hydrophobic interactions (Ozdal, Capanoglu, & Altay, 2013). The latter, known as covalent conjugation or adduction, involves the oxidation of polyphenols into highly reactive quinones and subsequent attachment of quinones to the side-chain nucleophiles such as lysine or thiols group of proteins (Cilliers & Singleton, 1991). The change in physicochemical and functional properties of proteins resulting from their interaction with polyphenols is dependent on the non-covalent or covalent nature of the interaction. The covalent conjugation is preferable due to its intrinsic strength (Curcio et al., 2012). For example, it was shown that the antioxidant capacity and thermal stability of covalent epigallocatechin gallate (EGCG)-zein complex were higher than those of non-covalent one (Liu, Ma, McClements, & Gao, 2017). In addition, the stability of emulsion stabilised by lactoferrin-caffeic covalent conjugate was higher than that of native lactoferrin stabilised emulsion (Liu, Sun, Yang, Yuan, & Gao, 2015). Similarly, Banerjee et al. (2013) revealed that the stability of foam stabilised by Polysorbate 20 (Tween 20)-β-lactoglobulin was improved by cross-linking β-lactoglobulin molecules with (+)-catechin. These improved properties of protein-polyphenol covalent complexes can make them better emulsifiers and encapsulants.

Although a large number of studies on the covalent conjugation between proteins and polyphenols have been reported, most of them were performed on animal-derived proteins including myoglobin (Kroll, Rawel, & Seidelmann, 2000), gelatin (Strauss & Gibson, 2004) and whey protein (Rawel, Kroll, & Hohl, 2001). The interactions between plant proteins and phenolic compounds have been studied to stabilise the protein foam (Sarker, Wilde, & Clark, 1995), prevention of haze formation in beer (Lopez & Edens, 2005). However, none of these studies cover the effect of these interactions or the products of the interactions on the interfacial, emulsifying and encapsulating properties. There is limited knowledge on the nature of the interaction between plant protein and phenolic compounds extracted from oilseeds and phenolic alcohol such as hydroxytyrosol and the physicochemical and functional properties of resulting covalent protein-phenolic adducts (Jiang et al., 2019; Kroll, Rawel, Rohn, & Czajka, 2001).

There is an increasing trend of using plant-based proteins as food ingredients (Sui et al., 2018; Tao et al., 2018) due to their healthy perception and less cost for their production compared to animal proteins (Nesterenko, Alric, Silvestre, & Durrieu, 2013). Use of plant proteisn as ingredients is also increasing due to increasing vegetarian and vegan dietary practices (Karaca, Low, & Nickerson, 2015). However, it is still a paucity of information on the nature of interaction between

plant protein and plant phenolic compounds extracted from oilseeds and phenolic alcohol such as hydroxytyrosol. The study on the physicochemical and functional properties of resulting plant protein-phenolic adducts also hasn't received its due attention.

Regarding the encapsulation of unstable hydrophobic compounds such as omega-3 rich oils, the encapsulating shell material has to be stable against mechanical force and/or elevated temperature to ensure the stability of the microcapsules. Otherwise, the hydrophobic compound (e.g. oil) can be easily released from the microcapsules, compromising the quality of the microcapsules. Hence, synthetic crosslinkers (e.g. glutaraldehyde) have been used to consolidate the crosslinking of protein component in the shell material. However, glutaraldehyde is not suitable for food application due to its toxic nature. Hence, transglutaminase is commonly used to enhance the mechanical crosslinking of protein component in microcapsule shells. However, it comes with a high cost and, also it does not have antioxidative property. For this reason, polyphenols, as natural crossing-linking agents, can be better alternatives. Furthermore, it has been demonstrated that the stability of emulsified fish oil against oxidation was enhanced by β-lactoglobulin-green tea polyphenol complexes (von Staszewski, Pizones Ruiz-Henestrosa, & Pilosof, 2014). However, there is a very little information on the use of plant protein-phenolic conjugates as shell materials to produce powdered oil microcapsules.

Complex coacervation is one of the most effective methods for encapsulation of omega-3 fatty acids-rich oils (Barrow, Nolan, & Jin, 2007). Complex coacervate-based microencapsulation system was found to provide better mechanical and oxidative stability of encapsulated omega-3 oils (Kaushik, Dowling, McKnight, Barrow, & Adhikari, 2016; Timilsena, Adhikari, Barrow, & Adhikari, 2016). However, the knowledge on complex coacervation between proteins that are covalently conjugated (with polyphenols) and polysaccharides is limited. The efficacies of the resulting complex coacervates to encapsulate omega-3 rich oils and other unstable hydrophobic compounds has received little attention. Typically, oil emulsification is the essential step of complex coacervation-based oil microencapsulation process (Wang, Adhikari, & Barrow, 2014). Therefore, a fundamental understanding of emulsifying and interfacial behaviour of protein-polyphenol adducts to be used as emulsifiers or encapsulating shell materials enables the optimisation of the emulsification and encapsulation process. The understanding of the nature and mechanism of formation of protein-polyphenol adducts provides 'science-based' (as opposed to 'trial and error') method for selecting these adducts as emulsifiers and encapsulants. Protein-gum complexes are found to have improved surface activity than the uncomplexed protein (Ducel, Richard, Popineau, & Boury, 2005). There are no studies that either confirm or disprove this in the case of protein-polyphenol adducts. Although there is some evidence that the inclusion of phenolic

compounds in the encapsulating wall materials can improve the physicochemical stability of encapsulated oil (Muhoza, Xia, & Zhang, 2019; Yekdane & Goli, 2019), there is no study on the use protein-polyphenol adducts to produce complex coacervate-based oil microcapsules. Also, there is no study that is carried out to understand the digestion of oil encapsulated in phenolic compound adducted protein/gum complex coacervates, even in simulated (*in vitro*) environment.

In this research, flaxseed has been chosen as the single major source of protein, polyphenols, oil, and gum. Flaxseed protein isolate (FPI) is shown to be a promising encapsulating material for oil encapsulation (Kaushik et al., 2016). FPI is nutritionally comparable to soy protein isolate in terms of amino acid profile (Madhusudhan & Singh, 1985) and possesses promising emulsifying property and good thermal stability. In addition, flaxseed is also rich in polyphenols (5.42 g per 100 g of seed). It is reported that ferulic acid is the major phenolic acid in flaxseed together with p-coumaric, and caffeic acid (Dabrowski & Sosulski, 1984). These phenolic acids and their derivatives are known as the source of antioxidant properties in flaxseed (Waszkowiak, Gliszczyńska-Świgło, Barthet, & Skręty, 2015). Due to the high level of unsaturated fatty acids (>75%), flaxseed oil is highly susceptible to oxidation during processing, handling and storage. Thus, a number of shell materials such as legume protein/maltodextrin (Can Karaca, Low, & Nickerson, 2013), gelatin/flaxseed mucilage (Mohseni & Goli, 2019), and whey proteins/alginate (Fioramonti, Stepanic, Tibaldo, Pavón, & Santiago, 2019) are used to produce solid or powder microcapsules of flaxseed oil. Flaxseed gum (FG) has also been found to be effective in protecting unsaturated fatty acid rich oil against oxidation when used as an encapsulating shell material (Hadad & Goli, 2019; Mohseni & Goli, 2019; Nikbakht Nasrabadi et al., 2019). This is because FG, a heteropolysaccharide comprising of neutral and acidic portions, can offer high emulsifying activity (Kaushik, Dowling, Adhikari, Barrow, & Adhikari, 2017). Native or non-conjugated FPI/FG complex coacervate has been used to encapsulate flaxseed oil (Kaushik et al., 2016).

Hydroxytyrosol (HT) is a phenolic alcohol found abundantly in olive oil. It has been reported that HT possesses a strong antioxidative activity and offers many health benefits including reducing systolic blood pressure (Covas, de la Torre, & Fitó, 2015), enhancing endothelial function (Valls et al., 2015), and alleviating inflammation (Lopez et al., 2017). However, very little information is available on the effects of covalent conjugation of proteins with HT on their emulsifying and encapsulating properties.

The knowledge gaps mentioned above underline the need for investigating the interaction, particularly the covalent conjugation, between FPI and phenolic compounds (i.e. flaxseed polyphenol (FPP) and HT). A greater understanding of the mechanism of the interaction and the

changes of physicochemical, interfacial, and emulsifying properties of covalently conjugated FPI (with phenolic compounds) would enable tailor the characteristics of FPI-phenolic adducts. This will broaden their application as emulsifiers and encapsulating shell materials of unstable, yet valuable, hydrophobic compounds. The mechanism of interaction and structure-function of the resulting adducts will provide basis for developing encapsulation systems and microcapsules almost entirely from the plant source.

1.2 Research hypotheses and research questions

The general hypothesis of this study is that protein-phenolic adduct can be good emulsifiers and encapsulants, provide high stability to oil-in-water emulsions, the resulting emulsions and microcapsule powders will have high stability against oxidation. The microcapsules will also have better control/targeted release property upon digestion.

Based on the above hypothesis, this Thesis addresses the following research questions.

1. What is the nature and extent of covalent conjugation (adduction) and crosslinking between plant protein and phenolic compounds?

2. How does the formation of adducts between plant protein and phenolic compounds affect the interfacial behaviour of protein at the oil/water interface. How does this interfacial behaviour is linked with emulsifying properties?

3. When used as encapsulants, can the protein-phenolic adducts provide higher encapsulation efficiency and oxidative stability to polyunsaturated fatty acids (PUFAs) rich oil than the protein?

4. How does the digestion of PUFA-rich oil encapsulated in phenolic compound adducted protein/gum complex coacervates differ from that of PUFA-rich oil encapsulated in unadducted protein/gum complex coacervates?

1.3 Research objectives

Based on the research questions listed above, the specific objectives of this Thesis are as follows.

1. To determine the nature and extent of covalent conjugation and crosslinking between FPI and phenolic compounds, including flaxseed polyphenols, ferulic acid, and HT.

2. To measure and interpret the interfacial behaviour (dynamic interfacial tension, protein adsorption interface and dilatational rheology) of FPI, FPI-phenolic adducts at the oil/water interface and their emulsifying properties.

3. To produce spray-dried flaxseed oil microcapsules using FPI, FPI-phenolic adducts/flaxseed gum complex coacervates and characterise their encapsulation efficiency, surface oil content and oxidative stability.

4. To measure and explain the digestion and release behaviour of flaxseed oil encapsulated in phenolic adducted and unadducted FPI-flaxseed gum complex coacervates.

1.4 Expected outcomes of Thesis

This Thesis is expected to provide substantially detailed understanding of how plant proteins and polyphenols interact (mechanism) and how the resulting protein-phenolic adducts can be used as emulsifiers and encapsulating shell materials. It is also expected to quantify with which the phenolic-protein adduction can improve stability of emulsions against oxidation. The finding of this research is expected to underscore the role of crosslinking of protein molecules by phenolic moieties to strengthening the structure of shell materials used for encapsulation. This study will provide underpinning science in developing entirely plant-based emulsifiers and encapsulating shell material for food applications.

1.5 Outline of Thesis

This Thesis is compiled into seven chapters. The research findings documented in Chapters 3 to 6 are in the format of accepted journal manuscript. The contents of Chapters 3, 4 and 5 are published. The content of the Chapter 6 is accepted for publication. The brief outline of each chapter is presented below.

Chapter 1 provides background information and highlights the current state of science and gaps in the knowledge in the discipline relevant to this study. The hypothesis, research questions, research objectives, outcomes from this thesis and the structure (outline) outlines of this Thesis are documented in this chapter.

Chapter 2 presents a critical review of the literature relevant to this Thesis. It provides relevant information such as composition and characteristics of flaxseed and its protein, polyphenols, gum, and oil. It reviews the available information on the interaction between proteins and phenolic compounds including mechanism and characteristics of resulting adducts and complexes. The literature on the interfacial behaviour of proteins and the relationship between their interfacial behaviour and emulsifying properties is also reviewed in condensed form. Pertinent literature on the formation of complex coacervates and their application in encapsulating omega-3 rich oils, the

have also been reviewed. The literature on the methods used and characterisation of the digestion and release of encapsulated oil (from microcapsules) has also been reviewed.

Chapter 3 documents the process of producing FPI-phenolic adducts and the effects of covalent adduction of FPI with phenolic compounds (FPP, FA and HT) on the physicochemical and functional properties of FPI. The assessed properties included amount of free amino, thiol and tryptophan content, molecular weight profile, conformational structure, thermal stability, and hydrophobicity. The improvement in antioxidative capacity has also been assessed and reported. The content of this chapter is published in *Food Chemistry* (Pham, Wang, Zisu, & Adhikari, 2019a)

Chapter 4 documents the effects of covalent conjugation of FPI with phenolic compounds, listed above, on its interfacial and emulsifying properties. The interfacial properties at the oil/water interface of the phenolic-FPI adducts (dynamic interfacial tension, adsorption kinetics, and dilatational rheology) are characterised. The emulsifying properties, stability against oxidation and surface charge (zeta potential), and droplet size of emulsions stabilised by FPI and FPI-phenolic adducts are characterised and elucidated. The content of this chapter is published in *Food Hydrocolloids* (Pham, Wang, Zisu, & Adhikari, 2019b)

Chapter 5 documents the process of producing FPI/FG and polyphenol-adducted FPI/FG complex coacervates and application of these complex coacervates to produce powder microcapsules of FO. The optimum conditions (pH and protein/gum ratio) for producing these were determined. Spray drying was used to produce the powder FO microcapsules. The most important physical properties of the microcapsules including water activity (a_w), glass transition temperature (T_g), particle size, surface oil content, microencapsulation efficiency and oxidative stability were determined. The surface elemental composition and morphology of the sprayed dried microcapsules were determined and is elucidated. The content of this chapter is published in *Food Hydrocolloids* (Pham, Wang, Zisu, Truong, & Adhikari, 2020).

Chapter 6 reports the results of *in-vitro* digestion of FO encapsulated in FPI and phenolic-adducted FPI/FG complex coacervate. The particle size, zeta potential and microstructure of digested microcapsules was measured at the end of oral, gastric, and intestinal stages. The digestion (hydrolysis) of the FPI and phenolic-adducted FPI, used as shell material, was determined in the gastric and intestinal phases. The release of oil from microcapsules at the end of each digestion stage and the release of free fatty acids at intestinal stage were measured and explained. The content of this chapter is accepted for publication in *Food Hydrocolloids.*

Chapter 7 presents the key findings and conclusions of experimental chapters in integral manner. It also lists the main contributions made by this study to the body of knowledge relevant to the field. Recommendations for future works, based on the experience gained during this study, are also presented in this chapter.

References

Banerjee, S., Chattopadhyay, P., Ghosh, A., Goyary, D., Karmakar, S., & Veer, V. (2013). Influence of process variables on essential oil microcapsule properties by carbohydrate polymer-protein blends. *Carbohydr Polym, 93*(2), 691-697.

Barrow, C. J., Nolan, C., & Jin, Y. (2007). Stabilization of highly unsaturated fatty acids and delivery into foods. *Lipid Technology, 19*(5), 108-111.

Can Karaca, A., Low, N., & Nickerson, M. (2013). Encapsulation of flaxseed oil using a benchtop spray dryer for legume protein-maltodextrin microcapsule preparation. *J Agric Food Chem, 61*(21), 5148-5155.

Cilliers, J. J., & Singleton, V. L. (1991). Characterization of the products of nonenzymic autoxidative phenolic reactions in a caffeic acid model system. *Journal of Agricultural and Food Chemistry, 39*(7), 1298-1303.

Covas, M.-I., de la Torre, R., & Fitó, M. (2015). Virgin olive oil: a key food for cardiovascular risk protection. *British Journal of Nutrition, 113*(S2), S19-S28.

Curcio, M., Parisi, O. I., Puoci, F., Altimari, I., Spizzirri, U. G., & Picci, N. (2012). Antioxidant polymers by free radical grafting on natural polymers. *Antioxidant Polymers: Synthesis, Properties, and Applications*, 153-178.

Dabrowski, K. J., & Sosulski, F. W. (1984). Composition of free and hydrolyzable phenolic acids in defatted flours of ten oilseeds. *Journal of Agricultural and Food Chemistry, 32*(1), 128-130.

Ducel, Richard, Popineau, & Boury. (2005). Rheological Interfacial Properties of Plant Protein-Arabic Gum[1020].pdf. *Biomacromolecules, 6*, 790-796.

Fioramonti, S. A., Stepanic, E. M., Tibaldo, A. M., Pavón, Y. L., & Santiago, L. G. (2019). Spray dried flaxseed oil powdered microcapsules obtained using milk whey proteins-alginate double layer emulsions. *Food Research International, 119*, 931-940.

Hadad, S., & Goli, S. A. H. (2019). Improving Oxidative Stability of Flaxseed Oil by Encapsulation in Electrospun Flaxseed Mucilage Nanofiber. *Food and Bioprocess Technology, 12*(5), 829-838.

Jiang, L., Liu, Y., Li, L., Qi, B., Ju, M., Xu, Y., . . . Sui, X. (2019). Covalent conjugates of anthocyanins to soy protein: Unravelling their structure features and in vitro gastrointestinal digestion fate. *Food Research International, 120*, 603-609.

Karaca, A. C., Low, N., & Nickerson, M. (2015). Potential use of plant proteins in the microencapsulation of lipophilic materials in foods. *Trends in Food Science & Technology, 42*(1), 5-12.

Kaushik, P., Dowling, K., Adhikari, R., Barrow, C. J., & Adhikari, B. (2017). Effect of extraction temperature on composition, structure and functional properties of flaxseed gum. *Food Chem, 215*, 333-340.

Kaushik, P., Dowling, K., McKnight, S., Barrow, C. J., & Adhikari, B. (2016). Microencapsulation of flaxseed oil in flaxseed protein and flaxseed gum complex coacervates. *Food Research International, 86*, 1-8.

Kroll, J., Rawel, H. M., Rohn, S., & Czajka, D. (2001). Interactions of glycinin with plant phenols–influence on chemical properties and proteolytic degradation of the proteins. *Molecular Nutrition & Food Research, 45*(6), 388-389.

Kroll, J., Rawel, H. M., & Seidelmann, N. (2000). Physicochemical properties and susceptibility to proteolytic digestion of myoglobin-phenol derivatives. *Journal of Agricultural and Food Chemistry, 48*(5), 1580-1587.

Liu, F., Ma, C., McClements, D. J., & Gao, Y. (2017). A comparative study of covalent and non-covalent interactions between zein and polyphenols in ethanol-water solution. *Food Hydrocolloids, 63*, 625-634.

Liu, F., Sun, C., Yang, W., Yuan, F., & Gao, Y. (2015). Structural characterization and functional evaluation of lactoferrin–polyphenol conjugates formed by free-radical graft copolymerization. *RSC Advances, 5*(20), 15641-15651.

Lopez, M., & Edens, L. (2005). Effective prevention of chill-haze in beer using an acid proline-specific endoprotease from Aspergillus niger. *Journal of Agricultural and Food Chemistry*, 53(20), 7944-7949.

Lopez, S., Montserrat-de la Paz, S., Lucas, R., Bermudez, B., Abia, R., Morales, J. C., & Muriana, F. J. G. (2017). Effect of metabolites of hydroxytyrosol on protection against oxidative stress and inflammation in human endothelial cells. *Journal of Functional Foods, 29*, 238-247.

Madhusudhan, K., & Singh, N. (1985). Isolation and characterization of the major fraction (12 S) of linseed proteins. *Journal of Agricultural and Food Chemistry, 33*(4), 673-677.

Mohseni, F., & Goli, S. A. H. (2019). Encapsulation of flaxseed oil in the tertiary conjugate of oxidized tannic acid-gelatin and flaxseed (Linum usitatissimum) mucilage. *International Journal of Biological Macromolecules, 140*, 959-964.

Muhoza, B., Xia, S., & Zhang, X. (2019). Gelatin and high methyl pectin coacervates crosslinked with tannic acid: The characterization, rheological properties, and application for peppermint oil microencapsulation. *Food Hydrocolloids, 97*, 105174.

Nesterenko, A., Alric, I., Silvestre, F., & Durrieu, V. (2013). Vegetable proteins in microencapsulation: A review of recent interventions and their effectiveness. *Industrial Crops and Products, 42*, 469-479.

Nikbakht Nasrabadi, M., Goli, S. A. H., Sedaghat Doost, A., Roman, B., Dewettinck, K., Stevens, C. V., & Van der Meeren, P. (2019). Plant based Pickering stabilization of emulsions using soluble flaxseed protein and mucilage nano-assemblies. *Colloids and Surfaces A: Physicochemical and Engineering Aspects, 563*, 170-182.

Ozdal, T., Capanoglu, E., & Altay, F. (2013). A review on protein–phenolic interactions and associated changes. *Food Research International, 51*(2), 954-970.

Pham, L. B., Wang, B., Zisu, B., & Adhikari, B. (2019a). Complexation between flaxseed protein isolate and phenolic compounds: Effects on interfacial, emulsifying and antioxidant properties of emulsions. *Food Hydrocolloids, 94*, 20-29.

Pham, L. B., Wang, B., Zisu, B., & Adhikari, B. (2019b). Covalent modification of flaxseed protein isolate by phenolic compounds and the structure and functional properties of the adducts. *Food Chemistry, 293*, 463-471.

Pham, L. B., Wang, B., Zisu, B., Truong, T., & Adhikari, B. (2020). Microencapsulation of flaxseed oil using polyphenol-adducted flaxseed protein isolate-flaxseed gum complex coacervates. *Food Hydrocolloids, 107*, 105944.

Rawel, H. M., Czajka, D., Rohn, S., & Kroll, J. (2002). Interactions of different phenolic acids and flavonoids with soy proteins. *Int J Biol Macromol, 30*(3-4), 137-150.

Rawel, H. M., Kroll, J., & Hohl, U. (2001). Model studies on reactions of plant phenols with whey proteins. *Molecular Nutrition & Food Research, 45*(2), 72-81.

Sarker, D. K., Wilde, P. J., & Clark, D. C. (1995). Control of surfactant-induced destabilization of foams through polyphenol-mediated protein-protein interactions. *Journal of Agricultural and Food Chemistry*, 43(2), 295-300.

Strauss, G., & Gibson, S. M. (2004). Plant phenolics as cross-linkers of gelatin gels and gelatin-based coacervates for use as food ingredients. *Food Hydrocolloids, 18*(1), 81-89.

Sui, X., Sun, H., Qi, B., Zhang, M., Li, Y., & Jiang, L. (2018). Functional and conformational changes to soy proteins accompanying anthocyanins: Focus on covalent and non-covalent interactions. *Food Chemistry, 245*, 871-878.

Tao, F., Jiang, H., Chen, W., Zhang, Y., Pan, J., Jiang, J., & Jia, Z. (2018). Covalent modification of soy protein isolate by (−)-epigallocatechin-3-gallate: effects on structural and emulsifying properties. *Journal of the Science of Food and Agriculture, 98*(15), 5683-5689.

Timilsena, Adhikari, R., Barrow, C. J., & Adhikari, B. (2016). Microencapsulation of chia seed oil using chia seed protein isolate-chia seed gum complex coacervates. *Int J Biol Macromol, 91*, 347-357.

Valls, R.-M., Farràs, M., Suárez, M., Fernández-Castillejo, S., Fitó, M., Konstantinidou, V., . . . Solà, R. (2015). Effects of functional olive oil enriched with its own phenolic compounds on endothelial function in hypertensive patients. A randomised controlled trial. *Food Chemistry, 167*, 30-35.

von Staszewski, M., Pizones Ruiz-Henestrosa, V. M., & Pilosof, A. M. R. (2014). Green tea polyphenols-β-lactoglobulin nanocomplexes: Interfacial behavior, emulsification and oxidation stability of fish oil. *Food Hydrocolloids, 35*, 505-511.

Wang, Adhikari, B., & Barrow, C. J. (2014). Optimisation of the microencapsulation of tuna oil in gelatin-sodium hexametaphosphate using complex coacervation. *Food Chem, 158*, 358-365.

Waszkowiak, K., Gliszczyńska-Świgło, A., Barthet, V., & Skręty, J. (2015). Effect of Extraction Method on the Phenolic and Cyanogenic Glucoside Profile of Flaxseed Extracts and their Antioxidant Capacity. *J Am Oil Chem Soc, 92*(11-12), 1609-1619.

Yekdane, N., & Goli, S. A. H. (2019). Effect of pomegranate juice on characteristics and oxidative stability of microencapsulated pomegranate seed oil using spray drying. *Food and Bioprocess Technology, 12*(9), 1614-1625.

CHAPTER 2

Literature Review

Complexation between protein and phenolic compounds and the application of the adducts and complex coacervates as emulsifiers and encapsulants

Complexation between protein and phenolic compounds and the application of the adducts and complex coacervates as emulsifiers and encapsulants

Abstract

The science of covalent conjugation between plant protein and phenolic compounds has received increasing interest due to the potential of adducts as emulsifiers and encapsulants. A sound understanding of science of complex coacervation between phenolic-adducted protein with polysaccharide gum is also important as they also have great potential as emulsifiers and encapsulating shell materials of unstable, yet nutritionally important polyunsaturated fatty acids (PUFAs).The complexing interaction between polyphenol, protein and gum and the physicochemical and functional properties of resulting adducts and complex coacervates are expected to depend on the characteristics of the interacting proteins, phenolic compounds and gums. Thus, this chapter reviews the recent advance in science of complexation (primarily covalent one) between plant proteins and phenolic compounds under alkaline condition including the mechanism involved and the effect of conjugation on the physicochemical and functional properties of protein-phenolic adducts. The nature of complex coacervation between the phenolic-adducted protein and plant gums and the efficacy of the resulting complex coacervates on emulsification and encapsulation of PUFA-rich oils have also been reviewed. This chapter also reviews the literature on the release and digestion of PUFA-rich oils encapsulated in protein-phenolic adducts and their complex coacervates. Oil seed, particularly flaxseed, is chosen as the model plant source for protein, polyphenols, oil, and gum. Hydroxytyrosol is chosen as a typical plant-based phenolic alcohol, and their relevant physicochemical properties are also reviewed.

Keywords: Flaxseed protein, phenolic compounds, gum, covalent conjugation, complex coacervation, hydroxytyrosol

2.1 Introduction

Covalent interaction between proteins and phenolic compounds has attracted increasing research as the resulting complexes or adducts can be used in food industry as emulsifiers and microencapsulating shell materials of sensitive compounds such as omega-3 rich oils. The covalent conjugation or adduction between protein and phenolic compounds has shown to significantly improve emulsifying and foaming properties (Sui et al., 2018), cream stability (Tao et al., 2018), antioxidative capacity (Liu, Sun, Yang, Yuan, & Gao, 2015), and thermal stability (Liu, Ma, McClements, & Gao, 2017) of various food products. For these reasons, the interaction between various phenolic compounds including phenolics (phenolic acids, flavonoids) (Sęczyk, Świeca, Kapusta, & Gawlik-Dziki, 2019) and polyphenols extracted from plants (Rawel, Czajka, Rohn, & Kroll, 2002a) and various proteins such as glycinin, trypsin inhibitor (Rawel et al., 2002a), myoglobin (Kroll, Rawel, & Seidelmann, 2000), gelatin (Strauss & Gibson, 2004) and whey protein (Rawel, Kroll, & Hohl, 2001a) have been studied.

There is an increasing trend of using plant proteins for food application (Sui et al., 2018; Tao et al., 2018) due to healthy and eco-friendly perception of plant proteins (Nesterenko, Alric, Silvestre, & Durrieu, 2013), and increasing vegetarian and vegan dietary practices from various reasons (Karaca, Low, & Nickerson, 2015). However, it is still dearth of research on the covalent conjugation between plant proteins with polyphenols extracted from oilseeds and phenolic alcohol such as hydroxytyrosol. This is gap in knowledge is clearly felt as currently there is lack of research on the application of these adducts as encapsulants and emulsifiers. The polyphenols from oil seeds known for their antioxidant (Alu'datt et al., 2016), anti-inflammatory, and anti-mutagenic properties (Khattab, Eskin, & Thiyam-Hollander, 2014). Hydroxytyrosol and similar phenolic alcohols are found abundantly in olive oil possessing. These phenolic alcohols possess strong antioxidative activity and provide many health benefits, including reducing systolic blood pressure (Covas, de la Torre, & Fitó, 2015), enhancing endothelial function (Valls et al., 2015), and alleviating inflammation (Lopez et al., 2017). Generally, the covalent interaction/conjugation between proteins and phenolic compounds can be induced by using free radical mediated grafting, enzymatic catalysis, and alkali-facilitated reaction (Prigent, Voragen, Visser, van Koningsveld, & Gruppen, 2007). Out of these, the free radical mediated grafting method is not preferred in food application due to the involvement of toxic chemical (H_2O_2) while the enzymatic method is found to be very limited (Ali, Homann, Khalil, Kruse, & Rawel, 2013; Liu et al., 2019). The covalent conjugation of phenolic compounds and proteins in alkaline condition is reported to be simple and efficient to synthesize protein-phenolic adducts (Liu et al., 2019).

It is well established that proteins have the ability to stabilise emulsions by adsorbing at the oil-water interface (Dickinson, 2010). It appears that the interaction of proteins with certain phenolic compounds can improve their emulsifying property. Thus, reports on the effect of covalent interaction of protein with phenolic compounds on the stability of oil-water emulsions are being published (Sui et al., 2018; Tao et al., 2018; Xu et al., 2019). Given the emulsifying property of proteins affects the their oil encapsulating efficacy (Di Giorgio, Salgado, & Mauri, 2019; Karaca, Nickerson, & Low, 2013; Shi, Beamer, Yang, & Jaczynski, 2018), few studies have undertaken to evaluate the effect of covalent conjugation between protein and phenolic compound on the efficacy of oil encapsulation and the bioavailability of encapsulated oil. Many microencapsulation methods have been developed to stabilise susceptible oils such as spray and freeze-drying of emulsions, fluidised bed drying, extrusion, and complex coacervation followed by spray drying (Kaushik, Dowling, Barrow, and Adhikari (2015b); the latter is regarded as one of the most effective techniques for microencapsulation of omega-3 rich-oils due to high oil loading and low surface oil content (Wang, Adhikari, & Barrow, 2019). To date, a wide range of complex coacervates has been used as wall materials for the microencapsulation of polyunsaturated fatty acids (PUFAs) rich-oils, among which whey protein and gelatin based complex coacervates are the most popular (Eratte, Dowling, Barrow, & Adhikari, 2018). Thus, with the increasing tendency of usage of plant-based food materials, the application of protein-phenolic conjugates derived from plant proteins as encapsulating shell materials will be healthy and sustainable option of producing microcapsules of sensitive and high value food compounds.

In this context, this chapter presents an overview the mechanisms through which proteins, especially those from oilseeds, interact with polyphenols. The interaction/conjugation occurring in alkaline condition will be reviewed in greater detail. Proteins and polyphenols extracted from flaxseed will be used as a model protein, polyphenols, polysaccharide gum. Flaxseed oil, which is rich in alpha-linolenic acid (omega-3) acid will also be used as the model oil. The nature of phenolic alcohols, particularly that of hydroxytyrosol, will be reviewed with respect to their antioxidative and ability to conjugate with plant proteins.

Thus, this chapter is organized in 9 sections. Section 1 provides the background information; section 2 presents the mechanism of interaction between proteins and phenolic compounds with greater focus on covalent interaction/conjugation under alkaline condition; section 3 covers the effects of covalent interaction on the physicochemical and functional properties (interfacial and emulsifying properties) of proteins; section 4 reviews the stabilisation of PUFAs-rich oils using protein/gum complex coacervates as wall material; section 5 presents the overview of microencapsulation of omega-3 rich oils using plant protein based complex coacervates; section 6

provides *in-vitro* digestion of oil microcapsules with greater focus on those produced using complex coacervates as shell material; section 7 and 8 provide the composition, physicochemical and functional properties of flaxseed and hydroxytyrosol, respectively; section 9 underscores the current research gaps and recommends for future research.

Scope and exclusion: The literature on the interaction between protein and phenolic compounds including the covalent conjugation is so large, thus this review only covers the interaction/conjugation occurring under the alkaline condition. In addition, although encapsulation of oil is carried out using various techniques, this review only covers the literature on microencapsulation carried out using protein/gum complex coacervation technique with more focus on complex coacervates produced using plant proteins.

2.2 The mechanism of covalent conjugation between proteins and phenolic compounds

It is known that the covalent conjugation/adduction between a phenolic compound and a protein under alkaline condition and oxygen exposure with the formation of quinone or semiquinone radical intermediates depending on the chemical structure of the phenolic compound. The former are formed from polyphenols with a catechol structure such as gallic acid, caffeic acid, myricetin, and quercetin (Rawel et al., 2002a; Strauss & Gibson, 2004). The latter are formed from monophenols such as ferulic, sinapic, and p-coumaric acids (Cilliers & Singleton, 1991; Rawel, Kroll, & Rohn, 2001b). Subsequently, these quinone or semiquinone radical intermediates react and/or cross-link with the side-chain nucleophiles of proteins (Figure 1). The interaction between flavonoid compounds with proteins takes place depending on the position of hydroxyl groups on their aromatic ring B and C (Rawel, Ranters, Rohn, & Kroll, 2004). The ortho-hydroxyl groups on ring B of flavonoids readily undergo covalent conjugation with proteins while hydroxyl groups on ring A of flavonoids were less reactive. Rawel, Rohn, and Kroll (2003) also found that quercetin has stronger affinity to conjugate with whey protein than rutin due to the presence of rhamnosylglucoside at 3-O position on the latter. However, fewer attempts are made to study the nature of the covalent interaction between plant protein with plant phenolic compounds derived from oil seeds and with phenolic alcohols such as hydroxytyrosol.

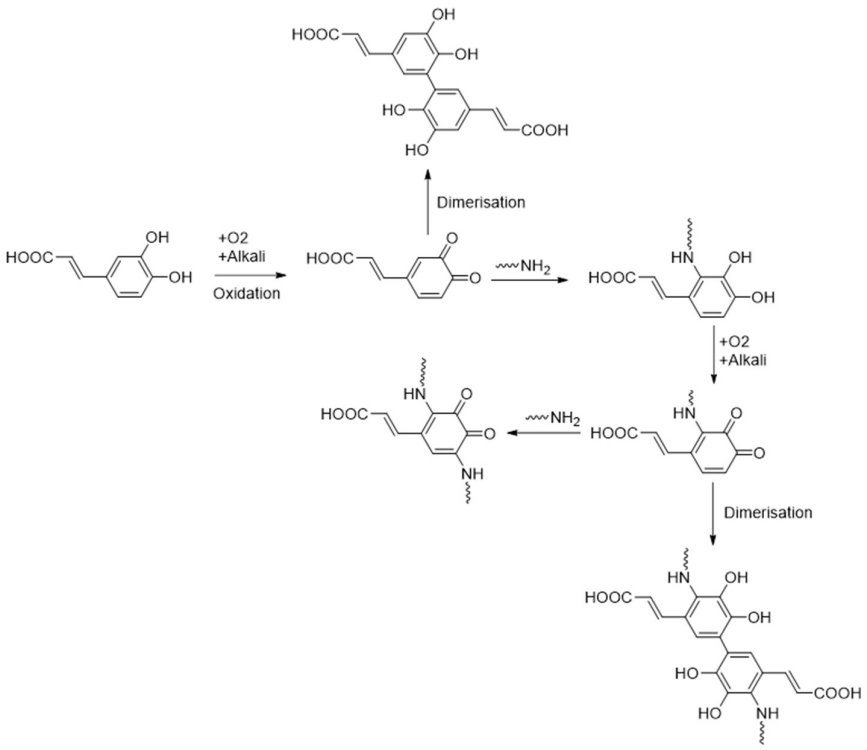

Figure 1. Mechanism of formation of conjugates/adducts between protein-phenolic acids under alkaline condition (Strauss & Gibson, 2004).

2.3 The effects of covalent conjugation of proteins with phenolic compounds on their physicochemical properties

The covalent conjugation between proteins and phenolic compounds affects the physicochemical properties of interacted proteins. The protein-phenolic conjugation typically affects the free amino and thiol groups and tryptophan contents, solubility, hydrophobicity, molecular weight, conformational structure, antioxidant activity, thermal stability, emulsion stability, and foaming capacity (Table 1). Many excellent reviews have covered these aspects in considerable detail (Keppler, Schwarz, & van der Goot, 2020; Liu et al., 2019; Quan, Benjakul, Sae-leaw, Balange, & Maqsood, 2019). Thus, this review focusses on reviewing and evaluating the effect of the covalent conjugation on the interfacial and emulsifying properties of proteins as these properties affect the emulsifying, oil microencapsulating and the digestion behaviour of the produced microcapsules.

Table 1: Effect of covalent conjugation between protein and phenolic compounds on the typical physicochemical properties of proteins.

Protein	Phenolic compounds	Effects on physicochemical properties	References
Animal-based proteins			
Whey protein isolate	Coffee, tea, potato, pear extract	↓ Free amino groups, tryptophan content, ↑ molecular weight, ↓ digestibility	Rawel et al. (2001a)
Whey protein isolate	Rosmarinic acid	↓ Free amino, thiol groups and tryptophan content, ↑ antioxidant capacity	Ali (2019)
Whey protein isolate	EGCG	↑ Molecular weight, cross-linking, ↑ foam and emulsion stability	Jia et al. (2016)
Myoglobin	O, p-hydroxyphenols, p-quinone, gallic acid, ferulic acid	↓ Free amino groups, ↑ hydrophobicity, ↓ solubility	Kroll and Rawel (2001)
Myoglobin	Chlorogenic acid, caffeic acid, p-quinone	↓ Solubility, ↑ molecular weight, ↓ digestibility	Kroll et al. (2000)
Lactoferrin	Chlorogenic acid	↑ Molecular weight, ↑ emulsion stability, cross-linking	Liu, Wang, Sun, McClements, and Gao (2016b)
BSA	Chlorogenic acid	↓ α-helix, ↑ β-strand, ↑ β-turn, ↓ hydrophobicity, ↓ digestibility	Rawel, Rohn, Kruse, and Kroll (2002b)
α-lactalbumin	EGCG	↑ Thermal stability, ↑ antioxidant activity, ↑ emulsion stability	Wang et al. (2014b)
Milk proteins	EGCG	↓ Free amino groups and sulfhydryl, ↓ solubility, ↑ thermal stability, ↑antioxidant activity, ↑emulsion stability	Wei, Yang, Fan, Yuan, and Gao (2015)
β-lactoglobulin	EGCG	↑ Molecular weight, cross-linking, ↑ antioxidant activity, ↑ emulsion stability	Tao et al. (2019)
β-lactoglobulin	5-Caffeoylquinic acid	↑ Hydrophobicity, ↑ thermal stability, ↑ antioxidant activity	Ali et al. (2013)
β-lactoglobulin	Allyl isothiocyanate	↓ Emulsion stability, ↑ foam stability	Rade-Kukic, Schmitt, and Rawel (2011)

β-Lactoglobulin	Caffeic acid	↑ β-sheets, ↓ coil, ↑ antioxidative capacity, ↑ thermal stability, ↑solubility, ↑ antioxidant activity	Abd El-Maksoud et al. (2018)
Ovotransferrin	Catechin	↑ Molecular weight, ↑ antioxidant activity	You, Luo, and Wu (2014)
Plant-based proteins			
Zein	EGCG	↓ α-helix, ↑ β-turn, ↑ thermal stability, ↑ antioxidant activity	Liu et al. (2017)
Soy glycinin	Myricetin, quercetin, chlorogenic and caffeic acid	↓ α-helix, ↑ β-strand, ↑ β-turn, ↑ thermal stability	Rawel et al. (2002a)
Soy protein isolate	Anthocyanins	↓ β-sheets, ↑ β-turns and coils, ↑ molecular weight, ↑ emulsion and foam stability, cross-linking	Sui et al. (2018)
Soy protein isolate	EGCG	↓ α-helix, ↑ β-sheet, ↑ molecular weight, ↑ emulsion stability, cross-linking	Tao et al. (2018)
Soy protein isolate	Anthocyanins	↓ α-helix and β-sheet, ↑digestibility	Jiang et al. (2019)
Pumpkin seed protein isolate	Pyrogallic acid	↑ Molecular weight, ↑ thermal stability, ↑ antioxidant activity, cross-linking	Yang, Wang, Wang, Xia, and Wu (2019)

2.3.1 Effect of covalent conjugation of protein with phenolic compounds on the free amino and thiol groups and tryptophan content

It has been reported that the number of free amino, thiol groups and tryptophan residuals of soy glycinin was reduced when it conjugated with phenolic compounds. Also, the extent of the decrease depends on the structure of participating phenolic compounds such as chlorogenic and caffeic acid (C_6-C_3 structure); gallic acid (C_6-C_1 structure); flavonoids, flavone, apigenin, kaempferol, quercetin and myricetin (C_6-C_3-C_6 structure) (Rawel et al., 2002a). The mechanism of this conjugation is elaborated by Strauss and Gibson (2004) in sufficient detail. Briefly, phenolic compounds are oxidised into ortho-quinone under the alkaline condition (pH 9.0) and in the presence of oxygen. The ortho-quinone then reacts with the nucleophile side chains of protein to form C-N (lysine, tryptophan) and C-S (cysteine) linkages (Figure 1). The conjugation of polyphenols from coffee and tea with whey protein was shown to bring about a sharp decrease in the number of free amino groups and tryptophan content in the adducts (Rawel et al., 2001a). The position of hydroxyl groups on phenolic compounds such as ortho-, para-, and meta-

hydroxyphenols was shown to affect their reactivity with myoglobin (Kroll & Rawel, 2001). It is shown that the ortho and para position on the hydroxyphenol possesses higher reactivity than meta position, leading to a greater reduction in the level of free amino groups in the conjugates (Kroll & Rawel, 2001). Rosmarinus acid has also found to have high degree of reactivity with whey protein isolate (WPI) reflected by the sharp reduction of free amino and thiol groups and tryptophan content (Ali, 2019).

2.3.2 Effect of covalent conjugation of protein with phenolic compounds on their molecular weight

The apparent change in molecular weight of protein due to conjugation with phenolic compounds can be quantified using various methods including sodium dodecyl sulfate-polyacrylamide gel electrophoresis (SDS-PAGE) (Jia et al., 2016; Liu et al., 2015; Rawel et al., 2002a) and the matrix-assisted laser desorption/ionization time of flight mass spectrometry (MALDI-TOF-MS) (Ali et al., 2013; Ishii et al., 2008; Kroll & Rawel, 2001). The protein adducted with phenolic compound shows increase in high molecular weight fraction and decrease in low molecular weight fraction in the SDS-PAGE electrophoresis (Figure 2A). However, the extent of change in molecular weight of the conjugated protein depends on the structure and molecular weight of the conjugated phenolic compound. A more detailed information on the change in molecular weight can be observed by their MALDI-TOF-MS chromatograms (Figure 2B), which reveal the appearance of new peaks (mass-to-charge ratio=m/z) corresponding to higher molecular weight fragments. Tandem mass spectrometry (MS/MS) analysis is used to determine the components of new peaks including the m/z of bound phenolic compounds (Abd El-Maksoud et al., 2018; Ishii et al., 2008; You et al., 2014). SDS-PAGE is also used to examine the degree of polyphenol-induced cross-linking of proteins. For example, Jia et al. (2016) used SDS-PAGE to determine EGCG induced cross-linking of WPI (Figure 2A). Similarly, Rawel et al. (2002b) showed the cross-linking of bovine serum albumin (BSA) when it was conjugated with chlorogenic acid under alkaline condition. Cross-linking was also observed in gelatine and lysozyme when crosslinked with various polyphenols including chlorogenic acid (Rawel, Kroll, & Riese, 2000; Strauss & Gibson, 2004). Anthocyanins and pyrogallic acid have recently been found to act as cross-linkers when they were conjugated with soy protein and pumpkin seed protein isolate, respectively under alkaline condition (Sui et al., 2018; Yang et al., 2019).

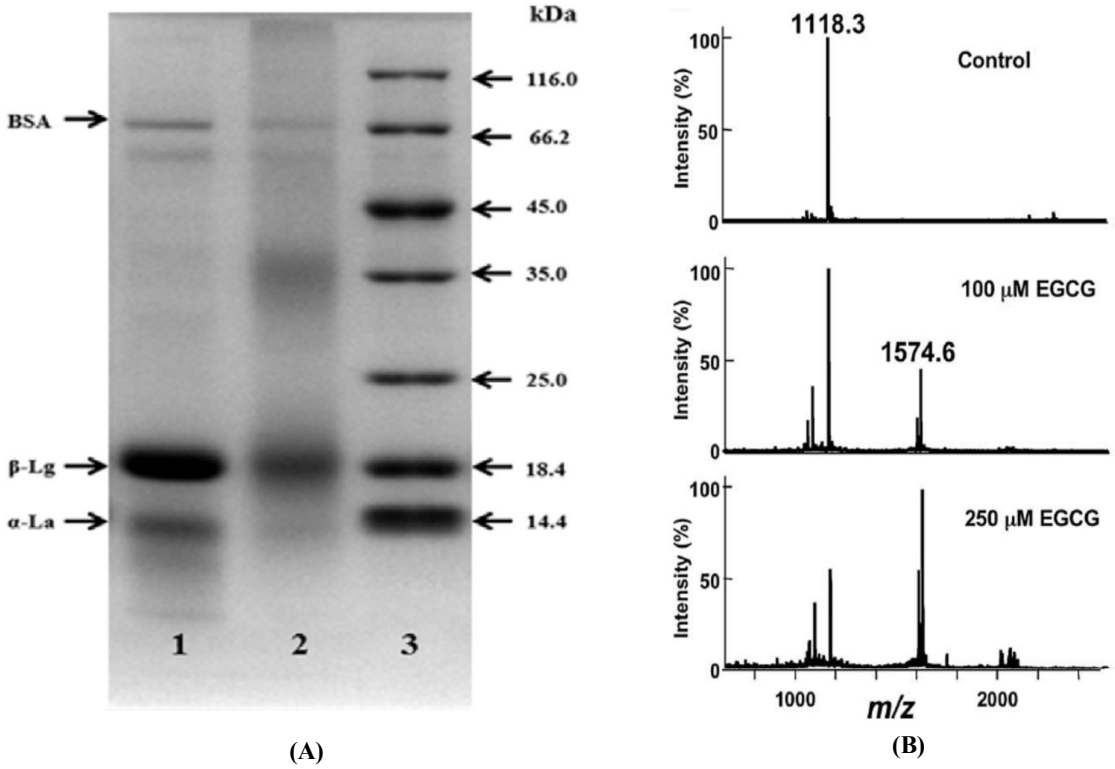

Figure 2. (A) Typical SDS-PAGE patterns of unmodified and EGCG conjugated WPI where crosslinking had occurred (Jia et al. (2016)). (B) MALDI-TOF-MS chromatogram of Calmodulin-dependent protein kinase II 281–289 (CaMKII) conjugated with EGCG (100, 250μM) (Ishii et al., 2008)

2.3.3 Effect of covalent conjugation of phenolic compounds on structural conformation of proteins

The conformational structure of intact (unmodified) and modified proteins is commonly determined by using many methods including Fourier-transform infrared spectroscopy (FTIR) and circular dichroism (CD). The secondary structure (α-helix, β-sheet, β-turn, and random coil) of proteins can change due to conjugation with phenolic compounds and this change can be qualitatively or quantitatively determined (Liu et al., 2017; Liu et al., 2015; Rawel et al., 2002a; Rawel et al., 2002b). The change in secondary structure of protein due to conjugation with phenolic compound also depends on the nature of the conjugated phenolic compounds. For instance, Rawel et al. (2002a) found an increase in α-helix when adduction between soy glycinin and caffeic and gallic acid occurred; while Liu et al. (2017) observed a decrease in α-helix and an increase in β-turn when zein protein and quercetagetin were conjugated. In another study, Tao et al. (2018) reported that the α-helix fraction decreased with a simultaneous increase in β-sheet structure of soy protein isolate (SPI) when it formed conjugates with EGCG. It was also reported that a decrease in α-helix, with a parallel increase in β-strand and turn of soy glycinin when it formed

conjugates with myricetin (Rawel et al., 2002a). Conversely, the conjugation of chlorogenic acid with BSA resulted in a reduction in α-helix with a parallel increase in the other secondary structures (Rawel et al., 2002b). Similarly, clear alteration of secondary structure was observed in various milk proteins when they were conjugated with EGCG (Wei et al., 2015).

2.3.4 Effect of covalent conjugation of phenolic compounds on the solubility and hydrophobicity of proteins

Solubility is important for using proteins as ingredient as it affects their emulsifying, foaming and encapsulating properties. The extent to which the solubility and hydrophobicity of proteins is affected due to conjugation with phenols depends on the structure and reactivity of the polyphenol involved. Rawel et al. (2002a) reported that the solubility of soy glycinin increased after covalent conjugation with quercetin. The increase in solubility depends on the chemical structure and physical conformation of the adducts produced. For example, the hydrophobic residues of proteins containing tryptophan can be blocked when they react with phenols and new hydrophilic groups (e.g., hydroxyl groups from phenols) are introduced to the protein chain (Rawel et al., 2002a). In contrast, Kroll and Rawel (2001) showed that solubility of polyphenol conjugated myoglobin decreased due to bonding of hydrophilic amino and thiol groups with phenolic compounds and/or introduction of non-polar groups by the adducted polyphenols. In this regard, Kroll et al. (2000) also reported that the solubility of myoglobin was decreased when it was conjugated with chlorogenic and caffeic acids and p-quinone.

It is reported that there is a reasonable correlation between hydrophobicity and insolubility as observed in milk and soy proteins (Hayakawa & Nakai, 1985). This phenomenon is also revealed in the case of gallic acid-modified myoglobin. The hydrophobicity of myoglobin was found to increase while its solubility decreased after its complexation with gallic acid (Kroll & Rawel, 2001). In contrast, the covalent conjugation of BSA with chlorogenic acid was observed to decrease its surface hydrophobicity (Rawel et al., 2002b). β-lactoglobulin when adducted with 5-caffeoylquinic acid also showed higher surface hydrophobicity in acidic pH compared to the native β-lactoglobulin (Ali et al., 2013). In other words, the solubility of these two adducts increased in the tested pH range.

2.3.5 Effect of covalent conjugation with phenolic compounds on the thermal stability of proteins

Proteins adducted with phenolic compounds tend to be more thermally stable than the unadducted ones. For instance, the thermal stability of soy glycinin was found to improve after conjugation with phenolic acids (e.g. chlorogenic and caffeic acid) and flavonoids (e.g. quercetin and

myricetin) (Rawel et al., 2002a). This increased thermal stability is reflected by the increase in the denaturation temperature and the denaturation enthalpy. In this context, Ali et al. (2013) found that the conjugation of lactoglobulin with caffeoylquinic acid increased its denaturation temperature yet less energy was required for unfold. Liu et al. (2017) reported that zein-EGCG conjugate had higher thermal stability than the unmodified zein as reflected in the increased denaturation temperature. The denaturation of lactoferrin was improved after conjugation with chlorogenic acid (CA) and EGCG due to the formation of irreversible aggregation resulting from the increase in the α-helix structure of lactoferrin (Liu, Wang, Ma, & Gao, 2016a). Similarly, the thermal stability of pumpkin seed protein isolate-pyrogallic acid conjugate was higher than that of native one (Yang et al., 2019).

2.3.6 Effect of covalent conjugation with phenolic compounds on the antioxidative property of proteins

Higher antioxidant capacity of phenolic compound conjugated proteins is one of their most desired functional properties. Most reviews in this theme suggest that antioxidant activity of proteins increases when they undergo covalent conjugation with phenolic compounds (Liu et al. (2019); Quan et al. (2019). It is commonly reported that the antioxidant activity of proteins is improved after covalent conjugation with phenolic compounds. The antioxidant activity of these conjugates is determined using DPPH (2,2-diphenyl-1-picrylhydrazyl) and ABTS (2,2′-Azino-bis(3-ethylbenzothiazoline-6-sulfonic acid)) scavenging activity and other reducing power tests. The extent of increase in antioxidant capacity of proteins after covalent conjugation with phenolic compounds depends on the nature (chemical structure) of the phenolics involved. For example, the EGCG-α-lactalbumin derivative had significantly higher antioxidative activity than the unmodified α-lactalbumin (Wang et al., 2014b). Similar improvement in antioxidative activity was observed in 5-caffeoylquinic acid-β-lactoglobulin, EGCG-lactoferrin, quercetagetin-zein conjugates (Ali et al., 2013; Liu et al., 2017).

2.3.7 Effect of covalent conjugation of proteins with phenolic compounds on their interfacial/emulsifying properties

The emulsifying activity of proteins depends on their ability to diffuse through the aqueous medium and adsorb at the oil/water interface (Amine, Dreher, Helgason, & Tadros, 2014). Since emulsions are inherently unstable due to the immiscible nature of continuous and dispersed phases, the interfacial tension at the oil/water interface has to be minimized to improve emulsion stability.

2.3.7.1 Effect of conjugation with phenolic compounds on the interfacial behaviour of proteins

Interfacial behaviour of proteins at oil/water interface is usually associated with their ability to adsorb at and occupy the oil/water interface. The extent of adsorption of proteins is commonly measured using interfacial tension (DIT), explained using adsorption kinetics and correlated to emulsifying capacity.

The interfacial rheology of the absorbed protein layer provides information on the behaviour of protein molecules at the interface. These interactions could be hydrophobic and/or van der Waals, both of which affect the stability of the emulsion. For example, the interfacial (dilatational) elasticity is inversely proportional to the coalescence (Tadros, 2013). Proteins, are inherently amphiphilic, which enables them to adsorb at the oil/water interface. The adsorption of a protein at the oil/water interface results into a decrease in the DIT over time, which itself is driven by its concentration gradient (Wang et al., 2012). The adsorption kinetics of protein at the oil/water interface can show three distinct stages (Graham & Phillips, 1979): (1) Diffusion of protein from the bulk to the layer adjacent to the interface; (2) adsorption of protein molecules to the interface, and (3) reorganisation. The native as well as (thermally and enzymatically) modified plant proteins including soy, lentil, pea, sunflower, and pumpkin are shown to exhibit the similar adsorption behaviour (Amine et al., 2014; Bučko et al., 2018; Ducel, Richard, Popineau, & Boury, 2004; Jarpa-Parra et al., 2015; Karefyllakis, Altunkaya, Berton-Carabin, van der Goot, & Nikiforidis, 2017). Studies aimed at determining the effect of protein-phenolic complexation on the interfacial properties of proteins have been undertaken; however, most of these studies have used non-covalent complexes (Karefyllakis et al., 2017; Rodríguez, von Staszewski, & Pilosof, 2015; von Staszewski, Pizones Ruiz-Henestrosa, & Pilosof, 2014). There is no information in the literature on the interfacial behaviour (diffusion, absorption and realignment) of plant protein-phenolic covalent conjugates at oil/water interface.

In the case of diffusion-controlled adsorption, the extent of diffusion of proteins to interface depends on the initial protein concentration, pH, and temperature. In order to determine the diffusion coefficient, a modified form of Ward and Tordai (1946), equation (1) is commonly used.

$$\pi = 2C_0KT\left(\frac{Dt}{3.142}\right)^{1/2} \qquad \text{(eq.1)}$$

where, $\pi = (\gamma - \gamma_0)$ is the interfacial pressure (mN m^{-1}), C_0 is the concentration of protein in the bulk phase (mol. m^{-3}), K is the Boltzamann constant (m^2 kg s^{-2} K^{-1}), T is the absolute temperature (K), D is diffusion coefficient (m^2 s^{-1}), and t is adsorption time (s), γ and γ_0 are the interfacial tension of solution and water at the oil-water interface respectively.

It was reported that the chlorogenic acid-sunflower protein non-covalent complex sowed higher surface pressure than the native sunflower protein at the oil/water interface (Karefyllakis et al., 2017). This increased surface pressure was attributed to the formation of hydrogen bonds between adjacent phenols bound to the protein molecules, which caused increased unfolding. This unfolding increased the intermolecular interaction between the adsorbed proteins leading to increased occupation of interface. In contrast, green tea polyphenols-β-lactoglobulin and other whey proteins' complexes showed a decrease in surface pressure as compared to the uncomplexed or free β-lactoglobulin and other whey proteins at the oil/water interface (von Staszewski et al., 2014). This behaviour was attributed to the unavailability of hydrophobic domains to migrate to the interface caused by the grafting of green tea polyphenols to the hydrophobic side chain of amino acids (Sausse, Aguié-Béghin, & Douillard, 2003).

The dilatational modulus (*E*) can be calculated based on the change in interfacial tension (γ) as a function of change in the oil-water interfacial area (*A*) as given by equation (2) (Ravera, Loglio, & Kovalchuk, 2010).

$$E = \frac{d\gamma}{dA/A} \qquad \text{(eq. 2)}$$

The dilatational modulus is a complex quantity comprised of real and imaginary parts represented by the dilatational elasticity (E′) and viscosity (E′′). E′ and E′′ (mN m^{-1}) are calculated by the Fourier transformation using equations (3) and (4), respectively (Cascão Pereira, Theodoly, Blanch, & Radke, 2003):

$$E' = \Delta\gamma \frac{A_0}{\Delta A} cos\emptyset \qquad \text{(eq. 3)}$$

$$E'' = \Delta\gamma \frac{A_0}{\Delta A} sin\emptyset \qquad \text{(eq. 4)}$$

where, ΔA (mm^2) and Δγ (mN m^{-1}) are the amplitude of change in the interfacial area and interfacial tension, respectively. ∅ is the phase shift between the sinusoidal perturbation of the interfacial tension and that of the interfacial area.

Karefyllakis et al. (2017) found that the interfacial layer of chlorogenic acid-sunflower protein complex showed greater elastic behaviour than that of native sunflower protein. Conversely, Rodríguez et al. (2015) and von Staszewski et al. (2014) reported that the dilatational property of the adsorbed complex layer decreased when compared with that of the native one.

2.3.7.2 Effect of conjugation of phenolic compounds with proteins on the emulsifying properties

The covalent conjugation between proteins and polyphenols can improve the stability of protein based-colloid systems and protein stabilised emulsions. For example, the stability of emulsion produced using caffeic-lactoferrin covalent conjugate as emulsifier was higher than that of native lactoferrin stabilized emulsion (Liu et al., 2015). Similarly, the improved stability was observed in emulsions stabilised by 5-Caffeoylquinic acid-milk whey protein, EGCG-α-lactalbumin, EGCG-WPI, EGCG-lactoferrin conjugates compared to those stabilised by the corresponding native proteins (Jia et al., 2016; Liu et al., 2016b; Rawel et al., 2002a; Wang et al., 2014b). Jia et al. (2016) and Wang et al. (2014b) reported that the emulsions stabilized EGCG-α-lactalbumin and EGCG-lactoferrin conjugates had smaller particle size than those stabilized by the corresponding native proteins. Conversely, the emulsion stabilised by β-lactoglobulin-allyl isothiocyanate conjugate was less stable than the one stabilized by β-lactoglobulin (Rade-Kukic et al., 2011). In addition, Liu et al. (2016b) noted that the emulsions stabilised by using EGCG-lactoferrin, and chlorogenic acid-lactoferrin conjugates had higher oxidative stability in comparison to the emulsions stabilised lactoferrin. von Staszewski et al. (2014) also reported that the oxidative stability of fish oil stabilised using β-lactoglobulin-green tea polyphenol complex was higher than that of oil stabilised by β-lactoglobulin. In general, most of the studies agreed on the positive effect of protein-phenolic conjugation on emulsion stability (Table 1); however, Rade-Kukic et al. (2011) reported that the emusion stabilised by the conjugates formed between β-lactoglobulin and allyl isothiocyanate had significantly poor emuslion stability than the one stabilised by β-lactoglobulin.

2.4 Stabilisation of polyunsaturated fatty acids (PUFAs) rich oils using protein/gum complex coacervates as wall material

Polyunsaturated fatty acids (PUFAs) such as omega-3(n-3) and omega-6(n-6) are nutritionally important (Abuajah et al., 2015). PUFAs reduce the risk of cardiovascular disease (Steffens, 1997), improve mental and visual functions (Li & Hu, 2009). They also reduce the risk of diabetes (Connor et al., 1993), arthritis (Kremer, 1996), autoimmune disorders (Calder, 2006) and colon cancer (Roynette, Calder, Dupertuis, & Pichard, 2004). Human body cannot synthesize PUFAs; thus, they have to be delivered, preferably as part of the diet. PUFAs are susceptible to suboptimal processing and storage stressors such as elevated temperature, oxygen, and light. The exposure of PUFAs with these factors results in an undesirable change in sensory (flavour and colour) and nutritional values (Comunian & Favaro-Trindade, 2016). This is because PUFAs readily undergo oxidation and produce harmful reaction products (Tao, 2015). The nutritional and functional values

of PUFAs can be enhanced if oxidation can be avoided or minimised (Alamed, McClements, & Decker, 2006).

In order to protect PUFAs from oxidation and to prolong their shelf-life, various protection methods including microencapsulation are implemented (Betoret, Betoret, Vidal, & Fito, 2011). Among these methods, microencapsulation is preferred as it readily covers the oil droplets and the technologies to carry it out are well developed (Betoret et al., 2011; Sanguansri & Augustin, 2016). Microencapsulation technology creates a matrix structure surrounding the PUFAs and offers a barrier against oxidative deterioration. Microencapsulation also masks the characteristic fishy smell of PUFAs and also helps deliver the PUFAs in a small serving (Nesterenko et al., 2013). For doing this, the encapsulating shell material has to be stable against mechanical force and temperature to keep the entrapped oil within the core. Otherwise, the oil will easily leak out from the microcapsules. For this purpose, the shell surrounding the microencapsulated PUFAs is chemically (glutaraldehyde) or enzymatically (transglutaminase) crosslinked to strengthen the shell structure.

However, glutaraldehyde is not suitable for food application due to its toxic nature and transglutaminase comes with a high cost. The polyphenols, as natural crossing-linking agents, can be "healthy" cross-linkers due to their strong cross-linking ability with protein. As stated above, the covalent conjugation between proteins with phenolic compounds can enhance their structural stability as at the same time improving antioxidant capacity, and thermal and emulsion stability. Therefore, there is a potential of using phenolic-conjugated proteins as encapsulants of PUFAs.

Many methods that are currently used to microencapsulate PUFAs capsules were reviewed by Ruiz, Ortiz, and Segura (2017) including spray-dried emulsions, freeze-dried emulsions, fluidized bed drying, extrusion, and complex coacervation. Of these methods, spray drying is most commonly used to produce microcapsules of PUFA-rich oils due to its affordability, reproducibility, and high scalability (Encina, Vergara, Gimenez, Oyarzun-Ampuero, & Robert, 2016). Creation of shell using complex coacervation is more effective in producing oil microcapsules with high payload and encapsulation efficiency (Timilsena, Wang, Adhikari, & Adhikari, 2017b). Complex coacervation also has the advantage of having mild processing conditions (Gouin, 2004). Complex coacervation is carried out pH and polymer concentration ranges within which best possible electrostatic interaction occurs between the oppositely charged proteins and polysaccharides and leads to phase separation (Figure 3A). The complex coacervation process is also affected primarily by the electrostatic interaction and also to some extent by van der Walls forces, hydrophobic interactions, and hydrogen bonding (Turgeon, Schmitt, & Sanchez,

2007). Complex coacervation between two oppositely charged polymers is induced by changing the pH and ionic strength within certain temperature range. In food systems, proteins and polysaccharides are commonly used biopolymers used for complex coacervation (Schmitt & Turgeon, 2011). In order to encapsulate the oil using protein/gum complex coacervates, the oil is firstly emulsified with protein solution. Secondly, the gum solution is added to the emulsion followed by pH adjustment to produce protein/gum coacervate stabilised emulsions or liquid microcapsules. Finally, the complex coacervate shell is crosslinked using appropriate crosslinker (e.g. transglutaminase) to consolidate the liquid capsules before spray/freeze drying to obtain oil powder microcapsules (Figure 3B) (Wang, Adhikari, & Barrow, 2014a).

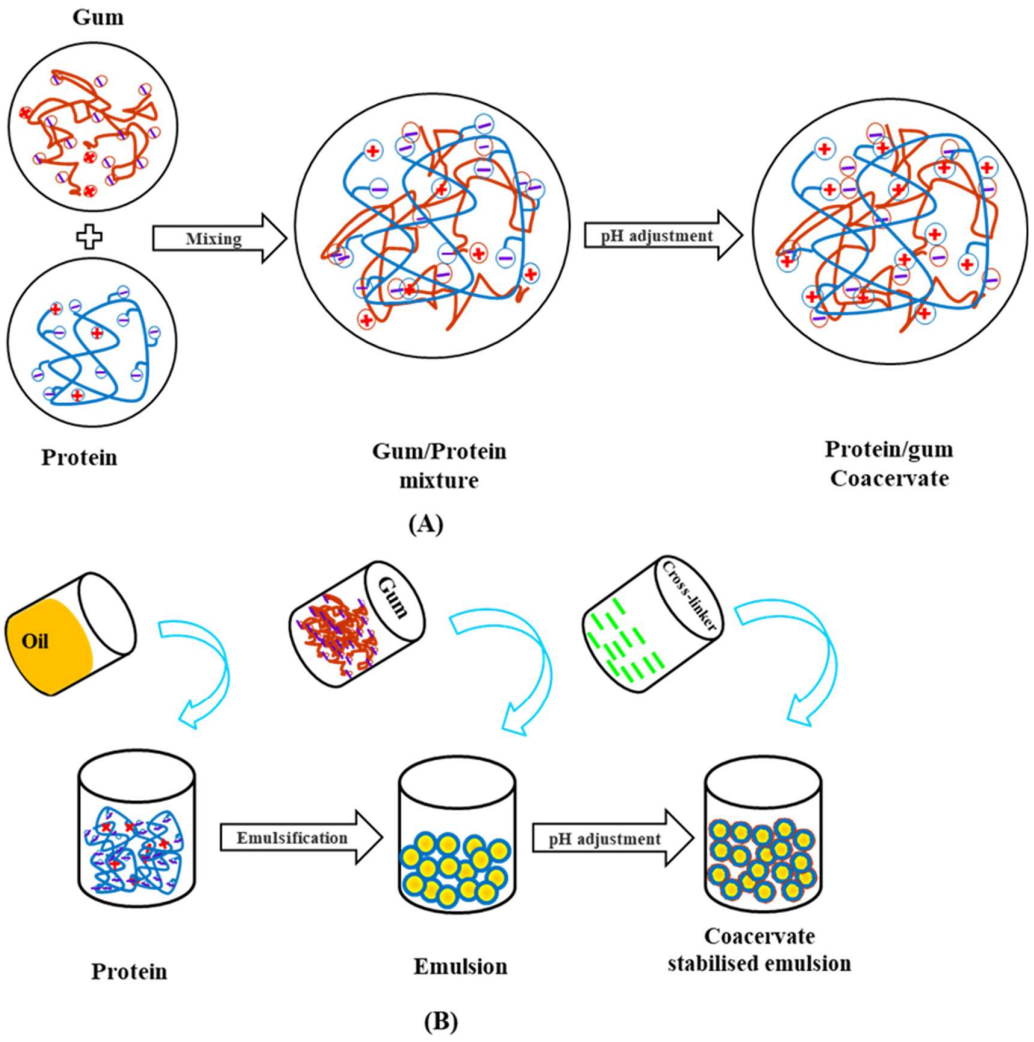

Figure 3. Schematic illustration of complex coacervation process between protein and polysaccharide gum with oil (B) and without oil (A).

2.5 Microencapsulation of PUFAs rich oil using plant based-wall materials

Recent developments on the microencapsulation of PUfFAs-rich oils using complex coacervation approach have been reviewed by Timilsena et al. (2017b) and Eratte et al. (2018). These reviews and the research cited there agree that physicochemical properties of encapsulated oil using complex coacervation is greatly affected by the core/wall ratio, drying methods in addition to the type of biopolymers used. These aspects of complex coacervation using plant-based biopolymers are summarised in Table 2. These data indicate that proteins and polysaccharide gums obtained from different sources required different conditions for complex coacervation and produce microcapsules with different surface oil content. It is reported that chia oil microcapsules produced using chia seed protein isolate (CPI)-chia seed gum (CG) achieved surface oil content of about 2% and higher encapsulation efficiency (94%) both of which were higher than in microcapsules produced using solely chia seed protein isolate (Timilsena, Adhikari, Barrow, & Adhikari, 2016). The optimum pH and CPI/CG ratio were found to be at 2.7 and 6.0, respectively. These values were 4.5 and 5.0 in the case of FPI-complex coacervates (Kaushik, Dowling, Barrow, & Adhikari, 2015a). The encapsulated oil produced using this FPI-FG complex coacervate had 2.8% surface oil and 87% encapsulation efficiency (Kaushik, Dowling, McKnight, Barrow, & Adhikari, 2016a). Jun-xia, Hai-yan, and Jian (2011) reported that the highest yield of complex coacervate using SPI and gum Arabic (GA) took place at pH of 4.0 and a SPI/GA ratio of 1.0.

Table 2: The optimum conditions for complex coacervation of various plant-based biopolymers and the surface oil content of corresponding microcapsules. SPI = Soy protein isolate, GA = Gum Arabic, CPI = Chia seed protein isolate, CG = Chia seed gum, FPI = Flaxseed protein isolate, FG = Flaxseed gum.

Protein (P)	Polysaccharides (Poly)	pH	P/Poly ratio	P+Poly/oil ratio	Surface oil (%)	Drying methods	References
SPI	GA	4.0	1:1	1:10	-	Freeze drying	Jun-xia et al. (2011)
SPI	GA	4.0	1.8:1	2.6:1	2.46	Spray drying	de Conto, Grosso, and Gonçalves (2013)
CPI	CG	2.7	6:1	2:1	2.1	Spray drying	Timilsena et al. (2016)
FPI	FG	3.1	3:1	2:1	2.78	Spray drying	Kaushik et al. (2016a)

Although various aspects of complex coacervation based-microencapsulation of PUFAs using plant proteins and gums has been studied, there is still a paucity of investigation on the efficacy of complex coacervates in which the protein component is covalently conjugated with phenolic

compounds. The incorporation of phenolic compounds in capsule shells was found to improve physicochemical properties of microcapsules in addition to improving their oxidative stability. For example, it was reported that the inclusion of sinapic acid in capsule walls improved the oxidative stability of encapsulated echium oil (Comunian et al., 2016). Muhoza, Xia, and Zhang (2019) also showed that the use of tannic acid as a cross-linker provided greater thermal stability of the oil encapsulated in gelatin-high methyl pectin coacervate. The improvements on some physicochemical and functional properties of microcapsules when phenolic compounds are incorporated in the wall matrix are presented in Table 3.

Table 3: The improvement of some physicochemical and functional of microcapsules when phenolic compounds were incorporated in the wall matrix. GA = Gum Arabic, HMP = High methyl pectin, FM = Flaxseed mucilage, XG = Xanthan gum, CC = Carboxymethyl chitosan.

Wall materials	Phenolic compounds	Improved properties	References
Gelatin/GA	Sinapic acid	Oxidative stability	Comunian et al. (2016)
Gelatin/HMP	Tannic acid	Oxidative and thermal stability	Muhoza et al. (2019)
Gelatin/FM	Tannic acid	Oxidative stability, low porosity	Mohseni and Goli (2019)
GA/XG	Pomegranate Juice	Oxidative stability, smooth surface structure	Yekdane and Goli (2019)
Zein/CC	Tea polyphenols	Antioxidant activities, colour stability	Ba et al. (2020)
Zein	Citric acid	Thermal and freeze-thaw stability	Teng et al. (2020)

2.6 *In-vitro* digestion of oil microcapsules produced using complex coacervates as shell material

A well-designed microencapsulation matrix facilitates the controlled-release oil in the digestion process to improve its bioavailability. As a rapid, cheap, convenient, and ethical method (Minekus et al., 2014), *in-vitro* digestion is commonly used to study the digestion behaviour of lipid at each stage of the gastrointestinal tract (Sarkar, Goh, Singh, & Singh, 2009; Sarkar, Horne, & Singh, 2010). In *in-vitro* digestion, food samples are subjected to simulated oral, gastric, and intestinal conditions, including electrolytes, enzymes, bile, and pH for a period of time. The composition of simulated fluids commonly used in the three different digestion stages is presented in Table 4 based on an international consensus (Minekus et al. (2014). Typical *in-vitro* static digestion experimental conditions at the oral, gastric and intestinal stages are described in Table 5.

Table 4: Composition of simulated digestion fluids: SSF = simulated salivary fluid, SGF = simulated gastric fluid (SGF), and SIF = simulated intestinal fluid. The final volume of each simulated fluid was made up to 500 mL with Milli-Q water (Minekus et al., 2014).

Constituent	Stock conc (M)	SSF (pH 7)		SGF (pH 3)		SIF (pH 7)	
		Volume of stock (mL)	Final conc (mM)	Volume of stock (mL)	Final conc (mM)	Volume of stock (mL)	Final conc (mM)
KCl	0.5	15.1	15.1	6.9	6.9	6.8	6.8
KH_2PO_4	0.5	3.7	3.7	0.9	0.9	0.8	0.8
$NaHCO_3$	1	6.8	13.6	12.5	25	42.5	85
NaCl	2			11.8	47.2	9.6	38.4
$MgCl_2(H_2O)_6$	0.15	0.5	0.15	0.4	0.12	1.1	0.33
$(NH_4)_2CO_3$	0.5	0.06	0.06	0.5	0.5		
NaOH	1						
HCl	6	0.09	1.1	1.3	15.6	0.7	8.4
$CaCl_2(H_2O)_2$	0.3	0.025	1.5	0.005	0.15	0.04	0.6

Table 5: Typical experimental condition in *in-vitro* static digestion. SF = simulated fluid (electrolytes), SSF = simulated salivary fluid, SGF = simulated gastric fluid (SGF), and SIF = simulated intestinal fluid. The final volume of each simulated fluid was made up to 500 mL with Milli-Q water (Minekus et al., 2014).

Components	Unit	Oral stage (SSF - pH 7)	Gastric stage (SGF - pH 3)	Intestinal stage (SIF - pH 7)
Sample	g or mL	5	10*	20**
SF	mL	3.5	7.5	11
Enzymes				
Salivary amylase (1.5KU mL^{-1})	mL	0.5		
Pepsin (25KU mL^{-1})	mL		1.6	
Pancreatin based on trypsin (0.8KU mL^{-1})	mL			5
$CaCl_2$ (0.3M)	mL	0.025	0.005	0.04
HCl (1M)	mL		0.2	
NaOH (1M)	mL			0.15
Fresh bile (0.16M)	mL			2.5
H_2O	mL	0.975	0.695	1.31

* Sample from the oral phase; ** Sample from the gastric phase

In-vitro digestion of oil microcapsules commonly includes the digestion of encapsulating wall and the subsequent release and lipolysis of encapsulated oil. It was been reported that the wall matrix had a strong influence on the digestion behaviour of encapsulated oils (Augustin et al., 2014). Thus, various wall materials have been investigated in order to develop effective oil delivery systems which can ensure the release and absorption of oil at the intestinal stage of digestion. Attempts have been made to modify proteins, when used as shell material, with other food ingredients such as polyphenols, polysaccharides to improve the stability, targeted release and bioavailability of hydrophobic core (Mohseni & Goli, 2019; Teng et al., 2020). According to Teng et al. (2020), the acid citric cross-linked zein capsule, when used as the wall material, was stable in gastric stage, and facilitated the delivery of β-carotene to intestinal stage, thus, improved its bioaccessibility. It has also been shown that the digestibility of proteins altered when they are conjugated with phenolic compounds. For example, the digestibility of BSA was slowed down when it was conjugated with chlorogenic acid (Rawel et al., 2002b). In contrast the digestibility of SPI increased when it was conjugated with black rice anthocyanins (Jiang et al., 2019).

The amount of released oil and free fatty acids (FFA) are commonly used as indicators of the extent of decomposition and the subsequent lipolysis of microcapsules (Timilsena et al., 2017). The rate and extent of lipolysis in the gastrointestinal tract were found to be strongly affected by the size, interfacial characteristics of the protein and the solid or liquid state of lipid (Augustin et al., 2014). Small microcapsules make it easy for the oils to be release and to be acted on by lipase due to their larger surface area and thinner membrane (Dong et al., 2011). Oil droplets can also be emulsified during lipid digestion which facilitates the migration of lipase to the oil droplets (Reis, Holmberg, Watzke, Leser, & Miller, 2009). The size of oil droplets also plays a critical role in lipolysis; for example, the smaller droplets are digested faster (Gallier & Singh, 2012). In the digestive system, 70-90% of the lipid in the food matrix gets digested in the small intestine by pancreatic lipases (Wickham, Wilde, & Fillery-Travis, 2002). The oil encapsulated in a double-layered complex coacervate system was shown to only partially release the oil during digestion due to interference of the polysaccharide component to the lipase (Mun, Decker, & McClements, 2007). Gumus, Decker, and McClements (2017) showed that proteins from lentil, pea, and faba, when used as wall materials, did not did not slow down the digestion of oil. Guimarães Drummond e Silva et al. (2017) demonstrated that the presence of phenolic compounds in flaxseed protein concentrate did not affect the hydrolytic action of pepsin and pancreatin. Conversely, it was shown that green tea polyphenols reduced the activity of digestive enzymes by as much as 54% (He, Lv, & Yao, 2007). Thus, if slow breakdown of protein shell is desired, their conjugation with phenolic compounds is expected to be a promising approach. This approach can be used

to customize/control the physiological digestion of lipids and thus help reduce the risk of diseases related to high fat consumption. However, this important aspect has not received its due attention.

2.7 Composition and physicochemical properties of flaxseed protein, polyphenol, gum, and oil

Flaxseed (*Linumusitatissimum L*.) is one of the most important oilseeds grown over the world with its production exceeding 2.9 million tonnes in 2016 (FAO, 2016). Although the composition of flaxseed is expected to vary depending on the variety, environment and soil (Daun, Barthet, Chornick, & Duguid, 2003); a typical flaxseed contains 20% protein, 41% fat, and 28% total dietary fibre of which about 9% is soluble Table 6 (Cui, 2000). Currently, flaxseed is mainly used for its oil due to its high alpha-linolenic acid (ALA) content (>50% of total fatty acids) (Green & Marshall, 1984) while the defatted meal is used as animal feed (Sielicka & Małecka, 2017) despite being rich in protein and polyphenols (Dabrowski & Sosulski, 1984; Oomah, Mazza, & Cui, 1994). It is also reported that flaxseed protein, polyphenol or their complexes have potential for reducing the risk of diabetes, colorectal cancer, and obesity (Arora et al., 2019; Thakur, Mitra, Pal, & Rousseau, 2009; Williams et al., 2007).

Table 6: Proximate composition in 100 g of flaxseed (Morris, 2003)

Nutrients	Amount per 100 g
Energy (kcal.)	450.0
Proteins (g)	20.0
Fat (g)	41.0
Total dietary fibre (g)	28

2.7.1 Flaxseed protein

The protein content in flaxseed varies from 10.5% to 31% of seed mass depending on the variety and growth environment (Oomah & Mazza, 1993). It is reported that the flaxseed protein has similar amino acid profile to soy protein (Madhusudhan & Singh, 1985). Flaxseed protein possesses a higher amount of branched-chain amino acids (BCAA) such as leucine, isoleucine, and valine and a lower amount of aromatic amino acids (AAA) such as tyrosine and phenylalanine compared to soy protein (Table 7). This leads to a high Fischer ratio (BCCA/AAA) which is associated with many health benefits of flaxseed (Wanasundara & Shahidi, 2003). Flaxseed protein also shows superior functional properties such as high oil holding and foaming capacity, emulsifying activity and good thermal stability (Kaushik et al., 2016b). It can be a protein of choice

for the vegetarian and vegan population. Flaxseed protein contains two main fractions: salt-soluble 11-12S globulins and water-soluble 1.2-6S albumins (Vassel & Nesbitt, 1945). The average molecular weight of flaxseed globulin is reported to be about 320 kDa while that of the albumin is in the range of 16-18 kDa (Chung, Lei, & Li-Chan, 2005). The molecular weight of globulin fraction, which contains five disulfide-linked subunits, varies from 11 to 61 kDa (Oomah & Mazza, 1993).

Table 7: Amino acid composition of flaxseed protein (g/100g protein)

Amino acid	**Brown flaxseed (Norlin)[1]**	**Yellow flaxseed (Omega)[1]**	**Soybean[2]**
Alanine (Ala)	4.4	4.5	4.1
Arginine (Arg)	9.2	9.4	7.3
Aspartic acid (Asp)	9.3	9.7	11.7
Cystine (Cys)	1.1	1.1	1.1
Glutamic acid (Glu)	19.6	19.7	18.6
Glycine (Gly)	5.8	5.8	4.0
Histidine (His)	2.2	2.3	2.5
Isoleucine (Ile)[a]	4.0	4.0	4.7
Leucine (Leu)[a]	5.8	5.9	7.7
Lysine (Lys)[a]	4.0	3.9	5.8
Methionine (Met)[a]	1.5	1.4	1.2
Phenylalanine (Phe)[a]	4.6	4.7	5.1
Proline (Pro)	3.5	3.5	5.2
Serine (Ser)	4.5	4.6	4.9
Threonine (Thr)[a]	3.6	3.7	3.6
Tryptophan (Trp)[a]	1.8	NR[b]	NR[b]
Tyrosine (Tyr)	2.3	2.3	3.4
Valine (Val)[a]	4.6	4.7	5.2

[a] Essential amino acids for humans; [b] Not reported; [1] Oomah and Mazza (1993); [2] Friedman and Levin (1989)

Extraction of flaxseed protein has mostly produced flaxseed protein concentrate rather than flaxseed protein isolate (Tirgar, Silcock, Carne, & Birch, 2017; Wang, Li, Wang, & Özkan, 2010). This is due to the interference of highly viscous flaxseed gum, which easily dissolves in water during protein extraction. The presence of gum leads to a low purity of extracted flaxseed protein. Subsequently, acidic isoelectric precipitation (AI) and micellization (MI) methods are performed to produce higher purity of extracted flaxseed protein (i.e. producing FPI) (Alu'datt et al., 2016;

Krause, Schultz, & Dudek, 2002; Oomah et al., 1994). It is reported that the solubility and emulsifying properties of FPI produced by AI can be as low as 50% compared to those produced by MI (Krause et al., 2002). The poor performance of the former could be due to the denaturation of protein during acid precipitation (Bramsnaes & Olsen, 1979).To avoid protein denaturation, a dialysis-based method was developed to produce FPI with higher solubility and emulsifying properties (Bustamante, Oomah, Rubilar, & Shene, 2017; Karaca, Low, & Nickerson, 2011).

2.7.2 Flaxseed polyphenols

Flaxseed is a rich source of polyphenols as it contains total phenolic content (TPC) of 5.42 g per 100 g seed (Hall & Shultz, 2001). The lignin of flaxseed hull contains a high concentration of phenolic compounds (Oomah, 2003). Phenolic compounds in flaxseed can be classified into two main phenolic groups: phenolic acids and their derivates, and complex lignans (Figure 4). Flaxseed is known to contain about 800 mg to 1000 mg phenolic acids, 500 mg esterified phenolic acids, and 300-500 mg etherified phenolic acids per 100 g of seed (Oomah, Kenaschuk, & Mazza, 1995). Figure 4 represents the chemical structure of the main phenolic compounds found in flaxseed. Ferulic acid (FA) is most abundant phenolic acid in flaxseed followed by p-coumaric and caffeic acid (Waszkowiak, Gliszczyńska-Świgło, Barthet, & Skręty, 2015).

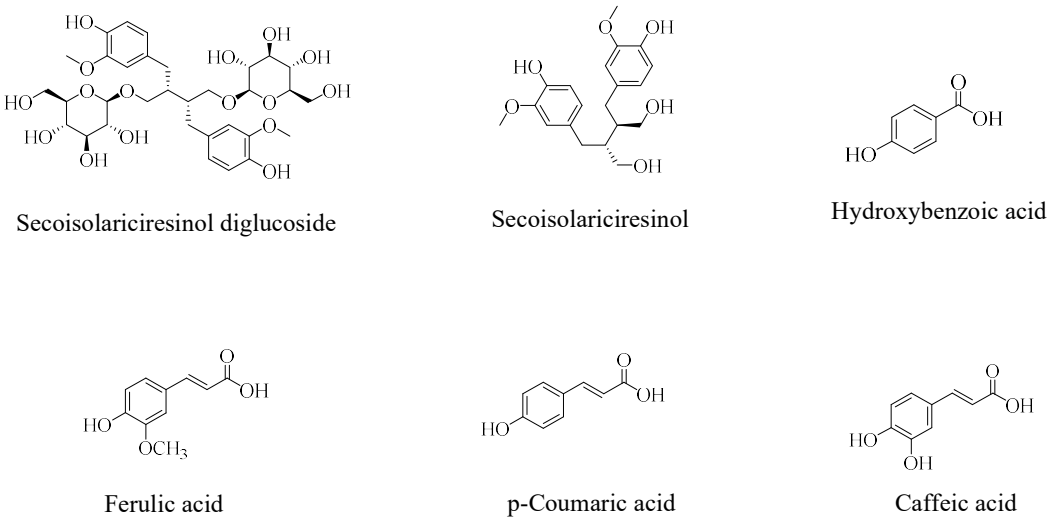

Figure 4. Chemical structure of typical phenolic compounds in flaxseed (Herchi et al., 2014)

Phenolic acids of flaxseed and their adducts are considered as the source of antioxidant properties in flaxseed (Harris & Haggerty, 1993). In addition, secoisolariciresinol diglucoside (SDG) is a complex phenols (lignan) and acts as a phytoestrogen and antioxidant (Touré & Xueming, 2010).It is reported that consumption of SDG reduces the risk of cardiovascular ailments and slows down the progression of some types of diabetes (Mueller, Eisner, Yoshie-Stark, Nakada, & Kirchhoff,

2010). Waszkowiak and Gliszczyńska-Świgło (2015) reported that the concentration of SDG, phenolic acids and their glucosides in phenolic extract depend on cultivar and the solvent used for extraction (Table 8). An ethanol-water mixture with the ethanol to water ratio of 60:40 (v/v) was found to achieve a high extraction yield of total phenolic content from flaxseed. Waszkowiak et al. (2015) showed that proteins get excreted along with polyphenol, which is a common problem in obtaining purer flaxseed polyphenol. Dabrowski and Sosulski (1984) reported that the trans-ferulic and trans-sinapic acid in ethanolic extract of defatted flaxseed flour (about 89% (w/w) of total phenolic acids) can be released under the alkaline condition. Recently, flaxseed polyphenols are used as preferred antioxidants to enhance the stability of flaxseed oil nanoemulsions stabilised by whey protein (Cheng et al., 2019).

Table 8: Phenolic compounds and their content (mg g^{-1}) in flaxseed extracts produced by ethanolic and aqueous extraction (Waszkowiak et al., 2015). SDG=secoisolariciresinol diglucoside, SECO=secoisolariciresinol,

Phenolic compounds	Ethanolic flaxseed extracts		Aqueous flaxseed extracts	
	Brown Szafi	Golden Oliwin	Brown Szafi	Golden Oliwin
SDG[a]	107.37 ± 3.00	77.96 ± 1.00	9.55 ± 0.13	10.80 ± 0.13
SECO[b]	21.74 ± 0.60	15.85 ± 0.20	2.11 ± 0.03	2.36 ± 0.03
p-Coumaric acid glucoside[a,c,e]	9.85 ± 0.14	9.77 ± 0.11	0.73 ± 0.04	1.68 ± 0.07
Caffeic acid glucoside[a,c,f]	2.18 ± 0.04	2.01 ± 0.01	0.17 ± 0.01	0.23 ± 0.01
Ferulic acid glucoside[a,c,g]	1.92 ± 0.21	1.82 ± 0.02	0.14 ± 0.01	0.20 ± 0.01
p-Coumaric acid[a]	1.30 ± 0.02	1.26 ± 0.02	0.16 ± 0.01	0.19 ± 0.01
p-Coumaric acid[b]	7.33 ± 0.09	7.78 ± 0.24	0.51 ± 0.02	0.68 ± 0.04
Ferulic acid[a]	9.04 ± 0.24	13.69 ± 0.14	0.76 ± 0.04	1.88 ± 0.05
Ferulic acid[b]	10.64 ± 0.12	14.45 ± 0.14	0.87 ± 0.01	1.81 ± 0.05
Caffeic acid[b]	2.77 ± 0.03	1.29 ± 0.02	0.12 ± 0.01	0.14 ± 0.00
p-Hydroxybenzoic acid[b]	1.60 ± 0.01	0.77 ± 0.03	0.13 ± 0.01	0.14 ± 0.01
p-Hydroxybenzoic acid[b,d,e]	0.90 ± 0.03	0.69 ± 0.12	ND	ND
Ferulic acid ester[b,d,g]	3.83 ± 0.42	1.80 ± 0.41	ND	ND
Total after alkaline hydrolysis[a]	131.65 ± 2.88	106.51 ± 1.11	11.50 ± 0.21	14.98 ± 0.17
Total after alkaline-acid hydrolysis[b]	48.80 ± 0.86	42.63 ± 0.80	3.73 ± 0.05	5.13 ± 0.07

ND not detected. [a] Present after alkaline hydrolysis of extract solution; [b] Present after alkaline and acid hydrolyses of extract solution; [c] Identified based on elution order of flax phenolics and its decline after acid hydrolysis; for details see; [d] Identified based on elution order of flax phenolics and formation conditions; for details see; [e] Quantified as p-coumaric acid; [f] Quantified as caffeic acid; [g] Quantified as ferulic acid

2.7.3 Flaxseed gum

FG is located on the outermost layer of seed coat (Mazza & Biliaderis, 1989) and its content in flaxseed varies from 3.5 to 9.4% of seed mass depending on the cultivar and environment (Cui, Mazza, & Biliaderis, 1994). It consists of neutral (NF; 25%) and acidic fractions (AF; 75%) with a certain amount of proteinaceous contaminant (Warr et al., 2003). The NF contains a high molecular weight arabinoxylan while the AF is primarily composed of a low molecular weight rhamnogalacturonan (Cui et al., 1994). Kaushik et al. (2017) showed that the composition of extracted FG in also depended on the temperature of the solvent (water) used and that the concentration of protein extracted along with FG increased from 4.4% (w/w) of the extract at 30oC to 15.1% of the extract at 90^{o}C. Thus, choice of a temperature is important to increase the purity of FG.

It is reported that FG solution shows higher viscosity than gum Arabic (GA) but lower than that of locust bean, guar, and xanthan gums (Mazza and Biliaderis, 1989). Mazza and Biliaderis (1989) showed that FG exhibits pseudoplastic behaviour at a concentration above 0.2% (w/v), below this concentration it showed Newtonian behaviour. The flow behaviour of FG is also dictated by the NF:AF ratio (Cui et al., 1994). These authors reported that the NF showed shear thinning behaviour above 0.5% concentration AF showed Newtonian behaviour up to 2% (w/v).

In recent years, FG has been commonly and widely used as an encapsulating wall material to encapsulate flaxseed oil. Most of the studies show that FG offers and effective protection against oxidation of flaxseed when used as an encapsulant (Hadad & Goli, 2019; Mohseni & Goli, 2019; Nikbakht Nasrabadi et al., 2019).

2.7.4 Flaxseed oil

Flaxseed oil (FO) accounts for approximately 40% of seed weight (Daun et al., 2003). FO contains 57% alpha-linoleic acid (ALA) and 16% linoleic acid of total fatty acids. The composition of fatty acids of FO also depends on varieties and the environment prevailing in its cultivation. The composition of extracted oil also depends on the extraction techniques used). FO is reported to reduce blood lipids and glomerular injury and mitigates the decline in renal function (Cunnane et al., 1993; Ingram et al., 1995). However, due to the high level of unsaturated fatty acids (~90%) (Table 10), FO is susceptible to suboptimal processing and storage stresses such as temperature, presence of oxygen, and light. This makes it highly unstable and oxidized quickly. For example, the oxidation stability index of FO (0.5-2 h) is lower than that of many other plant seed oils such

as chia seed oil (2.4 h), and canola oil (12-17 h) (Metrohm, 2004; Timilsena, Vongsvivut, Adhikari, & Adhikari, 2017a). Hence, it is essential to provide suitable protection of the FO against oxidation. For this reason, FO was encapsulated using various wall materials such as flaxseed gum (Hadad & Goli, 2019), gelatin/flaxseed mucilage (Mohseni & Goli, 2019) and milk whey proteins/alginate (Fioramonti, Stepanic, Tibaldo, Pavón, & Santiago, 2019). These studies revealed that the oxidative stability of encapsulated FO was successfully enhanced. However, the encapsulation process (electrospinning, homogenization and spray drying) induced the significant increment of primary oxidation product, suggested by increased hydroperoxide values.

2.8 Hydroxytyrosol

Although hydroxytyrosol (HT) is not a part of flaxseed, it was used in this thesis as a model phenolic alcohol. HT is a dihydroxy phenolic compound (Figure 5) and is present, in abundance in olive oil. HT is a strong antioxidant and has many health benefits, including reduction of systolic blood pressure (Covas et al., 2015), improvement of endothelial function (Valls et al., 2015), and alleviation of inflammation (Lopez et al., 2017). HT is used in meat as preservative because of its high antioxidative activity (Martínez, Ros, & Nieto, 2018). HT is one of the most effective oxidants among olive olive phenolics. It has been incorporated as antioxidant in emulsions stabilised by β-lactoglobulin and maltodextrin (Paradiso et al., 2016). However, to date, there is no study on the conjugation of HT with protein under alkaline condition.

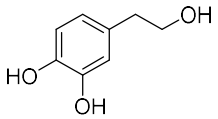

Figure 5: Chemical structure of hydroxytyrosol

2.9 Concluding remarks

There is an increasing body of research on covalent modification of proteins with phenolic compounds to enhance their physicochemical and functional properties. Protein-phenolic conjugates can be novel food ingredients with superior emulsifying and encapsulating properties. Thus, greater understanding of encapsulating and encapsulating properties of plant protein-phenolic adducts enables development of novel emulsions with improved stability and stability against oxidation and also microcapsules with higher payload and control delivery characteristics. The protein-phenol conjugates and their complex coacervates with plant gums can be suitable

emulsifiers and encapsulants for PUFA-rich oils. However, there is a lack of knowledge on the covalent conjugation between plant proteins and phenolic compounds, especially those obtained from oil seeds. Besides, the interaction between proteins and phenolic alcohols such as hydroxytyrosol has not been elucidated. There is a paucity of information on the efficacy of plan protein-phenolic adducts and also their complex coacervates with gums on emulsifying and encapsulating PUFAs-rich oils; particularly on stability, stability against oxidation and release and digestion of encapsulated oil in gastrointestinal tract.

Therefore, this chapter aims to underscore the above-stated knowledge gaps and limitations. In addition, this chapter highlights the potential use of flaxseed polyphenols and hydroxytyrosol as valuable phenolic compounds to covalently conjugate with plant proteins and utilize the resulting conjugates and their complex coavervates with plant gums as potential emulsifiers and encapsulations of PUFAs-rich oils.

References

Abd El-Maksoud, A. A., Abd El-Ghany, I. H., El-Beltagi, H. S., Anankanbil, S., Banerjee, C., Petersen, S. V., . . . Guo, Z. (2018). Adding functionality to milk-based protein: Preparation, and physico-chemical characterization of β-lactoglobulin-phenolic conjugates. *Food Chemistry, 241*, 281-289.

Abuajah, C. I., Ogbonna, A. C., & Osuji, C. M. (2015). Functional components and medicinal properties of food: a review. *J Food Sci Technol, 52*(5), 2522-2529.

Alamed, J., McClements, D. J., & Decker, E. A. (2006). Influence of heat processing and calcium ions on the ability of EDTA to inhibit lipid oxidation in oil-in-water emulsions containing omega-3 fatty acids. *Food Chemistry, 95*(4), 585-590.

Ali, M. (2019). Chemical, structural and functional properties of whey proteins covalently modified with phytochemical compounds. *Journal of Food Measurement and Characterization, 13*(4), 2970-2979.

Ali, M., Homann, T., Khalil, M., Kruse, H.-P., & Rawel, H. (2013). Milk whey protein modification by coffee-specific phenolics: effect on structural and functional properties. *Journal of Agricultural and Food Chemistry, 61*(28), 6911-6920.

Alu'datt, M. H., Rababah, T., Alhamad, M. N., Gammoh, S., Ereifej, K., Kubow, S., & Alli, I. (2016). Characterization and antioxidant activities of phenolic interactions identified in byproducts of soybean and flaxseed protein isolation. *Food Hydrocolloids, 61*, 119-127.

Amine, C., Dreher, J., Helgason, T., & Tadros, T. (2014). Investigation of emulsifying properties and emulsion stability of plant and milk proteins using interfacial tension and interfacial elasticity. *Food Hydrocolloids, 39*, 180-186.

Arora, T., Rudenko, O., Egerod, K. L., Husted, A. S., Kovatcheva-Datchary, P., Akrami, R., . . . Bäckhed, F. (2019). Microbial fermentation of flaxseed fibers modulates the transcriptome of GPR41-expressing enteroendocrine cells and protects mice against diet-induced obesity. *American Journal of Physiology-Endocrinology and Metabolism, 316*(3), E453-E463.

Augustin, M. A., Sanguansri, L., Rusli, J. K., Shen, Z., Cheng, L. J., Keogh, J., & Clifton, P. (2014). Digestion of microencapsulated oil powders: in vitro lipolysis and in vivo absorption from a food matrix. *Food & function, 5*(11), 2905-2912.

Ba, C., Fu, Y., Niu, F., Wang, M., Jin, B., Li, Z., . . . Li, X. (2020). Effects of environmental stresses on physiochemical stability of β-carotene in zein-carboxymethyl chitosan-tea polyphenols ternary delivery system. *Food Chemistry, 311*, 125878.

Betoret, E., Betoret, N., Vidal, D., & Fito, P. (2011). Functional foods development: Trends and technologies. *Trends in Food Science & Technology, 22*(9), 498-508.

Bramsnaes, F., & Olsen, H. S. (1979). Development of field pea and faba bean proteins. *Journal of the American Oil Chemists' Society, 56*(3), 450-454.

Bučko, S., Katona, J., Petrović, L., Milinković, J., Spasojević, L., Mucić, N., & Miller, R. (2018). The Influence of Enzymatic Hydrolysis on Adsorption and Interfacial Dilatational Properties of Pumpkin (Cucurbita pepo) Seed Protein Isolate. *Food Biophysics*, 1-9.

Bustamante, M., Oomah, B. D., Rubilar, M., & Shene, C. (2017). Effective Lactobacillus plantarum and Bifidobacterium infantis encapsulation with chia seed (Salvia hispanica L.) and flaxseed (Linum usitatissimum L.) mucilage and soluble protein by spray drying. *Food Chemistry, 216*, 97-105.

Calder, P. C. (2006). n− 3 polyunsaturated fatty acids, inflammation, and inflammatory diseases. *The American journal of clinical nutrition, 83*(6), S1505-1519S.

Cascão Pereira, L. G., Theodoly, O., Blanch, H. W., & Radke, C. J. (2003). Dilatational rheology of BSA conformers at the air/water interface. *Langmuir, 19*(6), 2349-2356.

Cheng, C., Yu, X., McClements, D. J., Huang, Q., Tang, H., Yu, K., . . . Deng, Q. (2019). Effect of flaxseed polyphenols on physical stability and oxidative stability of flaxseed oil-in-water nanoemulsions. *Food Chemistry, 301*, 125207.

Chung, Lei, B., & Li-Chan, E. (2005). Isolation and structural characterization of the major protein fraction from NorMan flaxseed (Linum usitatissimum L.). *Food Chemistry, 90*(1), 271-279.

Cilliers, J. J., & Singleton, V. L. (1991). Characterization of the products of nonenzymic autoxidative phenolic reactions in a caffeic acid model system. *Journal of Agricultural and Food Chemistry, 39*(7), 1298-1303.

Comunian, T. A., Boillon, M. R. G., Thomazini, M., Nogueira, M. S., de Castro, I. A., & Favaro-Trindade, C. S. (2016). Protection of echium oil by microencapsulation with phenolic compounds. *Food Research International, 88*, 114-121.

Comunian, T. A., & Favaro-Trindade, C. S. (2016). Microencapsulation using biopolymers as an alternative to produce food enhanced with phytosterols and omega-3 fatty acids: A review. *Food Hydrocolloids, 61*, 442-457.

Connor, W. E., Prince, M. J., Ullmann, D., Riddle, M., Hatcher, L., Smith, F. E., & Wilson, D. (1993). The Hypotriglyceridemic Effect of Fish Oil in Adult-Onset Diabetes without Adverse Glucose Control. *Annals of the New York Academy of Sciences, 683*(1), 337-340.

Covas, M.-I., de la Torre, R., & Fitó, M. (2015). Virgin olive oil: a key food for cardiovascular risk protection. *British Journal of Nutrition, 113*(S2), S19-S28.

Cui, S., W. (2000). *Polysaccharide Gums from Agricultural Products.pdf*: CRC Press.

Cui, W., Mazza, G., & Biliaderis, C. (1994). Chemical structure, molecular size distributions, and rheological properties of flaxseed gum. *Journal of Agricultural and Food Chemistry, 42*(9), 1891-1895.

Cunnane, S. C., Ganguli, S., Menard, C., Liede, A. C., Hamadeh, M. J., Chen, Z.-Y., . . . Jenkins, D. J. (1993). High α-linolenic acid flaxseed (Linum usitatissimum): some nutritional properties in humans. *British Journal of Nutrition, 69*(2), 443-453.

Dabrowski, K. J., & Sosulski, F. W. (1984). Composition of free and hydrolyzable phenolic acids in defatted flours of ten oilseeds. *Journal of Agricultural and Food Chemistry, 32*(1), 128-130.

Daun, J. K., Barthet, V. J., Chornick, T., & Duguid, S. (2003). Structure, composition, and variety development of flaxseed. *Flaxseed in human nutrition, 2*, 1-40.

de Conto, L. C., Grosso, C. R. F., & Gonçalves, L. A. G. (2013). Chemometry as applied to the production of omega-3 microcapsules by complex coacervation with soy protein isolate and gum Arabic. *LWT-Food Science and Technology, 53*(1), 218-224.

Di Giorgio, L., Salgado, P. R., & Mauri, A. N. (2019). Encapsulation of fish oil in soybean protein particles by emulsification and spray drying. *Food Hydrocolloids, 87*, 891-901.

Dickinson, E. (2010). Food emulsions and foams: Stabilization by particles. *Current Opinion in Colloid & Interface Science, 15*(1), 40-49.

Dong, Z., Ma, Y., Hayat, K., Jia, C., Xia, S., & Zhang, X. (2011). Morphology and release profile of microcapsules encapsulating peppermint oil by complex coacervation. *Journal of Food Engineering, 104*(3), 455-460.

Ducel, V., Richard, J., Popineau, Y., & Boury, F. (2004). Adsorption Kinetics and Rheological Interfacial Properties of Plant Proteins at the Oil− Water Interface. *Biomacromolecules, 5*(6), 2088-2093.

Encina, C., Vergara, C., Gimenez, B., Oyarzun-Ampuero, F., & Robert, P. (2016). Conventional spray-drying and future trends for the microencapsulation of fish oil. *Trends in Food Science & Technology, 56*, 46-60.

Eratte, D., Dowling, K., Barrow, C. J., & Adhikari, B. (2018). Recent advances in the microencapsulation of omega-3 oil and probiotic bacteria through complex coacervation: A review. *Trends in Food Science & Technology, 71*, 121-131.

FAO. (2016). Food and Agriculture Organisation

Fioramonti, S. A., Stepanic, E. M., Tibaldo, A. M., Pavón, Y. L., & Santiago, L. G. (2019). Spray dried flaxseed oil powdered microcapsules obtained using milk whey proteins-alginate double layer emulsions. *Food Research International, 119*, 931-940.

Friedman, M., & Levin, C. E. (1989). Composition of jimson weed (Datura stramonium) seeds. *Journal of Agricultural and Food Chemistry, 37*(4), 998-1005.

Gallier, S., & Singh, H. (2012). The physical and chemical structure of lipids in relation to digestion and absorption. *Lipid Technology, 24*(12), 271-273.

Gouin, S. (2004). Microencapsulation: industrial appraisal of existing technologies and trends. *Trends in Food Science & Technology, 15*(7), 330-347.

Graham, D., & Phillips, M. (1979). Proteins at liquid interfaces: I. Kinetics of adsorption and surface denaturation. *Journal of colloid and interface science, 70*(3), 403-414.

Green, A., & Marshall, D. (1984). Isolation of induced mutants in linseed (Linum usitatissimum) having reduced linolenic acid content. *Euphytica, 33*(2), 321-328.

Guimarães Drummond e Silva, F., Miralles, B., Hernández-Ledesma, B., Amigo, L., Iglesias, A. H., Reyes Reyes, F. G., & Netto, F. M. (2017). Influence of Protein–Phenolic Complex on the Antioxidant Capacity of Flaxseed (Linum usitatissimum L.) Products. *Journal of Agricultural and Food Chemistry, 65*(4), 800-809.

Gumus, C. E., Decker, E. A., & McClements, D. J. (2017). Gastrointestinal fate of emulsion-based ω-3 oil delivery systems stabilized by plant proteins: Lentil, pea, and faba bean proteins. *Journal of Food Engineering, 207*, 90-98.

Hadad, S., & Goli, S. A. H. (2019). Improving Oxidative Stability of Flaxseed Oil by Encapsulation in Electrospun Flaxseed Mucilage Nanofiber. *Food and Bioprocess Technology, 12*(5), 829-838.

Hall, C., & Shultz, K. (2001). *Phenolic antioxidant interactions.* Paper presented at the 92nd American Oil Chemists Society Annual Meeting and Expo. p. S88 Minneapolis, Minnesota: AOCS.

Harris, R., & Haggerty, W. (1993). Assays for potentially anticarcinogenic phytochemicals in flaxseed. *Cereal foods world (USA)*.

Hayakawa, S., & Nakai, S. (1985). Relationships of hydrophobicity and net charge to the solubility of milk and soy proteins. *Journal of Food Science, 50*(2), 486-491.

He, Q., Lv, Y., & Yao, K. (2007). Effects of tea polyphenols on the activities of α-amylase, pepsin, trypsin and lipase. *Food Chemistry, 101*(3), 1178-1182.

Herchi, W., Arr, aacute, ez, R., aacute, n, D., . . . ndez-Gutierrez, A. (2014). Phenolic Compounds in Flaxseed: a Review of Their Properties and Analytical Methods. An Overview of the Last Decade. *Journal of Oleo Science, 63*(1), 7-14.

Ingram, A. J., Parbtani, A., Clark, W. F., Spanner, E., Huff, M. W., Philbrick, D. J., & Holub, B. J. (1995). Effects of flaxseed and flax oil diets in a rat-5/6 renal ablation model. *American Journal of Kidney Diseases, 25*(2), 320-329.

Ishii, T., Mori, T., Tanaka, T., Mizuno, D., Yamaji, R., Kumazawa, S., . . . Akagawa, M. (2008). Covalent modification of proteins by green tea polyphenol (-)-epigallocatechin-3-gallate through autoxidation. *Free Radic Biol Med, 45*(10), 1384-1394.

Jarpa-Parra, M., Bamdad, F., Tian, Z., Zeng, H., Temelli, F., & Chen, L. (2015). Impact of pH on molecular structure and surface properties of lentil legumin-like protein and its application as foam stabilizer. *Colloids and Surfaces B: Biointerfaces, 132*, 45-53.

Jia, Z., Zheng, M., Tao, F., Chen, W., Huang, G., & Jiang, J. (2016). Effect of covalent modification by (−)-epigallocatechin-3-gallate on physicochemical and functional properties of whey protein isolate. *LWT - Food Science and Technology, 66*, 305-310.

Jiang, L., Liu, Y., Li, L., Qi, B., Ju, M., Xu, Y., . . . Sui, X. (2019). Covalent conjugates of anthocyanins to soy protein: Unravelling their structure features and in vitro gastrointestinal digestion fate. *Food Research International, 120*, 603-609.

Jun-xia, X., Hai-yan, Y., & Jian, Y. (2011). Microencapsulation of sweet orange oil by complex coacervation with soybean protein isolate/gum Arabic. *Food Chemistry, 125*(4), 1267-1272.

Karaca, A. C., Low, N., & Nickerson, M. (2011). Emulsifying properties of canola and flaxseed protein isolates produced by isoelectric precipitation and salt extraction. *Food Research International, 44*(9), 2991-2998.

Karaca, A. C., Low, N., & Nickerson, M. (2015). Potential use of plant proteins in the microencapsulation of lipophilic materials in foods. *Trends in Food Science & Technology, 42*(1), 5-12.

Karaca, A. C., Nickerson, M., & Low, N. H. (2013). Microcapsule production employing chickpea or lentil protein isolates and maltodextrin: physicochemical properties and oxidative protection of encapsulated flaxseed oil. *Food Chem, 139*(1-4), 448-457.

Karefyllakis, D., Altunkaya, S., Berton-Carabin, C. C., van der Goot, A. J., & Nikiforidis, C. V. (2017). Physical bonding between sunflower proteins and phenols: Impact on interfacial properties. *Food Hydrocolloids, 73*, 326-334.

Kaushik, P., Dowling, K., Barrow, C. J., & Adhikari, B. (2015a). Complex coacervation between flaxseed protein isolate and flaxseed gum. *Food Research International, 72*, 91-97.

Kaushik, P., Dowling, K., Barrow, C. J., & Adhikari, B. (2015b). Microencapsulation of omega-3 fatty acids: A review of microencapsulation and characterization methods. *Journal of Functional Foods, 19*, 868-881.

Kaushik, P., Dowling, K., McKnight, S., Barrow, C. J., & Adhikari, B. (2016a). Microencapsulation of flaxseed oil in flaxseed protein and flaxseed gum complex coacervates. *Food Research International, 86*, 1-8.

Kaushik, P., Dowling, K., McKnight, S., Barrow, C. J., Wang, B., & Adhikari, B. (2016b). Preparation, characterization and functional properties of flax seed protein isolate. *Food Chemistry, 197*(Pt A), 212-220.

Keppler, J. K., Schwarz, K., & van der Goot, A. J. (2020). Covalent modification of food proteins by plant-based ingredients (polyphenols and organosulphur compounds): A commonplace reaction with novel utilization potential. *Trends in Food Science & Technology, 101*, 38-49.

Khattab, R. Y., Eskin, M. N., & Thiyam-Hollander, U. (2014). Production of canolol from canola meal phenolics via hydrolysis and microwave-induced decarboxylation. *Journal of the American Oil Chemists' Society, 91*(1), 89-97.

Krause, J. P., Schultz, M., & Dudek, S. (2002). Effect of extraction conditions on composition, surface activity and rheological properties of protein isolates from flaxseed (Linum usitativissimum L). *Journal of the Science of Food and Agriculture, 82*(9), 970-976.

Kremer, J. M. (1996). Effects of modulation of inflammatory and immune parameters in patients with rheumatic and inflammatory disease receiving dietary supplementation of n-3 and n-6 fatty acids. *Lipids, 31*(1), S243-S247.

Kroll, J., & Rawel, H. M. (2001). Reactions of plant phenols with myoglobin: influence of chemical structure of the phenolic compounds. *Journal of Food Science, 66*(1), 48-58.

Kroll, J., Rawel, H. M., & Seidelmann, N. (2000). Physicochemical properties and susceptibility to proteolytic digestion of myoglobin− phenol derivatives. *Journal of Agricultural and Food Chemistry, 48*(5), 1580-1587.

Li, D., & Hu, X.-J. (2009). Fish and its multiple human health effects in times of threat to sustainability and affordability: are there alternatives? *Asia Pacific journal of clinical nutrition, 18*(4), 553-563.
Liu, F., Ma, C., McClements, D. J., & Gao, Y. (2017). A comparative study of covalent and non-covalent interactions between zein and polyphenols in ethanol-water solution. *Food Hydrocolloids, 63*, 625-634.
Liu, F., Sun, C., Yang, W., Yuan, F., & Gao, Y. (2015). Structural characterization and functional evaluation of lactoferrin–polyphenol conjugates formed by free-radical graft copolymerization. *RSC Advances, 5*(20), 15641-15651.
Liu, F., Wang, D., Ma, C., & Gao, Y. (2016a). Conjugation of polyphenols prevents lactoferrin from thermal aggregation at neutral pH. *Food Hydrocolloids, 58*, 49-59.
Liu, F., Wang, D., Sun, C., McClements, D. J., & Gao, Y. (2016b). Utilization of interfacial engineering to improve physicochemical stability of β-carotene emulsions: Multilayer coatings formed using protein and protein–polyphenol conjugates. *Food Chemistry, 205*, 129-139.
Liu, J., Yong, H., Yao, X., Hu, H., Yun, D., & Xiao, L. (2019). Recent advances in phenolic–protein conjugates: synthesis, characterization, biological activities and potential applications. *RSC Advances, 9*(61), 35825-35840.
Lopez, S., Montserrat-de la Paz, S., Lucas, R., Bermudez, B., Abia, R., Morales, J. C., & Muriana, F. J. G. (2017). Effect of metabolites of hydroxytyrosol on protection against oxidative stress and inflammation in human endothelial cells. *Journal of Functional Foods, 29*, 238-247.
Madhusudhan, K., & Singh, N. (1985). Isolation and characterization of the major fraction (12 S) of linseed proteins. *Journal of Agricultural and Food Chemistry, 33*(4), 673-677.
Martínez, L., Ros, G., & Nieto, G. (2018). Hydroxytyrosol: Health benefits and use as functional ingredient in meat. *Medicines, 5*(1), 13.
Mazza, G., & Biliaderis, C. (1989). Functional properties of flax seed mucilage. *Journal of Food Science, 54*(5), 1302-1305.
Metrohm, A. G. (2004). Oxidation stability of oils and fats – Rancimat method. *Metrohm application bulletin No, 204*, 1-4.
Minekus, M., Alminger, M., Alvito, P., Ballance, S., Bohn, T., Bourlieu, C., . . . Dupont, D. (2014). A standardised static in vitro digestion method suitable for food–an international consensus. *Food & function, 5*(6), 1113-1124.
Mohseni, F., & Goli, S. A. H. (2019). Encapsulation of flaxseed oil in the tertiary conjugate of oxidized tannic acid-gelatin and flaxseed (Linum usitatissimum) mucilage. *International Journal of Biological Macromolecules, 140*, 959-964.
Morris, D. H. (2003). Flax: A health and nutrition primer. *Flax Council of Canada, 3rd*, 11.
Mueller, K., Eisner, P., Yoshie-Stark, Y., Nakada, R., & Kirchhoff, E. (2010). Functional properties and chemical composition of fractionated brown and yellow linseed meal (Linum usitatissimum L.). *Journal of Food Engineering, 98*(4), 453-460.
Muhoza, B., Xia, S., & Zhang, X. (2019). Gelatin and high methyl pectin coacervates crosslinked with tannic acid: The characterization, rheological properties, and application for peppermint oil microencapsulation. *Food Hydrocolloids, 97*, 105174.
Mun, S., Decker, E. A., & McClements, D. J. (2007). Influence of emulsifier type on in vitro digestibility of lipid droplets by pancreatic lipase. *Food Research International, 40*(6), 770-781.
Nesterenko, A., Alric, I., Silvestre, F., & Durrieu, V. (2013). Vegetable proteins in microencapsulation: A review of recent interventions and their effectiveness. *Industrial Crops and Products, 42*, 469-479.

Nikbakht Nasrabadi, M., Goli, S. A. H., Sedaghat Doost, A., Roman, B., Dewettinck, K., Stevens, C. V., & Van der Meeren, P. (2019). Plant based Pickering stabilization of emulsions using soluble flaxseed protein and mucilage nano-assemblies. *Colloids and Surfaces A: Physicochemical and Engineering Aspects, 563*, 170-182.

Oomah, B., & Mazza, G. (1993). Flaxseed proteins—a review. *Food Chemistry, 48*(2), 109-114.

Oomah, B. D. (2003). Processing of flaxseed fiber, oil, protein, and lignan. *Flaxseed in human nutrition, 2*, 363-386.

Oomah, B. D., Mazza, G., & Cui, W. (1994). Optimization of protein extraction from flaxseed meal. *Food Research International, 27*(4), 355-361.

Oomah, D., B., Kenaschuk, O., E., & Mazza, G. (1995). Phenolic acid in flaxseed. *Journal of Agricultural and Food Chemistry, 43*, 2016-2019.

Paradiso, V. M., Di Mattia, C., Giarnetti, M., Chiarini, M., Andrich, L., & Caponio, F. (2016). Antioxidant Behavior of Olive Phenolics in Oil-in-Water Emulsions. *J Agric Food Chem, 64*(29), 5877-5886.

Prigent, S. V., Voragen, A. G., Visser, A. J., van Koningsveld, G. A., & Gruppen, H. (2007). Covalent interactions between proteins and oxidation products of caffeoylquinic acid (chlorogenic acid). *Journal of the Science of Food and Agriculture, 87*(13), 2502-2510.

Quan, T. H., Benjakul, S., Sae-leaw, T., Balange, A. K., & Maqsood, S. (2019). Protein–polyphenol conjugates: Antioxidant property, functionalities and their applications. *Trends in Food Science & Technology*.

Rade-Kukic, K., Schmitt, C., & Rawel, H. M. (2011). Formation of conjugates between β-lactoglobulin and allyl isothiocyanate: Effect on protein heat aggregation, foaming and emulsifying properties. *Food Hydrocolloids, 25*(4), 694-706.

Ravera, F., Loglio, G., & Kovalchuk, V. I. (2010). Interfacial dilational rheology by oscillating bubble/drop methods. *Current Opinion in Colloid & Interface Science, 15*(4), 217-228.

Rawel, H. M., Czajka, D., Rohn, S., & Kroll, J. (2002a). Interactions of different phenolic acids and flavonoids with soy proteins. *Int J Biol Macromol, 30*(3-4), 137-150.

Rawel, H. M., Kroll, J., & Hohl, U. (2001a). Model studies on reactions of plant phenols with whey proteins. *Molecular Nutrition & Food Research, 45*(2), 72-81.

Rawel, H. M., Kroll, J., & Riese, B. (2000). Reactions of chlorogenic acid with lysozyme: physicochemical characterization and proteolytic digestion of the derivatives. *Journal of Food Science, 65*(6), 1091-1098.

Rawel, H. M., Kroll, J., & Rohn, S. (2001b). Reactions of phenolic substances with lysozyme—physicochemical characterisation and proteolytic digestion of the derivatives. *Food Chemistry, 72*(1), 59-71.

Rawel, H. M., Ranters, H., Rohn, S., & Kroll, J. (2004). Assessment of the reactivity of selected isoflavones against proteins in comparison to quercetin. *Journal of Agricultural and Food Chemistry, 52*(16), 5263-5271.

Rawel, H. M., Rohn, S., & Kroll, J. (2003). Influence of a sugar moiety (rhamnosylglucoside) at 3-O position on the reactivity of quercetin with whey proteins. *International Journal of Biological Macromolecules, 32*(3-5), 109-120.

Rawel, H. M., Rohn, S., Kruse, H.-P., & Kroll, J. (2002b). Structural changes induced in bovine serum albumin by covalent attachment of chlorogenic acid. *Food Chemistry, 78*(4), 443-455.

Reis, P., Holmberg, K., Watzke, H., Leser, M. E., & Miller, R. (2009). Lipases at interfaces: A review. *Advances in colloid and interface science, 147-148*, 237-250.

Rodríguez, S. D., von Staszewski, M., & Pilosof, A. M. R. (2015). Green tea polyphenols-whey proteins nanoparticles: Bulk, interfacial and foaming behavior. *Food Hydrocolloids, 50*, 108-115.

Roynette, C. E., Calder, P. C., Dupertuis, Y. M., & Pichard, C. (2004). n-3 Polyunsaturated fatty acids and colon cancer prevention. *Clinical Nutrition, 23*(2), 139-151.
Ruiz, J. R., Ortiz, E. V., & Segura, M. C. (2017). Encapsulation of vegetable oils as source of omega-3 fatty acids for enriched functional foods. *Critical Reviews in Food Science and Nutrition, 57*(7), 1423-1434.
Sanguansri, L., & Augustin, M. A. (2016). Microencapsulation and delivery of omega-3 fatty acids. *Functional food ingredients and nutraceuticals, processing technologies*, 373-408.
Sarkar, A., Goh, K. K. T., Singh, R. P., & Singh, H. (2009). Behaviour of an oil-in-water emulsion stabilized by β-lactoglobulin in an in vitro gastric model. *Food Hydrocolloids, 23*(6), 1563-1569.
Sarkar, A., Horne, D. S., & Singh, H. (2010). Pancreatin-induced coalescence of oil-in-water emulsions in an in vitro duodenal model. *International dairy journal, 20*(9), 589-597.
Sausse, P., Aguié-Béghin, V., & Douillard, R. (2003). Effects of Epigallocatechin Gallate on β-Casein Adsorption at the Air/Water Interface. *Langmuir, 19*(3), 737-743.
Schmitt, C., & Turgeon, S. L. (2011). Protein/polysaccharide complexes and coacervates in food systems. *Advances in colloid and interface science, 167*(1), 63-70.
Sęczyk, Ł., Świeca, M., Kapusta, I., & Gawlik-Dziki, U. (2019). Protein-Phenolic Interactions as a Factor Affecting the Physicochemical Properties of White Bean Proteins. *Molecules (Basel, Switzerland), 24*(3), 408.
Shi, L., Beamer, S. K., Yang, H., & Jaczynski, J. (2018). Micro-emulsification/encapsulation of krill oil by complex coacervation with krill protein isolated using isoelectric solubilization/precipitation. *Food Chemistry, 244*, 284-291.
Sielicka, M., & Małecka, M. (2017). Enhancement of Oxidative Stability of Flaxseed Oil Through Flaxseed, Evening Primrose and Black Cumin Cake Extracts. *Journal of Food Processing and Preservation, 41*(4).
Steffens, W. (1997). Effects of variation feeds on nutritive in essential fatty acids in fish value of freshwater fish for human. *Aquaculture, 151*, 97-119
Strauss, G., & Gibson, S. M. (2004). Plant phenolics as cross-linkers of gelatin gels and gelatin-based coacervates for use as food ingredients. *Food Hydrocolloids, 18*(1), 81-89.
Sui, X., Sun, H., Qi, B., Zhang, M., Li, Y., & Jiang, L. (2018). Functional and conformational changes to soy proteins accompanying anthocyanins: Focus on covalent and non-covalent interactions. *Food Chemistry, 245*, 871-878.
Tadros, T. F. (2013). *Emulsion formation and stability*: John Wiley & Sons.
Tao, F., Jiang, H., Chen, W., Zhang, Y., Pan, J., Jiang, J., & Jia, Z. (2018). Covalent modification of soy protein isolate by (−)-epigallocatechin-3-gallate: effects on structural and emulsifying properties. *Journal of the Science of Food and Agriculture, 98*(15), 5683-5689.
Tao, F., Xiao, C., Chen, W., Zhang, Y., Pan, J., & Jia, Z. (2019). Covalent modification of β-lactoglobulin by (−)-epigallocatechin-3-gallate results in a novel antioxidant molecule. *International Journal of Biological Macromolecules, 126*, 1186-1191.
Tao, L. (2015). Oxidation of Polyunsaturated Fatty Acids and its Impact on Food Quality and Human Health. *Advances in Food Technology and Nutritional Sciences - Open Journal, 1*(6), 135-142.
Teng, M.-J., Wei, Y.-S., Hu, T.-G., Zhang, Y., Feng, K., Zong, M.-H., & Wu, H. (2020). Citric acid cross-linked zein microcapsule as an efficient intestine-specific oral delivery system for lipophilic bioactive compound. *Journal of Food Engineering, 281*, 109993.
Thakur, G., Mitra, A., Pal, K., & Rousseau, D. (2009). Effect of flaxseed gum on reduction of blood glucose and cholesterol in type 2 diabetic patients. *International Journal of Food Sciences and Nutrition, 60*(sup6), 126-136.

Timilsena, Adhikari, R., Barrow, C. J., & Adhikari, B. (2016). Microencapsulation of chia seed oil using chia seed protein isolate-chia seed gum complex coacervates. *Int J Biol Macromol, 91*, 347-357.
Timilsena, Vongsvivut, J., Adhikari, R., & Adhikari, B. (2017a). Physicochemical and thermal characteristics of Australian chia seed oil. *Food Chemistry, 228*, 394-402.
Timilsena, Y. P., Wang, B., Adhikari, R., & Adhikari, B. (2017b). Advances in microencapsulation of polyunsaturated fatty acids (PUFAs)-rich plant oils using complex coacervation: A review. *Food Hydrocolloids, 69*, 369-381.
Tirgar, M., Silcock, P., Carne, A., & Birch, E. J. (2017). Effect of extraction method on functional properties of flaxseed protein concentrates. *Food Chem, 215*, 417-424.
Touré, A., & Xueming, X. (2010). Flaxseed lignans: source, biosynthesis, metabolism, antioxidant activity, bio-active components, and health benefits. *Comprehensive reviews in food science and food safety, 9*(3), 261-269.
Turgeon, S. L., Schmitt, C., & Sanchez, C. (2007). Protein–polysaccharide complexes and coacervates. *Current Opinion in Colloid & Interface Science, 12*(4-5), 166-178.
Valls, R.-M., Farràs, M., Suárez, M., Fernández-Castillejo, S., Fitó, M., Konstantinidou, V., . . . Solà, R. (2015). Effects of functional olive oil enriched with its own phenolic compounds on endothelial function in hypertensive patients. A randomised controlled trial. *Food Chemistry, 167*, 30-35.
Vassel, B., & Nesbitt, L. (1945). The nitrogenous constituents of flaxseed II. The isolation of a purified protein fraction. *Journal of Biological Chemistry, 159*(3), 571-584.
von Staszewski, M., Pizones Ruiz-Henestrosa, V. M., & Pilosof, A. M. R. (2014). Green tea polyphenols-β-lactoglobulin nanocomplexes: Interfacial behavior, emulsification and oxidation stability of fish oil. *Food Hydrocolloids, 35*, 505-511.
Wanasundara, P., & Shahidi, F. (2003). Flaxseed proteins: potential food applications and process-induced changes. *Flaxseed in human nutrition*, 387-403.
Wang, Adhikari, B., & Barrow, C. J. (2014a). Optimisation of the microencapsulation of tuna oil in gelatin-sodium hexametaphosphate using complex coacervation. *Food Chem, 158*, 358-365.
Wang, B., Adhikari, B., & Barrow, C. J. (2019). Highly stable spray dried tuna oil powders encapsulated in double shells of whey protein isolate-agar gum and gellan gum complex coacervates. *Powder Technology, 358*, 79-86.
Wang, B., Li, D., Wang, L.-J., & Özkan, N. (2010). Effect of concentrated flaxseed protein on the stability and rheological properties of soybean oil-in-water emulsions. *Journal of Food Engineering, 96*(4), 555-561.
Wang, J.-M., Xia, N., Yang, X.-Q., Yin, S.-W., Qi, J.-R., He, X.-T., . . . Wang, L.-J. (2012). Adsorption and dilatational rheology of heat-treated soy protein at the oil–water interface: Relationship to structural properties. *Journal of Agricultural and Food Chemistry, 60*(12), 3302-3310.
Wang, X., Zhang, J., Lei, F., Liang, C., Yuan, F., & Gao, Y. (2014b). Covalent complexation and functional evaluation of (−)-epigallocatechin gallate and α-lactalbumin. *Food Chemistry, 150*, 341-347.
Ward, A., & Tordai, L. (1946). Time-dependence of boundary tensions of solutions I. The role of diffusion in time-effects. *The Journal of Chemical Physics, 14*(7), 453-461.
Warr, J., Michaud, P., Picton, L., Muller, G., Courtois, B., Ralainirina, R., & Courtois, J. (2003). Large-scale purification of water-soluble polysaccharides from flaxseed mucilage, and isolation of a new anionic polymer. *Chromatographia, 58*(5-6), 331-335.
Waszkowiak, K., & Gliszczyńska-Świgło, A. (2015). Binary ethanol–water solvents affect phenolic profile and antioxidant capacity of flaxseed extracts. *European Food Research and Technology, 242*(5), 777-786.

Waszkowiak, K., Gliszczyńska-Świgło, A., Barthet, V., & Skręty, J. (2015). Effect of Extraction Method on the Phenolic and Cyanogenic Glucoside Profile of Flaxseed Extracts and their Antioxidant Capacity. *J Am Oil Chem Soc, 92*(11-12), 1609-1619.

Wei, Z., Yang, W., Fan, R., Yuan, F., & Gao, Y. (2015). Evaluation of structural and functional properties of protein–EGCG complexes and their ability of stabilizing a model β-carotene emulsion. *Food Hydrocolloids, 45*, 337-350.

Wickham, M., Wilde, P., & Fillery-Travis, A. (2002). A physicochemical investigation of two phosphatidylcholine/bile salt interfaces: implications for lipase activation. *Biochimica et Biophysica Acta (BBA)-Molecular and Cell Biology of Lipids, 1580*(2), 110-122.

Williams, D., Verghese, M., Walker, L., Boateng, J., Shackelford, L., & Chawan, C. (2007). Flax seed oil and flax seed meal reduce the formation of aberrant crypt foci (ACF) in azoxymethane-induced colon cancer in Fisher 344 male rats. *Food and Chemical Toxicology, 45*(1), 153-159.

Xu, H., Zhang, T., Lu, Y., Lin, X., Hu, X., Liu, L., Wu, X. (2019). Effect of chlorogenic acid covalent conjugation on the allergenicity, digestibility and functional properties of whey protein. *Food Chemistry, 298*, 125024.

Yang, C., Wang, B., Wang, J., Xia, S., & Wu, Y. (2019). Effect of pyrogallic acid (1, 2, 3-benzenetriol) polyphenol-protein covalent conjugation reaction degree on structure and antioxidant properties of pumpkin (Cucurbita sp.) seed protein isolate. *LWT, 109*, 443-449.

Yekdane, N., & Goli, S. A. H. (2019). Effect of pomegranate juice on characteristics and oxidative stability of microencapsulated pomegranate seed oil using spray drying. *Food and Bioprocess Technology, 12*(9), 1614-1625.

You, J., Luo, Y., & Wu, J. (2014). Conjugation of ovotransferrin with catechin shows improved antioxidant activity. *Journal of Agricultural and Food Chemistry, 62*(12), 2581-2587.

CHAPTER 3

Covalent modification of flaxseed protein isolate by phenolic compounds and the structure and functional properties of the adducts

Published in *Food chemistry,* 2019, 293, 463-471.

Food Chemistry 293 (2019) 463–471

Contents lists available at ScienceDirect

Food Chemistry

journal homepage: www.elsevier.com/locate/foodchem

Covalent modification of flaxseed protein isolate by phenolic compounds and the structure and functional properties of the adducts

Loc Bao Pham[a], Bo Wang[b], Bogdan Zisu[c], Benu Adhikari[a,*]

[a] School of Science, RMIT University, Melbourne, Vic 3028, Australia
[b] Nu-Mega Ingredients Pty Ltd, Brisbane, Qld 4109, Australia
[c] Spraying Systems Co. Pty Ltd, Truganina, Vic 3029, Australia

ARTICLE INFO

Keywords:
Flaxseed protein
Phenolic compounds
Antioxidant
Hydroxytyrosol
Covalent bonding
Crosslinking

ABSTRACT

Covalent modification of flaxseed protein isolate by phenolic compounds including flaxseed polyphenols, ferulic acid, and hydroxytyrosol was studied under alkaline condition and in the presence of oxygen. The structure and function of the adducts was evaluated. The extent of covalent reaction and the physicochemical characteristics of flaxseed protein isolate-phenolic adducts were found to depend on the structure of the phenolic compounds. The decrease in free amino, thiol and tryptophan groups and increase in molecular weight were different. Crosslinks were found in flaxseed protein isolate-hydroxytyrosol adducts while ferulic acid and flaxseed polyphenols were unable to crosslink flaxseed proteins. The thermal stability and antioxidative capacity of the adducts were higher than those of flaxseed protein isolate. The structural conformation and hydrophobicity of the adducts were also found to depend on the nature of phenolic compounds. These adducts can be used in food formulations as natural antioxidants, emulsifiers and encapsulating shell materials.

1. Introduction

Proteins can undergo covalent and/or non-covalent interactions with phenolic compounds and these interactions can modify the functional properties of proteins such as solubility, emulsifying, gelling, thermal stability and antioxidant capacity (Liu, Sun, Yang, Yuan, & Gao, 2015; Strauss & Gibson, 2004). The covalent interaction between protein and polyphenol has attracted greater research attention due to the stability of modified products brought about by the intrinsic strength of covalent interaction (Curcio et al., 2012). The thermal stability, antioxidant activity and emulsion stability of proteins can be altered by making use of the nature of protein, phenolic compound and their interactions (Liu, Ma, McClements, & Gao, 2017; Rawel, Czajka, Rohn, & Kroll, 2002). For example, Liu et al. (2017) observed that the thermal stability and antioxidant activity of zein protein increased in the zein-epigallocatechin gallate (EGCG) conjugate. Similarly, Liu et al. (2015) and Rawel, Czajka, et al. (2002) also observed improved emulsifying and solubility behaviour in lactoferrin-caffeic acid and soy glycinin-phenolic acid adducts compared to that of proteins.

The covalent reaction between protein and phenolic compounds can be carried out using enzymatic or non-enzymatic oxidation methods (Prigent, Voragen, Visser, van Koningsveld, & Gruppen, 2007). Among the non-enzymatic oxidation methods, alkaline treatment is most commonly used. So far, quite different mechanisms have been proposed to explain the reaction or interaction between protein and phenolic compounds using some commonly available proteins (Kroll & Rawel, 2001; Rawel, Czajka, et al., 2002; Rawel, Kroll, & Hohl, 2001; Strauss & Gibson, 2004). It is commonly accepted that the reaction between phenolic compounds and proteins starts from the formation of quinone or semiquinone radical intermediates. The formation of these radical intermediates itself depends on the structural configuration of phenolic compounds. For example, quinone radical intermediates are usually formed from phenolic compounds such as caffeic acid, gallic acid, quercetin and myricetin which have catechol in their structure (Rawel, Czajka, et al., 2002; Strauss & Gibson, 2004). The semiquinone radical intermediates are formed from ferulic acid, *p*-coumaric acid, and sinapic acid which have monophenols in their structure (Cilliers & Singleton, 1991; Rawel, Kroll, & Rohn, 2001). Subsequently, these quinone or semiquinone radical intermediates react and/or crosslink with protein chains (shown as Fig. 1A, B). However, to date, vast majority of published literature reports the interactions between proteins and phenolic substances using phenolic acids, flavonoids and their adducts (Liu et al., 2017; Rawel, Czajka, et al., 2002). There is not much information on the reaction behaviour of phenolic alcohols and their adducts such as hydroxytyrosol (HT) with proteins. HT is a o-diphenol found abundantly in olive oil and it possesses strong antioxidative

* Corresponding author.
E-mail address: benu.adhikari@rmit.edu.au (B. Adhikari).

https://doi.org/10.1016/j.foodchem.2019.04.123
Received 12 December 2018; Received in revised form 27 April 2019; Accepted 30 April 2019
Available online 02 May 2019

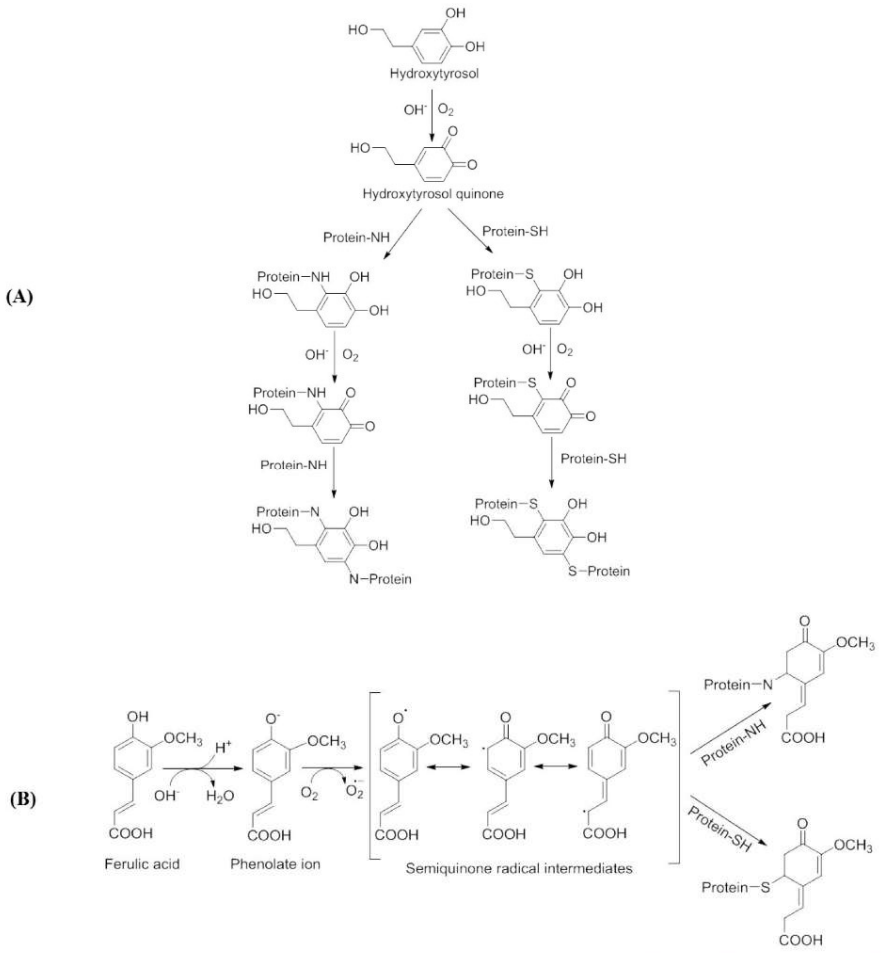

Fig. 1. Mechanism for the formation of FPI-HT (A) and FPI-FA (B) adduct. Adapted from Strauss and Gibson (2004) and Rawel, Kroll, and Rohn (2001). FPI = flaxseed protein isolate, FA = ferulic acid, HT = hydroxytyrosol.

activity and offers many health benefits including preventing cancer, protecting skin and eye, and easing inflammation (Martínez, Ros, & Nieto, 2018). On the other hand, although a large number of proteins such as glycinin, trypsin inhibitor (Rawel, Czajka, et al., 2002), myoglobin (Kroll, Rawel, & Seidelmann, 2000), gelatin (Strauss & Gibson, 2004) and whey protein (Rawel, Kroll, & Hohl, 2001) have been reported to react with phenolic compounds, most of these studies were performed using animal-based proteins. There still is a paucity of information on the nature of reaction between plant protein and plant phenolic compounds and the physicochemical characteristics of protein-phenolic adducts resulting from their reaction.

Flaxseed (*Linumusitatissimum* L.) is one of the most important oilseeds grown over the world with its production exceeding 2.9 million tonnes in 2016 (Food and Agriculture Organization, 2016). Currently, flaxseed is mainly used for its oil due to its high alpha-linolenic acid (ALA) content (> 50% of total fatty acids) (Daun, Barthet, Chornick, & Duguid, 2003) while the defatted meal is used as animal feed (Sielicka & Małecka, 2017) despite it being rich in protein and polyphenols (Dabrowski & Sosulski, 1984; Oomah, Mazza, & Cui, 1994). It is reported that the amino acid profiles and nutritional value of flaxseed protein is similar to those of soy protein (Madhusudhan & Singh, 1985). Flaxseed protein contains higher amount of branched chain amino acids (BCAA) such as isoleucine, leucine, and valine and a lower amount of aromatic amino acids (AAA) like phenylalanine and tyrosine compared to soy protein. This amino acid composition leads to a high Fischer ratio (BCCA/AAA) which helps to overcome the negative effect associated with burns, cancer, liver failure, and trauma (Wanasundara & Shahidi, 2003). Flaxseed protein also exhibits promising functional properties including high oil holding and foaming capacity, emulsifying activity and good thermal stability. It can be a protein of choice for the increasing vegetarian and vegan population. Flaxseed is also a rich source of polyphenols as it contains total phenolic content (TPC) of 5.42 g per 100 g seed. Flaxseed is known to contain about 800 mg–1000 mg phenolic acids, 500 mg esterified phenolic acids, and 300–500 mg etherified phenolic acids per 100 g of seed (Oomah, Kenaschuk, & Mazza, 1995). Ferulic acid (FA) was found to be a major phenolic acid in flaxseed together with *p*-coumaric, and caffeic acid (Waszkowiak, Gliszczyńska-Świgło, Barthet, & Skręty, 2015). These phenolic acids and their adducts were considered as the source of antioxidant properties in flaxseed.

In the above context, we studied the reaction between FPI and various phenolic compounds including FPP, FA and HT and the effect of this reaction on the physicochemical properties of FPI including the molecular weight, secondary structure, surface hydrophobicity, and

thermal and antioxidative stability. The nature and the mechanism of reaction between FPI and above polyphenols are explained making use of these physicochemical properties. This work shows that the FPI-phenolic adducts can be used as novel functional emulsifiers in various delivery systems used for the stabilisation of bioactive food ingredients.

2. Materials and methods

2.1. Materials

Flaxseed *sample* was obtained from Stoney Creek Oil Products Pty Ltd (Talbot, Victoria, Australia) and was stored at 4 °C before use. Trinitrobenzene sulfonic acid (TNBSA), 5,5′-dithio-bis-2-nitrobenzoic acid (DTNB), and ethylenediaminetetraacetic acid (EDTA) were purchased from Fisher Scientific (Loughborough Leicestershire, U.K.). Potassium ferricyanide, trichloroacetic acid, ferulic acid, Folin–Ciocalteu reagent, 8-Anilino-1-naphthalenesulfonic acid (ANS), *p*-coumaric acid, tryptophan, leucine, sodium dodecyl sulfate (SDS), (±)-6-Hydroxy-2,5,7,8-tetramethylchromane-2-carboxylic acid (trolox), 1,1-diphenyl-2-picrylhydrazyl (DPPH), and 2,20-azino-bis-3-ethylbenzthiazoline-6-sulphonic acid (ABTS) were purchased from Sigma Aldrich (Castle Hill, New South Wales, Australia). Hydroxytyrosol (HT, purity ≥ 95%) was purchased from AvaChem Scientific (San Antonio, Texas, USA). Mini-PROTEAN TGXTMprecast gel, Precision Plus Protein™ WesternC™ Blotting Standards (10–250 kDa), Tris/Glycine/SDS buffer, Coomassie Blue R-250 solution, Laemmli sample buffer, and 2-mercaptoethanol were purchased from Bio-Rad Incorporation (Gladesville, NSW, Australia).

2.2. Methods

2.2.1. Extraction of FPI

FPI was produced according to Oomah et al. (1994) with some modifications. Flaxseed gum was removed by stirring in Milli-Q water (1:18 w/w, 60 °C) for 2 h with the aid of ultrasonication. For doing this, ultrasonication at 400 W and 20 Hz (HD3400, Bandelin, Berlin, Germany) was performed for 2 min in every 20 min interval. After that, the seeds were filtrated and dehydrated at the ambient temperature for 48 h. These dried seeds were ground using a coffee grinder and defatted using hexane (1:6 w/v) for 2 cycles. This defatted-degummed flaxseed meal was sieved using a 150 μm sieve to remove non-protein non-gum residues. The sieved sample was air dried for 24 h. Finally, this defatted-degummed flaxseed flour was mixed with 0.1 M Tris buffer (pH 8.6) at a flour-to-buffer ratio of 1:16 (w/v). This slurry was stirred at 600 rpm for 16 h and centrifuged at 10,000 × *g* for 20 min. Then, the supernatant was collected and dialysed using a dialysing bag with molecular cut off weight of 6–8 kDa (Orange Scientific, Braine-l'Alleud, Belgium) against water for 48 h at 4 °C. This dialysed extract was freeze dried at −40 °C to obtain the FPI and was stored at 4 °C before use.

2.2.2. Extraction of flaxseed polyphenol

FPP was extracted from defatted degummed flaxseed meal according to Anwar and Przybylski (2012). In brief, the defatted degummed flaxseed flour was mixed with 60% (v/v) ethanol at the flour-to-ethanol ratio of 1:10 (w/v) and stirred at 750 rpm for 4 h at ambient temperature. Then, the slurry was centrifuged at 10,000 × *g* for 10 min to separate the residue and the supernatant. The residue was brought into the second extraction process and the supernatant from both extractions were pooled. The solvent was subsequently evaporated using a rotary vacuum evaporator (RC 2000, Buchi Corporation, Flawil, Switzerland) and the concentrated extract was freeze dried at −40 °C to prepare FPP powder. This FPP powder was stored at 4 °C before use.

2.2.3. Determination of chemical composition of FPI and FPP

Moisture, lipid, and ash contents of FPI were measured using AOAC methods 925.1, 920.85, and 923.03, respectively (AOAC, 2005). The total protein content of solid samples was measured by measuring nitrogen content and using a conversion factor of 6.25 (FP-2000, LECO Corporation, Saint Joseph, MI, U.S.A.) (Oomah, Der, & Godfrey, 2006). The protein content of aqueous protein solutions was determined by Bradford protein assay method using bovine serum albumin (BSA) as the standard.

The total phenolic content was determined using Folin–Ciocalteu method (Škerget et al., 2005) with minor modification. Briefly, 2.5 mL 0.1 N Folin–Ciocalteu reagent was added into 5 mL test tubes containing 0.5 mL samples. After 5 min, 2 mL Na_2CO_3 (7.5%, w/v) was added and the samples were incubated at 50 °C for 5 min. The absorbance of these mixtures was measured at 760 nm using a UV–Vis spectrophotometer (Lambda 35, Perkin Elmer, Llantrisant, U.K.). The total phenolic content of FPP is reported as ferulic acid equivalent. The main components (phenolic acids) of FPP were characterised using HPLC method (Waszkowiak et al., 2015).

2.2.4. Preparation of protein-phenolic adducts

FPI-FPP, FPI-FA, and FPI-HT adducts were produced following to Rawel, Czajka, et al. (2002). Firstly, the FPI solution was prepared by dispersing 1 g of FPI powder in 100 mL Milli-Q water at pH 9.0. Beforehand, the FPP was hydrolysed in 2 M NaOH for 2 h to break the large phenolic molecules (i.e., phenolic glycosides) to small ones (phenolic acids or flavonoids) and to facilitate its reaction with protein. After that, 0.3 mmol solution of phenolic compounds was added to the FPI solution. The pH of these mixtures as adjusted to 9.0 and agitated at 200 rpm for 24 h at ambient temperature in the presence of oxygen. To remove the unreacted phenolic compounds, these reacted mixtures were dialysed using dialysis bags with 6–8 kDa molecular weight cut off (Orange Scientific, Braine-l'Alleud, Belgium) against water for 20 h. The dialyzed FPI-phenolic adducts sample was finally freeze dried (− 40 °C) and stored at 4 °C before further analysis. In parallel, FPI (control) was prepared following the above listed procedure in the absence of phenolic compounds.

2.2.5. Determination of free amino, thiol and tryptophan contents

The free amino groups of protein-phenolic adducts were measured according to Adler-Nissen (1979) with minor modification. Briefly, 2 mg of each adduct sample was dissolved in 10 mL 0.1 M sodium bicarbonate buffer at pH 8.5. Subsequently, 0.25 mL TNBSA solution (0.01%, w/v) was added to 0.5 mL sample solution and incubated at 37 °C for 2 h. Finally, 0.25 mL 10% SDS and 0.125 mL 1 N HCl was added to each sample and their absorbance at 335 nm was measured using a UV–VIS spectrophotometer (Lambda 35, Perkin Elmer, Llantrisant, U.K.). The amount of free amino group was estimated using a calibration curve produced by using L-leucine solution.

The free thiol group was determined based on Liu et al. (2015). Firstly, 5,5-dithiobis nitro-benzoic acid (DTNB) reagent was prepared by dissolving 4 mg DTNB in 1 mL 50 mM Tris/HCl reaction buffer at pH 8.0 containing 1 mM EDTA. Secondly, 15 mg sample was dissolved in 5 mL reaction buffer containing 8 M urea and then 50 μl DTNB reagent was added. This reaction mixture was incubated at room temperature for 1 h and its absorbance was measured at 412 nm using the spectrophotometer listed above. The content of free thiol group was determined using Eq. (1):

$$SH = 73.53 \times A_{412}/C \quad (1)$$

where SH is the concentration of thiol group in nM per mg, A412 is the absorbance measured at 412 nm and C is the concentration of samples in mg/mL.

The tryptophan content in the samples was measured according to Rawel, Kroll, and Rohn (2001) with minor modification. Briefly, 5 mg of sample was suspended in 10 mL 8 M urea and the tryptophan content in the solution was measured using excitation and emission at the wavelengths of 295 nm and 300–500 nm, respectively using a florescence spectroscope (FlexStation 3, Molecular Devices Corporation,

Sunnyvale, CA, USA). The curve generated by L-tryptophan solution was used as the standard. The amount of protein bound with phenolic compounds was calculated using the decrease in free amino and thiol groups and tryptophan residue during the reaction.

2.2.6. Determination of molecular weight of FPI in protein-phenolic adducts

The sodium dodecyl sulfate-polyacrylamide gel electrophoresis (SDS-PAGE) analysis of protein and protein-phenolic adducts was performed using a 4–15% precast polyacrylamide gel under reducing condition. Briefly, sample solution (5 mg/mL) was mixed with loading buffer (95% Laemmli buffer and 5% 2-mercaptoethanol, w/w) at a sample-to-buffer ratio of 3:1 (v/v). This mixture was heated at 95 °C for 5 min and 12 µl sample was loaded into the precast gel. The SDS-PAGE test was run at 100 V for 90 min using Mini-PROTEAN Tetra Cell. Then the gel was removed and dyed with Coomassie Brilliant Blue R-250 solution for 24 h, followed by destaining with a mixture of acetic acid and methanol (6:4, v/v). Seven microliter WesternCTM blotting protein standard was used as a molecular weight maker.

The matrix-assisted laser desorption/ionization time of flight mass spectrometry (MALDI-TOF-MS) analysis of protein and protein-phenolic adducts was performed as follows: Firstly, 10 µl sample (1 mg/mL) was dissolved in 25 mM ammonium bicarbonate buffer at pH 8.0 containing 10 mM 2-mercapton ethanol. The sample solution was mixed with 10 µl matrix solution prepared by saturating sinapinic acid in 0.1% trifluoroaceticacid and 50% acetonitrile. Secondly, 1 µl of these samples was brought on to the target and was crystallised by air-drying for 30 min. Finally, samples were measured using an Auto Flex II TOF/TOF mass spectrometer (BrukerDaltonics, Billerica, MA, USA).

2.2.7. Characteristic infrared absorption bands of functional groups using Fourier transform infrared spectroscopy (FTIR)

The FTIR spectra of the samples were acquired in the range of 4000 to 400 cm^{-1}. Thirty-two scans were acquired and averaged at 4 cm^{-1} resolution. FTIR equipped with a MIRacel™ ZnSe single reflection ATR (Perkin-Elmer, Norwalk, CT, U.S.A.) was used for this purpose.

2.2.8. Determining the secondary structural features of FPI and its adducts

Circular dichroism (CD) spectra of the control FPI and its protein-phenolic adducts were obtained using the CD Spectropolarimeter 815 (Jasco International Co., Ltd., Tokyo, Japan). For this purpose, 8 µl of each sample solution (2.5 mg/mL) was prepared in sodium carbonate buffer at pH 8.0 and was loaded into a cylindrical quartz cell with an optical path length of 0.1 mm. The wavelength range of 180–260 nm was used to acquire the spectra with 3 accumulations and the secondary structural features of the samples were estimated using Dichroweb software (Lobley, Whitmore, & Wallace, 2002).

2.2.9. Determination of thermal behaviour of FPI and its FPI-phenolic adducts

Differential scanning calorimetry (DSC) is now commonly used to determine the irreversible unfolding or denaturation of proteins in food products including flaxseed protein. The denaturation temperature (T_d) and the denaturation enthalpy (ΔH) of FPI and FPI phenolic adducts were obtained by following Li-Chan and Ma (2002) approach with some modification. A modulated differential scanning calorimeter (DSC Q-2000, TA Instruments, New Castle, DE, U.S.A.) was used for this purpose. For this purpose, approximately 7 mg samples were loaded into an aluminium pan and hermetically sealed. These samples were heated from 25 °C to 180 °C at a rate of 10 °C/min under 20 mL/min nitrogen gas purge. Sealed empty pan was used as the control. The values of T_d and ΔH were acquired using Universal™ software (TA Instruments, New Castle, DE, U.S.A.).

The thermal stability of the unmodified (control) FPI and the FPI-phenolic adducts was also evaluated using Pyris 1 thermogravimetric analyser and associated Pyris™ software (Perkin Elmer Inc., Wellesley, MA, U.S.A.). Briefly, 5–7 mg sample was loaded into an aluminium pan and was heated from 35 °C to 750 °C at a rate of 10 °C/min under 20 mL/min nitrogen gas flow.

2.2.10. Determination of surface hydrophobicity

The hydrophobicity of the samples was measured according to Kato and Nakai (1980) with minor modification. Briefly, the sample solutions were prepared by dissolving the powder in 20 mM phosphate buffer solution at pH 7.4 and the mixture was stirred for 2 h at the ambient temperature. Then the dispersions were centrifuged at 1000 × *g* for 10 min and their supernatants were collected. A serial dilution of the supernatant was carried out to obtain 0.1–0.5 mg/mL protein concentration. Subsequently, 10 µl of 8 mM ANS solution, prepared in the same buffer solution, was added to 2 mL of the sample solution and the mixture was incubated at ambient temperature for 45 min. Finally, the fluorescence intensity (FI) of the samples at the above mentioned protein concentrations was measured at the excitation/emission wavelength of at 390/470 nm on a florescence spectrophotometer (CLARIOstar, BMG LABTECH GmbH, Ortenberg, Germany). The blank sample (protein without ANS) and the blank reagent (only buffer and ANS) were also prepared and their readings were used as relative fluorescence intensity (RFI). The protein concentration dependent initial slope of the RFI was computed using linear regression analysis and was used to calculate the protein surface hydrophobicity index (S_o).

2.2.11. Determination of antioxidative capacity of FPI and FPI-phenolic adducts

The solutions of FPI and FPI-phenolic adducts were prepared at the protein concentration of 0.5 mg/mL in Milli-Q water and their antioxidative capacity was evaluated in terms of free-radical scavenging activity and reducing power.

2,2-diphenyl-1-picrylhydrazyl (DPPH) scavenging activity: the DPPH scavenging activity of the samples was determined according to Gong et al. (2012) with some modifications. Briefly, 2 mL sample was added into 2 mL DPPH solution (1.75×10^{-4} M in methanol) and the mixture was placed in a dark room for 60 min. Subsequently, the DPPH content was quantified using a spectrophotometer (Lambda 35, Perkin Elmer, Llantrisant, U.K.) at 517 nm. The DPPH free radical activity was calculated and expressed as µmol Trolox equivalent (TE) per g of protein in the sample.

2,2′-Azino-bis(3-ethylbenzothiazoline-6-sulfonic acid (ABTS) scavenging activity: the ABTS scavenging activity of the samples was evaluated according to Siddhuraju (2006). In brief, 7 mM ABTS solution was prepared by dissolving 10 mg ABTS powder in 2.6 mL 2.45 mM potassium persulfate solution and the prepared ABTS solution was incubated at room temperature (22 ± 2 °C) from 12 to 16 h. This incubated ABTS solution was diluted with Milli-Q water until an absorbance of 7.0 ± 0.02 at 734 nm was achieved (Lambda 35, Perkin Elmer, Llantrisant, U.K.). In order to measure the ABTS scavenging activity of the samples, 1 mL sample was mixed with 3 mL diluted ABTS solution and incubated at room temperature (22 ± 2 °C) for 1 h. The ABTS concentration in the mixture was measured at 734 nm using a spectrophotometer listed above. The ABTS free radical activity was computed and expressed as µmol Trolox equivalent (TE) per g of protein in the sample.

Reducing power: The reducing power of samples was evaluated using the method described by Yıldırım, Mavi, and Kara (2001). Specifically, 1 mL sample was mixed with 2.5 mL 0.2 M sodium phosphate buffer (pH 6.6) followed by the addition of 2.5 mL potassium ferricyanide 1% (w/v). This mixture was incubated at 50 °C for 20 min and 2.5 mL trichloroacetic acid (10%, w/v) was added. The mixture was then centrifuged at 3000 × *g* for 10 min. Subsequently, 2.5 mL supernatant was collected and mixed with 0.5 mL Milli-Q water and 0.1 mL $FeCl_3$ solution (0.1%, w/v). The absorbance of the samples at 700 nm was measured and the reducing power of the sample was calculated, expressed as µmol Trolox equivalent (TE) per g of protein in the sample.

2.2.12. Statistical analysis

Experiments were conducted at least in triplicate and data were reported as mean ± standard deviation. The SPSS statistical software (version 24, SPSS Inc., Chicago, IL, USA) was used for the analysis of variance (ANOVA) in order to test the significance. Duncan test was carried out on the data sets using 95% significance level ($p < 0.05$).

3. Results and discussion

3.1. Chemical composition of FPI and FPP

The FPI extracted in this study contained 2.70 ± 0.04% (w/w) moisture, 93.60 ± 2.06% (w/w) protein, 2.10 ± 0.07% (w/w) lipid and 0.56 ± 0.07% (w/w) ash. The total phenolic content (TPC) of samples was expressed as mg ferulic acid equivalent (FAE) per 100 mg extract. It contained 113.6 ± 0.55 mg FAE per gram of extract. The ferulic acid and *p*-coumaric acid were found to be the major phenolic acids in the FPP accounted for 53.39 ± 0.48 mg and 5.86 ± 0.13 mg per g of extract, respectively.

3.2. Free amino, thiol and tryptophan contents in FPI and FPI-phenolic adducts

The free amino, thiol group and tryptophan contents of FPI (control) and FPI-phenolic adducts are shown in Table 1. As can be observed, the contents of these groups in FPI decreased significantly ($p < 0.05$) as a result of its covalent modification with phenolic compounds, especially with HT. This is because the HT was oxidised into *ortho*-quinone under the alkaline condition (pH 9.0) and in the presence of oxygen. The *ortho*-quinone then reacted with the nucleophile side chains of protein to form C–N and C–S linkages as shown in Fig. 1A (Strauss & Gibson, 2004). The reactions leading to the formation of FPI-FA and FPI-FPP adducts can be explained using the mechanism proposed by Rawel, Kroll, and Rohn (2001). Once the phenolate ion is formed, the ferulic acid is able to react with oxygen to produce semiquinone which subsequently bonds covalently with side chains of FPI (Fig. 1B).

The decrease in the number of free thiol group in FPI after its covalent modification with phenolic compounds can be explained according to the reaction mechanism proposed by Strauss and Gibson (2004). According to this mechanism, the free thiol groups of cysteine in FPI react with the oxidised phenolic compounds. Furthermore, the fluorescent intensity of FPI-phenolic adducts was lower than that of FPI indicating the fact that the formation of covalent bond had taken place between tryptophan and oxidised phenolic compounds. This is because the presence of urea had already destroyed non-covalent bonding such as hydrogen bonds (Rawel, Kroll, & Rohn, 2001). HT was able to bind with two or more protein molecules during modification suggesting that its reactivity with FPI was the highest among the phenolic compounds tested (Table 1). This can be attributed to i) the presence of higher number of hydroxyl group per unit mass of HT and ii) the distribution pattern of hydroxyl group on its aromatic rings (Rawel, Czajka, et al., 2002). In this regard, Kroll et al. (2000) also explained that the high reactivity of *p*-quinone with myoglobin was also due to these reasons. There was no significant difference ($p > 0.05$) on the amount of covalently bound FPI in FPI-FPP and FPI-FA adducts, most probably due to similar molecular weight of FPP and FA. FA has the molecular weight of 194 Da while FPP is a natural mixture of phenolic compounds including *trans*-ferulic acid (approximately 194 Da) and p-coumaric acid (approximately 164 Da) (Oomah et al., 1995). Accordingly, the ability of phenolic compounds to undergo modification with FPI depended on the nature of the phenolic compounds. This observation agrees well with that of Rawel, Kroll, and Rohn (2001) who reported that the crosslinking ability of dihydroxybenzenes (m-resorcinol, o-pyrocatechol and p-hydroquinone) with nucleophiles (lysine, tryptophan, tyrosine, cysteine) was higher than that with ferulic acid. Rawel, Czajka, et al. (2002) also reported that the extent of the decrease in the number of thiol group and tryptophan residues in glycinin varied depending on the structure of participating phenolic compounds.

3.3. Change in molecular weight of FPI due to reaction with phenolic compounds

The results of the SDS-PAGE carried out under reducing condition created by SDS and 2-mercaptoethanol are shown in Fig. 2A. No significant ($p > 0.05$) change in the molecular weight of FPI-FPP and FPI-FA adducts was observed, compared to that of FPI (control). Interestingly, the results obtained from MALDI-TOF-MS, presented below, do show that the molecular weight of modified FPI was different than that of the unmodified one. In the case of FPI-HT adduct, a decrease in intensity of bands in the 10–30 kDa range and the appearance of new bands in the 50–60 kDa range and above 70 kDa were observed. These SDS-PAGE results further confirm covalent modification of FPI with HT. Rawel and Rohn (2010) reported that the reaction between a phenolic compound and a protein depends primarily on the structure of phenolic compound. The structure of a phenolic compound determines its ability to autooxidise and produce redox active quinone under alkaline condition. This is because the presence of active quinone is a prerequisite for the interaction to take place with the side chains of a protein.

In order to investigate the effect of interaction of phenolic compounds with FPI and subsequent change in its molecular weight, MALDI-TOF-MS analysis was performed, and the result is shown in Fig. 2B. The data shows that there is slight increase in molecular weight around 20 kDa within the molecular weight range of 10–30 kDa in all the protein-phenolic adducts. This increase can be attributed to the reaction of low molecular weight phenolic compounds with FPI. Similar increase of molecular weight was also observed in the range of 40–55 kDa in all the protein-phenolic adducts. We wish to stress here that this change in molecular weight was not observed in SDS-PAGE data indicating the fact that MALDI-TOF-MS is a much more sensitive method. Moreover, a new peak was detected around 61 kDa in FPI-HT adduct which agrees well with the SDS-PAGE data presented above.

The MALDI-TOF-MS results can be used to describe the covalent reaction between FPI and phenolic compounds (Fig. 1). In the case of FPI-FA and FPI-FPP adducts, FA and FPP first formed the semiquinone and then attached onto the side chain of FPI. This led to the small increase in the molecular weight of covalently modified FPI in 10–30 kDa and 30–55 kDa ranges (Fig. 2B). In the case of oxidised HT, there was a decrease in 13 kDa with appearance of 60 kDa (Fig. 2B).

Table 1
The free amino group, thiol group, tryptophan residue contents in the control FPI and FPI-phenolic adducts (nmol/mg protein). FPI = flaxseed protein isolate, FPP = flaxseed polyphenols, FA = ferulic acid, HT = hydroxytyrosol.

Sample	Free amino group	Thiol group	Tryptophan	Bounded protein groups
FPI	929.85 ± 41.64a	40.39 ± 1.30a	71.69 ± 2.03a	–
FPI-FPP adduct	810.49 ± 24.04b	29.54 ± 1.50b	43.38 ± 4.37b	158.52 ± 16.26a
FPI-FA adduct	748.89 ± 65.68b	33.58 ± 0.46c	44.55 ± 5.26b	214.91 ± 30.82a
FPI-HT adduct	579.47 ± 13.33c	2.02 ± 0.37d	37.42 ± 2.54b	423.02 ± 29.42b

Different letters in the same column indicate significant differences ($p < 0.05$).

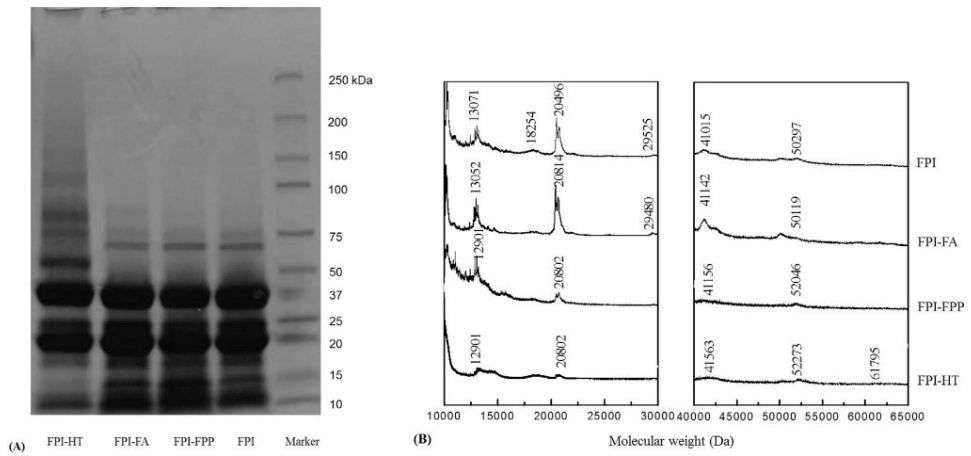

Fig. 2. SDS-PAGE (A) and MALDI-TOF-MS (B) analysis of the control FPI, FPI-FA, FPI-FPP, and FPI-HT adducts in the range of 10,000–30,000 and 40,000–65,000 Da. FPI = flaxseed protein isolate, FA = ferulic acid, FPP = flaxseed polyphenols, HT = hydroxytyrosol.

3.4. Conformation of FPI and phenolic compound reaction through FTIR

The FTIR spectra of FPI and its adducts are shown in Fig. 3A. These spectra show that there is no significant shift of amide I band (1600–1700 cm^{-1}) due to the reaction between FPI and phenolic compound. However, the change in the lower and upper wavelength number of amide II band in the FPI and its adducts were observed (1510–1580 and 1520–1531 cm^{-1} for FPI and FPI-phenolics adducts, respectively). It is now accepted that amide I band occurs due to stretching vibrations of C=O and C–N while amide II band occurs due to in-plane N–H bending and C–N, C–C stretching vibrations (Susi & Byler, 1986). The shift of the amide II band towards higher wavenumber further confirms the fact that chemical reaction has taken place between FPI and phenolic compounds (Jackson & Mantsch, 1995). The detailed secondary structural features of both modified and unmodified FPI are documented in the next section.

3.5. Conformational structure of FPI and FPI-phenolic adducts

The far UV-CD spectra of FPI and protein-phenolic adducts are presented in Fig. 3B. The spectra exhibited positive peaks in the wavelength range of 190–195 nm due to α-helix and β-strand structure and negative peaks in the wavelength range of 207–208 nm contributed by the α-helix structure. The positive peaks in between 190 and 195 nm suggest to an alteration in α-helix and β-strand content due to the chemical reaction. Changes of this nature on the secondary structures of the protein due to its interaction with phenolic compounds were also reported by Liu et al. (2017) and Rawel, Czajka, et al. (2002). These authors reported that the conjugation between zein and quercetagetin decreased in α-helix and increased in β-turn while the reaction of soy glycinin with caffeic and gallic acid marginally increased in α-helix content, respectively.

The percentage composition of individual secondary structure components of FPI and FPI-phenolic adducts estimated by CDSSTR method is shown in Fig. 3C. As can be observed, conformational structure of FPI was changed due to its reaction with phenolic compounds. These changes (structural features) are different in different FPI-phenolic adducts which could be attributed to different phenol type. In the case of FPI-FPP adduct, the increase in α-helix and β-strand ($p < 0.05$) were observed accompanied by a decrease in the unordered coil ($p < 0.05$). In the case of FPI-FA adduct, an increase in α-helix and β-turn ($p < 0.05$) was observed. In the case of FPI-HT adduct, a decrease in α-helix and an increase in β-turn occurred ($p < 0.05$).

3.6. Thermal stability of FPI-phenolic adducts

The onset (T_{onset}), peak (T_d) and endset (T_{endset}) denaturation temperature and the denaturation enthalpy (ΔH) of FPI and its adducts with phenolic compounds are presented in Table 2. The T_d (147 °C) of FPI is somewhat higher than the value 138.5 °C reported by Alu'datt, Rababah, and Alli (2014). This may be due to the presence of higher percentage of 11–12S globulin fraction in our FPI samples. Oomah and Mazza (1993) reported that the flaxseed protein was comprised of approximately 20% low molecular weight protein (1.6-2S albumin fraction) and 80% high molecular weight proteins (11-12S globulin fraction). It is not uncommon for highly compact globular proteins to have denaturation temperature as we have observed (Privalov & Gill, 1988). Similarly, Savadkoohi, Bannikova, Mantri, and Kasapis (2016) reported that the denaturation temperature of the soy proteins increased to 140 °C with the increase of its 11S globulin (glycinin) content to 80% (w/w). The T_d value of the protein-phenolic adducts was significantly higher than that of FPI ($p < 0.05$), suggesting that these adducts had improved thermal stability. Among these FPI-phenolic adducts, FPI-HT adduct exhibited the highest denaturation temperature (154.3 °C), which could be correlated with the conformational change in FPI when it was covalently modified by HT. It was reported by Alu'datt et al. (2014) that the thermal stability of flaxseed protein isolate was much higher in the presence of free and bound phenolic compounds. Rawel, Czajka, et al. (2002) also reported an increase of T_d and ΔH values in soy protein after it was covalently modified with polyphenols. However, the total energy required for the denaturation of FPI (control) and FPI in FPI-phenolic adducts was very close ($p > 0.05$). This observation agrees with that of Damodaran and Agyare (2013) and indicates to the insignificant contribution of non-covalent linkages arisen from the addition of carboxylic and hydroxyl groups to thermal stability.

The thermogravimetric analysis data of FPI and FPI-phenolic adducts are shown in Table 2. The initial degradation temperatures of FPI and its phenolic adducts were very close (about 259 °C) except for FPI-HT adducts (265 °C). This significantly higher degradation temperature of FPI-HT adduct indicates to its better thermal stability compared to FPI and its adducts with FPP and FA. The $D_{1/2}$ temperature at which half of the sample was decomposed followed the FPI < FPI-FA < FPI-FPP < FPI-HT order, which also agrees with the content of reactive groups and molecular weight data of FPI presented in earlier sections. The temperature at which maximum denaturation rate (MDRT) occurred was found to be around 315 °C which was similar ($p > 0.05$) for FPI, FPI-FA, and FPI-HT adducts. MDRT of FPI-FPP was significant the

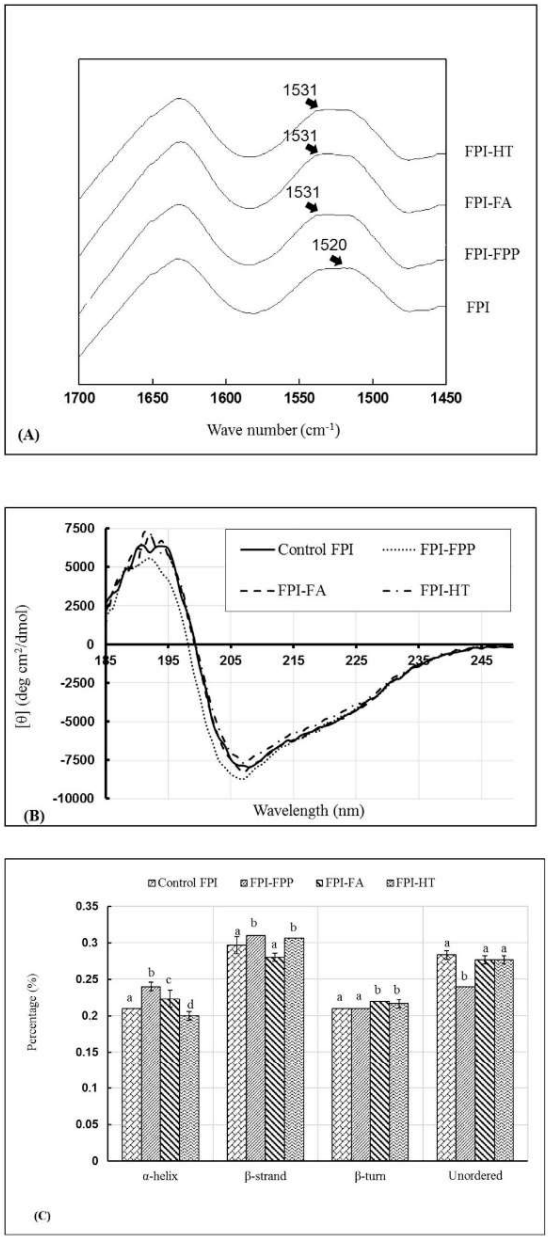

Fig. 3. FTIR (A) and Far UV (B) spectra, and secondary structure ratio (C) of control FPI, FPI-FPP, FPI-FA and FPI-HT adducts. FPI = flaxseed protein isolate, FPP = flaxseed polyphenols, FA = ferulic acid, HT = hydroxytyrosol.

lowest most probably due to the presence of thermally sensitive phenolic compounds in FPP mix.

3.7. Surface hydrophobicity of FPI and FPI-phenolic adducts

The surface hydrophobicity of FPI and FPI-phenolic adducts is shown in Table 3. Compared with FPI, a significant increase in surface hydrophobicity was observed in FPI-FPP and FPI-FA adducts. These results indicated that the formation of the adducts reduced the number of hydrophilic amino and thiol residues as they bonded with oxidised phenolic compounds. This modification also increased the non-polar groups containing aromatic rings (Kroll & Rawel, 2001). In this regard, Kroll et al. (2000) also reported a decreased solubility/increased surface hydrophobicity of myoglobin after its conjugation with chlorogenic and caffeic acid and *p*-quinone.

In the case of FPI-HT adduct, a significant ($p < 0.05$) decrease in the surface hydrophobicity was observed, which can be due to increased exposure of hydrophilic groups in FPI-HT adducts brought about by the conformational change (Rawel, Kroll, & Hohl, 2001). Hydrophobic residues of FPI such as tryptophan were blocked when it reacted with HT and new hydrophilic groups such as hydroxyl groups from HT were introduced to the protein chain (Rawel, Czajka, et al., 2002). This ultimately contributed to the decrease in the surface hydrophobicity of FPI-HT adduct. This observation is in accordance to Rawel, Rohn, Kruse, and Kroll (2002) who reported a decrease in surface hydrophobicity of bovine serum albumin after its reaction with chlorogenic acid.

3.8. Antioxidative capacity of FPI-phenolic adducts

The free radicals (DPPH and ABTS) scavenging activity and reducing power of the FPI-phenolic adducts are shown in Table 3, along with that of FPI. Compared with FPI, all FPI-phenolic adducts exhibited improved free radical scavenging and iron(III) reducing capacity. Specifically, the DPPH and ABTS radical scavenging activity of FPI-FPP and FPI-FA adducts was approximate 2.5 and 4.5 times higher than that of FPI, respectively. Similarly, the improved reducing power of all the adducts was also observed. Liu et al. (2015) found that after lactoferrin formed adducts with EGCG, chlorogenic acid, and gallic acid, the authors observed a significant increase in the antioxidative capacity of the protein. In this study, the extent of the improvement in the antioxidative capacity varied, depending on the nature of the reacting phenolic compounds. For example, FPI-FPP and FPI-FA adducts exhibited higher free radical scavenging activity and reducing power than FPI-HT adduct. Although there was no significantly difference in the DPPH scavenging activity between FPI-FA and FPI-FPP adducts, a significantly higher ABTS scavenging activity was observed in FPI-FA adduct.

4. Conclusion

This study shows that the covalent modification of FPI with phenolic compounds (FPP, FA, HT) significantly affected its molecular weight, structural conformation, surface hydrophobicity, thermal stability and antioxidant capacity. The extent and nature of covalent reaction between FPI and phenolic compounds varied, depending on the nature of the phenolics. The highest degree of reaction occurred between FPI and HT. FA and FPP interacted with the side chain of FPI which only marginally increased the molecular weight of FPI while HT crosslinked FPI and produced protein crosslinks with molecular mass > 60 kDa. The covalent modification of FPI with phenolic compounds altered conformational structure and surface hydrophobicity FPI. The FPI-FPP and FPI-FA were more hydrophobic while FPI-HT was more hydrophilic than FPI. Covalent modification of FPI with phenolic compounds significantly increased the denaturation temperature of the products. FPI-phenolic adducts also had significantly improved antioxidative capacity. These findings can be used to develop novel plant protein-phenolic adducts that can be preferably used as healthy antioxidants, emulsifiers and encapsulating shell materials for stabilisation of bioactive ingredients.

Declaration of Competing Interest

The authors do not have conflict of interest. All authors have agreed

Table 2
Thermal parameters of the control FPI and FPI-phenolic adducts by MDSC and TGA. T_d = denaturation temperature, ΔH = denaturation enthalpy, IDT = initial decomposition temperature, $D_{1/2}$ = the temperature for 50 wt% decomposition, MRDT = the temperature for the maximum rate of decomposition. FPI = flaxseed protein isolate, FPP = flaxseed polyphenols, FA = ferulic acid, HT = hydroxytyrosol.

Sample	T_{onset} (°C)	T_d (°C)	T_{endset} (°C)	ΔH (J/g)	IDT (°C)	$D_{1/2}$ (°C)	MRDT (°C)
FPI	142.41 ± 1.46a	147.06 ± 1.42a	152.46 ± 1.09a	6.88 ± 0.13a	259.31 ± 2.28a	376.0 ± 6.24a	317.33 ± 1.15a
FPI-FPP adduct	147.46 ± 0.99b	152.03 ± 0.94b	157.48 ± 0.98b	6.79 ± 0.22a	259.54 ± 3.11a	379.67 ± 2.52a	312.67 ± 2.30b
FPI-FA adduct	146.43 ± 0.75b	151.06 ± 0.73b	156.22 ± 0.71b	7.46 ± 0.52a	260.45 ± 1.98a	377.0 ± 1.0a	318.33 ± 1.15a
FPI-HT adduct	149.57 ± 0.18c	154.30 ± 0.21c	159.45 ± 0.22c	6.96 ± 0.61a	265.92 ± 3.60b	387.67 ± 4.04b	317.0 ± 2.64a

Different letters in the same column indicate significant differences ($p < 0.05$).

Table 3
Hydrophobicity index (S_0) and antioxidant capacity of the control FPI and FPI-phenolic adducts (μmol trolox per g protein). FPI = flaxseed protein isolate, FPP = flaxseed polyphenols, FA = ferulic acid, HT = hydroxytyrosol.

Sample	Hydrophobicity index (S_0)	DPPH· scavenging capacity	ABTS· scavenging capacity	Reducing power
FPI	120.63 ± 14.78a	44.83 ± 1.61a	143.30 ± 1.64a	10.91 ± 0.43a
FPI-FPP adduct	141.34 ± 8.50b	110.66 ± 4.84b	632.47 ± 3.57b	68.14 ± 1.57b
FPI-FA adduct	232.49 ± 10.83c	112.28 ± 4.05b	640.05 ± 4.98c	62.86 ± 1.03b
FPI-HT adduct	47.95 ± 1.18d	101.06 ± 2.68c	258.11 ± 0d	38.72 ± 4.88c

Different letters in the same column indicate significant differences ($p < 0.05$).

with the content and also agreed to submit the manuscript to Food Chemistry. This research did not receive any specific grant from funding agencies in the public, commercial, or not-for-profit sectors.

Appendix A. Supplementary data

Supplementary data to this article can be found online at https://doi.org/10.1016/j.foodchem.2019.04.123.

References

Adler-Nissen, J. (1979). Determination of the degree of hydrolysis of food protein hydrolysates by trinitrobenzenesulfonic acid. *Journal of Agricultural and Food Chemistry, 27*(6), 1256–1262.

Alu'datt, M. H., Rababah, T., & Alli, I. (2014). Effect of phenolic compound removal on rheological, thermal and physico-chemical properties of soybean and flaxseed proteins. *Food Chemistry, 146*, 608–613.

Anwar, F., & Przybylski, R. (2012). Effect of solvents extraction on total phenolics and antioxidant activity of extracts from flaxseed (Linum usitatissimum L.). *Acta Scientiarum Polonorum Technologia Alimentaria, 11*(3), 293–302.

AOAC (2005). *Official methods of analysis* (18th ed.). Arlington, VA: Association of Official Analytical Chemists.

Cilliers, J. J., & Singleton, V. L. (1991). Characterization of the products of nonenzymic autoxidative phenolic reactions in a caffeic acid model system. *Journal of Agricultural and Food Chemistry, 39*(7), 1298–1303.

Curcio, M., Parisi, O. I., Puoci, F., Altimari, I., Spizzirri, U. G., & Picci, N. (2012). Antioxidant polymers by free radical grafting on natural polymers. *Antioxidant Polymers: Synthesis, Properties, and Applications*, 153–178.

Dabrowski, K. J., & Sosulski, F. W. (1984). Composition of free and hydrolyzable phenolic acids in defatted flours of ten oilseeds. *Journal of Agricultural and Food Chemistry, 32*(1), 128–130.

Damodaran, S., & Agyare, K. K. (2013). Effect of microbial transglutaminase treatment on thermal stability and pH-solubility of heat-shocked whey protein isolate. *Food Hydrocolloids, 30*(1), 12–18.

Daun, J. K., Barthet, V. J., Chornick, T., & Duguid, S. (2003). Structure, composition, and variety development of flaxseed. *Flaxseed in Human Nutrition, 2*, 1–40.

Food and Agriculture Organization. (2016). URL http://www.fao.org/faostat/en/#data/QC Accessed 14.02.18.

Gong, Y., Hou, Z., Gao, Y., Xue, Y., Liu, X., & Liu, G. (2012). Optimization of extraction parameters of bioactive components from defatted marigold (Tagetes erecta L.) residue using response surface methodology. *Food and Bioproducts Processing, 90*(1), 9–16.

Jackson, M., & Mantsch, H. H. (1995). The use and misuse of FTIR spectroscopy in the determination of protein structure. *Critical Reviews in Biochemistry and Molecular Biology, 30*(2), 95–120.

Kato, A., & Nakai, S. (1980). Hydrophobicity determined by a fluorescence probe method and its correlation with surface properties of proteins. *Biochimica et Biophysica Acta (BBA)-Protein Structure, 624*(1), 13–20.

Kroll, J., & Rawel, H. M. (2001). Reactions of plant phenols with myoglobin: Influence of chemical structure of the phenolic compounds. *Journal of Food Science, 66*(1), 48–58.

Kroll, J., Rawel, H. M., & Seidelmann, N. (2000). Physicochemical properties and susceptibility to proteolytic digestion of myoglobin – Phenol derivatives. *Journal of Agricultural and Food Chemistry, 48*(5), 1580–1587.

Li-Chan, E. C. Y., & Ma, C.-Y. (2002). Thermal analysis of flaxseed (Linum usitatissimum) proteins by differential scanning calorimetry. *Food Chemistry, 77*(4), 495–502.

Liu, F., Ma, C., McClements, D. J., & Gao, Y. (2017). A comparative study of covalent and non-covalent interactions between zein and polyphenols in ethanol-water solution. *Food Hydrocolloids, 63*, 625–634.

Liu, F., Sun, C., Yang, W., Yuan, F., & Gao, Y. (2015). Structural characterization and functional evaluation of lactoferrin–polyphenol conjugates formed by free-radical graft copolymerization. *RSC Advances, 5*(20), 15641–15651.

Lobley, A., Whitmore, L., & Wallace, B. (2002). DICHROWEB: An interactive website for the analysis of protein secondary structure from circular dichroism spectra. *Bioinformatics, 18*(1), 211–212.

Madhusudhan, K., & Singh, N. (1985). Isolation and characterization of the major fraction (12 S) of linseed proteins. *Journal of Agricultural and Food Chemistry, 33*(4), 673–677.

Martínez, L., Ros, G., & Nieto, G. (2018). Hydroxytyrosol: Health benefits and use as functional ingredient in meat. *Medicines, 5*(1), 13.

Oomah, B., & Mazza, G. (1993). Flaxseed proteins—A review. *Food Chemistry, 48*(2), 109–114.

Oomah, B. D., Der, T. J., & Godfrey, D. V. (2006). Thermal characteristics of flaxseed (Linum usitatissimum L.) proteins. *Food Chemistry, 98*(4), 733–741.

Oomah, B. D., Mazza, G., & Cui, W. (1994). Optimization of protein extraction from flaxseed meal. *Food Research International, 27*(4), 355–361.

Oomah, D. B., Kenaschuk, O. E., & Mazza, G. (1995). Phenolic acid in flaxseed. *Journal of Agricultural and Food Chemistry, 43*, 2016–2019.

Prigent, S. V., Voragen, A. G., Visser, A. J., van Koningsveld, G. A., & Gruppen, H. (2007). Covalent interactions between proteins and oxidation products of caffeoylquinic acid (chlorogenic acid). *Journal of the Science of Food and Agriculture, 87*(13), 2502–2510.

Privalov, P. L., & Gill, S. J. (1988). Stability of protein structure and hydrophobic interaction. *Advances in protein chemistry: vol. 39*, (pp. 191–234). Elsevier.

Rawel, H. M., Czajka, D., Rohn, S., & Kroll, J. (2002a). Interactions of different phenolic acids and flavonoids with soy proteins. *International Journal of Biological Macromolecules, 30*(3–4), 137–150.

Rawel, H. M., Kroll, J., & Hohl, U. (2001a). Model studies on reactions of plant phenols with whey proteins. *Molecular Nutrition & Food Research, 45*(2), 72–81.

Rawel, H. M., Kroll, J., & Rohn, S. (2001b). Reactions of phenolic substances with lysozyme – physicochemical characterisation and proteolytic digestion of the derivatives. *Food Chemistry, 72*(1), 59–71.

Rawel, H. M., & Rohn, S. (2010). Nature of hydroxycinnamate-protein interactions. *Phytochemistry Reviews, 9*(1), 93–109.

Rawel, H. M., Rohn, S., Kruse, H.-P., & Kroll, J. (2002b). Structural changes induced in bovine serum albumin by covalent attachment of chlorogenic acid. *Food Chemistry, 78*(4), 443–455.

Savadkoohi, S., Bannikova, A., Mantri, N., & Kasapis, S. (2016). Structural modification in condensed soy glycinin systems following application of high pressure. *Food Hydrocolloids, 53*, 115–124.

Siddhuraju, P. (2006). The antioxidant activity and free radical-scavenging capacity of phenolics of raw and dry heated moth bean (Vigna aconitifolia)(Jacq.) Marechal seed extracts. *Food Chemistry, 99*(1), 149–157.

Sielicka, M., & Małecka, M. (2017). Enhancement of oxidative stability of flaxseed oil through flaxseed, evening primrose and black cumin cake extracts. *Journal of Food Processing and Preservation, 41*(4).

Škerget, M., Kotnik, P., Hadolin, M., Hraš, A. R., Simonič, M., & Knez, Ž. (2005). Phenols, proanthocyanidins, flavones and flavonols in some plant materials and their antioxidant activities. *Food Chemistry, 89*(2), 191–198.

Strauss, G., & Gibson, S. M. (2004). Plant phenolics as cross-linkers of gelatin gels and gelatin-based coacervates for use as food ingredients. *Food Hydrocolloids, 18*(1),

81–89.
Susi, H., & Byler, D. M. (1986). Resolution-enhanced fourier transform infrared spectroscopy of enzymes. *Methods in Enzymology, 130*, 290–311.
Wanasundara, P., & Shahidi, F. (2003). Flaxseed proteins: Potential food applications and process-induced changes. *Flaxseed in Human Nutrition*, 387–403.
Waszkowiak, K., Gliszczyńska-Świgło, A., Barthet, V., & Skręty, J. (2015). Effect of extraction method on the phenolic and cyanogenic glucoside profile of flaxseed extracts and their antioxidant capacity. *Journal of the American Oil Chemists' Society, 92*(11–12), 1609–1619.
Yıldırım, A., Mavi, A., & Kara, A. A. (2001). Determination of antioxidant and antimicrobial activities of Rumex crispus L. extracts. *Journal of Agricultural and Food Chemistry, 49*(8), 4083–4089.

CHAPTER 4

Complexation between flaxseed protein isolate and phenolic compounds: Effects on interfacial, emulsifying and antioxidant properties of emulsions

Published in *Food hydrocolloids,* 2019, 94, 20-29.

Food Hydrocolloids 94 (2019) 20–29

Contents lists available at ScienceDirect

Food Hydrocolloids

journal homepage: www.elsevier.com/locate/foodhyd

Complexation between flaxseed protein isolate and phenolic compounds: Effects on interfacial, emulsifying and antioxidant properties of emulsions

Loc B. Pham[a], Bo Wang[b], Bogdan Zisu[a], Benu Adhikari[a,*]

[a] School of Science, RMIT University, Melbourne, VIC, 3028, Australia
[b] Nu-Mega Ingredients Pty Ltd, Brisbane, QLD, 4109, Australia

ARTICLE INFO

Keywords:
Interfacial tension
Emulsion stability
Oxidative stability
Adsorption
Dilatational rheology

ABSTRACT

Interfacial and emulsifying properties of flaxseed protein isolate (FPI) and its phenolic complexes were studied, aiming to develop plant-based natural emulsifiers with improved interfacial and oxidative activity and adding value to the by-product of flaxseed oil production. Flaxseed polyphenols (FPP) and hydroxytyrosol (HT) were used as model phenolic compounds. The stability of emulsions produced using FPI, FPI-FPP and FPI-HT as emulsifiers was measured and correlated with their solubility and surface charge. The dynamic interfacial tension (DIT) and dilatational elasticity (E′) and viscosity (E″) were measured at flaxseed oil/water interface. The diffusion and penetration rate constants were calculated using DIT data. The complexation of FPI with FPP and HT significantly increased the diffusion rate constant at low FPI concentration (0.1 mg mL^{-1}). At higher FPI concentration (from 1 to 10 mg mL^{-1}), the DIT and penetration rate constant of FPI, FPI-FPP and FPI-HT were not different. The E' of interfacial layer of FPI was lower than that of FPI-HT interfacial layer but was higher than that of FPI-FPP interfacial layer. The E" of FPI-FPP and FPI-HT complexes was lower than that of FPI. FPI-stabilised emulsion with higher charge density had higher physical stability compared to the emulsions stabilised by FPI-phenolic complexes which had lower charge density. The emulsions stabilised by FPI-FPP and FPI-HT complexes had higher antioxidative stability compared to that of FPI stabilised emulsion. The emulsions stabilised by FPI-FPP and FPI-HT complexes had higher red and yellow hue than the emulsion stabilised by FPI.

1. Introduction

The interactions between proteins and polyphenols can enhance the stability of protein based colloid systems and protein stabilised emulsions. For example, the stability of emulsion produced using lactofferin-caffeic covalent conjugate as emulsifier was better than that of native lactofferin stabilised emulsion (Liu, Sun, Yang, Yuan, & Gao, 2015). Similarly, Banerjee et al. (2013) reported that the stability of Tween 20/β-lactoglobulin stabilised foam was improved by crosslinking β-lactoglobulin molecules with (+)-catechin at the adsorbed layer. However, the interaction between proteins and polyphenols may also bring undesirable effects on some functional properties of proteins. For instance, the complexation of green tea polyphenols and whey proteins reduced the interfacial tension and viscoelasticity of adsorbed layer, leading to the faster drainage of the foam (Rodríguez, von Staszewski, & Pilosof, 2015). Similarly, a compromised interfacial activity of β-lactoglobulin-green tea polyphenol complex was also reported compared to that of β-lactoglobulin (von Staszewski, Pizones Ruiz-Henestrosa, & Pilosof, 2014).

The change in functional properties of proteins arising from their interaction with polyphenols depends on the non-covalent or covalent nature of interaction. The non-covalent interaction includes hydrogen bonding, ionic and/or hydrophobic interaction (Ozdal, Capanoglu, & Altay, 2013). The covalent interaction involves the oxidation of polyphenols to quinones and the subsequent addition of nucleophiles such as lysine or thiol group on the side chain of proteins to quinones (Cilliers & Singleton, 1991). The covalent interaction is more desirable because it produces covalent complexes which are more stable (Curcio et al., 2012). It was reported that the thermal stability and antioxidant activity of covalently bonded zein-epigallocatechin gallate (EGCG) complex were improved compared to those of non-covalently bonded one. Thus, these beneficial properties of protein-polyphenol complexes can be utilised to improve the thermal property of proteins when they are used as encapsulant. For example, von Staszewski et al. (2014) showed that the stability of fish oil against oxidation was enhanced in the presence of green tea polyphenols in emulsions stabilised by β-lactoglobulin-green tea polyphenol complexes.

Flaxseed protein has comparable amino acid profile and nutritional

* Corresponding author.
E-mail address: benu.adhikari@rmit.edu.au (B. Adhikari).

https://doi.org/10.1016/j.foodhyd.2019.03.007
Received 26 November 2018; Received in revised form 5 March 2019; Accepted 5 March 2019
Available online 08 March 2019
0268-005X/

value to soy protein (Madhusudhan & Singh, 1985). More importantly, flaxseed protein possesses promising functional properties such as emulsifying property and good thermal stability (Kaushik et al., 2016). Despite these valuable properties flaxseed protein is poorly utilised and its major source (flaxseed meal) is commonly used as animal feed (Sielicka & Małecka, 2017). As consumers are increasingly drawn towards plant proteins (Can Karaca, Low, & Nickerson, 2013; Chen, Zhang, & Tang, 2016; Ma, Boye, & Simpson, 2016), it is expected that flaxseed protein will be used in many food formulations including food emulsions in the future.

Flaxseed is also a rich source of polyphenols as it contains total phenolic content (TPC) of 5.42 g per 100 g of seed. Flaxseed is known to contain about 800–1000 mg phenolic acids, 500 mg esterified phenolic acids, and 300–500 mg etherified phenolic acids per 100 g of seed (Hall & Shultz, 2001; Shahidi & Naczk, 2003). Dabrowski and Sosulski (1984) reported that the trans-ferulic, trans-sinapic and p-courmaric acid extracted from defatted flaxseed flour accounted for 89% (w/w) of total phenolic acids content. These phenolic acids and their derivatives were found to be the source of antioxidant properties in flaxseed (Waszkowiak, Gliszczyńska-Świgło, Barthet, & Skręty, 2015b).

There is not much information on the reaction behaviour of phenylethanoids and their derivatives such as hydroxytyrosol (HT) with proteins. HT is a dihydroxy phenolic compound found abundantly in olive oil. It has been reported that HT possesses strong antioxidative activity and offers many health benefits including reducing systolic blood pressure (Covas, de la Torre, & Fitó, 2015), enhancing endothelial function (Valls et al., 2015), and alleviating inflammation (Lopez et al., 2017).

Generally, the emulsifying activity of proteins is determined by diffusion and adsorption processes occurring at the oil/water interface (Amine, Dreher, Helgason, & Tadros, 2014). Emulsions are inherently unstable due to immiscible nature of continuous and dispersed phases. The interfacial tension between continuous and dispersed phase must be minimized in order to enhance their stability. The interfacial rheology of protein layer provides information on the interaction of protein molecules at the interface. These interactions could be hydrophobic or van der Waals and they could affect the stability of emulsion. For example, the interfacial elasticity is inversely proportional to the coalescence (Tadros, 2013). However, there is no information, in the literature, on the interfacial behaviour (diffusion, absorption and realignment) of flaxseed protein isolate (FPI) and flaxseed protein isolate (FPI)-polyphenol (PP) complexes at oil/water interface. It is expected that the complexation of FPI with polyphenols can greatly alter the oil-water interfacial properties and affect the emulsion stability.

In the above context, the objectives of this study were to measure and explain the effects of complexes formed between modifed FPI and phenolic compounds (FPP and HT) on oil/water interfacial and emulsifying properties as well as antioxidative stability of emulsions. In addition, the relationship between the interfacial behaviour of FPI at oil/water interface and emulsion stability stabilised by FPI alone is elucidated. The findings documented in this study can be used to produce protein-polyphenol complexes with better interfacial and antioxidative activities.

2. Material and methods

2.1. Materials

Flaxseed sample was obtained from Stoney Creek Oil Products Pty Ltd (Talbot, Victoria, Australia) and was stored at 4 °C before use. Ferulic acid (FA), Folin–Ciocalteu reagent, Florisil, sodium dodecyl sulfate (SDS) were purchased from Sigma Aldrich (Castle Hill, New South Wales, Australia). Hydroxytyrosol (HT, purity ≥ 95%) was purchased from AvaChem Scientific (San Antonio, Texas, USA).

2.2. Sample preparation

2.2.1. Extraction of flaxseed protein isolate, flaxseed polyphenols and flaxseed oil

FPI was extracted according to Oomah, Mazza, and Cui (1994) with some modifications. Firstly, flaxseed was degummed by soaking in Milli-Q water at 60 °C at a flaxseed-to-water ratio of 1:18 (w/w) for 2 h under agitation. In this step, ultrasonication (HD3400, Bandelin, Berlin, Germany) was used at 400 W and 20 Hz for 12 min to facilitate the removal of the gum. This degummed flaxseed sample was dehydrated at room temperature (22 ± 1 °C) for 48 h. It was grounded using a coffee grinder. The grounded flaxseed was defatted using hexane at a meal-to-hexane ratio of 1:6 (w/v) for 2 cycles. Subsequently, the defatted mass was dried in a fume hood at 22 ± 1 °C for 24 h. The defatted and degummed flaxseed meal was sieved using a 150 μm sieve to remove hull residues. FPI was extracted from this defatted degummed flaxseed flour using 0.1M Tris buffer at pH 8.6 for 16 h at room temperature (22 ± 1 °C). A flour-to-buffer ratio of 1:16 (w/v) was used for this purpose. After the centrifugation (10,000 × *g* for 20 min), the supernatant was dialysed using a dialysing bag with the cut off molecular weight of 6–8 kDa (Orange Scientific, Braine-l'Alleud, Belgium) against water for 48 h at 4 °C. This dialysed supernatant was freeze dried at −40 °C to obtain the FPI. These FPI samples were stored at 4 °C before use.

FPP was extracted from defatted and degummed flaxseed meal according to Anwar and Przybylski (2012). Briefly, the defatted degummed flaxseed flour was mixed with 60% (v/v) ethanol at the flour-to-ethanol ratio of 1:10 (w/v) and stirred for 4 h at the room temperature (22 ± 1 °C). The undissolved solid content in the mixture was removed by filtration (Whatman No.1, GE Healthcare, Chicago, IL, U.S.A.). This extraction process was performed once again and the permeates from both extractions were combined. The solvent was subsequently evaporated using a rotary vacuum evaporator (RC 2000; Buchi Corporation, Flawil, Switzerland) and the partially evaporated sample was freeze dried at −40 °C to obtain FPP powder. This FPP powder was stored at 4 °C before use.

Flaxseed oil (FO) was extracted using solvent extraction method as described by Zhang, Wang, Li, Li, and Özkan (2011) with minor modification. Briefly, the degummed flaxseed was grounded using a coffee grinder before oil extraction. The grounded sample was mixed with hexane (meal to hexane ratio 1:6, w/v) and stirred at 800 rpm at room temperature (22 ± 1 °C) for 6 h during which the hexane was changed every 3 h. The slurry was centrifuged at 10,000 × *g* for 20 min and the clear supernatant was recovered. Subsequently, the supernatant was evaporated at 40 °C to obtain the oil. In order to remove the impurities, FO was further processed using Gaonkar (1989)'s method with minor modification. Briefly, the FO was mixed with Florisil (100–200 mesh) with a FO:Florisil ratio of 10:1 (w/w) and stirred for 2 h, followed by a centrifugation at 10,000 × *g* for 30 min to obtain the treated oil. This process was repeated for 3 times. The finally treated FO was stored at 4 °C using N_2 as headspace gas until further use.

2.2.2. Preparation of protein-phenolic complexes

The FPI-phenolic (FPP and HT) complexes were produced according to Rawel, Kroll, and Rohn (2001). Firstly, 0.2 mg mL^{-1} FPP solution was hydrolysed using an equal volume of 2M NaOH solution for 2 h in order to break the large phenolic molecules (i.e., phenolic glycosides) to small ones (phenolic acids, flavonoids and secoisolariciresinol diglucoside) to facilitate the reaction between FPI and FPP. Subsequently, this hydrolysed sample was neutralised using 2M HCl. The FPI solution was prepared by dispersing 1 g FPI in 100 mL Milli-Q water at pH 9.0 using 1M NaOH. This dissolved FPI was mixed with 0.3 mmol phenolic compounds. The pH of this FPI and phenolic compound mixture was adjusted to 9.0. The mixture was agitated at 200 rpm for 24 h at ambient temperature in the presence of oxygen to facilitate the reaction. The protein-phenolic complexes obtained were dialysed against water

for 20 h using dialysis bags with cut off molecular weight of 6–8 kDa (Orange Scientific, Braine-l'Alleud, Belgium). Dialysis was carried out to remove the unbounded phenolic compounds and NaCl formed during the neutralisation process. The dialysed FPI-phenolic complex samples were freeze dried and the powders were stored at 4 °C before further analysis.

2.3. Methods

2.3.1. Determination of chemical composition of FPI and FPP

The proximate contents of moisture, lipid, and ash of FPI were measured using AOAC methods 925.1, 920.85, and 923.03, respectively (AOAC, 2005). The total protein content of solid samples was measured by measuring nitrogen content and using a conversion factor of 6.25 (FP-2000, LECO Corporation, Saint Joseph, MI, U.S.A.) (Oomah, Der, & Godfrey, 2006). The protein content of aqueous protein solutions was determined using Bradford protein assay using bovine serum albumin (BSA) as standard (Bradford, 1976).

The total phenolic content of FPP was determined using Folin–Ciocalteu method (Škerget et al., 2005) with minor modification. Briefly, 2.5 mL 0.1N Folin–Ciocalteu reagent was transferred to 5 mL test tubes containing 0.5 mL samples. After 5 min, 2 mL Na_2CO_3 solution (7.5%, w/v) was added and the samples were incubated at 50 °C for 5 min. The absorbance of these mixtures was measured at 760 nm using a UV–Vis spectrophotometer (LAMBDA 35, Perkin Elmer, Llantrisant, U.K). The total phenolic content of FPP is reported in terms of ferulic acid equivalence.

The main components of FPP were characterised using HPLC method (Waszkowiak & Gliszczyńska-Świgło, 2015a) with minor modification. Briefly, 20 μL of hydrolysed FPP solution was injected to the a reverse phase C18 column (Zorbax SB, 250 × 4.6 mm i.d, pore size 5 mm, USA) of a HPLC instrument (Agilent 1100 series, Agilent Technologies, Waldbronn, Germany). This separation test was carried out at 25 °C. A mixture of acetonitrile (solvent A) and 0.1% trifluoroacetic acid (solvent B) was used as mobile phase. The flow rate of the mobile phase was set at 0.7 mL min^{-1}. The concentration of solvent A was increased from 12 to 80% in 14 min and then decreased back to 12% in 1 min using a flow rate of 1 mL min^{-1}. After that, the flow rate was reduced to 0.7 mL min^{-1} in 1 min. The phenolic components in the eluting stream were detected at 280 nm using a UV detector.

2.3.2. Determination of solubility of FPI and its complexes

Solubility of FPI and its complexes with phenolic compounds was measured according to Timilsena, Adhikari, Barrow, and Adhikari (2016) with minor modifications. Fifty milligrams of FPI or its phenolic complexes was dispersed in 10 mL Milli-Q water and the pH of the mixture was adjusted from pH 2 to 9. These dispersions were stirred for 2 h and allowed to hydrate overnight at 4 °C. Subsequently, the dispersions were centrifuged at 5000 × *g* in 10 min. The supernatant was collected and protein content in the mixture was determined using Bradford assay.

2.3.3. Determination of zeta potential and particle size of FPI and its complexes

The zeta potential of FPI and its complexes was measured as a function of pH from 2.0 to 9.0 using dynamic light scattering (Zetasizer NanoZS, Malvern Instruments Ltd., Worcestershire, UK) at 25 °C. At the same time, the particle size distribution of FPI and its complexes with phenolic compounds was measured using the same instruments at pH 7.0. For both measurements, the test solution was diluted to the concentration of 0.1 mg mL^{-1} with Milli-Q water and the pH was adjusted using 0.1M HCl and/or 0.1M NaOH.

2.3.4. Measurement of dynamic interfacial tension and dilatational rheology

The dynamic interfacial tension (DIT) and dilatational rheological parameters of FPI and its complexes were measured at the oil/water interface using a drop profile tensiometer (PAT-1M, Sinterface Technology, Berlin, Germany). A drop of sample solution was formed at the tip of a straight stainless steel capillary which was immersed in a quartz cuvette containing 15 mL treated flaxseed oil. The dynamic interfacial tension was calculated using Laplace equation and was recorded as a function of time for 3 h after the formation of fresh drop at the capillary tip. The temperature, was controlled at 25 °C and the volume of the drop was maintained at a constant value during these tests. After 3 h, the drop was oscillated (harmonic perturbation) at different frequencies (0.005, 0.01, 0.05 and 0.1 Hz) at a constant amplitude of 7.5%. The dilatational modulus (E) was computed using the change in interfacial tension (γ) as a function of change in the oil-water interfacial area (A) as given by equation (1) (Ravera, Loglio, & Kovalchuk, 2010).

$$E = \frac{d\gamma}{dA/A} \tag{1}$$

The dilatational modulus is a complex quantity comprised of real and imaginary parts represented by the dilatational elasticity (E′) and viscosity (E″) respectively. E′ and E″ (mN m^{-1}) are calculated by the Fourier transformation using equations (2) and (3), respectively (Cascão Pereira, Theodoly, Blanch, & Radke, 2003):

$$E' = \Delta\gamma \frac{A_0}{\Delta A} cos\varnothing \tag{2}$$

$$E'' = \Delta\gamma \frac{A_0}{\Delta A} sin\varnothing \tag{3}$$

where, ΔA (mm^2) and Δγ (mN m^{-1}) are the amplitude of change in the interfacial area and interfacial tension, respectively. ∅ is the phase shift between the sinusoidal perturbation of the interfacial tension and that of the interfacial area.

2.3.5. Measurement of adsorption of FPI and its phenolic complexes at oil/water interface

The adsorption of FPI and its phenolic complexes at the oil/water interface occurs in three stages (Graham & Phillips, 1979a): diffusion of protein from the bulk phase to layer adjacent to the interface; adsorption of protein molecules to the interface and their reorganisation. In the case of diffusion-controlled adsorption, the diffusion rate constant of proteins onto the oil/water interface can be calculated using a modified Ward and Tordai (1946) equation (4).

$$\pi = 2C_0KT\left(\frac{Dt}{3.142}\right)^{1/2} \tag{4}$$

where, π is the interfacial pressure (mN m^{-1}), C_0 is the concentration of protein in the bulk phase (mol m^{-3}), K is the Boltzamann constant (m^2 kg s^{-2} K^{-1}), T is the absolute temperature (K), D is diffusion coefficient (m^2 s^{-1}) and t is absorption time (s). If the absorption of protein at the interface is controlled by diffusion, a plot of interfacial pressure $\pi = (\sigma_0 - \sigma_t)$ against square root of time ($t^{1/2}$) will be linear and the slope of this plot will be the diffusion rate constant (K_{diff}). Here, σ_0 and σ_t are the interfacial tension of pure water and protein at oil/water interface, respectively. The penetration and rearrangement of the adsorbed protein layer at the interface was calculated using equation (5) (Graham & Phillips, 1979b).

$$ln \tag{5}$$

where, π_f, π_t, and π_0 are the interfacial pressures (mN m^{-1}) at the final adsorption time of each step (10800 s), at a chosen time, and at the initial time (100 s), respectively. In practice, the plot represented by equation (5) produces two or more linear regions. The initial slope is known as penetration rate constant (K_p) (s^{-1}) (Graham and Phillips, 1979b).

2.3.6. Preparation of emulsions

Oil-in-water (o/w) emulsions of FO (10% v/v) were prepared using FPI and FPI-phenolic complexes as emulsifier at a fixed protein concentration of 5 mg mL^{-1}. Ultra-Turrax T-50 Homogenizer was used at 15,000 rpm for 4 min to make coarse emulsions. These coarse emulsions were homogenised using a microfluidiser (M-110L, Microfluidics, Newton, MA) at 12,000 Psi using 3 passes to obtain fine emulsions (Wang, Li, Wang, Adhikari, & Shi, 2010).

2.3.7. Determination of particle size and zeta potential of emulsions

The droplet size of the o/w emulsion was determined by using dynamic light scattering after 24 h of storage (ZS-90, Malvern Instruments, UK). The emulsions were diluted to 0.001% (oil fraction, v/v) with Milli-Q water to avoid multiple scattering effect. At the same time, the Zeta potential was measured using Smoluchowski model with the same instrument (Kirby & Hasselbrink, 2004).

2.3.8. Determination of emulsifying activity and emulsion stability indices

The emulsifying activity index (EAI) and emulsion stability index (ESI) of emulsions, where FPI and FPI-phenolic complexes were used as emulsifiers, were determined using turbidimetric method (Pearce & Kinsella, 1978). The absorbance was measured at 500 nm. Beforehand, these emulsions were diluted to 1000 times with Milli-Q water and mixed thoroughly using a vortex mixer. The turbidity of emulsion was calculated using equation (6) below.

$$T = 2.303 \times \frac{A}{L} \times D \tag{6}$$

where, T is the turbidity of emulsion (m^{-1}), A is the absorbance, D is the dilution factor, L is the light path length (m). EAI was calculated using equation (7) given below.

$$EAI = \frac{2 \times T_0}{\varnothing \times C \times 1000} \tag{7}$$

where, T_0 is the turbidity of fresh emulsion, ϕ is the volumetric fraction of oil, and C is the concentration of protein solution (mg mL^{-1}). The ESI was calculated using equation (8), given below.

$$ESI = \frac{A_0 \times A_t}{A_0} \times t \tag{8}$$

where t is the time interval (h), A_0 and A_t are the absorbance values at t = 0 and 24 h, respectively.

2.3.9. Measurement of lipid oxidation

The extent of lipid oxidation was measured at two temperatures (at 20 °C and 40 °C) throughout storage period. For primary oxidation products, hydroperoxides were measured according to Shantha and Decker (1994). Briefly, 0.3 mL of emulsion was mixed with 1.5 mL of isooctane/2-propanol (2:1, v/v), vortexed for 30 s for 3 times and centrifuged at 1000 × *g* for 2 min. Subsequently, 0.2 mL of the supernatant was transferred to test tubes and 2.8 mL of a mixed solution of methanol and 1-buthanol (3:1, v/v) was added. Finally, 0.03 mL of mixture of 3.94 M ammonium thiocyanate and ferrous iron solution (1:1, v/v) was added to these test tubes. The ferrous iron solution was freshly prepared by adding equal amount of 0.132 M $BaCl_2$ and 0.144 M Fe_2SO_4 in 0.4 M HCl. The absorbance was measured at 510 nm using a microplate reader (FLUOstar Omega, BMG Labtech, Cary, NC). The concentration of hydroperoxides was calculated using a standard calibration curve prepared with hydrogen peroxide.

For secondary oxidation products, thiobarbituric acid reactive substances (TBARS) was measured as described by (McDonald & Hultin, 1987) with minor modifications. Tricholoracetic acid (15%, v/v) and thiobarbituric acid 0.375% (w/v) were mixed in 0.25 M HCl to prepare the thiobarbituric acid (TBA) reagent. A hundred microliter of emulsion was taken and its volume was adjusted to 1 mL using Milli-Q water. Further 2 mL TBA was added to this mixture. This mixture was sealed in a vial flushed by N_2, placed in boiling water for 15 min and then cooled down to ambient temperature for 10 min and then centrifuged at 5000 × *g* for 15 min. After 10 min, the absorbance was measured at 532 nm using a microplate reader mentioned above. The concentration of the TBARS was calculated using a standard curve prepared with 1,1,3,3-tetraethoxypropane.

2.3.10. Measurement of colour parameters

The colour of fresh emulsions was measured using a colorimeter (Minolta CR 300, Minolta Corp, Osaka, Japan). This instrument was calibrated using a white standard porcelain plate. Fifteen millilitre emulsions were pipetted into a measurement cup placed under black background. The colour of the emulsion was expressed in terms of L^* (lightness), a^* (green to red) and, b^* (blue to yellow).

2.3.11. Statistical analysis

All the tests were conducted at least in triplicate and data is reported as mean ± standard deviation. The SPSS statistical software (version 24, SPSS Inc., Chicago, IL, USA) was used for analysis of variance (ANOVA) in order to test the significant difference between any two mean values. Duncan test was implemented on the data sets using 95% significance level ($p < 0.05$).

3. Result and discussion

3.1. Chemical composition of FPI and FPP

The FPI sample contained 2.70 ± 0.04% (w/w) moisture, 93.60 ± 2.06% (w/w) protein, 2.10 ± 0.07% (w/w) lipid and 0.56 ± 0.07% (w/w) ash. The total phenolic content (TPC) of samples was expressed as mg of ferulic acid equivalent (FAE) per g of extract. It contained 113.6 ± 0.55 mg FAE per g of extract. The ferulic acid and

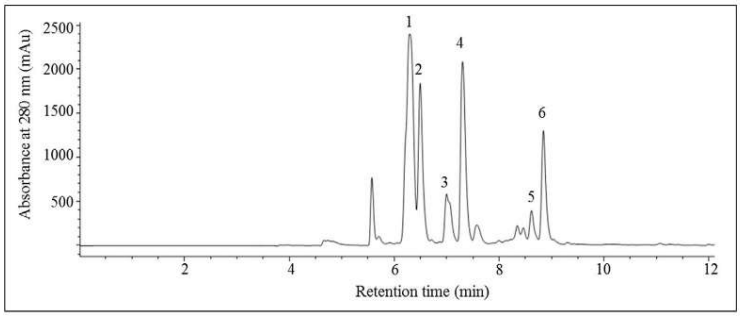

Fig. 1. HPLC chromatograms of alkaline hydrolysis FPP: (1) p-hydroxybenzoic acid, (2) p-coumaric acid glucoside, (3) ferulic acid glucoside, (4) secoisolariciresinol diglucoside (SDG), (5) p-coumaric acid, (6) ferulic acid.

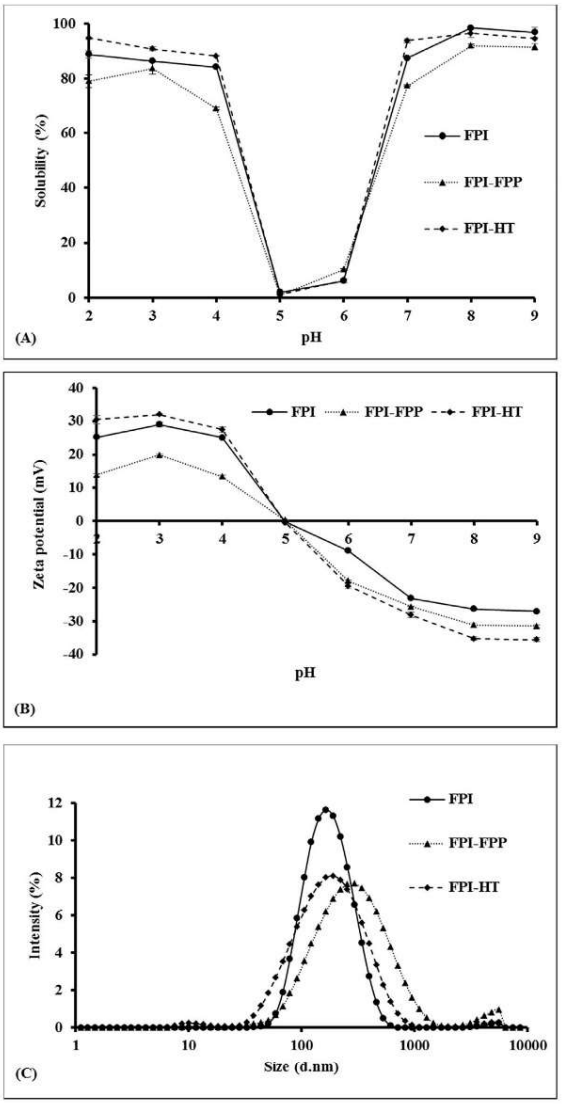

Fig. 2. (A) Solubility (B) Zeta potential as a function of pH of FPI, FPI-FPP and FPI-HT complexes and (C) intensity particle size distribution. FPI = flaxseed protein isolate (circle filled), FPP = flaxseed polyphenol (triangle filled), HT = hydroxytyrosol (diamond filled).

p-coumaric acid were found to be the major phenolic acids of FPP accounting for 53.39 ± 0.48 mg, 5.86 ± 0.13 mg per gram of extract, respectively (Fig. 1). Secoisolariciresinol diglucoside (SDG) was also found in considerable amount (98.41 ± 0.66 mg per gram of extract).

3.2. The physical properties of FPI and FPI-phenolic complexes

The solubility, zeta potential and particle size distribution of FPI, FPI-FPP and FPI-HT complexes are presented in Fig. 2. The solubility of FPI-HT (Fig. 2A) complex is higher than that of native FPI within the pH range of 2.0–9.0. This increased solubility of FPI-HT complex can be explained by the integral effect of conformational change in FPI due to complexation with HT. Hydrophobic residues of FPI such as tryptophan were blocked when they reacted with HT and new hydrophilic groups (e.g., hydroxyl groups) from HT were introduced to the protein chain. HT was oxidised to quinones under alkaline condition with the presence of oxygen and these quinones readily reacted with nucleophiles (tryptophan, lysine, and cysteine) of FPI to form the C—N and C—S linkages. This observation is in accordance with that of Rawel, Czajka, Rohn, and Kroll (2002) who reported that the solubility of soy glycinin was increased after its complexation with quercetin. However, the solubility of FPI-FPP complex was lower than that of unmodified FPI within the entire pH range tested. This decrease in solubility due to complex formation can be attributed to the decrease of hydrophilic amino and thiol residues as they bonded (formed complex) with oxidised phenolic compounds and/or increase of non-polar groups containing aromatic rings (Kroll & Rawel, 2001). In this regard, Kroll, Rawel, and Seidelmann (2000) also reported a decreased solubility of myoglobin upon its conjugation with chlorogenic and caffeic acids and p-quinone.

The variation of zeta potential FPI and its phenolic complexes with pH is presented in Fig. 2B. The FPI and its complexes with FPP and HT were neutral around pH 5.0 which is essentially the isoelectric point of FPI. This result was in good agreement with the lowest solubility of these three systems at this pH value (Fig. 2A). The surface charge of FPI increased after complexation with HT but decreased when it complexed with FPP at the pH values below its pI. The zeta potential values of FPI and its phenolic complexes, which can be used as indicator of solubility, were in the order of FPI-HT > FPI > FPI-FPP below the pI of FPI. However, both FPI-HT and FPI-FPP complexes showed higher surface charge compared to that of uncomplexed FPI at pH values above the pI. Similar variation of surface charge in soy glycinin and their complexes with phenolic acids, quercetin and myricetin was reported by Rawel et al. (2002). Their results showed that the change in surface charge in these systems was due to the reduction of positively charged amino groups and the introduction of negatively charged hydroxyl and carboxylic groups of phenolic compounds. These authors also showed that the extent of change in surface charge depends on the degree of complexation of proteins with the oxidised phenolic compounds.

The Z-average diameters of FPI, FPI-HT and FPI-FPP were 149.30 ± 2.00, 127.10 ± 1.10 and 210.02 ± 4.22 nm, respectively (Fig. 2C), suggesting that the size of FPI-phenolic complexes varied depending on the nature of phenolic compounds. Specifically, the reaction of FPI with HT and FPP folded and unfolded the protein chain slightly, which contributed to their decreased and increased size, respectively. The fact that the complexation of FPI with HT decreased the particle size agrees well with the observation made by Liu, Ma, McClements, and Gao (2017). These authors observed that the zein-polyphenol conjugates had smaller particle size compared to that of native zein. According to Schmitt, Bovay, Rouvet, Shojaei-Rami, and Kolodziejczyk (2007), the formation of covalent disulfide bond can decrease the particle size of the conjugate. These particle size data also agree well with the solubility as the more soluble complexes are expected to have smaller particle size than that of less soluble ones.

3.3. Effect of FPI-phenolic compound complexation on dynamic interfacial tension and adsorption kinetics

The DIT of FPI, FPI-FPP and FPI-HT complexes at the oil/water interface at different concentration (0.1–10 mg mL^{-1} of FPI) at pH 7.0 at 25 °C is presented in Fig. 3. The DIT of all these samples decreased with the increase of measurement time and protein concentration. The former observation can be associated with the protein adsorption at the oil/water interface and the latter one illustrates that the protein adsorption is driven by its concentration gradient (Wang et al., 2012). Among FPI, FPP and HT, FPI exhibited the strongest interfacial activity, followed by the FPP and HT. One should note that FPP exhibited similar but weaker interfacial activity compared to FPI, possibly due to the presence of a trace amount of FPI, which could not be separated from FPP during the extraction.

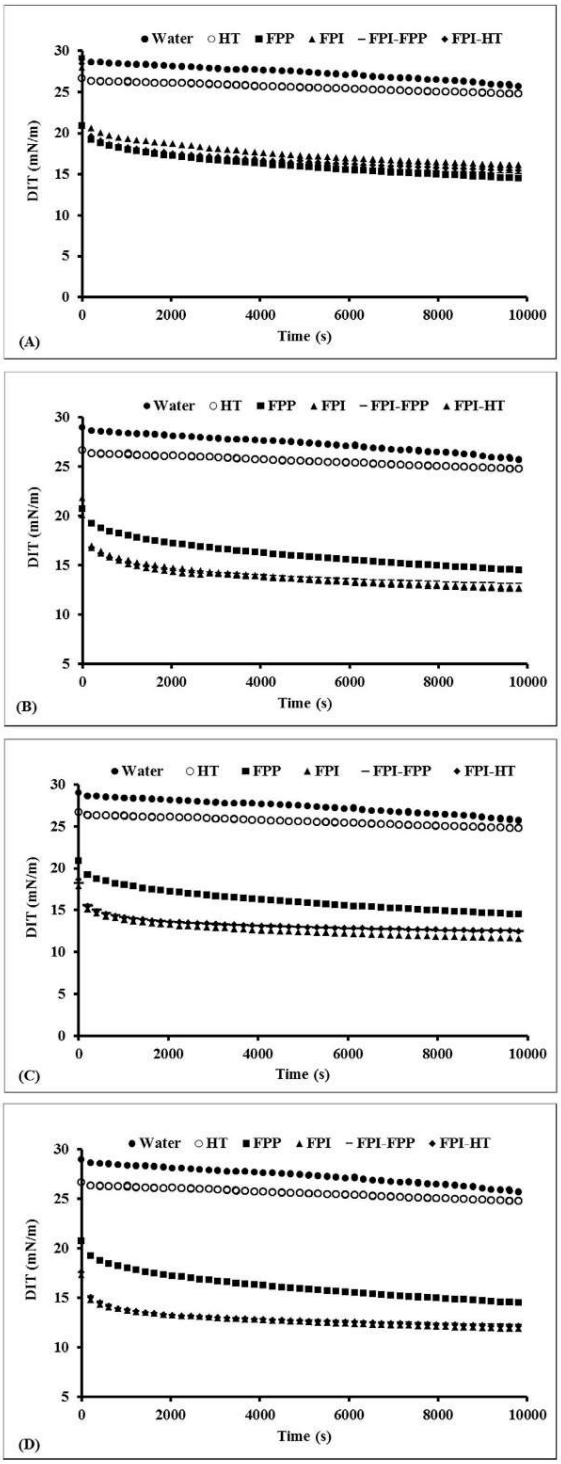

Fig. 3. DIT at flaxeed oil water (circle filled) in the presence of HT = hydroxytyrosol (circle), FPP = flaxseed polyphenol (square filled), FPI = flaxseed protein isolate (triangle filled), FPI-FPP (hyphen), and FPI-HT (diamond filled) complexes at different protein concentration of 0.1 mg mL^{-1} (A), 1 mg mL^{-1} (B), 5 mg mL^{-1} (C) and 10 mg mL^{-1} (D). Experiments were conducted at pH 7.0 and 25 °C.

As shown in Fig. 3, FPI and its phenolic complexes exhibited similar ($p > 0.05$) surface activity or interfacial tension lowering ability at protein concentrations from 5 mg mL^{-1} to 10 mg mL^{-1}. The interfacial tension of samples did not decrease further when their protein concentration was higher than 5 mg mL^{-1}, most probably due to saturation of oil/water interface by proteins. Therefore, this concentration (5 mg mL^{-1}) was chosen to characterise the emulsifying behaviour of FPI, FPI-FPP, and FPI-HT complexes. At low concentration of proteins (0.1 mg mL^{-1}), the adsorption of FPI and its phenolic complexes at the oil/water interface is controlled by diffusion. This diffusion process is particularly dominant at the early stage of adsorption of protein at the interface and it can be represented by the diffusion rate constant (K_{diff}). The K_{diff} values of FPI-FPP and FPI-HT are significantly ($p < 0.05$) higher than that of native FPI indicating that the greater surface activity of these complexes at the interface as compared to that of the uncomplexed native FPI at 0.1 mg mL^{-1} (Table 1). As discussed in **section 3.2**, the FPI-FPP was more hydrophobic. Thus, it adsorbed at the oil/water interface more effectively than FPI while in the case of FPI-HT, the decreased size contributed to its faster diffusion. In similar context, Palazolo, Mitidieri, and Wagner (2003) showed that the oil/water interfacial tension of soy protein isolate decreased more dramatically with higher dissociation degree and hydrophobicity. At higher protein concentrations (1–10 mg mL^{-1}), the evolution of the DIT of FPI, FPI-FPP and FPI-HT showed identical interfacial tension lowering behaviour (Fig. 3B, C, 3D). At these concentrations, the adsorption process of the proteins at the oil/water interface is not the diffusion controlled. The proteins migrate and adsorb to the interface very fast which results into sharp fall in DIT values immediately after the droplet or interface is formed. Therefore, it was not possible to calculate the k_{diff} value at protein concentration higher than 1 mg mL^{-1} using equation (4). This observation is in agreement with that of Liu, Zhao, Liu, and Zhao (2011) who reported that the adsorption of soy protein to the o/w interface at concentration > 1 mg mL^{-1} was not controlled by diffusion step which made it impossible to determine the k_{diff} value. At higher concentrations, the absorption of proteins to the oil/water interface is usually controlled by the penetration of protein at the interface. The rate constant of this process (k_p) was calculated and is presented in Table 1. As shown, k_p increased with the increase in protein concentration from 1 mg mL^{-1} to 5 mg mL^{-1}. However, the k_p value decreased slightly at 10 mg mL^{-1}. This is because high protein concentration facilitates their penetration to the oil/water interface and the interface saturates when the protein concentration attains its CMC value.

3.4. Effect of FPI-phenolic complexation to dilatational rheology of FPI

The evolution of the dilatational elasticity and viscosity at concentrations from 0.1 mg mL^{-1} to 10 mg mL^{-1} is shown in Fig. 4. As shown, the elasticity (E′) of the adsorbed layers of FPI, FPI-FPP and FPI-HT slightly increased with the increase of frequency at lower frequencies and almost remained unchanged at higher frequencies. This observation is in accordance with that of Bučko et al. (2018) who reported that the dilatational elasticity of pumpkin seed protein increased with the acceleration of oscillation frequency and tended to remain constant at higher frequencies. The dilatational viscosity (E") of all the three formulations decreased with the increase in frequency at all concentrations. This variation of E" with frequency agrees well with dilatational properties of sunflower protein-phenolic complexes

Table 1
The diffusion rate (K_{diff}) and penetration rate (K_p) constant and constan of FPI, FPI-FPP, and FPI-HT complexes at the oil/water interface. FPI = flaxseed protein isolate, FPP = flaxseed polyphenols, HT = hydroxytyrosol.

C_o ($mgmL^{-1}$)	FPI		FPI-FPP		FPI-HT	
	K_{diff} ($mNm^{-1}s^{-0.5}$)	$K_{p\ x\ 10^{-4}}$ (s^{-1})	K_{diff} ($mNm^{-1}s^{-0.5}$)	$K_{p\ x\ 10^{-4}}$ (s^{-1})	K_{diff} ($mNm^{-1}s^{-0.5}$)	$K_{p\ x\ 10^{-4}}$ (s^{-1})
0.1	0.684 ± 0.035 ^{a}	2.37 ± 0.01 ^{aA}	0.917 ± 0.011 ^{b}	2.46 ± 0.14 ^{aA}	0.817 ± 0.024 ^{c}	2.52 ± 0.2 ^{aA}
1	–	2.54 ± 0.09 ^{aA}	–	2.66 ± 0.02 ^{aA}	–	2.71 ± 0.02 ^{aA}
5	–	2.56 ± 0.23 ^{aA}	–	2.69 ± 0.13 ^{aA}	–	2.73 ± 0.12 ^{aA}
10	–	2.38 ± 0.01 ^{aA}	–	2.61 ± 0.09 ^{bA}	–	2.56 ± 0.08 ^{bA}

Different lowercase letters in the superscript of the same row and uppercase letters in the superscript of the same column indicate significant differences ($p < 0.05$).

reported by Karefyllakis, Altunkaya, Berton-Carabin, van der Goot, and Nikiforidis (2017). These observations suggest that the FPI and FPI-phenolic complexes at the oil/water interface behave more solid-like with increase of frequency. The dilatational viscosity of these three systems in current study continued to decrease with increase in frequency and tended to reach zero at 0.1 Hz. The highest dilatational viscosity, for all systems, was observed at frequencies < 0.005 Hz which can be explained by the mass transfer between the interfacial layer and the immediately adjacent layer. This mass transfer is the result of the time effect of long-time observation period (low frequency) (Rühs, Affolter, Windhab, & Fischer, 2013). Conversely, at high frequency (short observation period) there may be inadequate time for mass transfer of protein (and other diffusants) and the absorbed layers behaved as solid-like (Wojciechowski, 2013). In addition, the E′ value of the FPI layer at the interface was lower than that of the FPI-HT complex at all protein concentrations. This difference could be attributed to the more compact structure of the FPI-HT complex, due to the folding of the FPI chain (**section 3.2**) via the formation of hydrogen bonds between adjacent phenols bound to the protein molecules (Karefyllakis et al., 2017). In contrast, the native FPI had higher E′ value compared to that of FPI-FPP complex which could be ascribed to the less compact nature of FPI-FPP layer at the interface due to the larger particle size of FPI-FPP, compared with FPI (Fig. 2C). The E" values of all FPI-phenolic complexes were lower than that of native FPI at low frequencies (0.005–0.05 Hz) and very close to that of the latter at higher frequencies (0.05–0.1 Hz). These observations indicate that the complexation of FPI with the phenolic compounds alters the dilatational rheological behaviour of FPI. These changes are frequency dependent and the elasticity of the adsorbed layer can be increased or decreased depending on the nature of the complexing phenols.

3.5. Effect of FPI-phenolic complexation on emulsifying properties of FPI

The emulsifying properties of FPI, FPI-FPP, and FPI-HT complexes were characterised in terms of droplet size, zeta potential, emulsifying activity index (EAI) and emulsion stability index (ESI) after 24 h of formation of emulsion (Table 2). As shown, the dropet size of the emulsion stabilised by FPI-FPP complex was smaller than that of emulsions stabilsied by FPI and FPI-HT complex (Table 2), which was in a good agreement with the lower solubility of FPI-FPP (Fig. 2A). However, the zeta potetial of FPI stabilsed emulsion was significantly ($p < 0.05$) higher than that of emulsions stabilised by FPI-FPP and FPI-HT complexes. This result is different with the zeta potetial values of the FPI and its phenolic complexes alone at the neutral pH (Fig. 2B). The mechanism for this observation is unclear since the reaction between protein and phenolic compounds and the unfolding/folding of the protein at the oil/water interface are quite complex. Generally, it is accepted that a specific value of zeta potential (absulote value > 30 mV) is desired for an electrostatically stabilised emulsion. Thus, although there is no significant difference in the K_p value between FPI and its phenolic complexes, FPI could stabilise the oil/water interface more effectively due to higher surface charge in emulsions stabilised by it than stabilised by FPI-FPP and FPI-HT (Table 2). For example, the EAI of FPI-FPP stablished emulsion is about half compared to that of FPI stabilised one. In this study, we found the surface charge of the emulsion dropelts contributed more to the emuslion stability than their size. Similarly, von Staszewski et al. (2014) also reported that the stability of oil-in-water emulsion stabilised by sunflower protein-chlorogenic acid complex was higher than the stability of emuslion stabilised by the sunflower protein, despite having larger oil droplets.

3.6. Effect of FPI-phenolic reaction on the oxidation of oil-in-water emulsion

The evolution of hydroperoxides and TBARs values of emulsions stabilised by FPI, FPI-FPP and FPI-HT over storage time at 20 °C is shown in Fig. 5A and Fig. 5B. During the first 15 days of storage at 20 °C, the concentration of hydroperoxide and TBARs in FPI stabilised emulsions increased continuously. After 15 days storage, hydroperoxides and TBARs values of FPI-stabilsied emulsion were 19 and 10 times higher than the fresh emuslion, respectively.These observations are in line with those of Gumus, Decker, and McClements (2017). These authors observed similar trend of oxidation in the emulsions produced using lentil, pea, and faba bean proteins as emusifiers. The hydroperoxide vlues of FPI-FPP and FPI-HT stabilised emulions remained almost the same as those of freshly produced emulsions (day 0). The FPI-FPP stabilsied emulsions showed the lowest hydroperoxide values during 21-day storage indicating that this complex provided the best stability against oxidation. Similar result was observed in TBARS values, albeit they increased upon 15th and 18th day still remained well below that of FPI stabilised emulsions. In similar context, von Staszewski et al. (2014) reported that the oxidative stability of fish oil stabilised by β-lactoglobulin was enhanced in the presence of green tea polyphenols due to the formation of β-lactoglobulin-phenolic complex. A similar trend was observed in hydroperoxides and TBARs values in the emulsions stabilised by FPI and FPI-FPP and FPI-HT throughout storage at 40 °C (Fig. 5C and D). However, both hydroperoxide and TBARs values increased strongly in all emulsions at the initial stage (day 0–4) due to the accelerated lipid oxidation at the higher storage temperature. These observations indicate that FPI-phenolic complexes provide antioxidative effect to the emulsions they stabilise (Paradiso et al., 2016; Waszkowiak and Gliszczyriska-Swiglo, 2015a).

3.7. Effect of FPI - phenolic complexation on the colour of emulsions

It is of practical importance to quantify the difference in colour of emulsions stabilised by FPI, FPI-FPP and FPI-HT as these compounds have their inhernet colour. The colour parameters (L*, a*, and b*) of emulsions stabilised by FPI,FPI-FPP and FPI-HT are presented in Table 3. In particular, the lightness of emulsion stabablied by FPI-FPP and FPI-HT complexes increased significantly as compared to that of FPI stabilised emulsion. The yellowness parameter (b*) of emulsion stabilised by FPI-FPP and FPI-HT was higher than that of FPI stabilised emulsion. The redness paramter (a*) of emulsion stabilised by FPI-HT

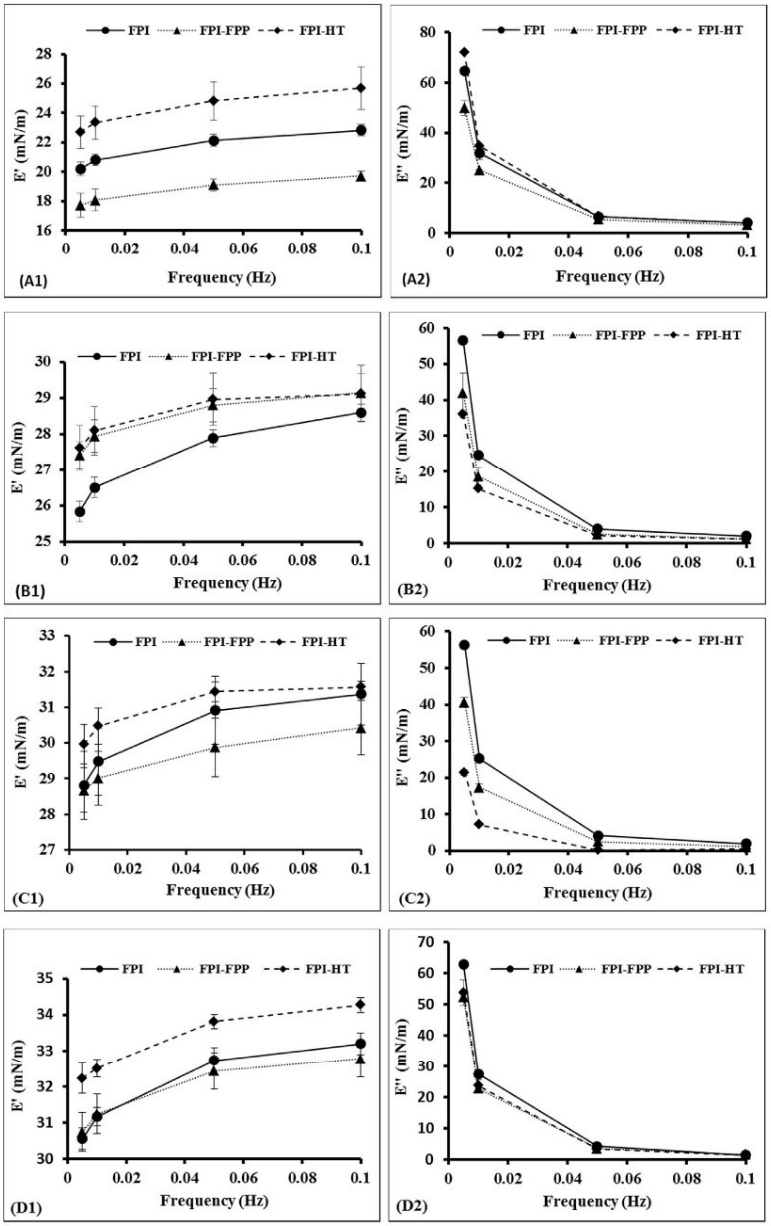

Fig. 4. Dilatational elasticity (E') (1) and viscosity (E") (2) of FPI (circle filled), FPI-FPP (triangle filled) and FPI-HT (diamond filled) complexes at oil/water interface at protein concentration of 0.1 mg mL^{-1} (A), 1 mg mL^{-1} (B), 5 mg mL^{-1} (C), and 10 mg mL^{-1} (D) as function of frequencies with 7.5% area change. FPI = flaxseed protein isolate, FPP = flaxseed polyphenols, HT = hydroxytyrosol.

Table 2
Emulsifying activity index (EAI), Emulsion stability index (ESI), Zeta potential and droplet size of emulsions stabilised by FPI, FPI-FPP and FPI-HT complexes. FPI = flaxseed protein isolate, FPP = flaxseed polyphenols, HT = hydroxytyrosol.

Formulations	EAI (m2/g)	ESI (h)	Zeta potential (mV)	Z-Average size (nm)
FPI	517.3 ± 3.9 ^{a}	742.0 ± 52.7 ^{a}	−36.9 ± 0.2 ^{a}	237.2 ± 1.3 ^{a}
FPI-FPP	229.5 ± 1.2 ^{b}	62.0 ± 1.7 ^{b}	−23.1 ± 1.4 ^{b}	213.9 ± 3.2 ^{b}
FPI-HT	347.3 ± 2.1 ^{c}	108.8 ± 4.1 ^{b}	−28.9 ± 0.8 ^{c}	238.0 ± 4.1 ^{a}

Different lowercase letters in the superscript of the same column indicate significant differences ($p < 0.05$).

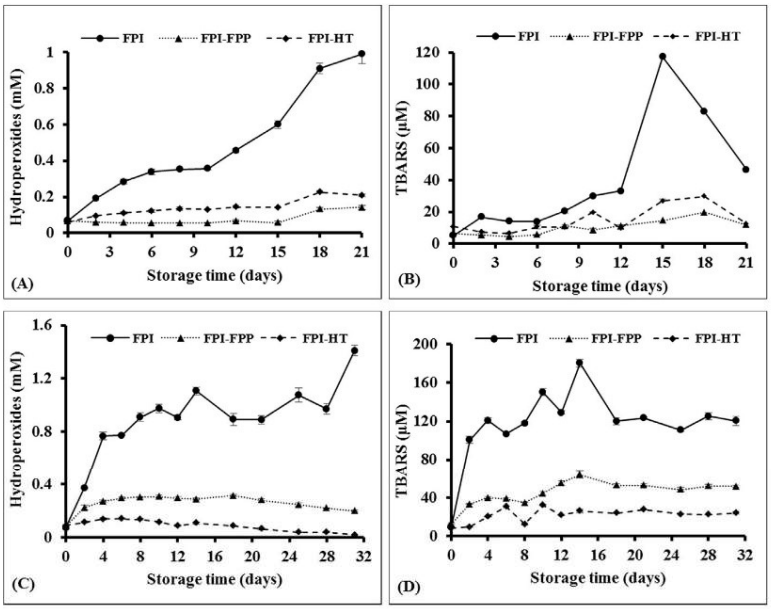

Fig. 5. Hydroperoxide and TBARS values of emulsions stabilised by FPI (circle filled), FPI-FPP (triangle filled), and FPI-HT (diamond filled) complexes at 20 °C (A & B) and 40 °C (C & D). FPI = flaxseed protein isolate, FPP = flaxseed polyphenol, HT = hydroxytyrosols.

Table 3
Colour of emulsions stabilised by FPI, FPI-FPP and FPI-HT complexes described by L*, a*, b* values. FPI = flaxseed protein isolate, FPP = flaxseed polyphenols, HT = hydroxytyrosol.

Formulations	L*	a*	b*
FPI	82.16 ± 0.79 [a]	−2.52 ± 0.15 [a]	3.66 ± 0.17 [a]
FPI-FPP	88.67 ± 0.54 [b]	−3.07 ± 0.10 [b]	7.05 ± 0.38 [b]
FPI-HT	87.30 ± 1.18 [c]	−0.51 ± 0.04 [c]	8.36 ± 0.28 [c]

Different lowercase letters in the superscript of the same column indicate significant differences ($p < 0.05$).

was found to be lower than the FPI-stabilsed emulsion. This increase in redness was due to the browning colour produced by the polymerisation of phenolic compounds in alkaline condition (Brenes-Balbuena, Garcia-Garcia, & Garrido-Fernandez, 1992).

4. Conclusion

This study shows that the complexation of FPI with phenolic compounds significantly alters the solubility of FPI depending on the nature of complexed phenolic compounds. The oil/water emulsion stabilising ability of FPI was better than that of FPI-FPP and FPI-HT complexes. The suprior emulsion stability of FPI stabilised emulsion correlated with its high surface charge density (zetapotential). The emulsions stabilised by FPI-FPP and FPI-HT complexes had significantly higher antioxidative stability compared to FPI stabilised emulsion. The emulsions produced by FPI-FPP and FPI-HT complexes had slightly higher red and yellow colour than those produced by FPI. This study highlights the mechanism of complexation of phenolic compounds, especially that of flaxseed polyphenols and hydroxytyrosol, with FPI. It also highlightes the advantages and limitations of the FPI-phenolic complexes when used as emulsifiers. Food systems almost invariably contain salt ions; hence, the effect of ions on the emulsifying and emulsion stabilising behaviours of FPI-phenolic complexes needs further study. The effect of folding and unfolding of protein chain on formation and characteristics of FPI− phenolic complexes also needs a systematic study.

Appendix A. Supplementary data

Supplementary data to this article can be found online at https://doi.org/10.1016/j.foodhyd.2019.03.007.

References

Amine, C., Dreher, J., Helgason, T., & Tadros, T. (2014). Investigation of emulsifying properties and emulsion stability of plant and milk proteins using interfacial tension and interfacial elasticity. *Food Hydrocolloids, 39*, 180–186.
Anwar, F., & Przybylski, R. (2012). Effect of solvents extraction on total phenolics and antioxidant activity of extracts from flaxseed (Linum usitatissimum L.). *ACTA Scientiarum Polonorum Technologia Alimentaria, 11*(3), 293–302.
AOAC (2005). *Official methods of analysis* (18th ed.). Arlington, VA: Association of Official Analytical Chemists.
Banerjee, S., Chattopadhyay, P., Ghosh, A., Goyary, D., Karmakar, S., & Veer, V. (2013). Influence of process variables on essential oil microcapsule properties by carbohydrate polymer-protein blends. *Carbohydrate Polymers, 93*(2), 691–697.
Bradford, M. M. (1976). A rapid and sensitive method for the quantitation of microgram quantities of protein utilizing the principle of protein-dye binding. *Analytical Biochemistry, 72*(1–2), 248–254.
Brenes-Balbuena, M., Garcia-Garcia, P., & Garrido-Fernandez, A. (1992). Phenolic compounds related to the black color formed during the processing of ripe olives. *Journal of Agricultural and Food Chemistry, 40*(7), 1192–1196.
Bučko, S., Katona, J., Petrović, L., Milinković, J., Spasojević, L., Mucić, N., et al. (2018). The influence of enzymatic hydrolysis on adsorption and interfacial dilatational properties of pumpkin (cucurbita pepo) seed protein isolate. *Food Biophysics*, 1–9.
Can Karaca, A., Low, N., & Nickerson, M. (2013). Encapsulation of flaxseed oil using a benchtop spray dryer for legume protein-maltodextrin microcapsule preparation. *Journal of Agricultural and Food Chemistry, 61*(21), 5148–5155.
Cascão Pereira, L. G., Theodoly, O., Blanch, H. W., & Radke, C. J. (2003). Dilatational rheology of BSA conformers at the air/water interface. *Langmuir, 19*(6), 2349–2356.
Chen, S., Zhang, N., & Tang, C.-H. (2016). Influence of nanocomplexation with curcumin on emulsifying properties and emulsion oxidative stability of soy protein isolate at pH 3.0 and 7.0. *Food Hydrocolloids, 61*, 102–112.
Cilliers, J. J., & Singleton, V. L. (1991). Characterization of the products of nonenzymic autoxidative phenolic reactions in a caffeic acid model system. *Journal of Agricultural and Food Chemistry, 39*(7), 1298–1303.
Covas, M.-I., de la Torre, R., & Fitó, M. (2015). Virgin olive oil: A key food for cardiovascular risk protection. *British Journal of Nutrition, 113*(S2), S19–S28.
Curcio, M., Parisi, O. I., Puoci, F., Altimari, I., Spizzirri, U. G., & Picci, N. (2012). Antioxidant polymers by free radical grafting on natural polymers. *Antioxidant*

Polymers: Synthesis, Properties, and Applications, 153–178.
Dabrowski, K. J., & Sosulski, F. W. (1984). Composition of free and hydrolyzable phenolic acids in defatted flours of ten oilseeds. *Journal of Agricultural and Food Chemistry, 32*(1), 128–130.
Gaonkar, A. G. (1989). Interfacial tensions of vegetable oil/water systems: Effect of oil purification. *Journal of the American Oil Chemists' Society, 66*(8), 1090–1092.
Graham, D., & Phillips, M. (1979a). Proteins at liquid interfaces: I. Kinetics of adsorption and surface denaturation. *Journal of Colloid and Interface Science, 70*(3), 403–414.
Graham, D., & Phillips, M. (1979b). Proteins at liquid interfaces: III. Molecular structures of adsorbed films. *Journal of Colloid and Interface Science, 70*(3), 427–439.
Gumus, C. E., Decker, E. A., & McClements, D. J. (2017). Impact of legume protein type and location on lipid oxidation in fish oil-in-water emulsions: Lentil, pea, and faba bean proteins. *Food Research International, 100*, 175–185.
Hall, C., & Shultz, K. (2001). Phenolic antioxidant interactions. *92nd American oil chemists society annual meeting and expo* (pp. S88). Minneapolis, Minnesota: AOCS.
Karefyllakis, D., Altunkaya, S., Berton-Carabin, C. C., van der Goot, A. J., & Nikiforidis, C. V. (2017). Physical bonding between sunflower proteins and phenols: Impact on interfacial properties. *Food Hydrocolloids, 73*, 326–334.
Kaushik, P., Dowling, K., McKnight, S., Barrow, C. J., Wang, B., & Adhikari, B. (2016). Preparation, characterization and functional properties of flax seed protein isolate. *Food Chemistry, 197*(Pt A), 212–220.
Kirby, B. J., & Hasselbrink, E. F. (2004). Zeta potential of microfluidic substrates: 1. Theory, experimental techniques, and effects on separations. *Electrophoresis, 25*(2), 187–202.
Kroll, J., & Rawel, H. M. (2001). Reactions of plant phenols with myoglobin: Influence of chemical structure of the phenolic compounds. *Journal of Food Science, 66*(1), 48–58.
Kroll, J., Rawel, H. M., & Seidelmann, N. (2000). Physicochemical properties and susceptibility to proteolytic digestion of myoglobin − phenol derivatives. *Journal of Agricultural and Food Chemistry, 48*(5), 1580–1587.
Liu, F., Ma, C., McClements, D. J., & Gao, Y. (2017). A comparative study of covalent and non-covalent interactions between zein and polyphenols in ethanol-water solution. *Food Hydrocolloids, 63*, 625–634.
Liu, F., Sun, C., Yang, W., Yuan, F., & Gao, Y. (2015). Structural characterization and functional evaluation of lactoferrin–polyphenol conjugates formed by free-radical graft copolymerization. *RSC Advances, 5*(20), 15641–15651.
Liu, L., Zhao, Q., Liu, T., & Zhao, M. (2011). Dynamic surface pressure and dilatational viscoelasticity of sodium caseinate/xanthan gum mixtures at the oil–water interface. *Food Hydrocolloids, 25*(5), 921–927.
Lopez, S., Montserrat-de la Paz, S., Lucas, R., Bermudez, B., Abia, R., Morales, J. C., et al. (2017). Effect of metabolites of hydroxytyrosol on protection against oxidative stress and inflammation in human endothelial cells. *Journal of Functional Foods, 29*, 238–247.
Ma, Z., Boye, J. I., & Simpson, B. K. (2016). Preparation of salad dressing emulsions using lentil, chickpea and pea protein isolates: A response surface methodology study. *Journal of Food Quality, 39*(4), 274–291.
Madhusudhan, K., & Singh, N. (1985). Isolation and characterization of the major fraction (12 S) of linseed proteins. *Journal of Agricultural and Food Chemistry, 33*(4), 673–677.
McDonald, R. E., & Hultin, H. O. (1987). Some characteristics of the enzymic lipid peroxidation system in the microsomal fraction of flounder skeletal muscle. *Journal of Food Science, 52*(1), 15–21.
Oomah, B. D., Der, T. J., & Godfrey, D. V. (2006). Thermal characteristics of flaxseed (Linum usitatissimum L.) proteins. *Food Chemistry, 98*(4), 733–741.
Oomah, B. D., Mazza, G., & Cui, W. (1994). Optimization of protein extraction from flaxseed meal. *Food Research International, 27*(4), 355–361.
Ozdal, T., Capanoglu, E., & Altay, F. (2013). A review on protein–phenolic interactions and associated changes. *Food Research International, 51*(2), 954–970.
Palazolo, G. G., Mitidieri, F., & Wagner, J. (2003). Relationship between interfacial behaviour of native and denatured soybean isolates and microstructure and coalescence of oil in water emulsions-effect of salt and protein concentration. *Food Science and Technology International, 9*(6), 409–419.
Paradiso, V. M., Di Mattia, C., Giarnetti, M., Chiarini, M., Andrich, L., & Caponio, F. (2016). Antioxidant behavior of olive phenolics in oil-in-water emulsions. *Journal of Agricultural and Food Chemistry, 64*(29), 5877–5886.
Pearce, K. N., & Kinsella, J. E. (1978). Emulsifying properties of proteins: Evaluation of a turbidimetric technique. *Journal of Agricultural and Food Chemistry, 26*(3), 716–723.
Ravera, F., Loglio, G., & Kovalchuk, V. I. (2010). Interfacial dilational rheology by oscillating bubble/drop methods. *Current Opinion in Colloid & Interface Science, 15*(4), 217–228.
Rawel, H. M., Czajka, D., Rohn, S., & Kroll, J. (2002). Interactions of different phenolic acids and flavonoids with soy proteins. *International Journal of Biological Macromolecules, 30*(3–4), 137–150.
Rawel, H. M., Kroll, J., & Rohn, S. (2001). Reactions of phenolic substances with lysozyme—physicochemical characterisation and proteolytic digestion of the derivatives. *Food Chemistry, 72*(1), 59–71.
Rodríguez, S. D., von Staszewski, M., & Pilosof, A. M. R. (2015). Green tea polyphenols-whey proteins nanoparticles: Bulk, interfacial and foaming behavior. *Food Hydrocolloids, 50*, 108–115.
Rühs, P. A., Affolter, C., Windhab, E. J., & Fischer, P. (2013). Shear and dilatational linear and nonlinear subphase controlled interfacial rheology of β-lactoglobulin fibrils and their derivatives. *Journal of Rheology, 57*(3), 1003.
Schmitt, C., Bovay, C., Rouvet, M., Shojaei-Rami, S., & Kolodziejczyk, E. (2007). Whey protein soluble aggregates from heating with NaCl: physicochemical, interfacial, and foaming properties. *Langmuir, 23*(8), 4155–4166.
Shahidi, F., & Naczk, M. (2003). *Phenolics in food and nutraceuticals*. CRC press.
Shantha, N. C., & Decker, E. A. (1994). *Rapid, sensitive, iron-based spectrophotometric methods for determination of perorlride values of food lipids*.
Sielicka, M., & Małecka, M. (2017). Enhancement of oxidative stability of flaxseed oil through flaxseed, evening primrose and black cumin cake extracts. *Journal of Food Processing and Preservation, 41*(4).
Škerget, M., Kotnik, P., Hadolin, M., Hraš, A. R., Simonič, M., & Knez, Ž. (2005). Phenols, proanthocyanidins, flavones and flavonols in some plant materials and their antioxidant activities. *Food Chemistry, 89*(2), 191–198.
von Staszewski, M., Pizones Ruiz-Henestrosa, V. M., & Pilosof, A. M. R. (2014). Green tea polyphenols-β-lactoglobulin nanocomplexes: Interfacial behavior, emulsification and oxidation stability of fish oil. *Food Hydrocolloids, 35*, 505–511.
Tadros, T. F. (2013). *Emulsion formation and stability*. John Wiley & Sons.
Timilsena, Y. P., Adhikari, R., Barrow, C. J., & Adhikari, B. (2016). Physicochemical and functional properties of protein isolate produced from Australian chia seeds. *Food Chemistry, 212*, 648–656.
Valls, R.-M., Farràs, M., Suárez, M., Fernández-Castillejo, S., Fitó, M., Konstantinidou, V., et al. (2015). Effects of functional olive oil enriched with its own phenolic compounds on endothelial function in hypertensive patients. A randomised controlled trial. *Food Chemistry, 167*, 30–35.
Wang, Li, D., Wang, L.-J., Adhikari, B., & Shi, J. (2010). Ability of flaxseed and soybean protein concentrates to stabilize oil-in-water emulsions. *Journal of Food Engineering, 100*(3), 417–426.
Wang, J.-M., Xia, N., Yang, X.-Q., Yin, S.-W., Qi, J.-R., He, X.-T., et al. (2012). Adsorption and dilatational rheology of heat-treated soy protein at the oil–water interface: Relationship to structural properties. *Journal of Agricultural and Food Chemistry, 60*(12), 3302–3310.
Ward, A., & Tordai, L. (1946). Time-dependence of boundary tensions of solutions I. The role of diffusion in time-effects. *The Journal of Chemical Physics, 14*(7), 453–461.
Waszkowiak, K., & Gliszczyńska-Świgło, A. (2015a). Binary ethanol–water solvents affect phenolic profile and antioxidant capacity of flaxseed extracts. *European Food Research and Technology, 242*(5), 777–786.
Waszkowiak, K., Gliszczyńska-Świgło, A., Barthet, V., & Skręty, J. (2015b). Effect of extraction method on the phenolic and cyanogenic glucoside profile of flaxseed extracts and their antioxidant capacity. *Journal of the American Oil Chemists Society, 92*(11–12), 1609–1619.
Wojciechowski, K. (2013). Surface activity of saponin from Quillaja bark at the air/water and oil/water interfaces. *Colloids and Surfaces B: Biointerfaces, 108*, 95–102.
Zhang, Z.-S., Wang, L.-J., Li, D., Li, S.-J., & Özkan, N. (2011). Characteristics of flaxseed oil from two different flax plants. *International Journal of Food Properties, 14*(6), 1286–1296.

CHAPTER 5

Microencapsulation of flaxseed oil using polyphenol-adducted flaxseed protein isolate-flaxseed gum complex coacervates

Published in *Food Hydrocolloids,* 2020, 107, 105944.

Food Hydrocolloids 107 (2020) 105944

Contents lists available at ScienceDirect

Food Hydrocolloids

journal homepage: http://www.elsevier.com/locate/foodhyd

Microencapsulation of flaxseed oil using polyphenol-adducted flaxseed protein isolate-flaxseed gum complex coacervates

Loc B. Pham [a], Bo Wang [b], Bogdan Zisu [c], Tuyen Truong [a], Benu Adhikari [a,*]

[a] School of Science, RMIT University, Melbourne, VIC, 3028, Australia
[b] Australian Catholic University, Sydney, NSW, 2060, Australia
[c] Spraying Systems Co Pty Ltd, Truganina, VIC, 3029, Australia

ARTICLE INFO

Keywords:
Flaxseed oil
Flaxseed polyphenols
Hydroxytyrosol
Complex coacervates
Lipid oxidation
Microencapsulation

ABSTRACT

This study aimed to evaluate the applicability of polyphenol-adducted flaxseed protein isolate (FPI)-flaxseed gum (FG) complex coacervates to encapsulate flaxseed oil (FO). FPI was covalently adducted with flaxseed polyphenol (FPP) or hydroxytyrosol (HT). β-sheet was major secondary structure of FPI and its covalent conjugation with polyphenols further increased the β-sheet content. The extent of increase of this ordered structure was found to depend on the type of aducted polyphenol. Subsequently, complex coacervation between polyphenol adducted FPI and FG was studied in terms of optimum complex coacervation pH and protein-to-gum ratio. Compared to FPI and FPI-polyphenol adducts, FPI/FG, (FPI-FPP)/FG and (FPI-HT)/FG complex coacervates had significantly higher random coil and significantly lower β-sheet contents suggesting that these complex coacervates had less ordered structure. Finally, the spray-dried microcapsule powders of FO were produced using FPI/FG, (FPI-FPP)/FG and (FPI-HT)/FG as shell materials. Physicochemical properties of these microcapsules, including surface oil, microencapsulation efficiency and stability against oxidation, were determined. The optimum pH for complex coacervation between FPI/FG, (FPI-FPP)/FG and (FPI-HT)/FG was very close (4.6 ± 0.1) and the optimum protein-to-gum ratio of 6.0 was also identical. All these microcapsules had irregular shape with wrinkled surface morphology. The microcapsules produced using (FPI-HT)/FG complex coacervates had lowest surface oil (1%, w/w) and highest microencapsulation efficiency (95.4%). The microcapsules encapsulated using (FPI-FPP)/FG complex coacervates had the highest stability against oxidation as measured by peroxide value and *p*-anisidine value. Overall the complex coacervates produced using polyphenol adducted FPI and FG were found to be better than FPI/FG complex coacervates as encapsulating shell materials for oxygen-sensitive oil.

1. Introduction

Microencapsulation technologies are commonly used in contemporary food industry to prevent the exposure of susceptible hydrophobic materials to environmental stresses such as oxygen, light and elevated temperature. In the case of sensitive plant oils from flaxseed, grapeseed and walnut, microcapsule shell materials create a physical barrier surrounding the hydrophobic core and provide significant level of protection against oxidative deterioration. The encapsulated oil can be converted into solid microcapsules, which facilitates handling, masking the odour/off-flavour and imparting control-released property (Gharsallaoui, Roudaut, Chambin, Voilley, & Saurel, 2007). Kaushik, Dowling, Barrow, and Adhikari (2015a) reviewed advantages and limitations of technologies used to encapsulate omega-3 oils including spray- and freeze-drying of emulsions, fluidised bed drying, extrusion and complex coacervation followed by spray drying. Among these technologies, the complex coacervation-followed by spray drying technology has shown many advantages such as affordability, reproducibility and scalability (Encina, Vergara, Gimenez, Oyarzun-Ampuero, & Robert, 2016), and produces powdered microcapsules with high oil loading and minimal surface oil (Timilsena, Adhikari, Barrow, & Adhikari, 2016).

Generally, good mechanical strength and thermal stability are required in the shell materials to keep the hydrophobic core "entrapped" and to prevent it from leaking out from the microcapsules. Chemicals and enzymes such as glutaraldehyde transglutaminase are used to date to crosslink the protein component of shell materials and to improve their mechanical strength. However, glutaraldehyde is not suitable for food application due to its toxic nature (Heck, Faccio, Richter, &

* Corresponding author.
E-mail address: benu.adhikari@rmit.edu.au (B. Adhikari).

https://doi.org/10.1016/j.foodhyd.2020.105944
Received 6 November 2019; Received in revised form 28 March 2020; Accepted 13 April 2020
Available online 19 April 2020

Thöny-Meyer, 2013). In this context, the interaction or reactivity between protein and phenolic compounds can be harnessed to improve the strength of the protein network (Lopez & Edens, 2005; Sarker, Wilde, & Clark, 1995). Furthermore, the presence of polyphenols in the shell matrix can impart antioxidative activity to the shell. For example, Binsi et al. (2017) examined microencapsulation of fish oil by using sage polyphenol to stabilize the caseinate/gum Arabic shell. This matrix provided an increased protection to the encapsulated oil against oxidation. Thus, it is of practical importance to explore further the inclusion of polyphenols in the shell matrix of microcapsules to enhance their protective function.

Dairy proteins and gelatin are so far the most widely used proteins to encapsulate polyunsaturated fatty acids (PUFAs) containing oils (Goyal et al., 2015; Pourashouri et al., 2014). However, plant proteins such as soybean, pea and cereal proteins are increasingly attracting research interest due to their green and healthy images to the consumers (Nesterenko, Alric, Silvestre, & Durrieu, 2013). Among various plant proteins, flaxseed protein isolate (FPI) is a promising encapsulating material for the oxygen-sensitive oil as it has suitable emulsifying property and good thermal stability (Kaushik et al., 2016). In addition, flaxseed also has high phenolic content (5.42 g per 100 g of seed) which can be potentially used as protein crosslinker (Dabrowski and Sosulski (1984). Flaxseed also contains phenolic acids such as ferulic, p-coumaric and caffeic acid which are the source of antioxidant properties (Waszkowiak, Gliszczyńska-Świgło, Barthet, & Skręty, 2015).

Flaxseed is still primarily used as a source of oil due to its high alpha-linolenic acid (ALA) content (>50% of total fatty acids) (Daun, Barthet, Chornick, & Duguid, 2003). Attempts have been made to improve the oxidative stability of encapsulated flaxseed oil by using lentil protein/maltodextrin (Avramenko, Chang, Low, & Nickerson, 2016), legume protein/maltodextrin (Can Karaca, Low, & Nickerson, 2013) and zein protein (Quispe-Condori, Saldaña, & Temelli, 2011) as shell materials. In another context, hydroxytyrosol (HT), a phenolic alcohol found abundantly in olive oil, is reported to possess intense antioxidative activity. It offers many health benefits, including reducing systolic blood pressure (Covas, de la Torre, & Fitó, 2015), enhancing endothelial function (Valls et al., 2015) and alleviating inflammation (Lopez et al., 2017). HT has a potential to form adducts with proteins including FPI as it is able to crosslink them and produce adducts with antioxidant properties (Pham, Wang, Zisu, & Adhikari, 2019b). Therefore, it is of scientific and practical importance to understand the complex coacervation occurring between polyphenol adducted protein and polysaccharide gum and the efficacy of their complex coacervates as encapsulants of oxygen sensitive compounds including PUFAs. It is hypothesized that the complex coacervates produced between polyphenol adducted FPI and FG can better encapsulate the flaxseed oil when it is used as a model PUFAs.

Here in, we report the complex coacervation behaviour of FPI-polyphenol (i.e. FPI-FPP and FPI-HT) adducts including optimum pH and adduct/FG ratio together with the complex coacervation behaviour of un-adducted (free) FPI. We also report the efficacy of complex coacervates of these adducts as shell material to produce powder microcapsules of oxygen-sensitive oil (e.g., flaxseed oil).

2. Materials and methods

2.1. Materials

Flaxseed was obtained from Stoney Creek Oil Products Pty Ltd (Talbot, Victoria, Australia) and was stored at 4 °C before use. Ferulic acid, Folin-Ciocalteu reagent, Bradford reagent, ammonium thiocyanate, ferrous sulfate, barium chloride and *p*-anisidine were purchased from Sigma Aldrich (Castle Hill, New South Wales, Australia). Hydroxytyrosol (HT, purity ≥ 95%) was purchased from AvaChem Scientific (San Antonio, Texas, USA).

2.2. Extraction of FPI, FPP, FG gum and flaxseed oil

FPI was extracted using Oomah, Mazza, and Cui (1994)'s method with minor modification as reported earlier (Pham, Wang, Zisu, & Adhikari, 2019a). Briefly, flaxseed was firstly degummed by soaking the seeds in Milli-Q water at 60 °C for 2 h at a flaxseed-to-water ratio of 1:18 (w/w) under continuous agitation. In this step, ultrasonication (HD3400, Bandelin, Berlin, Germany) was used at 400 W and 20 Hz for 12 min to facilitate the removal of the gum. The degummed flaxseed sample was air-dried for 48 h and then ground using a coffee grinder. The ground flaxseed was defatted twice using hexane at a degummed flaxseed meal-to-hexane ratio of 1:6 (w/v). The defatted degummed samples were dried in a fume hood for 24 h to remove hexane residue. The residual hull was separated from the defatted degummed flours using a 150 μm sieve. FPI was then extracted from the defatted degummed flaxseed flour by using 0.1M Tris buffer at a flour-to-buffer ratio of 1:16 (w/v) at pH 8.6 for 16 h. The undissolved residue was removed by centrifugation (at 10,000×*g* for 20 min) and the supernatant was dialysed (for 48 h at 4 °C) using a dialysing bag with a cut-off molecular weight of 6–8 kDa (Orange Scientific, Braine-l'Alleud, Belgium). Milli-Q water was used as a dialysing medium. The dialysed supernatant was freeze-dried at −40 °C to obtain the FPI powder and it was stored at 4 °C before use.

Flaxseed oil was extracted using hexane as described by Zhang, Wang, Li, Li, and Özkan (2011) with minor modification. Briefly, the degummed flaxseed was ground into a fine meal using a coffee grinder. This ground meal was mixed with hexane at the meal-to-hexane ratio 1:6 (w/v) and stirred at 800 rpm at 22 ± 1 °C for 6 h. Hexane was changed every 3 h during extraction. The slurry was centrifuged at 10,000×*g* for 20 min and the supernatant was collected. Subsequently, the solvent was evaporated at 40 °C using a rotary vacuum evaporator (RC 2000; Buchi Corporation, Flawil, Switzerland) to obtain the oil.

Flaxseed polyphenols (FPP) were extracted from defatted degummed flaxseed meal according to Anwar and Przybylski (2012)'s method. Briefly, the meal was mixed with 60% (v/v) ethanol at a flour-to-ethanol ratio of 1:10 (w/v) and stirred for 4 h at 22±1 °C. The undissolved fraction was removed by filtration (Whatman No.1, GE Healthcare, Chicago, IL, U.S.A.). This extraction process was performed once again and the filtrate from both extractions was combined. The solvent was subsequently removed using a rotary vacuum evaporator (RC 2000; Buchi Corporation, Flawil, Switzerland) and freeze-dried at −40 °C to obtain FPP powder. This FPP powder was stored at 4 °C before use.

Flaxseed gum (FG) was extracted from whole flaxseed as proposed by Cui, Mazza, and Biliaderis (1994) with minor modification. Briefly, the flaxseed was added to Milli-Q water at a flaxseed-to-water ratio of 1:18 and the mixture was heated at 60 °C. After 2h continuous agitation, the soaked seeds were filtered to remove the seed and the extracted gum was centrifuged at 10,000×*g* for 30 min to obtain mucilage as supernatant. The mucilage was precipitated from the supernatant by adding absolute ethanol at a mucilage solution-to-ethanol ratio of 1:2 (v/v). Finally, the precipitated gum was decanted, freeze-dried at −40 °C and stored at 4 °C for further use.

2.3. Determination of the proximate composition of FPI and FG

Moisture, lipid, and ash contents of FPI were measured using AOAC methods 925.1, 920.85 and 923.03, respectively (AOAC, 2005). The total protein content of solid samples was measured by measuring nitrogen content and using a conversion factor of 6.25 (FP-2000, LECO Corporation, Saint Joseph, MI, U.S.A.) (Oomah, Der, & Godfrey, 2006). The carbohydrate content was measured by subtracting the other components from 100%.

2.4. Preparation of protein-phenolic adducts

FPI-FPP and FPI-HT adducts were prepared following our recent

work (Pham et al., 2019b) with minor modification. Firstly, 10 g FPI was dispersed in 1000 mL Milli-Q water and the pH was adjusted to 9.0. Then 3 mmol phenolic compound was added. FPP was hydrolysed beforehand using 2M NaOH for 2 h to facilitate its reaction with protein. The above-mentioned molar concentration of FPP is expressed as ferulic acid equivalent determined by Folin–Ciocalteu method (Škerget et al., 2005). This hydrolysis step broke down large phenolic molecules (i.e., phenolic glycosides) to more reactive small ones (phenolic acids or flavonoids). These mixtures were stirred at 200 rpm for 24 h at ambient temperature in the presence of oxygen to enable the reaction between phenolic compounds and FPI. The pH of these mixtures was frequently checked and adjusted to 9.0 during agitation. After 24h, these reacted mixtures were dialysed using dialysis bags with a cut-off molecular weight range of 6–8 kDa (Orange Scientific, Braine-l'Alleud, Belgium) against water for 20 h to remove the unreacted phenolic compounds. The dialysed FPI-phenolic adduct sample was finally freeze-dried (−40 °C) and stored at 4 °C before further use.

2.5. Determination of optimum pH and protein/gum ratio for complex coacervation

The optimum pH and protein/gum ratio for complex coacervation were determined using zeta-potential and optical density values for FPI/FG, FPI-FPP/FG and FPI-HT/FG mixtures as a function of pH. For this purpose, the protein/gum ratios of 0.5, 1 to 10 with an increment of 1, 12, 15, 20 and 25 (w/w) were prepared the final total solid content of 0.3% (w/w).

The zeta-potential value was measured using a Zetasizer (ZS-90, Malvern instruments Ltd, Malvern, Worcestershire, UK) and calculated using a Zetasizer Nano software v3.30.

Optical density values of individual polymers and their mixture in the pH range of 2–7 were determined using Nakagawa and Nagao (2012)'s method with minor modification. The light absorption of these dispersions was recorded at 400 nm using a UV spectrophotometer (LAMBDA 35, PerkinElmer, Llantrisant, U.K). The pH value at which the highest optical density was observed was considered to be the optimum pH. In this test, the dispersions originally containing 0.3% (w/w) solids were diluted 200 times to avoid high turbidity and viscosity. The pH of the dispersion was adjusted as required using 0.1M HCl or 0.1 N NaOH.

2.6. Preparation of liquid microcapsules using FPI, FPI-phenolic adducts/FG complex coacervates

FPI or FPI-phenolic adduct solutions were prepared separately by dissolving 15 g FPI and FPI-phenolic adducts in water to obtain 250 g solution. FG solution was prepared by dissolving 2.5 g FG in water to obtain 250 g solution. In order to encapsulate the oil *in situ* while the complex coacervates were formed, the FPI or FPI-phenolic adduct solutions were mixed with 8.75 g flaxseed oil and the mixture was homogenised (Ultra-Turrax T-50 Homogenizer, IKA-Werke, Staufen, Germany) at 15,000 rpm for 4 min to prepare the coarse emulsions. These coarse emulsions were subsequently homogenised using a microfluidiser (M-110L, Microfluidics, Newton, MA) at 12,000 psi for 3 passes to produce fine emulsions (Wang, Li, Wang, Adhikari, & Shi, 2010). Then, 250 g FG solution was slowly added to these fine emulsions and agitated at 800 rpm. The temperature of this process was maintained at 40 °C to facilitate the agitation as the high viscosity of FG at the ambient temperature makes it harder to agitate (Timilsena, Adhikari, et al., 2016). The pH of the mixed emulsions was adjusted to their optimum values (section 2.4) using 1M HCl to induce complex coacervation. The concentrations of protein and gum solutions in the final mixture before the dehydration step was at 3 and 0.5% (w/w), respectively in all formulations. The core-to-wall ratio of these formulations was 1:2 (w/w). The liquid microcapsules formed in this way were cooled down to 5 °C to facilitate the migration of complex coacervates from the aqueous phase to the oil-water interface and cover the oil droplets (Wang, Adhikari, & Barrow, 2014). For consolidating the shell of microcapsules formed by the FPI-FG and FPI-phenolic adduct-FG complex coacervates, 50 mL (2%, w/v) transglutaminase solution was added to the liquid microcapsules at 5 °C and the mixture was further agitated for 24 h to complete the crosslinking process. The temperature of these liquid microcapsules was brought to 25 °C before they were spray dried.

2.7. Spray drying

The liquid microcapsules produced in section 2.5 were spray dried using a bench-top spray dryer (LabPlant, SD-Basic, England) equipped with a twin-fluid atomizing nozzle of 0.5 mm diameter. Compressed air was used as the atomizing fluid operating at pressure of 0.35 MPa. Liquid microcapsule samples were diluted twice to reduce their viscosity and to facilitate the atomization. The stability of the liquid microcapsules was not affected by this dilution step. The inlet and outlet temperature used were 200 and 112 ± 2 °C, respectively. The flow rate of the feed was controlled at 8 mL/min. Due to the relatively high viscosity of the feed (Fig. 3A), the outlet temperature of spray drier was maintained at 112 ± 2 °C to reduce the residual moisture content of the dried microcapsules to a desirable range. These spray-dried solid microcapsules were store at 4 °C until further use.

2.8. Determination of particle size of re-constituted microcapsules

The droplet size of emulsions and liquid microcapsules was determined using dynamic light scattering method (Mastersizer 3000, Malvern Instruments Ltd., Malvern, UK). Deionised water was used as the dispersant, and the droplet size was expressed as surface mean ($d_{3,2}$) and volume mean ($d_{4,3}$) using equations (1) and (2), respectively.

$$\mathbf{d}_{3,2} = \frac{\sum_{i=1} \mathbf{n_i}.\mathbf{d_i^3}}{\sum_{i=1} \mathbf{n_i}.\mathbf{d_i^2}} \quad (1)$$

$$\mathbf{d}_{4,3} = \frac{\sum_{i=1} \mathbf{n_i}.\mathbf{d_i^4}}{\sum_{i=1} \mathbf{n_i}.\mathbf{d_i^3}} \quad (2)$$

Reconstituted dispersion was prepared by dispersing 0.5 g spray-dried sample into 150 mL Milli-Q water. This dispersion was agitated at 200 rpm for 30 min before measuring the particle size.

2.9. Determination of viscosity of emulsion and liquid microcapsules

The viscosity of emulsion and liquid microcapsules was obtained through steady-shear flow measurement, using a rheometer (Discovery HR-1, TA Instruments Ltd., U.S.) equipped with a 40 mm stainless steel parallel plate. The gap was set at 1 mm, and the temperature was maintained at 25 °C. The viscosity was computed from the shear stress-shear rate curve in of 0–120 s^{-1} shear rate range.

2.10. Determination of physicochemical properties of microcapsules

2.10.1. Moisture content and water activity

Moisture content of spray-dried microcapsule was determined gravimetrically using an air-force oven at 105 °C for 12h (Klaypradit & Huang, 2008). The water activity (a_w) of microcapsules was measured using a water activity meter (Aqualab CX-2, Decagon Devices, Inc., Pullman, WA, USA).

2.10.2. Surface oil and total oil contents of microcapsules

The surface oil content (in wt. %) of microcapsule powder was measured according to Liu, Low, and Nickerson (2010)'s method. Briefly, 1 g microcapsule was added into 30 mL hexane and the mixture was vortexed for 60 s. Then, the oil-containing hexane was filtered into a pre-weighted rotating flask through a filter paper (No.1, GE Healthcare, Chicago, IL, U.S.A). Hexane was removed from the extracted oil by

evaporation using the rotary evaporator. The mass of the extracted oil was measured gravimetrically after heating it at 105 °C for 30 min to remove the remaining solvent. The total oil content of microcapsules was measured according to Klinkesorn, Sophanodora, Chinachoti, Decker, and McClements (2006). One gram of microcapsule was dispersed in 4 mL Milli-Q water and vortexed for 2 min. Then 25 mL of hexane/isopropanol (3:1, v/v) mixture was added to the dispersion and stirred at 300 rpm for 15 min followed by centrifugation at 15,000×*g* for 2 min. The clear upper phase was collected, and the lower aqueous phase was re-extracted with the same amount of solvent. The organic phase of both cycles was combined and filtered through Na_2SO_4 to remove the aqueous residue. Finally, the solvent was evaporated at 40 °C using the rotary vacuum evaporator and the oil was dried at 105 °C for 30 min to remove the remaining solvent.

2.10.3. Encapsulation efficiency

The encapsulation efficiency (EE, %) of the microcapsule powders was calculated making use of surface oil and the total oil contents using equation (3) (Anwar & Kunz, 2011).

$$\mathbf{EE} = \frac{(\mathbf{Total\ \ oil} - \mathbf{Surface\ \ oil})}{\mathbf{Total\ \ oil}} \times 100\% \quad (3)$$

2.10.4. Glass transition temperature

The glass transition temperature (T_g) of powder microcapsules was measured using a differential scanning calorimeter (DSC Q-2000, TA Instruments, New Castle, DE, U.S.A.). Briefly, 7 mg sample was loaded into an aluminum pan and hermetically sealed. Samples were heated from −20 to 130 °C at a rate of 10 °C/min under 20 mL/min nitrogen gas purge in the first cycle and cooled from 130 °C to −20 °C at the same rate. Second heating cycle was performed from −20 °C to 150 °C at the same heating and gas purge rates. T_g values were acquired at mid-point of the inflection section of thermogram using Universal™ software (TA Instruments, New Castle, DE, U.S.A.). A sealed empty pan was used to correct the baseline.

2.11. Determination of surface morphology of microcapsules

The surface morphology of spray-dried microcapsules was acquired using a scanning electron microscope (FEI Quanta 200 ESEM, Japan). Spray-dried capsules were coated with a thin layer of gold for 2 min using a gold sputter (Sputter coater, Agar Aids, England). The micrographs were acquired at an accelerating voltage of 30 kV.

2.12. Determination of surface composition of solid microcapsules

The elemental surface composition of solid microcapsules including carbon (C), nitrogen (N), and oxygen (O) was acquired using X-ray photoelectron spectroscopic (XPS) technique (Porras-Saavedra et al., 2018). For this, microcapsules were placed in a sample holder, kept in a vacuum chamber (2×10^{-8} mbar) for 24 h. The sample was scanned using an X-ray photoelectron spectrometer (K-alpha, Fischer Scientific, USA) equipped with a monochromatic X-ray source (Al K-alpha). The spectra were analysed using the Thermo Scientific Avantage software (v 5.9, Thermo Fisher Scientific, USA).

2.13. Oxidative stability of solid microcapsules

The FO microcapsule powders were stored at 40 °C for 4 weeks. Prior to analysing oxidative stability, the FO was extracted from the powder using the "total oil extraction method" (section 2.9.2) and then dried using nitrogen flush. The oxidative stability was measured in terms of peroxide and *p*-Anisidine values of the encapsulated FO in 1-week interval.

2.13.1. Peroxide value

The peroxide value (PV) of encapsulated oil was measured according to a method described by Shantha and Decker (1994) and Mancuso, McClements, and Decker (1999) with minor modifications. In brief, 10 mg extracted oil was weighed and transferred into a 5 mL test tube. Then, 3 mL methanol-butanol blend (2:1, v/v) was added to the test tube as the solvent and the mixture was vortexed to dissolve the oil. Subsequently, 15 μL 3.94 M ammonium thiocyanate solution and15 μL 0.072 M ferrous chloride solution were sequentially added to the test tube. The final mixture was vortexed and kept in a dark chamber for 20 min and then its absorbance was measured at 510 nm using the UV spectrometer. PV of reagents was also measured in the absence of to use as a blank. The PV was calculated using equation (4) and expressed as milliequivalents of O_2/kg oil.

$$PV = \frac{(A_s - A_b) \times m}{(55.84 \times m_0)} \quad (4)$$

where, PV is peroxide value of oil (meq. O_2/kg oil), A_s and A_b are absorbance values of sample and blank, respectively. Similarly, m is slope of Fe^{+3} standard curve (1–20 μg), m_0 is mass of the sample (g) and 55.84 is the atomic weight of iron.

2.13.2. p-Anisidine value

The *p*-Anisidine value (*p*-AV) of encapsulated oil was determined using the American Oil Chemists' Society (AOCS) Method Cd 18–90, AOCS (1998). Briefly, 500 mg extracted oil was dissolved in 25 mL iso-octane. Then, 5 mL of iso-octane dissolved oil was mixed with 1 mL p-anisidine reagent prepared by dissolving 0.25 g p-anisidine powder in 100 mL glacial acetic acid. This mixture was shaken vigorously for 10 min and its absorbance was measured at 350 nm using the UV spectrometer. The iso-octane solvent was used as the reference (blank). The *p*-AV of sample was calculated using equation (5).

$$p - AV = \frac{25 \times (1.2A_s - A_b)}{m} \quad (5)$$

where, *p*-AV is anisidine value (AU_{350}/g oil), A_b is absorbance of oil dissolved in isooctane; A_s is absorbance of oil solution with p-anisidine; m is the mass of oil (g).

2.14. Determination of secondary structure of protein in adducts and complex coacervates

FTIR spectra of FPI, FPI-phenolic adducts and their coacervates with FG were acquired at 4 cm^{-1} resolution with 128 scans using a PerkinElmer spectrometer with a diamond ATR (PerkinElmer, Norwalk, CT, U.S.A.). The spectra were analysed using Origin software (Version 9, Origin Lab, MA, USA) to quantify the secondary structure composition. Briefly, Fourier self deconvolution (FSD) of the spectrums was performed with the gamma of 5 and the smoothing factor of 0.1 (Jackson & Mantsch, 1995), followed by the straight baseline subtraction of the Amide I region at 1600–1700 cm^{-1} (Carbonaro & Nucara, 2010). Subsequently, the processed curve was fitted using Gaussian function and the peaks were assigned to the individual secondary structure of protein following the approach adapted by Jackson and Mantsch (1995) and Mizutani, Matsumura, Imamura, Nakanishi, and Mori (2003).

2.15. Statistical analysis

Tests were conducted at least in triplicate and data is reported as average ± standard deviation. The SPSS statistical software (version 24, SPSS Inc., Chicago, IL, USA) was used for analysis of variance (ANOVA) to test the significant difference between two mean values. Duncan test was implemented on the data sets at 95% significance level ($p < 0.05$).

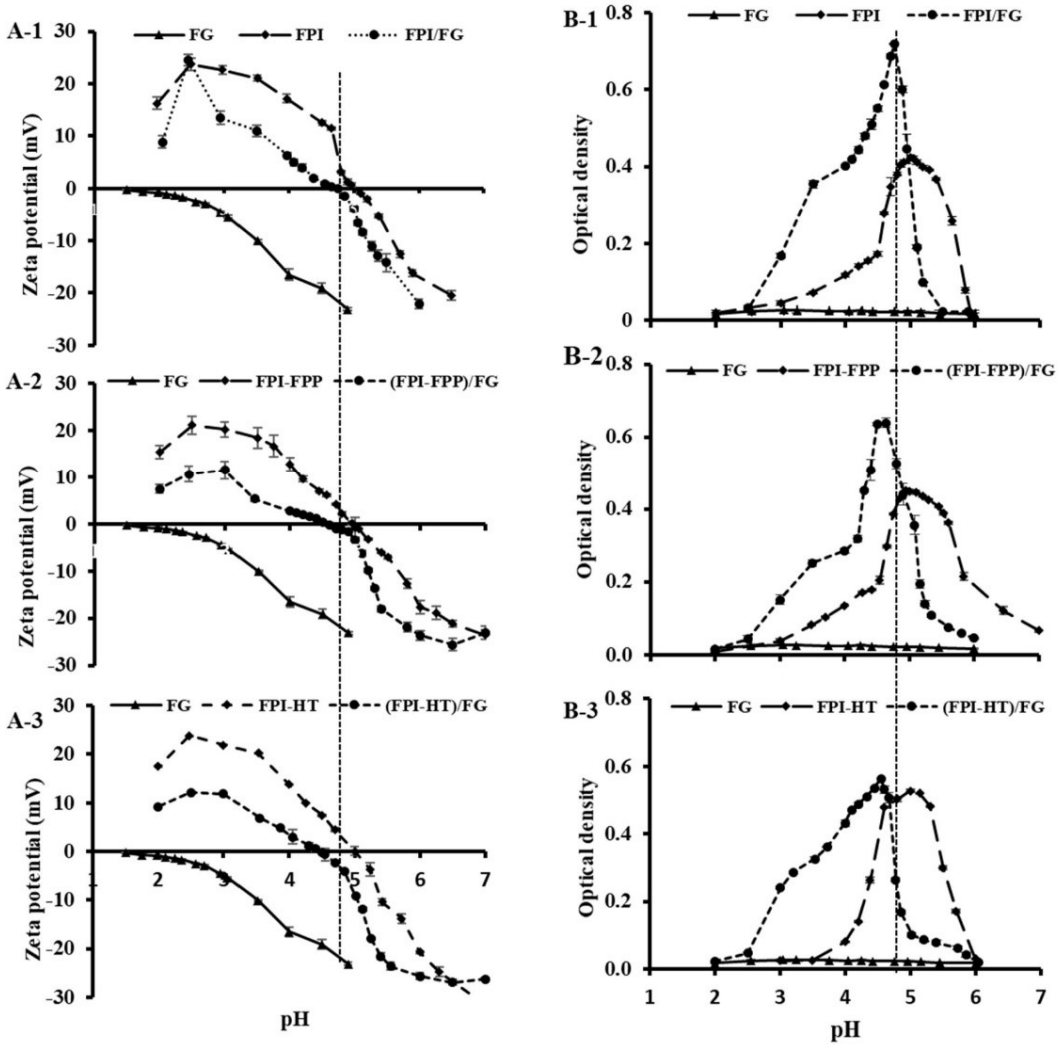

Fig. 1. Zeta potential (A), and optical density (B) of FPI (1), FPI-FPP (2), and FPI-HT (3) with FG at a protein/gum ratio of 6 and total solid content of 0.3% (w/w) as a function of pH. FPI = flaxseed protein isolate, FPP = flaxseed polyphenols, HT = hydroxytyrosol, FG = flaxseed gum.

3. Result and discussion

3.1. Chemical composition of FPI and FG

The FPI contained 2.70 ± 0.04% (w/w) moisture, 93.60 ± 2.06% (w/w) protein, 2.10 ± 0.07% (w/w) lipid and 0.56 ± 0.07% (w/w) ash. The FG contained 5.32 ± 0.17% (w/w) moisture, 12.66 ± 0.52% (w/w) protein, 1.11 ± 0.13% (w/w) lipid, 78.02 ± 0.50 carbohydrate and 2.89 ± 0.30% (w/w) ash.

3.2. Optimum pH for complex coacervation between FPI and phenolic compound adducted FPI with FG

The optimum pH for complex coacervation between FPI or between phenolic compound adducted FPI with FG was determined using their zeta potential and the optical density values (Fig. 1). FPI showed an isoelectric point (pI) at pH 5.0 below which it was positively charged (Fig. 1A). FG was negatively charged above pH 2.0. The pI of the mixture of the FPI/FG, (FPI-FPP)/FG, and (FPI-HT)/FG was observed at pH of 4.75, 4.65, and 4.55 respectively, suggesting that some of the amino groups in the FPI chain were blocked due to its covalent reaction with FPP and HT (Pham et al., 2019a). The pI values of FPI-FG and phenolic adducted-FPI-FG mixtures were further confirmed by their optical density values (Fig. 1B). This is because the highest optical density of protein-polysaccharides mixed solution occurred at the pH where the electrostatic charge was neutralized. These data suggest that the optimum pH for complex coacervation in FPI/FG, (FPI-FPP)/FG and (FPI-HT)/FG systems was 4.7, 4.6, and 4.5 respectively. The optimum pH at which complex coacervation occurred between FPI and FG was different than the optimum pH reported by Kaushik, Dowling, Barrow, and Adhikari (2015b), possibly be due to the difference in protein extraction method used. In this study, FPI was subjected to dialysis while Kaushik et al. (2015b) did not dialyse their FPI and thus their purity was lower (90.6%) than ours (93.6%).

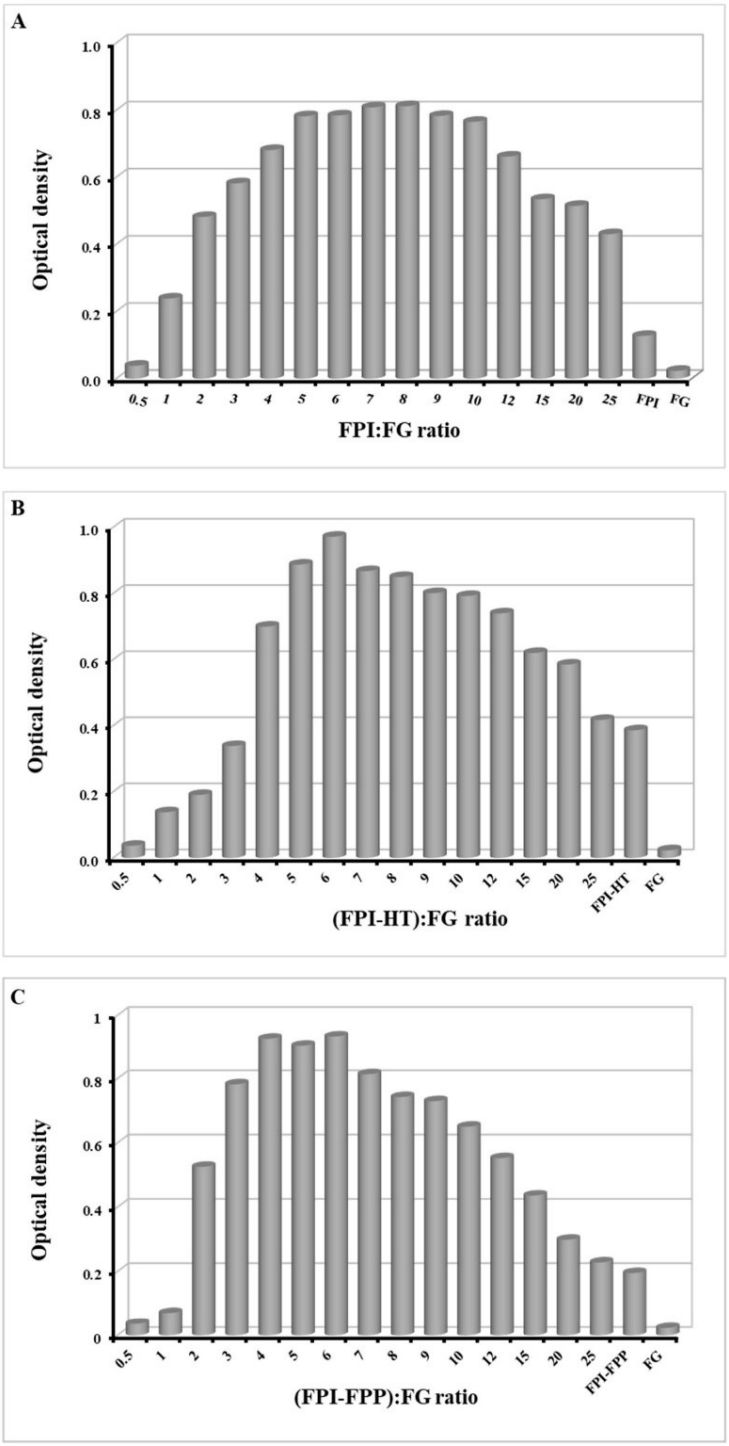

Fig. 2. Optical density of FPI (A), FPI-FPP (B) and FPI-HT (B) with FG at pH of 4.75, 4.65, and 4.55 respectively at total solid content of 0.3% (w/w) as a function of protein/gum ratio at their optimum pH. FPI = flaxseed protein isolate, FPP = flaxseed polyphenols, HT = hydroxytyrosol, FG = flaxseed gum.

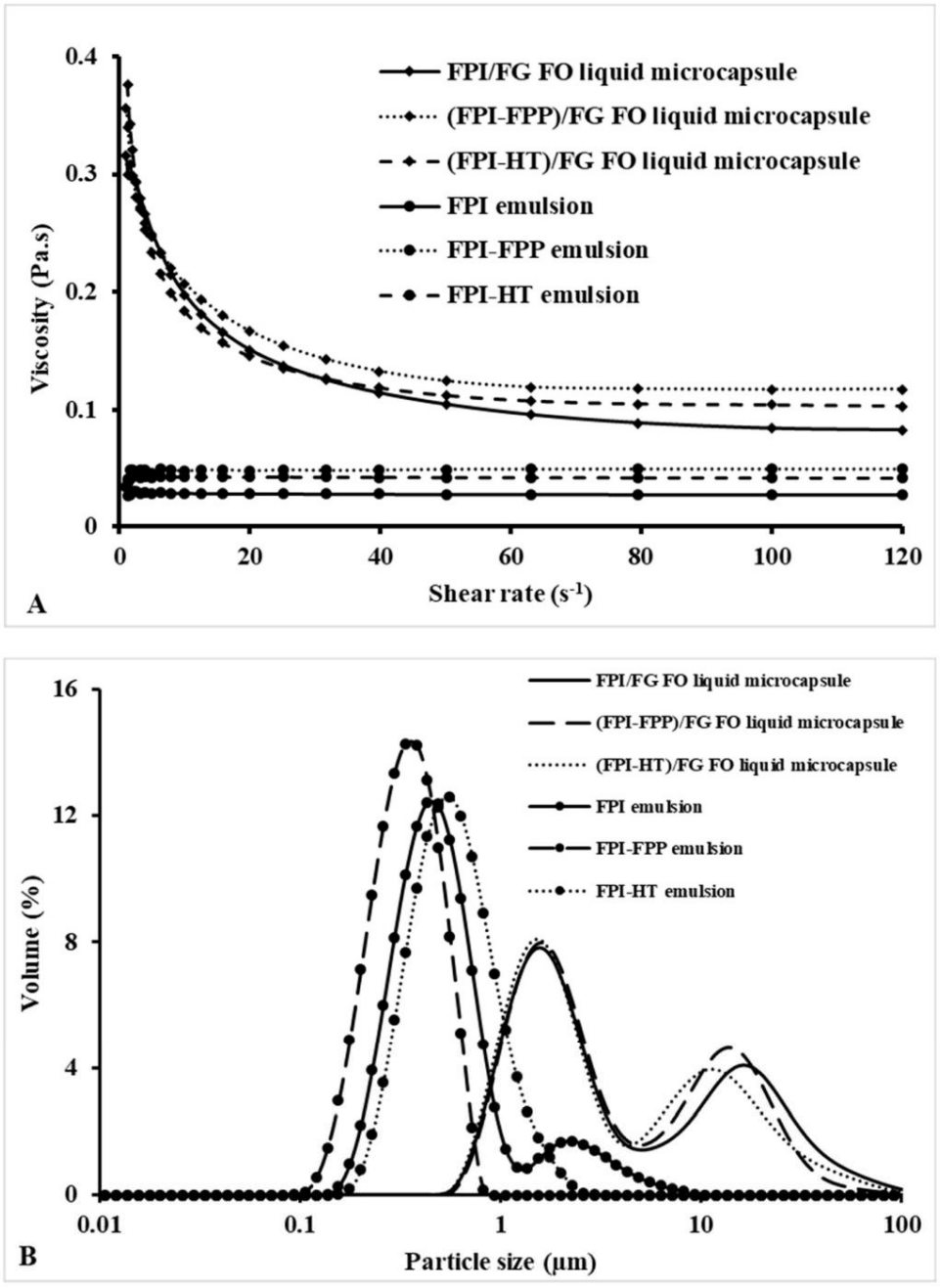

Fig. 3. Apparent viscosity measured in 0–120 shear rate (s^{-1}) range (A) and particle size distribution (B) of emulsions stabilised by FPI, FPI-FPP, and FPI-HT and liquid microcapsules produced by FPI/FG, (FPI-FPP)/FG, and (FPI-HT)/FG at pH of 4.75, 4.65, and 4.55 respectively with an oil/encapsulant ratio of 0.5 and a protein/gum ratio of 6. FPI = flaxseed protein isolate, FPP = flaxseed polyphenols, HT = hydroxytyrosol, FG = flaxseed gum, FO = flaxseed oil.

3.3. *Optimal ratio for complex coacervation between FPI, (FPI-FPP), and (FPI-HT) and FG*

The optical density values of FPI/FG and phenolic-adducted FPI/FG at various protein-to-gum ratios (0.5–25, w/w) at their respective optimum complex coacervation pHs are presented in Fig. 2. The optimum protein-to-gum ratio of 6 was observed in all three formulations. The optimum FPI-to-FG ratio is different than the one reported by Kaushik et al. (2015b), possibly due to significantly higher protein content in FPI used in this study. Interestingly, this ratio was quite close

Table 1
Physicochemical properties of microcapsules produced using FPI/FG, (FPI-FPP)/FG, and (FPI-HT)/FG. FPI = flaxseed protein isolate, FPP = flaxseed polyphenols, HT = hydroxytyrosol, FG = flaxseed gum.

Formulations	Moisture (%)	Water activity (%)	Glass transition (T_g, °C)	Particle size (μm)		Surface oil content (%)	Encapsulation efficiency (%)
				[d 4,3]	[d 3,2]		
FPI/FG	2.66 ± 0.09 ^{a}	0.16 ± 0 ^{a}	110.4 ± 1.7 ^{a}	5.11 ± 0.1 ^{a}	1.42 ± 0 ^{a}	2.8 ± 0.4 ^{a}	87.8 ± 1.7 ^{a}
FPI-FPP/FG	2.79 ± 0.33 ^{a}	0.16 ± 0 ^{a}	115.9 ± 1.3 ^{b}	3.46 ± 0.06 ^{b}	1.38 ± 0.01 ^{b}	3.5 ± 0.3 ^{a}	85.5 ± 1.4 ^{a}
FPI-HT/FG	2.89 ± 0.20 ^{a}	0.14 ± 0.01 ^{b}	121.2 ± 1.3 ^{c}	3.79 ± 0.01 ^{c}	1.43 ± 0 ^{a}	1.0 ± 0.3 ^{b}	95.4 ± 1.5 ^{b}

Different lowercase letters in the superscript of the same column indicate significant differences ($p < 0.05$).

to the optimum protein-to-gum ratio between chia seed protein isolate and chia seed gum (Timilsena, Wang, Adhikari, & Adhikari, 2016).

3.4. Viscosity and particle size of emulsion and liquid microcapsules

The viscosity of emulsions stabilised by FPI, (FPI-FPP), and (FPI-HT) and liquid microcapsules produced by FPI/FG, (FPI-FPP)/FG, and (FPI-HT)/FG as a function of shear rate is presented in Fig. 3A. All tested FO-in-water emulsions exhibited Newtonian behaviour and their viscosity values were in FPI < (FPI-HT) < (FPI-FPP) order. This slight increase in viscosity of emulsions stabilised by phenolic compound adducted FPI can be attributed to the change in the structure of FPI after conjugation with FPP and HT (Pham et al., 2019b). Similar Newtonian flow behaviour was observed in FO-in-water emulsions stabilised by WPI (Campelo et al., 2017) and avocado oil-in-water emulsion stabilised by WPI/-maltodextrin (Bae & Lee, 2008). The mean droplet size of FPI-FPP stabilised emulsion was significantly smaller than the ones prepared with FPI and FPI-HT (Fig. 3A) which can be attributed to its higher viscosity Carneiro, Tonon, Grosso, and Hubinger (2013).

Once the complex coacervation occurred between FPI, (FPI-HT), (FPI-FPP) and FG *in situ*, the liquid microcapsules showed shear thinning behaviour within the tested shear rate range and their apparent viscosity at each shear rate was higher than their respective emulsions. This can be attributed to attractive electrostatic interactions between the proteins and gum at optimum pH (Weinbreck, Wientjes, Nieuwenhuijse, Robijn, & de Kruif, 2004). This observation is consistent with that of Wang, Li, Wang, and Adhikari (2011) who showed that the presence of flaxseed gum increased the apparent viscosity of oil-in-water emulsion stabilised by soy protein isolate. The liquid microcapsules stabilised by (FPI-FPP)/FG and (FPI-HT)/FG showed shear thinning behaviour until the shear rate of 80 s^{-1} while the one stabilised by FPI/FG showed this behaviour until 100 s^{-1}, above these shear rates they showed Newtonian behaviour. Similar to their emulsions, the viscosity of these liquid capsules followed FPI/FG < (FPI-HT)/FG < (FPI-FPP/FG) order (Fig. 3B).

3.5. Other physical properties of microcapsules

Moisture content, a_w, T_g, particle size, surface oil content, and microencapsulation efficiency of spray dried microcapsules are presented in Table 1. The moisture content of all powders was quite similar and was below 3% which is safe moisture content in food powders (Bhandari & Adhikari, 2008). The a_w of all the microcapsule powder was also below 0.2 and is also falls within a desirable (Velasco, Dobarganes, & Márquez-Ruiz, 2003). T_g values of all powders were significantly different ($p < 0.05$) and were higher in the microcapsule powders produced using polyphenol adducted FPI/FG complex coacervates. The T_g of microcapsule produced using (FPI-HT)/FG was the highest (121.2 °C) which corroborates with its lowest a_w (0.14). The $d_{4,3}$ of microcapsules was significantly different ($p < 0.05$) and it was the lowest in microcapsules produced using (FPI-FPP)/FG. It was also observed that increased number of FO microcapsules agglomerated during spray drying when FPI/FG was used as shell materials. This result also agrees well with the droplet size distribution of corresponding liquid microcapsules produced by FPI/FG, (FPI-FPP)/FG, and (FPI-HT)/FG (Fig. 3).

It can be seen from Table 1 that the surface oil content in microcapsules produced using (FPI-HT)/FG was significantly lower ($p < 0.05$) than those produced using FPI/FG and (FPI-HT)/FG. As a consequence, the oil encapsulation efficiency in microcapsules produce using (FPI-HT)/FG was also highest. This can be explained by the higher solubility of (FPI-HT) than (FPI-FPP) and FPI in aqueous phase and also the ability of FPI-HT to produce denser shell due to crosslinking (Pham et al., 2019a). In this context, Bajaj et al. (2017) also showed that increased solubility of pea protein isolate improved the encapsulation efficiency of flaxseed oil. The microcapsules produced using (FPI-FPP)/FG showed higher surface oil content than those produced using (FPI-HT)/FG which could be due to lower solubility of FPI-FPP adduct and inability of FPI and FPP to crosslink to form dense structure (Anwar & Kunz, 2011).

Table 2
Surface nitrogen content and surface coverage of protein in microcapsules produced using FPI/FG, (FPI-FPP)/FG, and (FPI-HT)/FG acquired by XPS. FPI = flaxseed protein isolate, FPP = flaxseed polyphenols, HT = hydroxytyrosol, FG = flaxseed gum.

Formulations	Nitrogen (w_t %)	Surface coverage of protein (%) *
FPI/FG	5.90 ± 0.31 ^{a}	36.9 ± 1.9 ^{a}
FPI-FPP/FG	5.65 ± 0.37 ^{a}	35.3 ± 2.3 ^{a}
FPI-HT/FG	7.88 ± 0.26 ^{b}	49.2 ± 1.6 ^{b}

Different lowercase letters in the superscript of the same column indicate significant differences ($p < 0.05$).
* Surface coverage of protein was calculated by using a conversion factor of 6.25.

3.6. Surface elemental composition of microcapsules

The relative elemental composition (C, O, and N) on the surface of microcapsules is presented in Table 2. The distribution of protein on the surface of powders was calculated using the N concentration using a conversion factor of 6.25 (Drusch et al., 2012). As shown in the table, there was a significantly higher proportion of FPI on the surface of microcapsule powder produced using (FPI-HT)/FG than FPG/FG and (FPI-FPP)/FG. This highest surface protein content also explains why this formulation had the lowest surface free oil content (Table 1). In an earlier study, we reported that FPI-HT adducts had much higher solubility in aqueous medium compared to FPI and FPI-FPP adducts (Pham et al., 2019a). This improved solubility might have facilitated the migration of FPI-HT adducts to oil/water interface and increased their interfacial concentration (Sikorski (2001)). The higher concentration of FPI-HT adducts at oil/water interface is expected to result into stronger/thicker shell which would significantly lower the surface oil content in the microcapsule powder.

3.7. Morphological characteristics of solid microcapsules

The surface morphology of FO microcapsules produced by using FPI/FG, (FPI-FPP)/FG and (FPI-HT)/FG complex coacervates as shell materials is shown in Fig. 4. All of the microcapsules showed irregular shape with wrinkled and uneven surface which are typical characteristics of spray-dried powder containing polymeric materials (Vehring, Foss, &

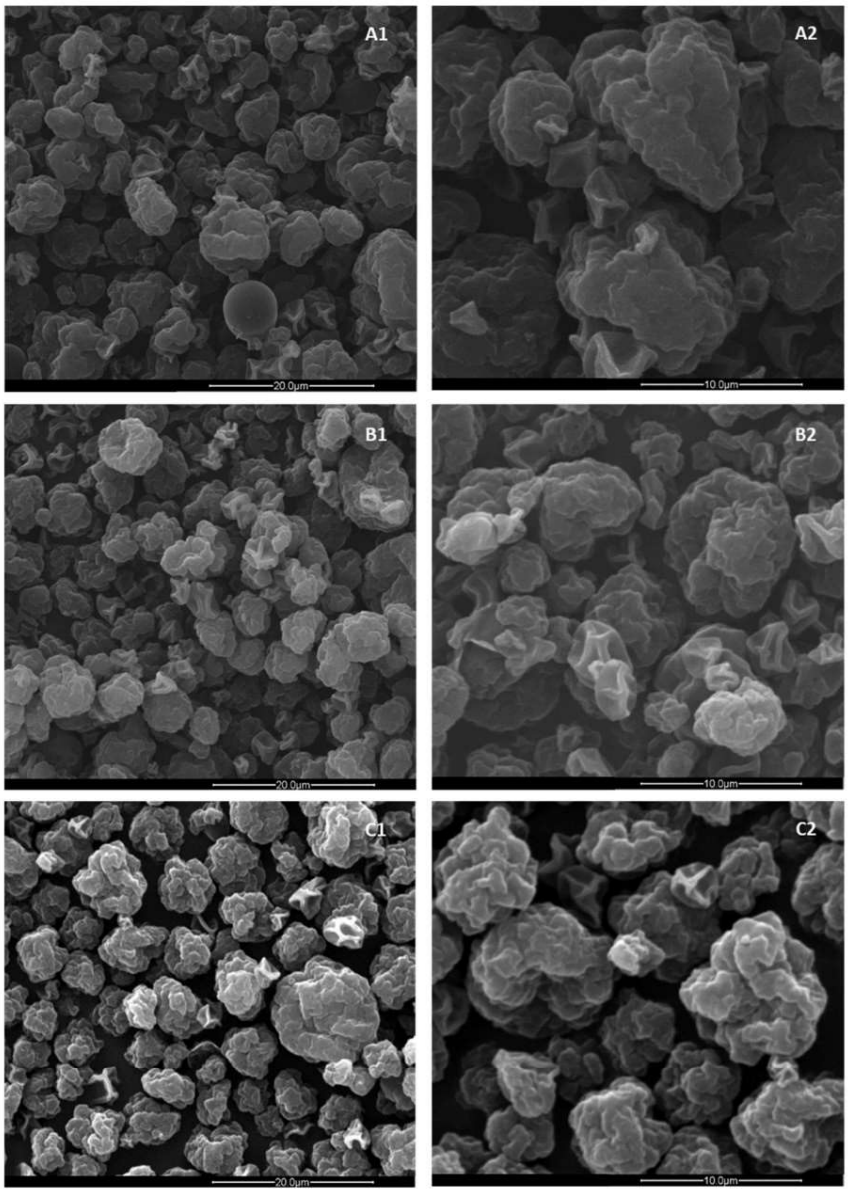

Fig. 4. SEM images of spray dried microcapsules produced by FPI/FG (A), (FPI-FPP)/FG (B), and (FPI-HT)/FG (C) complex coacervates at different magnification levels. Figures with subscript 1 and 2 have a scale bar of 20 and 10 μm, respectively. FPI = flaxseed protein isolate, FPP = flaxseed polyphenols, HT = hydroxytyrosol, FG = flaxseed gum.

Lechuga-Ballesteros, 2007). However, no cracks were observed on their surface, indicating that these shell materials can offer protection against leakage. Qualitatively observed particle size of these microcapsules followed FPI/FG > FPI-HT/FG > FPI-FPP/FG, which is in good agreement with the particle size data (Table 1).

3.8. *Oxidative stability of encapsulated flaxseed oil*

Oxidative stability of both unencapsulated and encapsulated FO evaluated in terms of hydroperoxide value (PV) and *p*-Anisidine value (p-AV) by storing at 40 °C for 4 weeks is presented in Fig. 5. The unencapsulated FO showed significantly higher PV and *p*-AV values than the encapsulated ones after one-week storage, indicating the protective effect of these complex coacervation-based shell materials against oxidation of FO. Similar protective effect of complex coacervates as shell materials has been reported in previous studies in the case of orange, krill, and chia seed oil. (Jun-xia, Hai-yan, & Jian, 2011; Kermasha, Aziz, Gill, & Neufeld, 2018; Timilsena, Adhikari, et al., 2016). Interestingly, the solid microcapsules showed higher PV values than unencapsulated FO at week zero. The p-AV value of the microcapsules was higher than

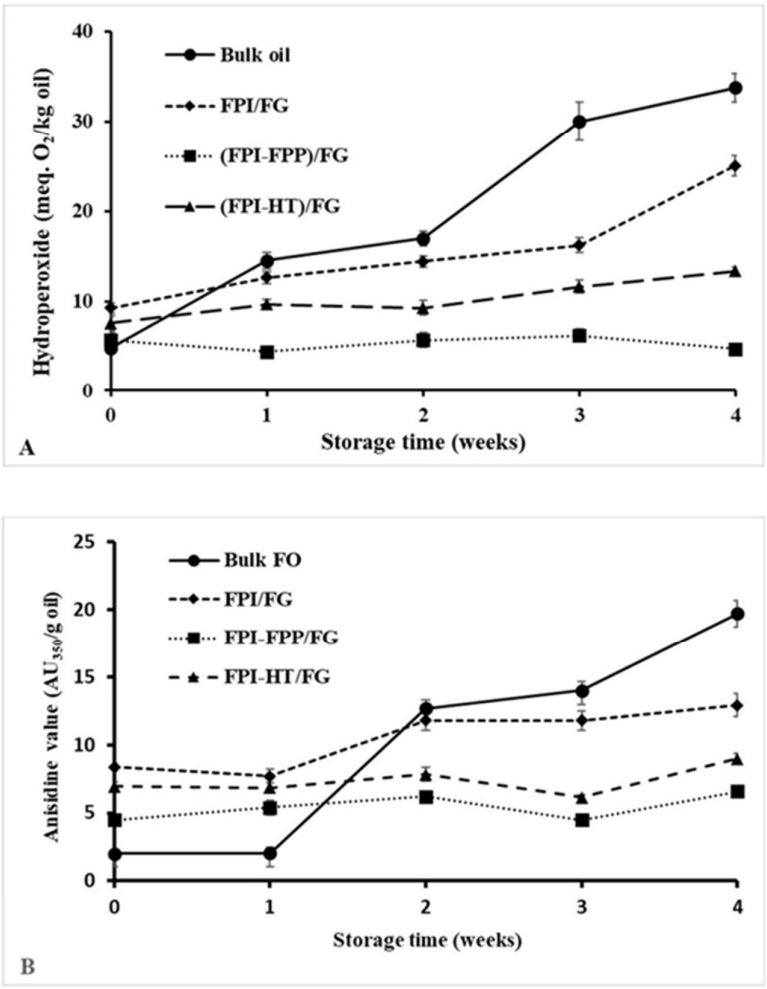

Fig. 5. Changes in peroxide value (A) and p-anisidine value (B) of unencapsulated (bulk oil) and encapsulated FO oil in FPI/FG, (FPI-FPP)/FG, (FPI-HT)/FG microcapsules at 40 °C over 4 weeks of storage. FPI = flaxseed protein isolate, FPP = flaxseed polyphenols, HT = hydroxytyrosol, FG = flaxseed gum, FO = flaxseed oil.

the unencapsulated oil up to week 1. This can be ascribed to the impact of high temperature during spray drying which appears to cause the formation of oxidation products (Reineccius, 2001). Tonon, Grosso, and Hubinger (2011) also reported that the PV of encapsulated FO increased with increasing inlet air temperature which is due to the greater availability of energy for oxidation. Another reason for this is that the

Table 3
Secondary structural features of FPI, FPI-pheolic adducts and their complex coacervate with FG. FPI = flaxseed protein isolate, FPP = flaxseed polyphenols, HT = hydroxytyrosol, FG = flaxseed gum.

	α-Helix (%)	β-Sheet (%)	β-Turn (%)	Random Coil (%)
FPI and FPI/FG complex coacervates				
FPI	21.51 ± 0.72 ^{a}	58.45 ± 0.63 ^{a}	18.51 ± 0.22 ^{a}	1.52 ± 0.12 ^{a}
FPI at pH 4.7	28.28 ± 1.97 ^{b}	52.73 ± 1.27 ^{b}	18.99 ± 0.70 ^{a}	0 ^{b}
FPI/FG	30.96 ± 0.44 ^{b}	43.30 ± 0.75^{c}	13.13 ± 0.66 ^{b}	12.61 ± 0.98 ^{c}
FPI-FPP adducts and (FPI-FPP)/FG complex coacervates				
FPI-FPP	9.92 ± 0.12 ^{a}	68.01 ± 0.19 ^{a}	22.08 ± 0.08 ^{a}	0 ^{a}
FPI-FPP at pH 4.6	39.99 ± 1.88 ^{b}	36.45 ± 1.88 ^{b}	23.55 ± 1.59 ^{a}	0 ^{a}
(FPI-FPP)/FG	26.96 ± 1.92 ^{c}	28.16 ± 0.95 ^{c}	12.96 ± 1.64 ^{b}	31.93 ± 1.23 ^{b}
FPI-HT adducts and (FPI-FPP)/FG complex coacervates				
FPI-HT	16.95 ± 0.52 ^{a}	73.15 ± 0.95 ^{a}	9.89 ± 1.47 ^{a}	0 ^{a}
FPI-HT at pH 4.5	6.86 ± 0.47 ^{b}	68.31 ± 0.86 ^{b}	24.84 ± 1.33 ^{b}	0 ^{a}
(FPI-HT)/FG	5.82 ± 0.81 ^{b}	21.15 ± 0.82 ^{c}	17.70 ± 0.37 ^{c}	54.42 ± 1.25 ^{b}

Different lowercase letters in the superscript of the same column within same group indicate significant differences ($p < 0.05$).

homogenisation was found to induce the hydroperoxide in FO during the emulsification process as it significantly increases the oil-water interfacial rea (Kuhn & Cunha, 2012). It can be seen from Fig. 5 that FO encapsulated in (FPI-FPP)/FG and (FPI-HT)/FG had lower values of PV and p-AV than those encapsulated in FPI/FG, indicating that the FPI-phenolic adducts used as shell material improved the oxidative stability FO compared to FPI alone. This result agrees well with the improvement of the antioxidant capability of FPI when it was adducted with FPP or HT in our previous study (Pham et al., 2019b). Microcapsules produced using (FPI-FPP)/FG complex coacervates showed significantly lower PV and p-AV values than those encapsulated in (FPI-HT)/FG complex coacervates even though the former had significantly higher surface oil content and lower encapsulation efficiency. This can be attributed to higher antioxidative activity of (FPI-FPP) adducts than that of (FPP-HT) ones (Pham et al., 2019b). This result also indicates that (FPI-FPP)/FG complex coacervates are promising shell materials for oxygen-sensitive oils.

3.9. *Effect of complex coacervation on the secondary structure of FPI and FPI-phenolic adducts*

As shown in Table 3, β-sheet was the major secondary structure in FPI (58.45 ± 0.63%) while random coil only accounted for 1.52 ± 0.12%, suggesting its ordered structure. It is similar to the secondary structure of legume protein in Carbonaro, Maselli, and Nucara (2012)'s study, where no unordered random coil structure was observed. When FPI was adducted with FPP, α-helix of FPI was reduced as it converted to β-sheet and β-turn. In the case of FPI-HT adducts, both α-helix and β-turn of FPI were converted to β-sheet. Interestingly, no random coil structure was observed in these protein-phenolic adducts, indicating the ordered structure of FPI was further reinforced by the covalent reaction. These changes in secondary structure of FPI, due to the covalent conjugation with phenolic compounds, depend on the nature of phenolic compounds as they induced folding/unfolding of FPI chain differently (Pham et al., 2019b). When the pH of FPI and FPI-phenolic adducts was adjusted from neutral to the pH at which complex coacervation occurred, the β-sheet content of all samples significantly decreased which could be due to disruption of hydrogen bonds in the acidic condition (Chourpa, Ducel, Richard, Dubois, & Boury, 2006).

In the case of complex coacervates produced using FPI/FG and polyphenol-aducted FPI/FG, significant decrease of almost all the ordered structure, particularly β-sheet, into random coil was observed (shown in Table 3) and this phenomenon was the most noticeable in (FPI-HT)/FG complex coacervate. This observation indicates that the charge-driven attachment of polysaccharides onto protein chain led to a product with a less ordered structure. It is reported in the literature that the level of decrease in ordered structure (particularly β-sheet) and increase in disordered structure (particularly radom coil) in complex coacervates depends on the nature of protein and gum used. Mekhloufi, Sanchez, Renard, Guillemin, and Hardy (2005) reported a decrease of the α-helix content of β-Lactoglobulin when it formed complex coacervate with Acacia gum while in Chourpa et al. (2006) 's study, decrease of random coil structures was observed in the pea globulin-gum Arabic complex coacervates.

4. Conclusion

This study shows that the complex coacervates of polyphenol (e.g., FPP, HT) adducted plant protein (e.g., FPI) and gum (e.g., FG) can be used as effective shell materials to encapsulate hydrophobic and oxygen-sensitive oils (e.g., FO). The covalent modification of protein by polyphenolic compounds altered the optimum complex coacervation pH and protein-to-gum ratio. The microcapsules of FO encapsulated in (FPI-HT)/FG FO had lower surface oil content and higher encapsulation efficiency while those encapsulated using (FPI-FPP)/FG complex coacervates had the highest stability against oxidation. The microcapsules produced using FPI/FG, (FPI-FPP)/FG and (FPI-HT)/FG complex coacervates showed similar irregular shape and wrinkled surface morphology.

Declaration of competing interest

We declare that the authors have no conflict of interest. All the authors have agreed to the content documented in this paper and also agreed to submit the manuscript to Food Hydrocolloids. It is not submitted, in part or in whole, to any other journals.

CRediT authorship contribution statement

Loc B. Pham: Investigation, Data curation, Writing - original draft, Writing - review & editing, Methodology, Visualization. **Bo Wang:** Supervision, Writing - review & editing, Methodology. **Tuyen Truong:** Supervision, Project administration. **Benu Adhikari:** Conceptualization, Supervision, Writing - review & editing, Resources, Project administration.

Appendix A. Supplementary data

Supplementary data to this article can be found online at https://doi.org/10.1016/j.foodhyd.2020.105944.

References

Anwar, S. H., & Kunz, B. (2011). The influence of drying methods on the stabilization of fish oil microcapsules: Comparison of spray granulation, spray drying, and freeze drying. *Journal of Food Engineering, 105*(2), 367–378.

Anwar, F., & Przybylski, R. (2012). Effect of solvents extraction on total phenolics and antioxidant activity of extracts from flaxseed (Linum usitatissimum L.). *ACTA Scientiarum Polonorum Technologia Alimentaria, 11*(3), 293–302.

AOAC. (2005). *Official methods of analysis* (18th ed.). Arlington, VA: Association of Official Analytical Chemists.

AOCS. (1998). *Official methods and recommended practices of the American Oil Chemists* (Vol. 5). Society. *AOCS*, 2-93.

Avramenko, N. A., Chang, C., Low, N. H., & Nickerson, M. T. (2016). Encapsulation of flaxseed oil within native and modified lentil protein-based microcapsules. *Food Research International, 81*, 17–24.

Bae, E., & Lee, S. (2008). Microencapsulation of avocado oil by spray drying using whey protein and maltodextrin. *Journal of Microencapsulation, 25*(8), 549–560.

Bajaj, P. R., Bhunia, K., Kleiner, L., Joyner, H. S., Smith, D., Ganjyal, G., et al. (2017). Improving functional properties of pea protein isolate for microencapsulation of flaxseed oil. *Journal of Microencapsulation, 34*(2), 218–230.

Bhandari, B. R., & Adhikari, B. P. (2008). Water activity in food processing and preservation. In *Drying technologies in food processing* (Vol. 1)Oxford, UK: Blackwell Publishing.

Binsi, P. K., Nayak, N., Sarkar, P. C., Jeyakumari, A., Muhamed Ashraf, P., Ninan, G., et al. (2017). Structural and oxidative stabilization of spray dried fish oil microencapsulates with gum Arabic and sage polyphenols: Characterization and release kinetics. *Food Chemistry, 219*, 158–168. https://doi.org/10.1016/j.foodchem.2016.09.126. http://www.ncbi.nlm.nih.gov/pubmed/27765212.

Campelo, P. H., Junqueira, L. A., Resende, J. V.d., Zacarias, R. D., Fernandes, R. V.d. B., Botrel, D. A., et al. (2017). Stability of lime essential oil emulsion prepared using biopolymers and ultrasound treatment. *International Journal of Food Properties, 20* (sup1), S564–S579.

Can Karaca, A., Low, N., & Nickerson, M. (2013). Encapsulation of flaxseed oil using a benchtop spray dryer for legume protein-maltodextrin microcapsule preparation. *Journal of Agricultural and Food Chemistry, 61*(21), 5148–5155. https://doi.org/10.1021/jf400787j. http://www.ncbi.nlm.nih.gov/pubmed/23663097.

Carbonaro, M., Maselli, P., & Nucara, A. (2012). Relationship between digestibility and secondary structure of raw and thermally treated legume proteins: A fourier transform infrared (FT-IR) spectroscopic study. *Amino Acids, 43*(2), 911–921.

Carbonaro, M., & Nucara, A. (2010). Secondary structure of food proteins by Fourier transform spectroscopy in the mid-infrared region. *Amino Acids, 38*(3), 679–690.

Carneiro, H. C. F., Tonon, R. V., Grosso, C. R. F., & Hubinger, M. D. (2013). Encapsulation efficiency and oxidative stability of flaxseed oil microencapsulated by spray drying using different combinations of wall materials. *Journal of Food Engineering, 115*(4), 443–451. https://doi.org/10.1016/j.jfoodeng.2012.03.033.

Chourpa, I., Ducel, V., Richard, J., Dubois, P., & Boury, F. (2006). Conformational modifications of α gliadin and globulin proteins upon complex coacervates formation with gum Arabic as studied by Raman microspectroscopy. *Biomacromolecules, 7*(9), 2616–2623. https://doi.org/10.1021/bm060131d.

Covas, M.-I., de la Torre, R., & Fitó, M. (2015). Virgin olive oil: A key food for cardiovascular risk protection. *British Journal of Nutrition, 113*(S2), S19–S28.

Cui, W., Mazza, G., & Biliaderis, C. (1994). Chemical structure, molecular size distributions, and rheological properties of flaxseed gum. *Journal of Agricultural and Food Chemistry, 42*(9), 1891–1895.

Dabrowski, K. J., & Sosulski, F. W. (1984). Composition of free and hydrolyzable phenolic acids in defatted flours of ten oilseeds. *Journal of Agricultural and Food Chemistry, 32*(1), 128–130.

Daun, J. K., Barthet, V. J., Chornick, T., & Duguid, S. (2003). Structure, composition, and variety development of flaxseed. *Flaxseed in Human Nutrition, 2*, 1–40.

Drusch, S., Serfert, Y., Berger, A., Shaikh, M., Rätzke, K., Zaporojtchenko, V., et al. (2012). New insights into the microencapsulation properties of sodium caseinate and hydrolyzed casein. *Food Hydrocolloids, 27*(2), 332–338.

Encina, C., Vergara, C., Gimenez, B., Oyarzun-Ampuero, F., & Robert, P. (2016). Conventional spray-drying and future trends for the microencapsulation of fish oil. *Trends in Food Science & Technology, 56*, 46–60.

Gharsallaoui, A., Roudaut, G., Chambin, O., Voilley, A., & Saurel, R. (2007). Applications of spray-drying in microencapsulation of food ingredients: An overview. *Food Research International, 40*(9), 1107–1121. https://doi.org/10.1016/j.foodres.2007.07.004.

Goyal, A., Sharma, V., Sihag, M. K., Tomar, S., Arora, S., Sabikhi, L., et al. (2015). Development and physico-chemical characterization of microencapsulated flaxseed oil powder: A functional ingredient for omega-3 fortification. *Powder Technology, 286*, 527–537.

Heck, T., Faccio, G., Richter, M., & Thöny-Meyer, L. (2013). Enzyme-catalyzed protein crosslinking. *Applied Microbiology and Biotechnology, 97*(2), 461–475. https://doi.org/10.1007/s00253-012-4569-z.doi:10.1007/s00253-012-4569-z.

Jackson, M., & Mantsch, H. H. (1995). The use and misuse of FTIR spectroscopy in the determination of protein structure. *Critical Reviews in Biochemistry and Molecular Biology, 30*(2), 95–120.

Jun-xia, X., Hai-yan, Y., & Jian, Y. (2011). Microencapsulation of sweet orange oil by complex coacervation with soybean protein isolate/gum Arabic. *Food Chemistry, 125*(4), 1267–1272.

Kaushik, Dowling, K., Barrow, C. J., & Adhikari, B. (2015a). Microencapsulation of omega-3 fatty acids: A review of microencapsulation and characterization methods. *Journal of Functional Foods, 19*, 868–881. https://doi.org/10.1016/j.jff.2014.06.029.

Kaushik, P., Dowling, K., Barrow, C. J., & Adhikari, B. (2015b). Complex coacervation between flaxseed protein isolate and flaxseed gum. *Food Research International, 72*, 91–97. https://doi.org/10.1016/j.foodres.2015.03.046.

Kaushik, P., Dowling, K., McKnight, S., Barrow, C. J., Wang, B., & Adhikari, B. (2016). Preparation, characterization and functional properties of flax seed protein isolate. *Food Chemistry, 197*(Pt A), 212–220. https://doi.org/10.1016/j.foodchem.2015.09.106. http://www.ncbi.nlm.nih.gov/pubmed/26616943.

Kermasha, S., Aziz, S., Gill, J., & Neufeld, R. (2018). Microencapsulation of esterified krill oil, using complex coacervation. *Journal of Microencapsulation, 35*(1), 36–48.

Klaypradit, W., & Huang, Y.-W. (2008). Fish oil encapsulation with chitosan using ultrasonic atomizer. *Lebensmittel-Wissenschaft und -Technologie- Food Science and Technology, 41*(6), 1133–1139. https://doi.org/10.1016/j.lwt.2007.06.014. http://www.sciencedirect.com/science/article/pii/S0023643807002368.

Klinkesorn, U., Sophanodora, P., Chinachoti, P., Decker, E. A., & McClements, D. J. (2006). Characterization of spray-dried tuna oil emulsified in two-layered interfacial membranes prepared using electrostatic layer-by-layer deposition. *Food Research International, 39*(4), 449–457.

Kuhn, K. R., & Cunha, R. L. (2012). Flaxseed oil – whey protein isolate emulsions: Effect of high pressure homogenization. *Journal of Food Engineering, 111*(2), 449–457. https://doi.org/10.1016/j.jfoodeng.2012.01.016. http://www.sciencedirect.com/science/article/pii/S0260877412000362.

Liu, S., Low, N., & Nickerson, M. T. (2010). Entrapment of flaxseed oil within gelatin-gum Arabic capsules. *Journal of the American Oil Chemists' Society, 87*(7), 809–815.

Lopez, M., & Edens, L. (2005). Effective prevention of chill-haze in beer using an acid proline-specific endoprotease from Aspergillus Niger. *Journal of Agricultural and Food Chemistry, 53*(20), 7944–7949.

Lopez, S., Montserrat-de la Paz, S., Lucas, R., Bermudez, B., Abia, R., Morales, J. C., et al. (2017). Effect of metabolites of hydroxytyrosol on protection against oxidative stress and inflammation in human endothelial cells. *Journal of Functional Foods, 29*, 238–247. https://doi.org/10.1016/j.jff.2016.12.033. http://www.sciencedirect.com/science/article/pii/S1756464616304327.

Mancuso, J. R., McClements, D. J., & Decker, E. A. (1999). The effects of surfactant type, pH, and chelators on the oxidation of salmon oil-in-water emulsions. *Journal of Agricultural and Food Chemistry, 47*(10), 4112–4116.

Mekhloufi, G., Sanchez, C., Renard, D., Guillemin, S., & Hardy, J. (2005). pH-induced structural transitions during complexation and coacervation of β-lactoglobulin and acacia gum. *Langmuir, 21*(1), 386–394.

Mizutani, Y., Matsumura, Y., Imamura, K., Nakanishi, K., & Mori, T. (2003). Effects of water activity and lipid addition on secondary structure of zein in powder systems. *Journal of Agricultural and Food Chemistry, 51*(1), 229–235.

Nakagawa, K., & Nagao, H. (2012). Microencapsulation of oil droplets using freezing-induced gelatin–acacia complex coacervation. *Colloids and Surfaces A: Physicochemical and Engineering Aspects, 411*, 129–139. https://doi.org/10.1016/j.colsurfa.2012.07.010. http://www.sciencedirect.com/science/article/pii/S0927775712004815.

Nesterenko, A., Alric, I., Silvestre, F., & Durrieu, V. (2013). Vegetable proteins in microencapsulation: A review of recent interventions and their effectiveness. *Industrial Crops and Products, 42*, 469–479. https://doi.org/10.1016/j.indcrop.2012.06.035.

Oomah, B. D., Der, T. J., & Godfrey, D. V. (2006). Thermal characteristics of flaxseed (Linum usitatissimum L.) proteins. *Food Chemistry, 98*(4), 733–741.

Oomah, B. D., Mazza, G., & Cui, W. (1994). Optimization of protein extraction from flaxseed meal. *Food Research International, 27*(4), 355–361.

Pham, L. B., Wang, B., Zisu, B., & Adhikari, B. (2019a). Complexation between flaxseed protein isolate and phenolic compounds: Effects on interfacial, emulsifying and antioxidant properties of emulsions. *Food Hydrocolloids, 94*, 20–29.

Pham, L. B., Wang, B., Zisu, B., & Adhikari, B. (2019b). Covalent modification of flaxseed protein isolate by phenolic compounds and the structure and functional properties of the adducts. *Food Chemistry, 293*, 463–471.

Porras-Saavedra, J., Alamilla-Beltrán, L., Lartundo-Rojas, L., de Jesús Perea-Flores, M., Yáñez-Fernández, J., Palacios-González, E., et al. (2018). Chemical components distribution and morphology of microcapsules of paprika oleoresin by microscopy and spectroscopy. *Food Hydrocolloids, 81*, 6–14.

Pourashouri, P., Shabanpour, B., Razavi, S. H., Jafari, S. M., Shabani, A., & Aubourg, S. P. (2014). Impact of wall materials on physicochemical properties of microencapsulated fish oil by spray drying. *Food and Bioprocess Technology, 7*(8), 2354–2365.

Quispe-Condori, S., Saldaña, M. D. A., & Temelli, F. (2011). Microencapsulation of flax oil with zein using spray and freeze drying. *Lebensmittel-Wissenschaft und -Technologie- Food Science and Technology, 44*(9), 1880–1887. https://doi.org/10.1016/j.lwt.2011.01.005.

Reineccius, G. A. (2001). The spray drying of food ingredients. In *The encapsulation of food ingredients* (pp. 151–184). Leatherhead Publ.

Sarker, D. K., Wilde, P. J., & Clark, D. C. (1995). Control of surfactant-induced destabilization of foams through polyphenol-mediated protein-protein interactions. *Journal of Agricultural and Food Chemistry, 43*(2), 295–300.

Shantha, N. C., & Decker, E. A. (1994). *Rapid, sensitive, iron-based spectrophotometric methods for determination of peroxide values of food lipids.*

Sikorski, Z. E. (2001). Functional properties of proteins in food systems. *Chemical and Functional Properties of Food Proteins*, 113–135.

Škerget, M., Kotnik, P., Hadolin, M., Hraš, A. R., Simonič, M., & Knez, Ž. (2005). Phenols, proanthocyanidins, flavones and flavonols in some plant materials and their antioxidant activities. *Food Chemistry, 89*(2), 191–198. https://doi.org/10.1016/j.foodchem.2004.02.025.

Timilsena, Adhikari, R., Barrow, C. J., & Adhikari, B. (2016a). Microencapsulation of chia seed oil using chia seed protein isolate-chia seed gum complex coacervates. *International Journal of Biological Macromolecules, 91*, 347–357. https://doi.org/10.1016/j.ijbiomac.2016.05.058. http://www.ncbi.nlm.nih.gov/pubmed/27212219.

Timilsena, Y. P., Wang, B., Adhikari, R., & Adhikari, B. (2016b). Preparation and characterization of chia seed protein isolate–chia seed gum complex coacervates. *Food Hydrocolloids, 52*, 554–563. https://doi.org/10.1016/j.foodhyd.2015.07.033.

Tonon, R. V., Grosso, C. R. F., & Hubinger, M. D. (2011). Influence of emulsion composition and inlet air temperature on the microencapsulation of flaxseed oil by spray drying. *Food Research International, 44*(1), 282–289. https://doi.org/10.1016/j.foodres.2010.10.018.

Valls, R.-M., Farràs, M., Suárez, M., Fernández-Castillejo, S., Fitó, M., Konstantinidou, V., & Solà, R. (2015). Effects of functional olive oil enriched with its own phenolic compounds on endothelial function in hypertensive patients. A randomised controlled trial. *Food Chemistry, 167*, 30–35. https://doi.org/10.1016/j.foodchem.2014.06.107. http://www.sciencedirect.com/science/article/pii/S0308814614010061.

Vehring, R., Foss, W. R., & Lechuga-Ballesteros, D. (2007). Particle formation in spray drying. *Journal of Aerosol Science, 38*(7), 728–746.

Velasco, J., Dobarganes, C., & Márquez-Ruiz, G. (2003). Variables affecting lipid oxidation in dried microencapsulated oils. *Grasas Y Aceites, 54*(3), 304–314.

Wang, Adhikari, B., & Barrow, C. J. (2014). Optimisation of the microencapsulation of tuna oil in gelatin-sodium hexametaphosphate using complex coacervation. *Food Chemistry, 158*, 358–365. https://doi.org/10.1016/j.foodchem.2014.02.135. http://www.ncbi.nlm.nih.gov/pubmed/24731355.

Wang, Y., Li, D., Wang, L.-J., & Adhikari, B. (2011). The effect of addition of flaxseed gum on the emulsion properties of soybean protein isolate (SPI). *Journal of Food Engineering, 104*(1), 56–62.

Wang, Li, D., Wang, L.-J., Adhikari, B., & Shi, J. (2010). Ability of flaxseed and soybean protein concentrates to stabilize oil-in-water emulsions. *Journal of Food Engineering, 100*(3), 417–426. https://doi.org/10.1016/j.jfoodeng.2010.04.026.

Waszkowiak, K., Gliszczyńska-Świgło, A., Barthet, V., & Skręty, J. (2015). Effect of extraction method on the phenolic and cyanogenic glucoside profile of flaxseed extracts and their antioxidant capacity. *Journal of the American Oil Chemists Society, 92*(11–12), 1609–1619. https://doi.org/10.1007/s11746-015-2729-x. http://www.ncbi.nlm.nih.gov/pubmed/26640278.

Weinbreck, F., Wientjes, R. H., Nieuwenhuijse, H., Robijn, G. W., & de Kruif, C. G. (2004). Rheological properties of whey protein/gum Arabic coacervates. *Journal of Rheology, 48*(6), 1215–1228.

Zhang, Z.-S., Wang, L.-J., Li, D., Li, S.-J., & Özkan, N. (2011). Characteristics of flaxseed oil from two different flax plants. *International Journal of Food Properties, 14*(6), 1286–1296.

CHAPTER 6

In-vitro digestion of flaxseed oil encapsulated in phenolic compound adducted flaxseed protein isolate-flaxseed gum complex coacervates

accepted for publication in *Food Hydrocolloids*

In-vitro digestion of flaxseed oil encapsulated in phenolic compound adducted flaxseed protein isolate-flaxseed gum complex coacervates

Loc B. Pham[a], Bo Wang[b], Bogdan Zisu[c], Tuyen Truong[a], Benu Adhikari[a*]

[a] School of Science, RMIT University, Melbourne, VIC 3028, Australia

[b] School of Behavioural and Health Science, Australian Catholic University, Sydney, NSW 2060, Australia

[c] Spraying Systems Co Pty Ltd, Truganina, VIC 3029, Australia

*Corresponding author; phone: +61 399259940, email:benu.adhikari@rmit.edu.au

Abstract

Two phenolic compounds, flaxseed polyphenol (FPP) and hydroxytyrosol (HT), were covalently adducted with flaxseed protein isolate (FPI) and then complex coacervated with flaxseed gum (FG). Flaxseed oil (FO) was microencapsulated using these complex coacervates as wall materials. The release of FO from these microcapsules and its digestion were studied using an *in vitro* digestion model. Most of the encapsulated oil (66-80%) was released in the intestinal stage, and 5-17% was released in the gastric stage. The proteolytic degradation of FPI from microcapsule shell and release of FO in the intestinal phase was slowed down by adduction to FPP but not to HT. The release of FO was highest (80%) in (FPI-HT)/FG/FO microcapsule, and 38.5% of released oil was lipolysed into free fatty acids. (FPI-FPP)/FG/FO microcapsules released the lowest amount of oil (66.3%) of which 28.9% was lipolysed. These findings suggest that the phenolic compound-adducted FPI/FG complex coacervates can be promising encapsulating shell materials that can remain intact in the gastric phase and deliver the encapsulant to intestinal phase.

Keywords: Flaxseed oil; Flaxseed polyphenols; Hydroxytyrosol; Complex coacervate; Microencapsualtion; *in-vitro* digestion

1. Introduction

Polyunsaturated fatty acids (PUFAs) such as omega-3 and omega-6 are known as important functional ingredients (Abuajah, Ogbonna, & Osuji, 2015) as their intake as part of diet can significantly improve visual function (Li & Hu, 2009), and prevent chronic diseases such as cardiovascular disease (Steffens, 1997), diabetes (Connor et al., 1993), arthritis (Kremer, 1996), autoimmune disorders (Calder, 2006) and colon cancer (Roynette, Calder, Dupertuis, & Pichard, 2004). However, PUFAs readily undergo oxidation, which leads to undesirable changes in sensorial (flavour and colour) and nutritional values of food products in which they are incorporated (Comunian & Favaro-Trindade, 2016). In order to avoid or minimise lipid oxidation, PUFA-rich oil is microencapsulated which creates physical barrier surrounding the oil and protects it against the external environmental stresses (Betoret, Betoret, Vidal, & Fito, 2011; Sanguansri & Ann Augustin, 2006). Moreover, appropriately designed encapsulating shell can help deliver and release the PUFA-rich oils in the small intestinal where 70-90% lipid is digested by pancreatic lipases (Wickham, Wilde, & Fillery-Travis, 2002). For this purpose, oil microcapsules are required to remain structurally and functionally intact in the acidic gastric environment and able to reach the small intestine.

In-vitro digestion has been widely used to study the digestion behaviour of foods including microencapsulated oils. It uses simulated fluids and mechanical actions to mimic the environment of each stage of gastrointestinal tract (Minekus et al., 2014; Sarkar, Horne, & Singh, 2010). During *in-vitro* digestion, encapsulated oil is released from the shell matrix by the combined action of water, pH and/or enzyme (Kong & Singh, 2009) and the released oil is lipolysed. Thus, the amount of the released oil and the free fatty acids (FFA) formed due to lipolysis are used as the indicators of the extent of digestion of microencapsulated oil (Timilsena, Wang, Adhikari, & Adhikari, 2017). Generally, the rate and extent of lipolysis of encapsulated oils in the gastrointestinal tract depend on the size of the microcapsules and the characteristics of the oil-digestive fluid interface (Augustin et al., 2014). The digestibility of entrapped oils can be controlled by appropriately designing the microencapsulation matrix (Gallier & Singh, 2012; Ghasemi Fard et al., 2020). For example, small microcapsules and thin shell hasten the release of oil to the digestive media as they offer a large surface area and less resistance to disintegration (Gallier & Singh, 2012). Since the lipid digestion relies on lipolytic action of pancreatic lipases, which are only active at the oil-water interface, encapsulation of oil can modulate this interfacial process (Golding et al., 2011). Moreover, the non-lipid components of food matrix can prolong the release of the oil, thus modulate its digestibility. For example, the digestion of encapsulated oil was substantially slowed down with

the presence of dietary fibres (Shen, Apriani, Weerakkody, Sanguansri, & Augustin, 2011). The release of encapsulated oil was slowed down from the microcapsules in which protein-polysaccharide complex coacervates were used as shell materials (Timilsena, Adhikari, Barrow, & Adhikari, 2017). Guimarães Drummond e Silva et al. (2017) demonstrated that the presence of phenolic compounds in flaxseed protein concentrate did not affect the hydrolytic action of pepsin and pancreatin. He, Lv, and Yao (2007) reported a significant decrease in the activities of α-amylase trypsin and lipase enzymes due to intake of green tea polyphenols.

We previously reported the process of synthesis of covalent conjugates using flaxseed protein isolate (FPI) and phenolic compounds including hydroxytyrosol (HT) and flaxseed polyphenols (FPP) (Pham, Wang, Zisu, & Adhikari, 2019b). The polyphenol-adducted FPI was then complex coacervated with flaxseed gum (FG). Subsequently, the complex coacervates formed between polyphenol-adducted FPI and FG were used to encapsulate flaxseed oil (FO) (Pham, Wang, Zisu, Truong, & Adhikari, 2020). The oxidative stability of FO was significantly improved due to the presence of phenolic compounds in the microcapsule wall. It is of interest to investigate how the shell of microcapsules produced using (polyphenol-adducted) protein-gum complex coacervates are digested and how the encapsulated oil is released. There is a paucity of information in the literature regarding the digestions of such microcapsules and the release of oil and further lipolytic breakdown of the released oil.

Thus, in this study, FO was used as the model oil and (polyphenol adducted) FPI/FG complex coacervates were used as model shell materials to encapsulate FO. Then, the breakdown of the shell and release and further lipolytic digestion of FO were studied using an *in-vitro* digestion system.

2. Materials and methods

2.1 Materials

Flaxseed sample was donated by Stoney Creek Oil Products Pty Ltd (Talbot, Victoria, Australia) and was stored at 4 ºC before use. Ferulic acid (FA), Folin-Ciocalteu reagent were purchased from Sigma Aldrich (Castle Hill, New South Wales, Australia). Hydroxytyrosol (HT, purity ≥ 95%) was purchased from AvaChem Scientific (San Antonio, Texas, USA). Mini-PROTEAN TGXTM precast gel, Precision Plus Protein™ WesternC™ Blotting Standards (10-250 kDa),

Tris/Glycine/SDS buffer, Coomassie Blue R-250 solution, Laemmli sample buffer, and 2-mercaptoethanol were purchased from Bio-Rad Incorporation (Gladesville, NSW, Australia).

2.2 Extraction of FPI, FO, FPP, FG and preparation of phenolic adducted FPI

The details of protocols used to extract and purify FPI, FO, FPP and FG and synthesising phenolic compound-adducted FPI and its complex coacervates with FG are reported in our previous papers (Pham, Wang, Zisu, & Adhikari, 2019a; Pham et al., 2019b). Those protocols are briefly presented here. FPI was prepared according to Oomah, Mazza, and Cui (1994) with minor modification. Flaxseed was soaked in Milli-Q water at 60 ºC (flaxseed-to-water ratio = 1:18, w/w) for 2 h under agitation to extract flaxseed gum. A probe-type sonicator (HD3400, Bandelin, Berlin, Germany) operating at 400 W and 20 Hz was used during the agitation stage for about 12 min to speed up the extracton of the gum. The degummed flaxseed sample was ground, air dried for 48 h in the fume hood and defatted using hexane (meal-to-hexane ratio = 1:6, w/v) for 3 h and air-dried for 24 h under a fume hood. The defatted- degummed flaxseed meal was sieved (150 µm sieve) to remove hull residues. Finally, the defatted-degummed flaxseed flour was mixed with 0.1 M Tris buffer (flour-to-buffer ratio = 1:16, w/v) maintained at pH 8.6 and stirred for 6 h at 800 rpm. After centrifugation (10,000× g for 20 min), the supernatant was dialysed using bags with molecular weight of 6-8 kDa (Orange Scientific, Braine-l'Alleud, Belgium) against Milli-Q water for 48 h at 4ºC. The dialysed sample was freeze-dried (-40ºC, 12 Pa) to obtain FPI powder.

FO was extracted from degummed flaxseed using hexane (Zhang, Wang, Li, Li, & Özkan, 2011). The degummed flaxseed was finely ground, mixed with hexane (meal-to-hexane ratio = 1:6, w/v), and stirred (800 rpm) at room temperature for 6 h. This mixed slurry was centrifuged (10,000×g for 20 minutes) supernatant was recovered. The residual hexane was evaporated at 40 ºC to obtain the FO.

FPP was extracted from the defatted-degummed flaxseed meal, according to Anwar and Przybylski (2012). The defatted-degummed meal was mixed with 60% (w/v) ethanol (meal-to-ethanol ratio = 1:10, w/v), and stirred at 600 rpm for 4 h at the room temperature. After this, the mixture was filtered (Whatman No.1, GE Healthcare, Chicago, IL, U.S.A.), and the filtrate was recovered. The methanol in the filtrate was evaporated (rotary vacuum evaporator, RC2000, Buchi, Switzerland) and then freeze-dried to obtain FPP powder.

FG was extracted as mentioned above in the degumming protocol according to Cui, Mazza, and Biliaderis (1994). The gum extract was centrifuged at 10,000×g for 30 min and the supernatant

was recovered. The gum was precipitated from the supernatant by adding absolute ethanol (supernatant-to-ethanol ratio = 1:2, v/v). The precipitated gum was collected, and freeze-dried (-40°C, 12 Pa).

The phenolic compounds (FPP and HT) were covalently adducted (conjugated) with FPI, according to Rawel, Czajka, Rohn, and Kroll (2002) as we have reported earlier (Pham et al., 2019b). Briefly, both FPI and phenolic compounds (FPP and HT) were individually dispersed in Milli-Q water, mixed in required ratio and the pH of the mixture was adjusted to pH 9.0 to facilitate covalent conjugation of phenolic compounds with FPI. The conjugation step was carried out for 24 h agitating at 200 rpm at the room temperature in the presence of oxygen. The reacted mixture was dialysed (molecular weight cut off 6-8 kDa) against water for 20 h to remove the unreacted polyphenolic compounds. These FPI-phenolic adducts were finally freeze-dried (-40^{o}C, 12 Pa) to convert into powder.

2.3 Preparation of FO microcapsules using phenolic compound adducted-FPI/FG complex coacervates

FO was encapsulated using (FPI-FPP)/FG and (FPI-HT)/FG complex coacervates. Briefly, 8.75 g FO was individually emulsified in 250 g FPI and phenolic adducted FPI solutions (6%, w/w) using Ultra-Turrax (15,000 rpm, 4 min). These coarse emulsions were further homogenised using a microfluidiser (M-110L, Microfluidics, Newton, MA) at 82 MPa for 3 passes to produce fine emulsions. Then, 250 g FG solution (1% w/w) was slowly added to these fine emulsions and the mixture was agitated at 800 rpm. The pH of the mixture was adjusted to optimum complex coacervation pH (4.6 and 4.5 for FPI-FPP/FG and FPI-HT/FG, respectively) using 1 M HCl to induce complex coacervation and to produce liquid microcapsules. The optimum ratio of FPI/FG and phenolic adducted-FPI/FG was 6:1 (w/w) and the core-to-wall ratio in these formulations was 1:2 (w/w) (Pham et al., 2020).

The liquid microcapsules were cooled down to 5^{o}C and 50 mL transglutaminase solution (2%, w/v) was added to crosslink the protein component of the shell. This crosslinking process required 24 h with slow and continuous agitation. These transglutaminase-crosslinked microcapsules were spray dried using a bench-top spray dryer (LabPlant, SD-Basic, England). The liquid microcapsules were diluted by 2 times with Milli-Q water to reduce its viscosity to facilitate the atomisation and spray drying. The inlet and outlet temperatures of the drying air were set at 200 ^{o}C and 112±2 ^{o}C, respectively (Pham et al., 2020).

2.4 Preparation of simulated digestive fluids and in-vitro digestion of FO microcapsules

Simulated digestive fluids including salivary (SSF), gastric (SGF), and intestinal (SGF) fluids for oral, gastric, and intestinal stages were prepared according to international consensus report (Minekus et al., 2014) as shown in Table 1. This protocol follows adult digestion and the tests were carried out at physiological temperature (37 ºC).

2.4.1 Simulated oral digestion

Two grams of FO microcapsules were dispersed in Milli-Q water to obtain 5.0 mL dispersion. This dispersion was mixed with 3.5 mL SSF and 1.5 mL SSF containing α-amylase (1500 U/mL) was added. Then, 25 µL 0.3 M $CaCl_2(H_2O)_2$ solution was added and the volume of the mixture was adjusted to 10 mL with 0.975 mL Milli-Q water. This final mixture was agitated at 100 rpm for 2 min at pH 7.0.

2.4.2 Simulated gastric digestion

Ten millilitres of oral bolus were mixed with 7.5 mL SGF and 1.6 mL SGF containing porcine pepsin (25,000 U/mL) was added. Then, 5 µL 0.3 M $CaCl_2$ solution and 0.695 mL Milli-Q water were added to the mixture. The pH of the final mixture was adjusted to 3.0 with 1 M HCl, and stirred at 100 rpm for 2 h.

2.4.3 Simulated intestinal digestion

Twenty millilitres gastric digesta was mixed with 11.0 mL SIF solution and then 5.0 mL SIF containing trypsin (800 U/mL) was added. Then, 2.5 mL 160 mM fresh bile salt solution, 0.04 mL of 0.3 M $CaCl_2$ solution and 1.31 mL of Milli-Q water was added to the mixture. The pH of the final mixture was adjusted to 7.0 with 0.15 mL of 1 M NaOH. It was agitated at 100 rpm for 2 h.

Table 1: Formulation of simulated digestion fluids: SSF = simulated salivary fluid, SGF = simulated gastric fluid (SGF), and SIF = simulated intestinal fluid. The final volume of each simulated fluid was made up to 500 mL with Milli-Q water. Conc=concentration.

Constituent	Stock conc (M)	SSF (pH 7)		SGF (pH 3)		SIF (pH 7)	
		Volume of stock (mL)	Final conc (mM)	Volume of stock (mL)	Final conc (mM))	Volume of stock (mL)	Final conc (mM)
KCl	0.5	15.1	15.1	6.9	6.9	6.8	6.8
KH_2PO_4	0.5	3.7	3.7	0.9	0.9	0.8	0.8
$NaHCO_3$	1	6.8	13.6	12.5	25	42.5	85
NaCl	2			11.8	47.2	9.6	38.4
$MgCl_2(H_2O)_6$	0.15	0.5	0.15	0.4	0.12	1.1	0.33
$(NH_4)_2CO_3$	0.5	0.06	0.06	0.5	0.5		
NaOH	1						
HCl	6	0.09	1.1	1.3	15.6	0.7	8.4
$CaCl_2(H_2O)_2$	0.3	0.025	1.5	0.005	0.15	0.04	0.6

2.4.4 Determination of particle size and zeta potential of digesta

The particle size of the digested samples at the end of each digestion stage was determined using dynamic light scattering technology (Mastersizer 3000B, Malvern Instruments Ltd., Malvern, Worcestershire, UK). Deionised water was used as the dispersant and the surface-mean ($d_{3,2}$) and volume-mean ($d_{4,3}$) were recorded.

The zeta-potential value of digesta at the end of each digestion stage was measured using a Zetasizer (ZS-90, Malvern instruments Ltd, Malvern, Worcestershire, UK). The digesta samples were diluted at 500 times with their respspective simulated fluids before measurment. The zetapotential values were calculated using the Smoluchowski model (Smoluchowski, 1921) by the associated software (DTS 5.10, Malvern Instruments Ltd., Malvern, Worcestershire, UK).

2.5 Proteomic analysis

2.5.1 Quantification of free amino groups in digesta

The extent of proteolysis of protein component of the microcapsule wall during each digestion stage was quantified by measuring the free NH_2 group (Dekkers, Kolodziejczyk, Acquistapace, Engmann, & Wooster, 2016). For this purpose, o-phthaldialdehyde (OPA) spectrophotometric assay was conducted at 0, 15, 30, 60, 90 and 120 min in the gastric and intestinal digestion stages, respectively. Briefly, the OPA reagent was prepared by dissolving 80 mg o-phthaldialdehyde in

50 mL 0.1 M sodium tetraborate buffer (pH 9.7–10), followed by addition of 5 mL 20 wt% sodium dodecyl sulphate and 0.2 mL of 2 M 2-mercaptoethanol stock solution. The volume of OPA reagent was adjusted to 100 mL with Milli-Q water. To determine the amount of free NH_2 group released from the digested sample, 0.04 mL sample was mixed with 2 mL OPA reagent and this mixture was incubated for 2 min at room temperature. Absorbance of the incubated sample was measured at 340 nm using a UV-Vis spectrophotometer (LAMBDA 35, Perkin Elmer, Llantrisant, UK). The amount of NH_2 was calculated using a standard curve which was established using 0-10 mM L-leucine solution.

2.5.2 Determination of molecular weight of protein in the digesta

The change of molecular weight of the protein component of the microcapsule shell due to proteolysis was determined using sodium dodecyl sulphate-polyacrylamide gel electrophoresis (SDS-PAGE). The SDS-PAGE test was performed on gastric and intestinal digesta collected at 0, 15, 30, 60, 90 and 120 min using a precast polyacrylamide gel (4-15%) under reducing condition. The digested sample solution (1% w/v) was mixed with loading buffer prepared by mixing 95% Laemmli buffer with 5% 2-mercaptoethanol (v/v) at a sample-to-buffer ratio of 3:1 (v/v). This mixture (12 µL) was loaded into the precast gel after heating at 95°C for 5 min. 7 µL WesternCTM blotting protein standard was used as a molecular weight marker. The gel electrophoresis was performed at 100 V for 90 min using Mini-PROTEAN Tetra Cell. Once the electrophoresis was complete, the gel was removed and stained with Coomassie Brilliant Blue R-250 solution for 24 h followed by destaining with an acetic acid/methanol mixture (6:4, v/v).

2.6 Determination of lipolysis of digesta

2.6.1 Quantification of released oil

The amount of released oil was measured at the end of each digestion stage according to Eratte, Dowling, Barrow, and Adhikari (2017) with minor modification. Each digested sample was mixed with 75 mL hexane and the mixture was vortexed for 60 s. Then, the hexane containing oil was filtered into a pre-weighted flask through a filter paper (No.1, GE Healthcare, Chicago, IL, U.S.A). The filtrate was evaporated using a rotary evaporator to remove hexane and recover the oil. The recovered oil was heated at 105 ºC for 30 min to ensure complete removal of residual solvent and the oil mass was measured. The amount of oil released from the digested microcapsule was expressed as percentage of the total oil of the intact microcapsule.

2.6.2 Quantification of released free fatty acids

The amount of free fatty acids (FFA) released, due to lipolysis, in the intestinal stage of digestion was determined by titrating with 0.1 M NaOH solution at an endpoint of pH 7.0 (stat 842 Titrando, Metrohm Ltd, Herisau, Switzerland) at 37°C, as described by Li and McClements (2010). The amount of consumed NaOH was recorded and used to calculate the percentage of FFA produced (Equation (1).

$$FFA\ (\%) = \frac{(V_{NaOH} \times m_{NaOH} \times M_{Lipid})}{W_{Lipid} \times 2} \times 100 \qquad (1)$$

Where, V_{NaOH} and m_{NaOH} are the volume (mL) and molarity of NaOH used to titrate the FFA released, W_{Lipid} is the total weight (g) of oil in the digested sample. M_{Lipid} is the molecular weight of triacylglycerol (g/mol) calculated using the average composition of extracted FO (Holčapek, Jandera, Zderadička, & Hruba, 2003). A replicate sample digested in lipase-free SIF was used as the control and these digesta were also titrated. The volume of NaOH consumed by the control sample was subtracted from the volume of NaOH consumed by the test sample to calculate amount of FFA released.

The relase of FFA as a function of time (FFA_t) modelled using a first-order reaction kinetics model Equation (2), as was used by (Ye, Cui, Zhu, & Singh, 2013).

$$FFA_t = FFA_{max}\ (1 - e^{-k\,t}) \qquad (2)$$

Where, FFA_{max} can be considered as the "pseudo-equilibrium. k (min^{-1}) is the constant of first-order reaction kinetics and t is the time (min). Equation 2 was fitted with FFAt verus t data using least sequre method given by Equation (3).

$$f_{min} = \sum_{t=0}^{t=120} \lfloor FFA_t\ (E) - \ FFA_t\ (P) \rfloor^2 \qquad (3)$$

Where, f_{min} is the function to be minimised. $FFA_t(E)$ and $FFA_t(P)$ are experimental and predicted values of FFAt; t = 120 indicates upper limit time used (min).

2.7 Observation of change of microstructure of microcapsules during digestion

The microstructure of digested sample at the end of each digestion stage was observed using a confocal laser scanning microscope (CLSM) and a scanning electron microscope (SEM). In the case of CLSM, 15 µL Fast green and Nile red in acetone (1%, w/v) were added to 1 mL digesta to stain the protein and lipids components, respectively. These stained samples were mixed well and

placed in the dark for 1 h prior to imaging using a Nikon A1R confocal microscope (Nikon Co. Ltd., Tokyo, Japan) with laser excitation wavelengths at 488 nm and 633 nm. For SEM observation, the samples obtained at the end of each digestion stage were freeze-dried, and their surface microstructure was acquired (FEI Quanta 200 ESEM, Japan). The samples were coated with a thin layer of gold for 2 min using a gold sputter (Sputter coater, Agar Aids, England). The micrographs were acquired at an accelerating voltage of 30 kV.

2.8 Statistical analysis

Tests were conducted in triplicate unless otherwise specified and the results are reported as average ± standard deviation. The SPSS statistical software (version 24, SPSS Inc., Chicago, IL, USA) was used for the analysis of variance (ANOVA) in order to test the significant difference between two mean values. Duncan test was implemented on the data sets at 95% confidence level ($p < 0.05$).

3. Results and discussion

3.1 Particle size, zeta potential and microstructure of digesta

3.1.1Particle size and size distribution

The change in particle size and the uniformity (span value) during the digestion process is shown in Figure 1. The oral and gastric digesta showed bimodal size distribution while the SIF digesta showed a multimodal size distribution with new peaks appearing in 50-1000 μm range. In addition, the major population size (mode) of SOF and SGF digesta was approximately 3 μm while that for SIF was around 10 μm. These observations indicate that the coalescence/flocculation occurred in the simulated intestinal digestion stage (Sarkar, Goh, Singh, & Singh, 2009), resulting from the disintegration of matrix wall followed by the release of oil which will be further explained in section 3.1.3.

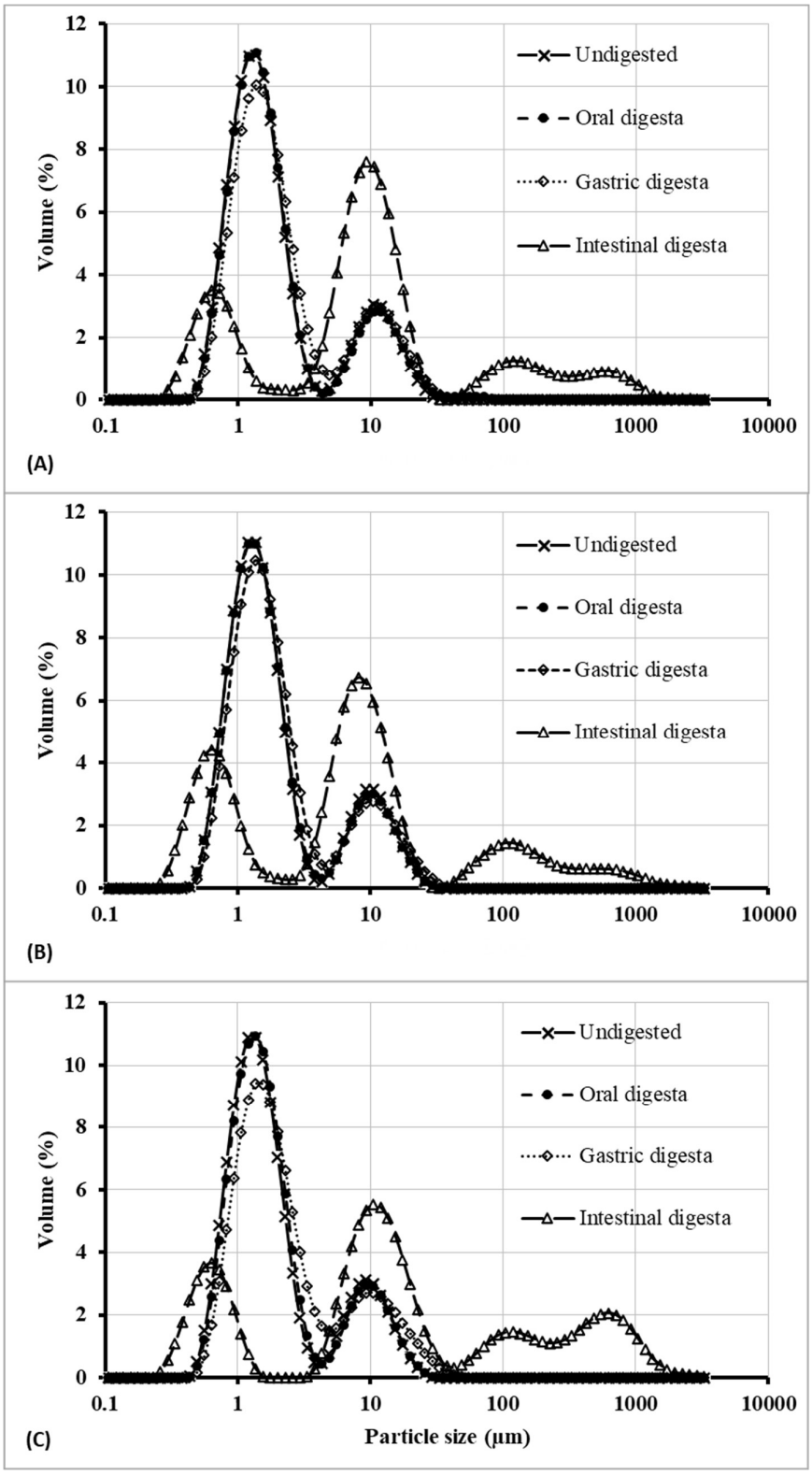

Figure 1. Particle size distribution of undigested and digested microcapsules (A= FPI/FG/FO, B= (FPI-FPP)/FG/FO, C= (FPI-HT)/FG/FO) at the end of each digestion stage. FPI=flaxseed protein isolate, FPP=flaxseed polyphenols, HT=hydroxytyrosol, FG=flaxseed gum. FO= flaxseed oil.

Table 2 presents the change of mean particle diameter ($d_{4,3}$ and $d_{3,2}$) of all digested microcapsules at the end of each digestion stage. As can be observed, the mean particle diameter and span values of all the digesta of the oral stage were similar ($p > 0.05$) to those of undigested microcapsules. These results indicated that the shell of the microcapsules remained intact during the oral digestion. This can be attributed to the indigestible nature of FG to the α-amylase. Also, the contact time (2 min) between the samples and SSF in this stage is too short to induce any significant changes in particle size. It also appears that the wall materials provide sufficient resistance to swelling in this stage. This finding agrees with that of Timilsena et al., (2017), where the chia seed oil microcapsules produced using protein isolate-chia seed gum complex coacervate also retained their original sizes during oral digestion.

The volume-mean diameter ($d_{4,3}$) and span values of all the digested samples in the gastric stage were similar ($p > 0.05$) to their corresponding values in the oral stage. However, their surface mean diameters ($d_{3,2}$) of samples in gastric digestion stage was significantly ($p < 0.05$) higher than in oral digestion stage. This increase in $d_{3,2}$ suggested that the wall materials of these microcapsules experienced a certain degree of hydrolysis in the gastric conditions, leading to the swelling of microcapsules and release of oil (discussed in section 3.1.3). The extent of increase in particle size (i.e. breaking down of microcapsule shell) at the gastric phase in this study was substantially lower than observed by Timilsena et al., (2017). These authors reported that the particle size of microcapsules in gastric condition was 10 times higher than that in oral one. This indicates that the shells produced using FPI-FG complex coacervates (with or without conjugation with phenolic compounds) are more resistant to proteolysis than the ones produced using chia seed protein-chia seed gum complex coacervates. At the end of SIF digestion, both diameters ($d_{4,3}$ and $d_{3,2}$) and span values of all microcapsules were significantly ($p < 0.05$) larger than their corresponding values in the gastric stage. This increase in particle size and broadening of size distribution can be attributed to further hydrolysis of the microcapsule shell in the intestinal stage that intensified the breakdown of the microcapsule and release of oil. As a result, the coalescence/flocculation of oil occurred faster, which led to the formation of bigger particles.

The $d_{4,3}$ and $d_{3,2}$ values of (FPI-HT)/FG/FO capsule were highest among the tested microcapsules at gastric and intestinal stages, suggesting that the highest degree of proteolysis occurred in this microcapsule. In contrast, the (FPI-FPP)/FG/FO showed the lowest degree of proteolysis, as indicated by its smallest mean diameters ($d_{4,3}$ and $d_{3,2}$). This implies that the FPP is able to provide better protection to the protein component of complex coacervates against proteolysis than HT. The different level of resistance of FPP and HT to proteolysis during digestion can be explained

from the difference in solubility of the coacervates. We have shown in our previous work that the solubility of FPI-HT adduct was much higher than that of FPI-FPP (Pham et al., 2019a). The lower solubility of FPP-FPP adduct could have hindered the access of protease in comparison to FPI-HT adduct.

Table 2: Mean droplet size ($d_{3,2}$ and $d_{4,3}$) and span of digested microcapsules at the end of oral, gastric, and intestinal stages. FPI=flaxseed protein isolate, FPP=flaxseed polyphenols, HT=hydroxytyrosol, FG=flaxseed gum. FO= flaxseed oil.

Microcapsule	Undigested			Oral phase			Gastric phase			Intestinal phase		
	$D_{4,3}$ (μm)	$D_{3,2}$ (μm)	Span	$D_{4,3}$ (μm)	$D_{3,2}$ (μm)	Span	$D_{4,3}$ (μm)	$D_{3,2}$ (μm)	Span	$D_{4,3}$ (μm)	$D_{3,2}$ (μm)	Span
FPI/FG/FO	3.49 ± 0.01aA	1.46 ± 0.01aA	6.83 ± 0.02aA	3.87 ± 0.07aA	1.48 ± 0.01aB	7.1 ± 0.05aA	4.01 ±0.1aA	1.64 ± 0aC	6.35 ± 0.24aA	70.3 ± 9.41aB	2.32 ± 0aD	21.87 ± 4.29aB
FPI-FPP/FG/FO	3.39 ± 0.02bA	1.45 ± 0aA	6.46 ± 0bA	3.39 ± 0.03bA	1.46 ± 0.01bA	6.40 ± 0.02bA	3.71 ± 0.11bA	1.58± 0.01bB	6.29 ± 0.21aA	65.7 ± 5.3aB	1.86 ± 0.08bC	19.35 ± 1.67aB
FPI-HT/FG/FO	3.24 ± 0.02cA	1.46 ± 0aA	3.94 ± 0cA	3.28 ±0.03bA	1.50 ± 0.02cA	5.74 ± 0.03cA	4.21 ± 0.11aA	1.74 ± 0cB	6.02 ± 0.64aA	149.3 ± 15.06bB	2.25 ± 0.07aB	45.11 ± 1.7bB

Different lowercase letters in the superscript of the same column and uppercase letters in the superscript of the same row indicate significant differences ($p < 0.05$).

3.1.2 The surface charge of digested microcapsules

The zeta potential data of digested microcapsules shows that their surface charge has altered substantially during the digestion process (Figure 2). In the oral digestion stage, all the digested microcapsules showed quite similar zeta potential values (approximately -12 mV); most probably due to the fact that zeta potential of the simulated salivary/oral fluid itself was -15.36 mV due to the presence of α-amylase and other negatively charged moieties (Figure 2). In the gastric digestion stage, the addition of highly acidic SGF (pH 3.0) to the boluses significantly reduced the magnitude and charge of zeta potential. It is worth noting that both FPI and phenolic-FPI adducts exhibit positive net charge in pH range 3.0-4.0 (Pham et al., 2020).

The simulated intestinal fluid was of neutral pH; thus, this increase of pH of a medium increased negative zeta potential values in all tested capsules compared to that in oral and gastric digestion stages (Figure 2). This tendency can be attributed to the negative charge of both FPI, phenolic-FPI adducts and FG, that formed the shell of microcapsules at the neutral pH (Pham et al., 2020). The presence of bile salt can also increase the negative charge at the water-oil interface (Nik, Wright, and Corredig (2011). In addition, the formation of FFA due to lipolysis (section 3.3.2) could also have contributed to the negative charge at the intestinal digestion stage (Tokle, Lesmes, Decker, & McClements, 2012).

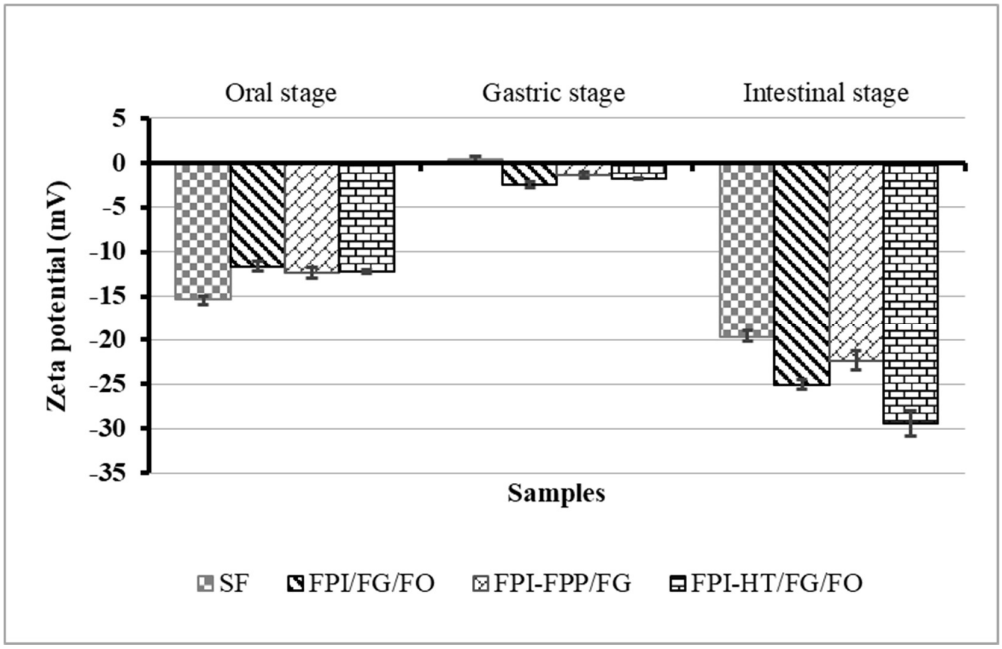

Figure 2: The surface charge (zeta potential) digesta simulated digestion conditions: SF=simulation fluids; FPI=flaxseed protein isolate, FPP=flaxseed polyphenols, HT=hydroxytyrosol, FG=flaxseed gum. FO= flaxseed oil.

3.1.3 The microstructure of digested microcapsules

The CLSM and SEM images of the digesta captured at the end of each digestion stage are shown in Figure 3 and Figure 4, respectively. The microstructure of all the microcapsules remained more or less intact in the oral digestion stage (Figure 3O1-O3) compared with the undigested microcapsules (Figure 3U and 4U). The CLSM micrographs reveal that the microcapsules were slightly aggregated during gastric digestion; however, the extent of aggregation was not substantial enough to alter the particle size. As mentioned earlier (section 3.1.1), the variation in particle size ($d_{3,2}$) of microcapsules at the end of oral and gastric stages was not significant. The fact that the surface morphology of microcapsules at the end of oral and gastric stages (observed through SEM) was quite similar also corroborates the similarity in their microstructure observed through CLSM. Interestingly, CLSM images showed increased intensity and area of red coloured zone (Figure 3G1-G3), indicating the fact that encapsulated oil started to release in the gastric digestion stage.

At the end of intestinal digestion, the release of encapsulated FO from all microcapsules was quite prominent both in CLSM (Figure 3I) and SEM micrographs (Figure 4I). The shell of microcapsules was completely disintegrated during the intestinal digestion as indicated by the absence of green-coloured zone in CLSM images and completely ruptured and distorted surface in SEM images. These changes in the microstructure (CLSM) and surface morphology (SEM) corroborate with the substantially increased particle size ($d_{4,3}$ and $d_{3,2}$) (section 3.1.1) in samples at the end of intestinal digestion. These results also indicate that disintegration of shell and release of oil occurred mostly in the intestinal rather than in the gastric phase. This can be attributed to the ability of phenolic-FPI conjugates to resist the proteolysis of FPI in gastric phase. The size of digested (FPI-HT)/FG/FO microcapsules (Figure 3I) was significantly bigger than that of (FPI-FPP)/FG/FO and FPI/FG/FO microcapsules, which also agrees with particle size data (section 3.1.1). This observation further confirmed that the degree of hydrolysis of the shell of (FPI-HT)/FG/FO capsule was the highest among all the tested samples.

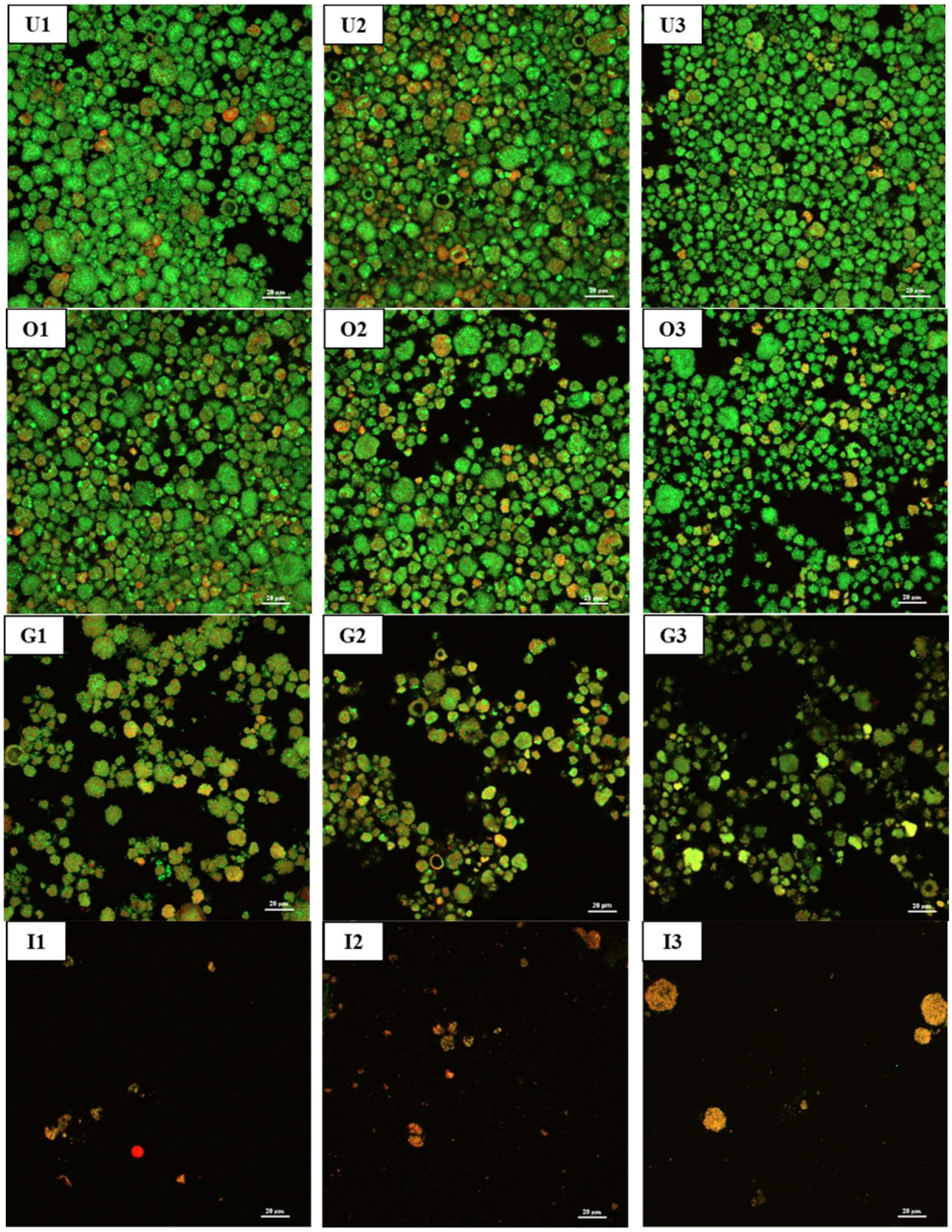

Figure 3: CLSM images of digested samples at the end of each digestion stage: U=undigested samples, O=oral digesta, G=gastric digesta, I=intestinal digesta, 1=FPI/FG/FO, 2=FPI-FPP/FG/FO, 3=FPI-HT/FG/FO. FPI=flaxseed protein isolate, FPP=flaxseed polyphenols, HT=hydroxytyrosol, FG=flaxseed gum. FO= flaxseed oil.

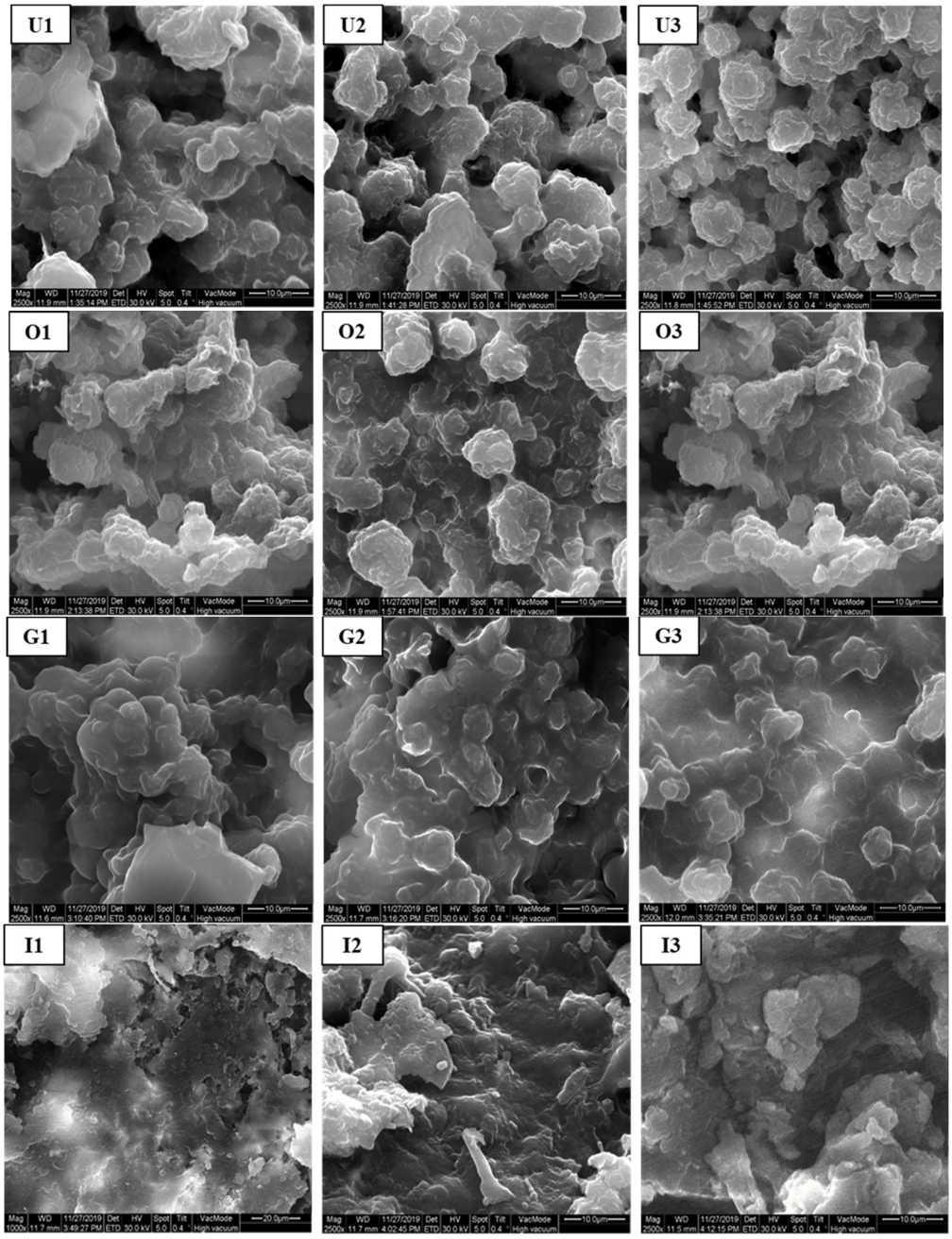

Figure 4: SEM images of freeze-dried digested samples at the end of each digestion stage: U=undigested samples, O=oral digesta, G=gastric digesta, I=intestinal digesta, 1=FPI/FG/FO, 2=FPI-FPP/FG/FO, 3=FPI-HT/FG/FO. FPI=flaxseed protein isolate, FPP=flaxseed polyphenols, HT=hydroxytyrosol, FG=flaxseed gum. FO= flaxseed oil.

3.2 Proteolysis during digestion

3.2.1 Concentration of free amino groups in digested samples

The extent of proteolysis of the microcapsule shell during digestion as indicated by the concentration of free amino group (NH_2), is shown in Figure 5. An increase of NH_2 concentration was observed in simulated fluids in all the samples, right from the start of gastric digestion. The formation of NH_2 was fast within the first 30 min (10 mM, Figure 5) of gastric digestion as indicated by the increase of environmental pH. It then became slower during the subsequent 30 to 120 min of digestion and the NH_2 concentration increased only to 12 mM at 120 min. This slower formation of NH_2 in later part of gastric digestion can be due to the increase of pH that hindered the activity of pepsin (Dekkers et al., 2016). According to Piper and Fenton (1965), the maximum proteolytic activity of pepsin occurs at pH 2.0, and it decreases to 70% of its maximum value at pH 4.5. The concentration of NH_2 during gastric digestion was similar ($p>0.05$) among the microcapsules, indicating a very low degree of protein digestion. This observation also corroborates with the negligible change volume-mean diameter ($d_{4,3}$) (Table 2) as there was no disintegration of the shell in the gastric stage. The concentration of NH_2 in samples at the end of the intestinal stage was significantly higher than that gastric stage, indicating the breakdown of the protein component of the microcapsule shell. This sharp increase in proteolysis of protein component in the intestinal stage is due to the combined proteolytic effect of pancreatin enzyme (lipase, amylase, and protease) (Karaca, Nickerson, & Low, 2013). It has also been reported that the bile salt present in the SIF also destabilises protein structure, making it more susceptible to hydrolysis by proteases (Gass, Vora, Hofmann, Gray, & Khosla, 2007).

During intestinal digestion, the concentration of NH_2 in (FPI-HT)/FG/FO was the highest (59.7 mM) among all the microcapsule powders, implying the highest digestibility of this matrix. This further corroborates the change in particle size and microstructure of the microcapsules during digestion (section 3.1). The fast degradation of (FPI-HT)/FG shell can be due to the fact that the conjugation of HT to FPI has altered the protein conformational structure to make it more susceptible to the proteolysis (Pham et al., 2019b; Xu et al., 2019). In this context, Jiang et al. (2019) studied the digestion of anthocyanins-soy protein isolate (SPI) conjugate and reported that it was more susceptible to hydrolysis than SPI due to unfolding of its structure (decrease in α-helix content). In contrast, the NH_2 concentration in digested FPI/FG/FO and (FPI-FPP)/FG/FO samples was quite similar (Figure 5). We observed in our previous work that the FPI and FPI-FPP had more compact structure than FPI-HT (Pham et al., 2019b). A decrease in digestibility of protein after its adduction with phenolic compounds has also been reported in the literature. For example, Rawel,

Kroll, and Riese (2000) showed that the digestibility of bovine serum albumin significantly decreased after its covalent conjugation with chlorogenic acid.

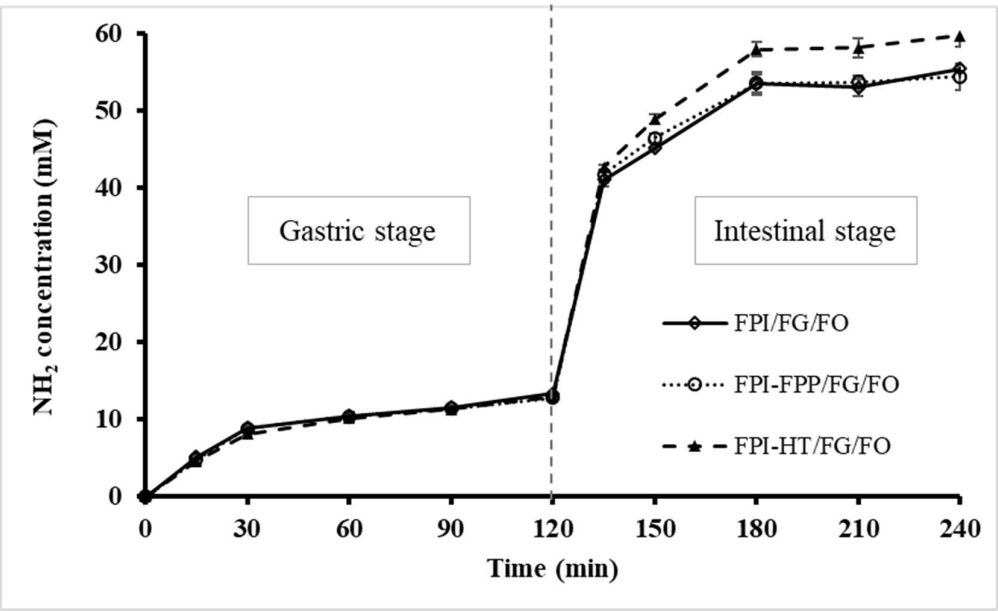

Figure 5: The concentration of free amino group (NH_2) (mM) in digesta as a function of time during gastric and intestinal digestion. FPI=flaxseed protein isolate, FPP=flaxseed polyphenols, HT=hydroxytyrosol, FG=flaxseed gum. FO= flaxseed oil

3.2.2 Change of molecular weight of protein

The change of molecular weight of FPI during digestion is shown in Figure 6. During the oral digestion, no significant molecular weight change was observed (lane O vs. U), suggesting no proteolysis occurred in this stage. In the gastric stage, FPI was hydrolysed into smaller fractions with MW ranging from 10 to 15 kDa (lanes G1-G5) by pepsin. The formation of these small molecular weight fractions was observed after 15 min of digestion in all microcapsules and the MW distribution of protein in all the samples was found to be similar in the gastric digestion stage. This observation is in accordance with the small yet similar level of increase in NH_2 concentration during the digestion stage. Overall, although the MW of protein in all microcapsules during the gastric phase, their shell structure did not seem to be ruptured as indicated by more or less intact particle size. This could be attributed small degree of hydrolysis of FPI due to its relatively strong resistance to gastric digestion. At the end of intestinal digestion, only the protein fractions with molecular weight < 10 kDa were observed in the microcapsule powders (Lanes I1- I5), suggesting

the protein was further hydrolysed to smaller peptides. Due to the limited sensitivity of SDS-PAGE test, the extent of protein hydrolysis in the intestinal digestion stage could not be revealed.

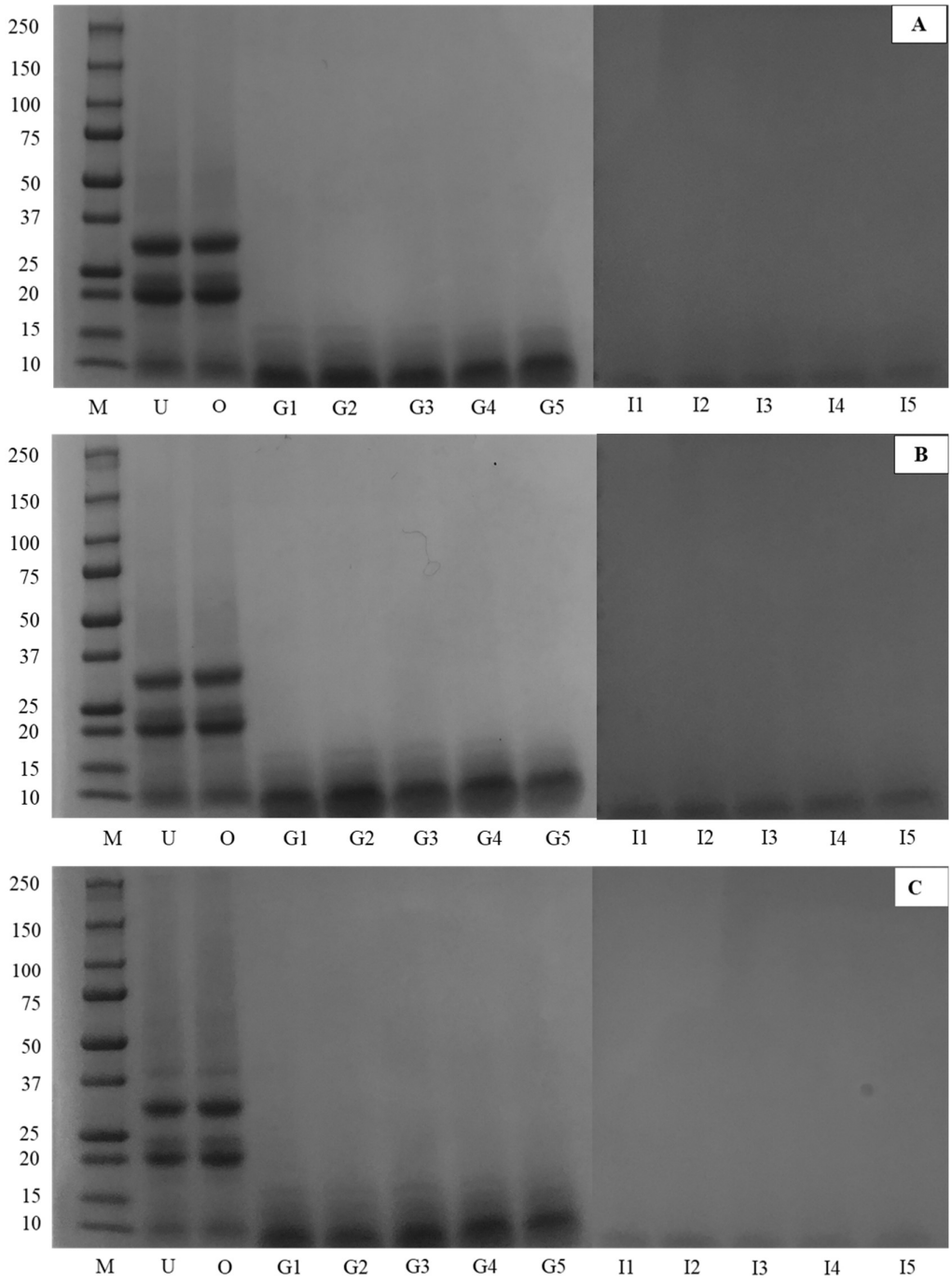

Figure 6: SDS-PAGE (under reducing conditions) of digested samples (A=FPI/FG/FO, B=FPI-FPP/FG/FO, C=FPI-HT/FG/FO) over the time during gastrointestinal digestion. M=marker, U=undigested, O=oral phase, G=gastric phase, I=intestinal phase, 1=15min, 2=30min, 3=60min, 4=90min, 5=120min. FPI=flaxseed protein isolate, FPP=flaxseed polyphenols, HT=hydroxytyrosol, FG=flaxseed gum. FO= flaxseed oil.

3.3 Release of oil and lipolysis during digestion

3.3.1 Release of oil

The release of encapsulated FO from microcapsules in oral, gastric and intestinal stages is shown in Figure 7. The vast majority of encapsulated oil (66-80%) from the microcapsules was released in the intestinal stage. The release of oil in gastric stage range from 5 to 17%. It is worth noting that the oil (2-9 %) released during the oral digestion was the surface oil. The release of oil in the gastric stage is due to some degree of proteolysis of FPI by pepsin, which made the shell more porous and allowed the oil to release. The fact that most of the oil was released in intestinal digestion stage agrees well with the sharp increase of NH_2 concentration and decrease of molecular weight of protein both of which favour the disintegration of microcapsule shell structure. This pattern of release of encapsulated oil is similar to one observed by Eratte et al. (2017) where 10 and 40% of the encapsulated tuna oil was released in gastric and intestinal stages, respectively from whey protein isolate-gum Arabic complex coacervate shell material.

Among microcapsules, (FPI-HT)/FG/FO released the highest amount of oil during intestinal digestion. This confirms the susceptibility of the FPI-HT conjugate to proteolysis due to the unfolded structure of protein component resulting from covalent conjugation with HT (Pham et al., 2019b). The lowest amount of oil was released from (FPI-FPP)/FG/FO powder which can be attributed to its folded structure (Pham et al., 2019b). As mentioned earlier, that the solubility of FPI-FPP adduct in aqueous medium was much lower compared to that of FPI and FPI-HT adduct (Pham et al., 2019a). The lower solubility of FPI-FPP matrix in SIF is expected to slow down the proteolysis and breakdown of matrix which would slow down the release of encapsulated oil. In similar context, Can Karaca, Low, and Nickerson (2013) reported that the low solubility of legume protein caused slow release of oil encapsulated in legume protein/maltodextrin matrix.

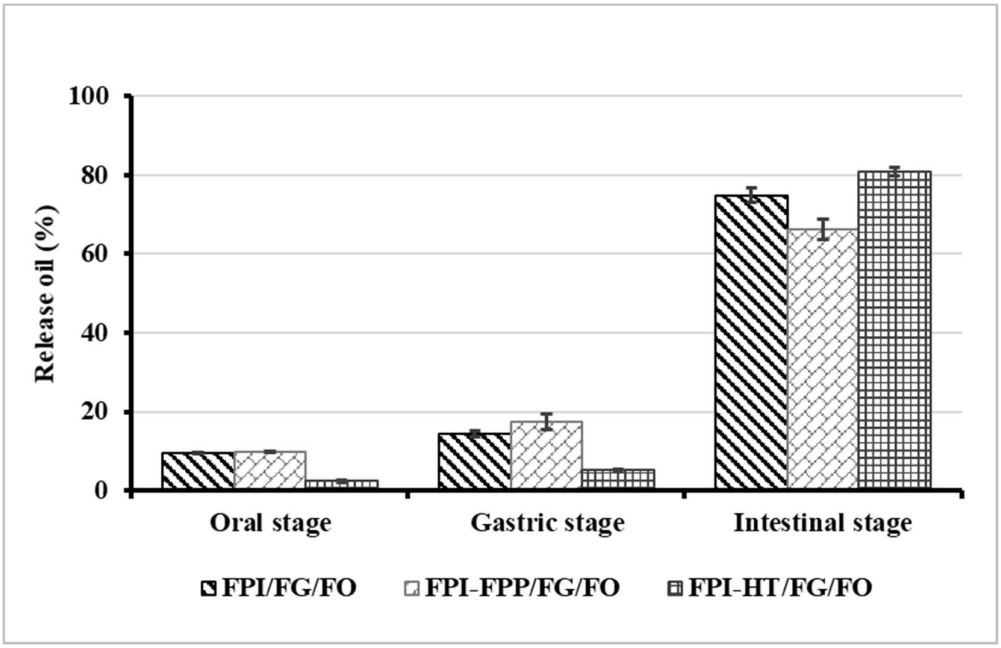

Figure 7: The amount of released oil from digested microcapsule at the end of each digestion stages. FPI=flaxseed protein isolate, FPP=flaxseed polyphenols, HT=hydroxytyrosol, FG=flaxseed gum. FO= flaxseed oil

3.3.2 Lipolysis of encapsulated oil

The release of free fatty acids (FFA) due to the lipolysis of released oil from microcapsules is shown in Figure 8. As can be observed, the first order kinetics model (Equation 2) followed the experimental data with 0.7-3.5% average absolute error. The FFAmax and k values obtained by fitting Equation (2) to experimental data to each microcapsule type is given in Table 3. The rate of release of FFA at 10 and 20 min were determined by equation (4) given below and are listed in Table 3 to support the discussion.

$$R_t = k\, FFA_{max}\, e^{-k\,t} \qquad (4)$$

It can be observed that lipolysis immediately started after the hydrolysis of the shell matrix started to occur and the released oil came in contact with pancreatin (intestinal stage). A sharp increase of FFA content was observed in the microcapsules within the first 10 min digestion as indicated by the rate release of FFA from each microcapsule type (Table 3). This could be due to the high concentration of lipase at the start of digestion, and its unhindered adsorption at the oil-water interface (Mun, Decker, & McClements, 2007). When rates of release of FFA in 10 and 20 minutes are compared, it can be observed that the rate of lipolysis decreased significantly after 20 min in all the samples, possibly because of the decline of lipase activity. Troncoso, Aguilera, and McClements (2012) reported competitive adsorption of FFA on oil/water interface, which can

interfere with lipase activity. The highest release of FFA (FFA_{max}) was observed in (FPI-HT)/FG/FO (38.5%) while the lowest release was observed in (FPI-FPP)/FG/FO (28.9%), which agrees with the extent of proteolysis and release of oil during the intestinal digestion.

As can be observed, the rate of release of FFA in both 10 min and 20 min is highest in (FPI-HT)/FG/FO, lowest in (FPI-FPP)/FG/FO and that of FPI/FG/FO remains in between. Overall, the released FFA content in these microcapsules was found to follow (FPI-HT)/FG/FO > FPI/FG/FO > (FPI-FPP)/FG/FO order which agrees with the patterns of breakdown of their respective microcapsule shell and release of oil.

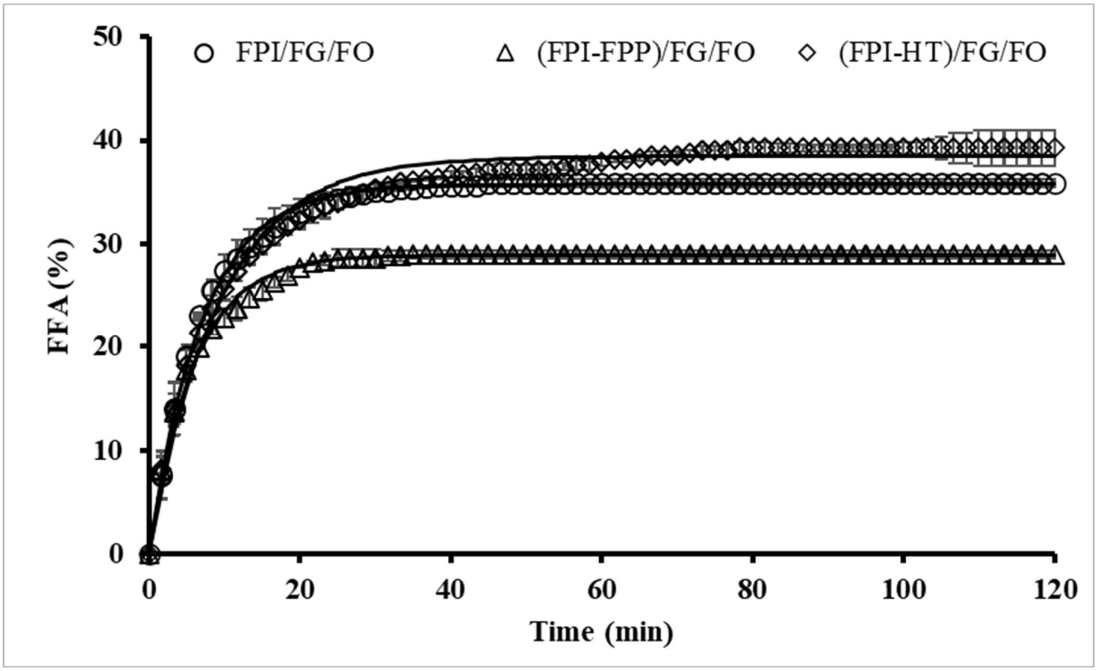

Figure 8: The release of free fatty acids (FFA) as a function of time during intestinal phase. Open symbols indicate the experimental curves while solid lines indicate the fitting curves (Equation 2). FPI=flaxseed protein isolate, FPP=flaxseed polyphenols, HT=hydroxytyrosol, FG=flaxseed gum. FO= flaxseed oil.

Table 3: Kinetic parameters describing the formation/release of FFA from microcapsules calculated using equation (2) and (4). FFA_{max} is the amount of FFA (%) released at the "pseudo-equilibrium". k is the constant of first-order reaction kinetics. R_{10} and R_{20} are the rate of release of FFA at 10 and 20 min, respectively. FPI=flaxseed protein isolate, FPP=flaxseed polyphenols, HT=hydroxytyrosol, FG=flaxseed gum. FO= flaxseed oil.

Microcapsule	R^2	FFA_{max} (%)	k	R_{10} (min^{-1})	R_{20} (min^{-1})
FPI/FG/FO	0.997	35.8 ± 0.9a	0.143 ± 0.004a	1.224 ± 0.002a	0.294 ± 0.01a
(FPI-FPP)/FG/FO	0.993	28.9 ± 0.3b	0.169 ± 0.004b	0.902 ± 0.001b	0.167 ± 0.006b
(FPI-HT)/FG/FO	0.976	38.5 ± 0.2c	0.109 ± 0.008c	1.406 ± 0.003c	0.475 ± 0.038c

Different lowercase letters in the superscript of the same column indicate significant differences ($p < 0.05$).

4. Conclusion

The particle size and microstructure of all the microcapsules produced using FPI/FG, (FPI-FPP)/FG and (FPI-HT)/FG as shell matrix were affected to a lesser degree in in gastric stage and only small quantity (5 to 17%) of FO was released. Breakdown of these matrices occurred mostly in intestinal stage due to breakdown of the protein component. Most of the encapsulated oil (FO) (66-80%) was released and further hydrolysed into FFA in the intestinal stage. Among the three microcapsule systems (FPI-HT)/FG microcapsule had the highest and (FPI FPP)/FG had the lowest FFA release. Thus, (FPI-FPP)/FG is a promising wall material to provide controlled release of hydrophobic ingredients such as omega-3 oils in the intestinal stage of digestion.

References

Abuajah, C. I., Ogbonna, A. C., & Osuji, C. M. (2015). Functional components and medicinal properties of food: a review. *J Food Sci Technol, 52*(5), 2522-2529.

Anwar, F., & Przybylski, R. (2012). Effect of solvents extraction on total phenolics and antioxidant activity of extracts from flaxseed (Linum usitatissimum L.). *ACTA Scientiarum Polonorum Technologia Alimentaria, 11*(3), 293-302.

Augustin, M. A., Sanguansri, L., Rusli, J. K., Shen, Z., Cheng, L. J., Keogh, J., & Clifton, P. (2014). Digestion of microencapsulated oil powders: in vitro lipolysis and in vivo absorption from a food matrix. *Food & function, 5*(11), 2905-2912.

Betoret, E., Betoret, N., Vidal, D., & Fito, P. (2011). Functional foods development: Trends and technologies. *Trends in Food Science & Technology, 22*(9), 498-508.

Calder, P. C. (2006). n− 3 polyunsaturated fatty acids, inflammation, and inflammatory diseases. *The American journal of clinical nutrition, 83*(6), S1505-1519S.

Can Karaca, A., Low, N., & Nickerson, M. (2013). Encapsulation of flaxseed oil using a benchtop spray dryer for legume protein-maltodextrin microcapsule preparation. *J Agric Food Chem, 61*(21), 5148-5155.

Comunian, T. A., & Favaro-Trindade, C. S. (2016). Microencapsulation using biopolymers as an alternative to produce food enhanced with phytosterols and omega-3 fatty acids: A review. *Food Hydrocolloids, 61*, 442-457.

Connor, W. E., Prince, M. J., Ullmann, D., Riddle, M., Hatcher, L., Smith, F. E., & Wilson, D. (1993). The Hypotriglyceridemic Effect of Fish Oil in Adult-Onset Diabetes without Adverse Glucose Control. *Annals of the New York Academy of Sciences, 683*(1), 337-340.

Cui, W., Mazza, G., & Biliaderis, C. (1994). Chemical structure, molecular size distributions, and rheological properties of flaxseed gum. *Journal of Agricultural and Food Chemistry, 42*(9), 1891-1895.

Dekkers, B., Kolodziejczyk, E., Acquistapace, S., Engmann, J., & Wooster, T. (2016). Impact of gastric pH profiles on the proteolytic digestion of mixed βlg-Xanthan biopolymer gels. *Food & function, 7*(1), 58-68.

Eratte, D., Dowling, K., Barrow, C. J., & Adhikari, B. P. (2017). In-vitro digestion of probiotic bacteria and omega-3 oil co-microencapsulated in whey protein isolate-gum Arabic complex coacervates. *Food Chemistry, 227*, 129-136.

Gallier, S., & Singh, H. (2012). The physical and chemical structure of lipids in relation to digestion and absorption. *Lipid Technology, 24*(12), 271-273.

Gass, J., Vora, H., Hofmann, A. F., Gray, G. M., & Khosla, C. (2007). Enhancement of Dietary Protein Digestion by Conjugated Bile Acids. *Gastroenterology, 133*(1), 16-23.

Ghasemi Fard, S., Loh, S. P., Turchini, G. M., Wang, B., Elliott, G., & Sinclair, A. J. (2020). Microencapsulated Tuna Oil Results in Higher Absorption of DHA in Toddlers. *Nutrients, 12*(1), 248.

Golding, M., Wooster, T. J., Day, L., Xu, M., Lundin, L., Keogh, J., & Clifton, P. (2011). Impact of gastric structuring on the lipolysis of emulsified lipids. *Soft Matter, 7*(7), 3513-3523.

Guimarães Drummond e Silva, F., Miralles, B., Hernández-Ledesma, B., Amigo, L., Iglesias, A. H., Reyes Reyes, F. G., & Netto, F. M. (2017). Influence of Protein–Phenolic Complex on the Antioxidant Capacity of Flaxseed (Linum usitatissimum L.) Products. *Journal of Agricultural and Food Chemistry, 65*(4), 800-809.

He, Q., Lv, Y., & Yao, K. (2007). Effects of tea polyphenols on the activities of α-amylase, pepsin, trypsin and lipase. *Food Chemistry, 101*(3), 1178-1182.

Holčapek, M., Jandera, P., Zderadička, P., & Hruba, L. (2003). Characterization of triacylglycerol and diacylglycerol composition of plant oils using high-performance liquid chromatography–atmospheric pressure chemical ionization mass spectrometry. *Journal of Chromatography A, 1010*(2), 195-215.

Jiang, L., Liu, Y., Li, L., Qi, B., Ju, M., Xu, Y., . . . Sui, X. (2019). Covalent conjugates of anthocyanins to soy protein: Unravelling their structure features and in vitro gastrointestinal digestion fate. *Food Research International, 120*, 603-609.

Karaca, A. C., Nickerson, M., & Low, N. H. (2013). Microcapsule production employing chickpea or lentil protein isolates and maltodextrin: physicochemical properties and oxidative protection of encapsulated flaxseed oil. *Food Chem, 139*(1-4), 448-457.

Kong, F., & Singh, R. P. (2009). Digestion of Raw and Roasted Almonds in Simulated Gastric Environment. *Food Biophysics, 4*(4), 365-377.

Kremer, J. M. (1996). Effects of modulation of inflammatory and immune parameters in patients with rheumatic and inflammatory disease receiving dietary supplementation of n-3 and n-6 fatty acids. *Lipids, 31*(1), S243-S247.

Li, D., & Hu, X.-J. (2009). Fish and its multiple human health effects in times of threat to sustainability and affordability: are there alternatives? *Asia Pacific journal of clinical nutrition, 18*(4), 553-563.

Li, Y., & McClements, D. J. (2010). New mathematical model for interpreting pH-stat digestion profiles: Impact of lipid droplet characteristics on in vitro digestibility. *Journal of Agricultural and Food Chemistry, 58*(13), 8085-8092.

Minekus, M., Alminger, M., Alvito, P., Ballance, S., Bohn, T., Bourlieu, C., . . . Dupont, D. (2014). A standardised static in vitro digestion method suitable for food–an international consensus. *Food & function, 5*(6), 1113-1124.

Mun, S., Decker, E. A., & McClements, D. J. (2007). Influence of emulsifier type on in vitro digestibility of lipid droplets by pancreatic lipase. *Food Research International, 40*(6), 770-781.

Nik, A. M., Wright, A. J., & Corredig, M. (2011). Impact of interfacial composition on emulsion digestion and rate of lipid hydrolysis using different in vitro digestion models. *Colloids and Surfaces B: Biointerfaces, 83*(2), 321-330.

Oomah, B. D., Mazza, G., & Cui, W. (1994). Optimization of protein extraction from flaxseed meal. *Food Research International, 27*(4), 355-361.

Pham, L. B., Wang, B., Zisu, B., & Adhikari, B. (2019a). Complexation between flaxseed protein isolate and phenolic compounds: Effects on interfacial, emulsifying and antioxidant properties of emulsions. *Food Hydrocolloids, 94*, 20-29.

Pham, L. B., Wang, B., Zisu, B., & Adhikari, B. (2019b). Covalent modification of flaxseed protein isolate by phenolic compounds and the structure and functional properties of the adducts. *Food Chemistry, 293*, 463-471.

Pham, L. B., Wang, B., Zisu, B., Truong, T., & Adhikari, B. (2020). Microencapsulation of flaxseed oil using polyphenol-adducted flaxseed protein isolate-flaxseed gum complex coacervates. *Food Hydrocolloids, 107*, 105944.

Piper, D., & Fenton, B. H. (1965). pH stability and activity curves of pepsin with special reference to their clinical importance. *Gut, 6*(5), 506.

Rawel, H. M., Czajka, D., Rohn, S., & Kroll, J. (2002). Interactions of different phenolic acids and flavonoids with soy proteins. *Int J Biol Macromol, 30*(3-4), 137-150.

Rawel, H. M., Kroll, J., & Riese, B. (2000). Reactions of chlorogenic acid with lysozyme: physicochemical characterization and proteolytic digestion of the derivatives. *Journal of Food Science, 65*(6), 1091-1098.

Roynette, C. E., Calder, P. C., Dupertuis, Y. M., & Pichard, C. (2004). n-3 Polyunsaturated fatty acids and colon cancer prevention. *Clinical Nutrition, 23*(2), 139-151.

Sanguansri, L., & Ann Augustin, M. (2006). Microencapsulation and delivery of omega-3 fatty acids. In *Functional food ingredients and nutraceuticals: Processing technologies* (pp. 297-327): CRC Press.

Sarkar, A., Goh, K. K. T., Singh, R. P., & Singh, H. (2009). Behaviour of an oil-in-water emulsion stabilized by β-lactoglobulin in an in vitro gastric model. *Food Hydrocolloids, 23*(6), 1563-1569.

Sarkar, A., Horne, D. S., & Singh, H. (2010). Pancreatin-induced coalescence of oil-in-water emulsions in an in vitro duodenal model. *International dairy journal, 20*(9), 589-597.

Shen, Z., Apriani, C., Weerakkody, R., Sanguansri, L., & Augustin, M. A. (2011). Food matrix effects on in vitro digestion of microencapsulated tuna oil powder. *Journal of Agricultural and Food Chemistry, 59*(15), 8442-8449.

Smoluchowski, M. v. (1921). Handbuch der Elektrizität und des Magnetismus. *Band II, Barth-Verlag, Leipzig*.

Steffens, W. (1997). Effects of variation feeds on nutritive in essential fatty acids in fish value of freshwater fish for human. *Aquaculture, 151*, 97-119

Timilsena, Y. P., Adhikari, R., Barrow, C. J., & Adhikari, B. (2017). Digestion behaviour of chia seed oil encapsulated in chia seed protein-gum complex coacervates. In *Food Hydrocolloids* (Vol. 66, pp. 71-81).

Timilsena, Y. P., Wang, B., Adhikari, R., & Adhikari, B. (2017). Advances in microencapsulation of polyunsaturated fatty acids (PUFAs)-rich plant oils using complex coacervation: A review. *Food Hydrocolloids, 69*, 369-381.

Tokle, T., Lesmes, U., Decker, E. A., & McClements, D. J. (2012). Impact of dietary fiber coatings on behavior of protein-stabilized lipid droplets under simulated gastrointestinal conditions. *Food & function, 3*(1), 58-66.

Troncoso, E., Aguilera, J. M., & McClements, D. J. (2012). Fabrication, characterization and lipase digestibility of food-grade nanoemulsions. *Food Hydrocolloids, 27*(2), 355-363.

Wickham, M., Wilde, P., & Fillery-Travis, A. (2002). A physicochemical investigation of two phosphatidylcholine/bile salt interfaces: implications for lipase activation. *Biochimica et Biophysica Acta (BBA)-Molecular and Cell Biology of Lipids, 1580*(2), 110-122.

Xu, H., Zhang, T., Lu, Y., Lin, X., Hu, X., Liu, L., . . . Wu, X. (2019). Effect of chlorogenic acid covalent conjugation on the allergenicity, digestibility and functional properties of whey protein. *Food Chemistry, 298*, 125024.

Ye, A., Cui, J., Zhu, X., & Singh, H. (2013). Effect of calcium on the kinetics of free fatty acid release during in vitro lipid digestion in model emulsions. *Food Chemistry, 139*(1-4), 681-688.

Zhang, Z.-S., Wang, L.-J., Li, D., Li, S.-J., & Özkan, N. (2011). Characteristics of flaxseed oil from two different flax plants. *International Journal of Food Properties, 14*(6), 1286-1296.

CHAPTER 7

General Discussion, Conclusion and Recommendation

7.1 Introduction

This Thesis aimed to study the effect of covalent conjugation between plant protein and plant phenolic compounds on the physicochemical and functional properties of the plant protein, and the application of these conjugates/adducts as emulsifiers and encapsulants of omega-3 rich oils. It also aimed gaining insights into the complex coacervation of these protein-phenolic adducts with plant polysaccharide gums. Then efficacy of these plant protein-phenolic adducts-gum complex coacervates in encapsulating omega-3 oil and delivery to the intestinal stage of digestion were also investigated. It was hypothesised that the plant protein-phenolic adducts and their complex coacervates with gum can be suitable emulsifiers of oil-in-water emulsions; and suitable encapsulating shell materials of omega-3 rich oils. Also, the application of plant protein-phenolic adducts and their complex coacervates with gum as emulsifiers and encapsulants can improve the oxidation stability of these emulsions and microcapsules. The outcomes of this Thesis contribute to the science of covalent conjugation between plant proteins and plant phenolic compounds and demonstrate the suitability of these adducts as natural emulsifiers/encapsulants of hydrophobic compounds due to their unique interfacial, emulsifying, encapsulating properties. This Thesis provides greater understanding of the digestion behaviour of omega-3 rich oil encapsulated in plant protein-phenolic compound-gum complex coacervate. Flaxseed was chosen as the plant source of protein, gum, oil and polyphenol whereas hydroxytyrosol (HT) was used as small molecular weight phenolic compound. Flaxseed protein isolate (FPI)-phenolic adducts were prepared by incubating FPI with flaxseed polyphenol (FPP), ferulic acid (FA), and HT under alkaline condition (pH 9.0) in the presence of oxygen. The findings of this Thesis are presented in chapters 3 to 6.

This Thesis commenced with the investigation of the effects of covalently interacted FPI-FPP, FPI-FA, and FPI-HT adducts on the physicochemical and functional properties of FPI (Chapter 3). The results revealed that the alteration of physicochemical and functional properties of FPI due to adduction depended on the nature of phenolic compounds tested; for example, HT was able to cross-link protein molecules of FPI. These findings provided greater insights in developing many other plant protein-phenolic adducts as emulsifiers and encapsulants. Examination of the interfacial and emulsifying properties of the adducts (Chapter 4) showed that FPI-phenolic adducts had weak stability at oil-water interface, and thus, resulted into poor emulsion stability. However, the emulsions stabilised by phenolic-adducted FPI had significantly higher stability against oxidation compared to that of FPI-stabilised emulsion. When the FPI-plant phenolic adducts formed complex coacervates with flaxseed gum (FG) (Chapter 5), the covalent conjugation altered the optimum conditions of the complex coacervation. As encapsulating shell materials, the FPI-

phenolic adducts and their complex coacervates with FG altered the properties of spray-dried flaxseed oil (FO) microcapsules depending on the nature of phenolic compounds incorporated. Overall, the FPI-phenolic adducts and FPI-phenolic adduct-FG complex coacervates successfully produced FO microcapsules; of which FPI-HT adducts acted as superior wall material (Chapter 5). The digestion behaviour of complex FO encapsulated in FPI-phenolic adduct-FG complex coacervates was different in oral, gastric and intestinal digestion stages, depending on nature of the phenolic-FPI adducts involved (Chapter 6). The highest degree of lipolysis was observed in the FPI-HT/FG/FO microcapsule (Chapter 6). The lowest degree of lipolysis was observed in the FPI-FPP/FG/FO microcapsule.

Findings documented Thesis provide insights into the effects of phenolic covalent conjugation on the physicochemical and functional properties of plant proteins and the applicability of these modified proteins (adducts) to formulate emulsifiers and encapsulating shell materials for hydrophobic bioactive compounds, including omega-3 rich oils which will impart desirable stability against oxidation and controlled/targeted release properties during digestion.

7.2 Key findings

This study was designed to understand the changes of physicochemical and functional properties of plant protein (FPI as model) when covalently conjugated with phenolic compounds, including FPP, FA, and HT. The conjugation of different phenolic compound with FPI is expected to alter the interfacial and emulsifying properties of FPI differently. Once the fundamental interfacial and emulsifying properties of the FPI-phenolic adducts and their complex coacervates with FG were quantified, this information was used to produce FO microcapsules using complex coacervates Finally, the digestion behaviour of these FO microcapsules was examined. The ensuring sections, present the key findings of this study.

7.2.1 Effect of covalent conjugation of FPI with phenolic compounds (FPP, FA, HT) on its physicochemical and functional properties

Reaction between FPI and FFP, FA and HT was carried out under alkaline condition (pH 9.0) with the presence of oxygen. The physicochemical and functional properties of FPI-phenolic adducts were characterised and compared with the unmodified FPI. The findings of this work are documented in Chapter 3.

The degree of covalent conjugation between FPI and phenolic compounds and the physicochemical properties of FPI-phenolic adducts were found to depend on the structure of the

phenolic compounds used. The extent of decrease in free amino, thiol and tryptophan groups and an increase in the apparent molecular weight of FPI due to conjugation and cross-linking was different. The cross-linking of protein molecules was observed in FPI-HT adduct while FA and FPP were unable to cross-link with FPI. The ability of HT to cross-link two protein molecules of FPI was attributed to the dihydroxybenzenes structure of HT rendering it to be oxidised to quinone and subsequently bound to the nucleophiles in the side chain of FPI. The HT that was found to the side chain of FPI was re-oxidised and dimerised to form a cross-link (Strauss & Gibson, 2004). The ability of FA and FPP to covalently bind with side chain of FPI molecule but unable to cross-link was due to hydroxycinnamic structure of FA, abundance of p-coumaric acid in FPP. Thus, FA and FPP were oxidised into phenolate ions and subsequently formed semiquinone radical intermediate which ultimately reacted with nucleophiles of the side chain of FPI (Kroll & Rawel, 2001). The thermal stability of the FPI-phenolic adducts was higher than that of the pure FPI, perhaps due to the increase of hydroxyl groups in the adducts (Damodaran & Agyare, 2013). The stability of all adducts against oxidation was improved compared to the native FPI due to innate antioxidant activity of phenolic compounds. In addition, the structural conformation and hydrophobicity of FPI-phenolic adducts were also found to depend on the nature of phenolic compounds. For example, the hydrophobicity of FPI-HT adduct decreased while that of FPI-FPP and FPI-FA increased compared to that of pure FPI. These finding indicates that the interfacial and emulsifying properties of the FPI-phenolic adducts are likely to be affected by their hydrophobic/hydrophilic nature vis a vis that of pure FPI.

7.2.2 Investigation of the interfacial and emulsifying properties of FPI-phenolic adducts

The interfacial behaviour of FPI-phenolic adducts was investigated in terms of the dynamic interfacial tension (DIT), dilatational elasticity (E′) and viscosity (E″) while their emulsifying characteristics were evaluated using emulsifying activity and emulsion stability as indicators. The solubility and surface charge were used to explain the stability of emulsions stabilised by FPI, FPI-FPP and FPI-HT adducts (Chapter 4). Regarding interfacial properties, the FPPI adducted with phenolic compounds significantly increased the diffusion rate constant when the FPI concentration was low (0.1 mg mL^{-1}). The dynamic interfacial tension (DIT) values and penetration rate constants of the FPI, FPI-FPP and FPI-HT adducts were not different at higher FPI concentration (1 to 10 mg mL^{-1}). Structural flexibility of FPI-phenolic adducts at oil-water interface was different as indicated by the difference in their dilatational rheological behaviours. For example, in comparison to unconjugated FPI, the FPI-HT adduct absorbed at oil-water interface had more compact structure due to cross-linking of FPI molecules with HT which resulted into higher E′

value. In contrast, the larger molecular structure of FPI-FPP adduct led to a less compact structure, which resulted into lower E′ value. Experimental data documented in this chapter shows that dilatational rheological behaviour of the absorption films at the oil-water interface did not necessarily reflect on the stability of macroscopic emulsions as indicated by the higher stability of FPI-stabilised emulsion than that of FPI-phenolic adducts stabilised ones. The emulsions stabilised by FPI-FPP and FPI-HT adducts had higher stability against oxidation compared to that of FPI stabilised one. These findings highlight the fact that advantages and limitations of the phenolic-FPI adducts have to be carefully considered when they are used as emulsifiers. The phenolic compound dependent solubility, hydrophobicity and of plant protein-phenolic adducts are expected to affect their effectiveness as encapsulants.

7.2.3 Microencapsulation of FO using phenolic adducted FPI-FG complex coacervates

The FPI-phenolic adducts were used as shell material to encapsulate FO. For this purpose, the optimum conditions for producing complex coacervates of FPI-phenolic adducts with FG were determined. Then, the complex coacervates were used to produce liquid microcapsules of FO followed by spray drying to produce solid FO microcapsules. Spray-dried FO microcapsules were produced using phenolic-adducted FPI/FG and FPI/FG (control). The properties of the FO microcapsules produced in this way were found to be influenced by the nature of the FPI-phenolic adducts (Chapter 5).

The optimum pH for complex coacervation of FPI, FPI-FPP, and FPI-HT with FG was quite narrow (4.6±0.1) and their optimum protein-to-gum ratio was also similar (6:1). These optimum parameters were determined through zeta potential, optical density of the complex coacervates. Spray-dried microcapsule powders had irregular shape with wrinkled surface morphology. The (FPI-HT)/FG complex coacervate was found to be the most effective encapsulant of FO with the lowest surface oil (1%, w/w) and highest microencapsulation efficiency (95.4%). These superior properties, compared to that of FPI, can be contributed by the improved solubility of FPI-HT adduct and its ability to produce denser shell surround the oil droplets due to cross-linking. The (FPI-FPP)/FG/FO microcapsule had the highest stability against oxidation as indicated by the lowest peroxide value and *p*-anisidine values, which is due to the inherent antioxidant activity of FPP. These findings suggested that FPI-phenolic adduct-FG complex coacervates can be preferred over FPI or other single plant protein matrix encapsulating shell materials for oxygen-sensitive oil.

7.2.4 In-vitro digestion behaviour of FO encapsulated in phenolic-adducted FPI/FG complex coacervates

The *in-vitro* digestion of FO microcapsules produced using phenolic-adducted FPI/FG and FPI/FG (control) complex coacervates was investigated using an adult *in vitro* digestion system. Degree of proteolysis of encapsulating shell and the extent of lipolysis of encapsulated FO were evaluated (Chapter 6). The result showed that the release of encapsulated FO from the microcapsules was prolonged. As expected, the degree of proteolysis of protein in the shell and lipolysis of oil were found to be dependent on the characteristics of the shell materials.

When used as encapsulating shell materials of for FO, both (FPI-HT)/FG and (FPI-FPP)/FG complex coacervates showed significant resistance against proteolysis in the simulated oral and gastric conditions, resulting in a small amount of released oil and almost unchanged particle size and microstructure. Majority of encapsulated FO was successfully released in the simulated intestinal stage due to the intensive disintegration of the shell materials. In particular, the highest amount of release of oil (80%) and formation of free fatty acids (FFA) (38.5 %) were observed in the (FPI-HT)/FG/FO microcapsule, which is due to the improved solubility and structural flexibility of FPI-HT adduct. These promoted the access of lipase to the oil-water interface. Meanwhile, the (FPI-FPP)/FG/FO microcapsule had the lowest released oil (66.3 %) and formation of FFA (28.9%); which attributed to reduced solubility and the compact structure of the FPI-FPP adduct. The rate of release of FFA was also highest in (FPI-HT)/FG/FO microcapsule and lowest in (FPI-FPP)/FG/FO microcapsule. These findings suggested that these two unique complex coacervates can be potentially used as a promising delivery vehicle for lipophilic compounds to deliver to intestinal stage of digestion.

7.3 Contribution made by this Thesis to the body of knowledge

This Thesis has made the following contributions to the body of knowledge.

1. Some phenolic compounds, such as HT can cross-link plant proteins (e.g. FPI) while others such as FPP simply covalently conjugate at the side chain but cannot cross-link.

2. It has shown that the changes in physicochemical and functional properties of plant proteins due to their covalent conjugation with phenolic compounds depends on the nature of phenolic compounds tested. For example, interfacial dilutional elasticity and viscosity of plant protein-phenolic adducts can be higher or lower depending on the nature of the adducted phenolic compounds. The dilatational viscosity of FPI-phenolic adducts was lower than that of unmodified FPI.

3. The stability of oil-water emulsions may not improve when phenolic compound adducted plant proteins are used as emulsifiers; however, the stability against oxidation will surely be improved.

4. Phenolic compound-adducted plant proteins can be effective encapsulating shell materials for unstable hydrophobic compounds e.g. omega-3 rich oils. The complex coacervates produced using these adducts with plant gums (e.g. FG) can be suitable encapsulants to deliver hydrophobic compounds (e.g. FO) to intestinal stage of digestion.

5. The flaxseed protein-polyphenol conjugates developed in this study have high oxidative stability. Thus, they can be used as emulsifiers to produce salad dressing, mayonnaise, and ice cream. This could extend the shelf life of these products. The flaxseed protein-polyphenol adduct/flaxseed gum complex coacervates produced in this study can be used as a highly stable wall matrix for microencapsulation of omega-3 oils. These microcapsules can be used to fortify yoghurt, cereal bar, and fruit juice in order to improve their stability and extend their shelf life.

7.4 Recommendations for future research

The author wished to carry out the following work as part of the thesis; however, due to time constraint it was not possible; thus, they are recommended for future study.

1. Complex coacervates were used to encapsulate the omega-3 oil rich FO; however, however, the interfacial behaviour (dynamic interfacial tension, dilatational elasticity and viscosity, rate of diffusion to the oil-water interface) of complex coacervate at the oil-water interface was not studied due to time constraint. Sound understanding of these properties will help quantify and explain the emulsifying properties of these complex coacervates.

2. It was found that HT readily cross-links with plant proteins (e.g. FPI). The covalent conjugation was carried out between FPI and HT and the resultant cross-linked adducts were used as emulsifiers. It would be of great practical implication if in situ cross-linking was carried out after the oil is emulsified by protein.; i.e. HT is used similar to the transglutaminase.

3. These plant protein-phenolic adducts can be used to co-encapsulate oils and probiotic bacteria for developing novel functional foods. A systematic study in this area and product developed in this way would have benefits of antioxidants, essential oils, and beneficial bacteria.

4. The FO microcapsules produced in this study can be incorporated into food products such as salad dressings, yoghurt, cereal bar, and fruit juice. Such study will help broaden the application of these novel ingredients in many commonly and widely produced and consumed foods.

5. There is common perception that the presence of phenolic compounds in food ingredients introduces some degree of bitterness. Thus, future works in this area should consider including sensory evaluation aspects to determine if bitterness is introduced and if so to what degree.

References

Damodaran, S., & Agyare, K. K. (2013). Effect of microbial transglutaminase treatment on thermal stability and pH-solubility of heat-shocked whey protein isolate. *Food Hydrocolloids, 30*(1), 12-18.

Kroll, J., & Rawel, H. M. (2001). Reactions of plant phenols with myoglobin: influence of chemical structure of the phenolic compounds. *Journal of Food Science, 66*(1), 48-58.

Strauss, G., & Gibson, S. M. (2004). Plant phenolics as cross-linkers of gelatin gels and gelatin-based coacervates for use as food ingredients. *Food Hydrocolloids, 18*(1), 81-89.